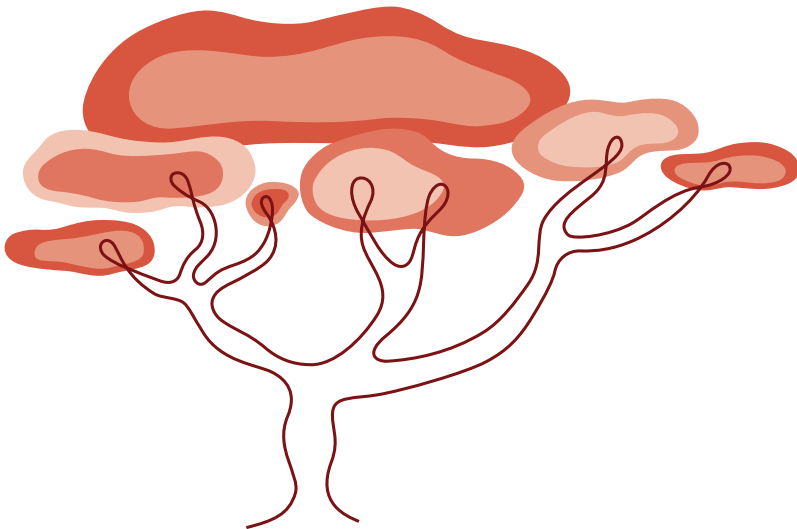# Optimizing visceral leishmaniasis treatment in Eastern Africa

Understanding the pharmacokinetics and pharmacodynamics in a pediatric and malnourished population

Luka Verrest

Optimizing visceral leishmaniasis treatment in Eastern Africa

Understanding the pharmacokinetics and pharmacodynamics
in a pediatric and malnourished population

Optimizing visceral leishmaniasis treatment in Eastern Africa

Understanding the pharmacokinetics and pharmacodynamics
in a pediatric and malnourished population

**Optimalisatie van de behandeling van viscerale leishmaniasis
in Oost-Afrika**

Begrip van de farmacokinetiek en farmacodynamiek
in een pediatrische en ondervoede populatie

(met een samenvatting in het Nederlands)

Proefschrift

ter verkrijging van de graad van doctor aan de
Universiteit Utrecht
op gezag van de
rector magnificus, prof.dr. H.R.B.M. Kummeling,
ingevolge het besluit van het college voor promoties
in het openbaar te verdedigen op

donderdag 16 maart 2023 des ochtends te 10.15 uur

door

Luka Verrest

geboren op 31 januari 1991
te Bergen op Zoom

Promotoren:

Prof. dr. A.D.R. Huitema
Prof. dr. J.H. Beijnen

Copromotor:

Dr. T.P.C. Dorlo

Beoordelingscommissie:

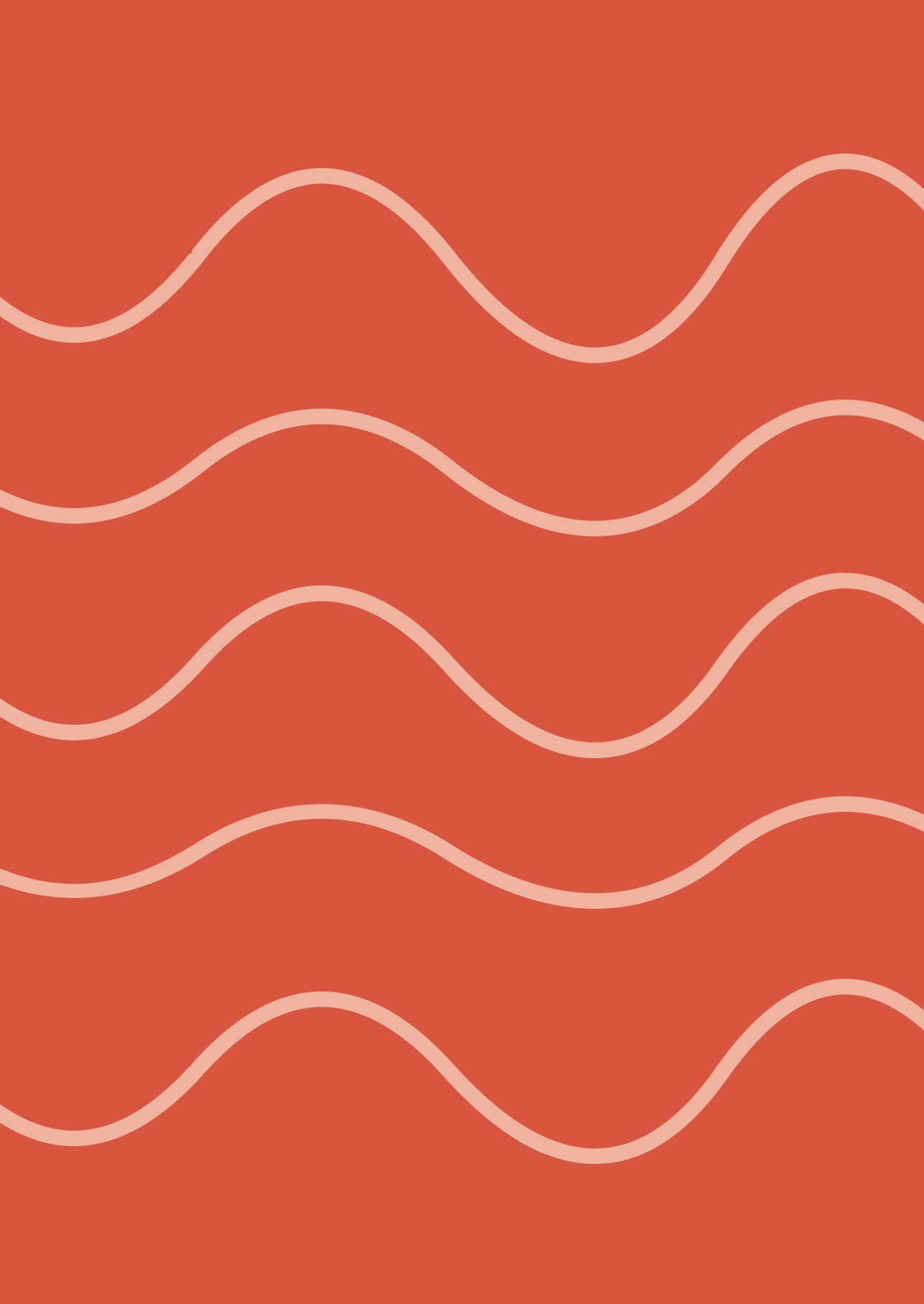Prof. dr. J. Frenkel (voorzitter)
Prof. dr. L. Friberg
Prof. dr. B.C.P. Koch
Prof. dr. A.K. Mantel - Teeuwisse
Prof. dr. A.C.G. Egberts

Table of contents

Preface

Preface

Visceral leishmaniasis (VL) is a neglected tropical disease caused by the *Leishmania* parasite, transmitted by sand flies, mainly affecting vulnerable and poor people in remote areas of low-income countries. The VL infection affects mainly the spleen, liver and bone marrow, where the parasites typically suppress the cellular immune response, preventing the patients' ability to clear the infection. Clinical manifestations of the disease are fever, weight loss, enlargement of the spleen and liver, and anemia. Over 95% of patients will eventually die when left untreated[1]. In the past five years, over 90 000 new cases have been reported globally, with the highest burden in Eastern Africa, where the disease mainly affects children[2]. Leishmaniasis is classified by the World Health Organization (WHO) as one of the neglected tropical diseases in critical need for disease control and elimination. Development of more effective and user-friendly treatment and diagnostics, especially for Eastern Africa, is one of research priorities set by the WHO[3].

Since 2010, a combination treatment of sodium stibogluconate (SSG) and paromomycin has been the standard of care for VL in Africa[4], which showed a final cure rate of 91.4% in a clinical trial setting[5], but is expected to be lower in general clinical practice. This treatment is far from optimal, since it entails hospitalization during the whole treatment period with painful injections twice daily and the risk of potentially life-threatening antimony-related toxicities such as cardiotoxicity, hepatotoxicity and pancreatitis. Although most patients seem initially cured by the end of treatment, most patients that do not reach final cure relapse after treatment, which is a particularly long-term event that can occur within 12 months or even longer after treatment and is difficult to predict.

To improve treatment of VL in Eastern Africa, treatment should be effective, affordable and easy to use in remote areas where most of these patients are living, while minimizing the risks of toxicities. New chemical entities that might meet these criteria are currently under development at preclinical stages. Until these agents reach the market, a (new) combination of drugs already used in monotherapy for VL treatment might be a fast way to improve therapy, preferably without the highly toxic SSG component. By using a combination therapy, efficacy can be improved, while minimizing the risks of emerging resistance and toxicities when lower doses or shorter treatment duration are used compared to monotherapies. In this regard, paromomycin and miltefosine, the only oral drug available for treatment of VL, are favorable treatment options because of their relatively good safety profile and suitability for use in remote areas. Various monotherapy and combination therapy regimens have been evaluated, but resulted however in unsatisfactory efficacy in Africa, with high variability between geographical regions where VL is endemic[5-7].

Reasons for unsatisfactory and variable efficacy between geographical regions might be patient related, i.e., typically patients are malnourished to a variable extent, are severely sick and often suffer from co-infections. These factors might influence the pharmacokinetics of the antileishmanial drugs and consequently the drug exposure, as well as the ability of the patient to clear the parasite by the hosts' immune system, as typically the cellular response is suppressed by the VL infection. Moreover, children are the mainstay of the population affected by VL, particularly in Eastern Africa, a vulnerable population that responds less adequate to VL treatment.

To improve VL treatment in Eastern Africa, dosing should be adjusted to Eastern African patients with the typical characteristics described above, in order to obtain adequate drug exposure in this population. Whereas underexposure can lead to diminished efficacy, overexposure can lead to higher rates of toxicity. Additionally, a better understanding of the parasite dynamics is needed to understand the interplay between growth of *Leishmania* parasites, exposure-response relationships of different VL drugs and the effect of the patients' immune system on parasite clearance. This knowledge can be useful to predict treatment efficacy of different therapies, in patients with different degrees of infection and different stages of immune impairment. Furthermore, this knowledge might even be useful to predict long-term treatment response already during or early after treatment by the identification of predictors of relapse.

Objectives of this thesis

In this thesis, we aim to improve VL treatment in Eastern African patients in two ways: 1) to characterize the pharmacokinetics of paromomycin and miltefosine in Eastern African patients to optimize dosing, in different Eastern African regions, in malnourished patients, and in pediatrics as well as adults, and 2) to characterize *Leishmania* parasite dynamics to understand exposure-response relationships of VL drugs and the effect of the hosts' immune system on parasite response and clinical outcome, and to identify early biomarkers to predict long-term treatment outcome.

Thesis outline

Chapter 1 introduces the importance of pharmacokinetic studies to optimize drug treatment of neglected tropical diseases by two systematic reviews. The added benefit of population-based pharmacokinetic studies is evaluated, as well as the impact of malnutrition on the pharmacokinetics of drugs used to treat poverty-related diseases. To assess whether the observed striking variability in VL treatment efficacy is related to drug pharmacokinetics, the pharmacokinetics of paromomycin and miltefosine in Eastern African VL patients are characterized and compared to their pharmacokinetics in Indian VL patients and Eastern African PKDL patients in **chapter 2**. Covariates are analyzed to assess whether variability in pharmacokinetics is influenced by the patients' nutritional status or manifestations of the disease. In **chapter 3**, blood parasite load is evaluated as a biomarker to represent the degree of *Leishmania* infection in the patient. The usefulness of this biomarker to predict clinical relapse in VL patients is evaluated. A *Leishmania* parasite dynamics model is developed to characterize *in vivo* parasite growth, drug-induced parasite clearance and parasite suppression after treatment, to identify drug exposure-response relationships and relationships between blood parasite load or blood parasite exposure and clinical relapse.

References

1. World Health Organization. Leishmaniasis [Internet]. 2022 [cited 2022 Oct 13]. Available from: https://www.who.int/news-room/fact-sheets/detail/leishmaniasis
2. Ruiz-Postigo JA, Jain S, Mikhailov A, Valadas S, Warusavithana S, Osman M, et al. Global leishmaniasis suveillance: 2019-2020, a baseline for the 2030 roadmap. Wkly Epidemiol Rec. 2021;35:19.
3. World Health Organization. Ending the neglect to attain the Sustainable Development Goals - A road map for neglected tropical diseases 2021–2030. 2020;(February 2019):1–13. Available from: https://www.who.int/neglected_diseases/Revised-Draft-NTD-Roadmap-23Apr2020.pdf?ua=1
4. Organization WH. Control of the leishmaniases. Report of a meeting of the WHO Expert Committee on the Control of Leishmaniases, Geneva. 2010; Available from: https://apps.who.int/iris/bitstream/handle/10665/44412/WHO_TRS_949_eng.pdf?sequence=1
5. Musa A, Khalil E, Hailu A, Olobo J, Balasegaram M, Omollo R, et al. Sodium stibogluconate (SSG) & paromomycin combination compared to SSG for visceral leishmaniasis in East Africa: A randomised controlled trial. PLoS Negl Trop Dis. 2012;6(6):e1674.
6. Wasunna M, Njenga S, Balasegaram M, Alexander N, Omollo R, Edwards T, et al. Efficacy and Safety of AmBisome in Combination with Sodium Stibogluconate or Miltefosine and Miltefosine Monotherapy for African Visceral Leishmaniasis: Phase II Randomized Trial. PLoS Negl Trop Dis. 2016;10(9):e0004880.
7. Hailu A, Musa A, Wasunna M, Balasegaram M, Yifru S, Mengistu G, et al. Geographical variation in the response of visceral leishmaniasis to paromomycin in East Africa: A multicentre, open-label, randomized trial. PLoS Negl Trop Dis. 2010;4(10):e709.

Chapter 1

Pharmacokinetics of treatment
for neglected tropical diseases

Chapter 1.1

Lack of clinical pharmacokinetic studies to optimize
the treatment of neglected tropical diseases:
A systematic review

Luka Verrest, Thomas P.C. Dorlo

Abstract

Introduction: Neglected tropical diseases (NTDs) affect more than one billion people, mainly living in developing countries. For most of these NTDs treatment is suboptimal. To optimize treatment regimens, clinical pharmacokinetic studies are required where they have not been previously conducted to enable the use of pharmacometric modelling and simulation techniques in their application, which can provide substantial advantages.

Objectives: Our aim was to provide a systematic overview and summary of all clinical pharmacokinetic studies in NTDs and to assess the use of pharmacometrics in these studies, as well as to identify which of the NTDs or which treatments have not been sufficiently studied.

Methods: PubMed was systematically searched for all clinical trials and case reports until end of 2015 that described the pharmacokinetics of a drug in the treatment of any of the NTDs in patients or healthy volunteers.

Results: Eighty-two pharmacokinetic studies were identified. Most studies included small patient numbers (only 5 studies included >50 subjects), and only 9 (11%) studies included pediatric patients. A large part of the studies was not very recent; 56% of studies were published before 2000. Most studies applied non-compartmental analysis methods for pharmacokinetic analysis (62%). Twelve studies used population-based compartmental analysis (15%) and 8 (10%) additionally performed simulations or extrapolation. For 10 out of the 17 NTDs, none or only very few pharmacokinetic studies could be identified.

Conclusions: For most NTDs adequate pharmacokinetic studies are lacking and population-based modeling and simulation techniques have not generally been applied. Pharmacokinetic clinical trials that enable population pharmacokinetic modeling are needed to make better use of the available data. Simulation-based studies should be employed to enable the design of improved dosing regimens and more optimally use the limited resources to effectively provide therapy in this neglected area.

Key points
- Neglected tropical diseases affect a major part of the global population, but treatments have generally not been optimized.
- Here we provide a comprehensive systematic overview of performed pharmacokinetic studies in all 17 neglected tropical diseases, advantages and drawbacks of different methodologies, and gaps in pharmacokinetic research through which neglected tropical diseases therapeutics can be further improved.
- For most neglected tropical diseases adequate pharmacokinetic studies were found lacking or completely absent, pediatric patients have largely been ignored, and population-based modeling and simulation techniques have not generally been applied.
- To more optimally use the limited available resources in this neglected area, more emphasis should be given to simulation-based pharmacokinetic studies enabling the design of improved dosing regimens.

1.   Introduction

Neglected tropical diseases (NTDs) represent a wide range of infectious afflictions, which are prevalent mostly in tropical and subtropical countries and have one common characteristic: they all affect people living in deep poverty. All NTDs are heavily debilitating, causing life-long disability, which can be directly fatal if left untreated. At the moment, over 1.4 billion people are affected by at least one NTD, and they are the cause of death for over 500 000 people annually[1,2]. There are currently 17 NTDs as defined by the World Health Organization (WHO), which include protozoal, bacterial, helminth, and viral infections[1]. An overview of their transmission, geography and burden of disease is provided in Table 1.1.1. Collectively, the NTDs belong to the most devastating of communicable diseases, not only in terms of global health burden (47.9 million disability-adjusted life-years)[3,4], but also in terms of impact on development and overall economic productivity in low- and middle-income countries[3,5].

The currently available treatments for NTDs are an outdated arsenal generally considered to be insufficient for NTD control and elimination[5]. Many of the currently available drugs were developed over 50 years ago and many of them exhibit high toxicity[5]. For example, the only available drug to treat late-stage human African trypanosomiasis (HAT or sleeping sickness) caused by T.b. rhodesiense is melarsoprol, an arsenic compound, developed in the 1940s, which is itself lethal to 5% of treated patients due to post-treatment reactive encephalopathy[6]. In many regions pentavalent antimony-containing compounds are still the treatment of choice for visceral and cutaneous leishmaniasis, which have been in use since the 1930s. Therapeutic failure is generally thought to result from sub-therapeutic dosing and shortened treatment durations[7]. As a consequence, clinical antimonial drug resistance in Leishmania has yield the drug useless in various geographical regions. At the same time, the upper limit of dosing of antimonials is limited by severe toxicities, such as pancreatitis and cardiotoxicity[7,8]. Examples like these emphasize the role of dose optimization and pharmacokinetic (PK) studies for treatments against NTDs, where there is often only a small therapeutic window between treatment failure, engendering drug resistance and drug toxicity.

In spite of the urgent need for new, safer and more efficacious treatments for NTDs, there is insufficient interest from the pharmaceutical industry to invest in drug development for these diseases because of the limited financial incentive. This paradigm has led to a fatal imbalance in drug development: although NTDs account for 12% of the global disease burden, only 1% of all approved drugs during the past decade was developed for these diseases. None of these approved drugs were a new chemical entity, and just 0.5% of all clinical trials in the past decade were dedicated to NTDs[9].

1.1

Table 1.1.1 Summary of neglected tropical diseases and global burden. DALYs: disability-adjusted life years.

Disease	Endemic areas	Causative agents	Transmission	Deaths per year	DALYs (in millions)
Protozoa infections					
Chagas disease	Latin America	Trypanosoma cruzi	triatomine bug	10 300	0.55
Human African trypanosomiasis	Africa	Trypanosoma brucei gambiense, T. brucei rhodesiense	tsetse fly	9 100	0.56
Leishmaniasis	Indian subcontinent, Asia, Africa, Mediterranean basin, South America	Visceral: Leishmania donovani, L. infantum; Cutaneous: L. major, L. tropica, L. braziliensis, L. mexicana and other Leishmania spp.	phlebotomine sandflies	51 600	3.32
Bacterial infections					
Buruli ulcer	Africa, South America and Western Pacific regions	Mycobacterium ulcerans	unknown	n.d.	n.d.
Leprosy	Africa, America, South-east Asia, Eastern Mediterranean, Western Pacific	Mycobacterium leprae	unknown	n.d.	0.006
Trachoma	Africa, Middle East, Mexico, Asia, South America, Australia	Chlamydia trachomatis	direct or indirect contact with an infected person	-	0.33
Endemic treponematoses	Global distribution	Treponema pallidum, T. carateum	skin contact	n.d.	n.d.
Helminthes					
Cysticercosis/taeniasis	Worldwide, mainly Africa, Asia and Latin America	Taenia solium, Taenia saginata, diphyllobothrium latum	ingestion of infected pork	1 200	0.5
Dracunculiasis	Chad, Ethiopia, Mali, South Sudan	Dracunculus medinensis	contaminated water	n.d.	n.d.
Echinococcosis	Global distribution	Echinococcus granulosus, Echinococcus multilocularis	faeces of carnivores	1 200	0.14
Foodborne trematodiases	South-east Asia, Central and South America	Clonorchis spp., Opisthorchis spp., Fasciola spp., and Paragonimus spp., Echinostoma spp., Fasciolopsis buski, Metagonimus, Metagonimus spp., Heterophyidae	contaminated food	-	1.88
Lymphatic filariasis	Africa, Asia, Central and Southern America	Wuchereria bancrofti, Brugia malayi, B.timori	mosquitos	-	2.78

1.1

Table 1.1.1 (continued)

Disease	Endemic areas	Causative agents	Transmission	Deaths per year	DALYs (in millions)
Onchocerciasis	Africa, Latin America, Yemen	Onchocerca volvulus	black flies	-	0.49
Schistosomiasis	Africa, South-America, Middle East, East-Asia, Laos, Cambodia	Schistosoma haematobium, S. guineensis, S. intercalatum, S. japonicum, S. mansoni, S. mekongi	contaminated water	11 700	3.31
Soil-transmitted helminthiases	Global distribution	Ascaris lumbricoides, Trichuris trichiura, Necator americanus, Ancylostoma duodenale	human faeces	2 700	5.19
Viral infectons					
Dengue	Asian and Latin American countries	Dengue fever virus (genus: Flavivirus)	mosquito	14 700	0.83
Rabies	Global distribution, mainly Africa, Asia, Latin America and Western Pacific	Rabies virus (genus: Lyssavirus)	animals, mostly domestic dogs	26 400	1.46

Summary of neglected tropical diseases, including endemic areas, causative agents, way of transmission and estimated global burden expressed in deaths per year and disability- adjusted life years (DALYs). Numbers are based on the Global Burden of Disease Study 2010 (4). n.d.= not determined.

Due to the lack of innovation as a result of the absence of financial incentives and the continued use of drugs developed many decades ago, dose-optimization studies or studies in specific patient populations particularly affected by NTDs (e.g., pediatric or HIV-co-infected patients) have rarely been reported. While a comprehensive and quantitative overview is currently lacking, only few clinical trials on NTDs appear to have included studies on the PK of the therapeutic compounds that were under clinical investigation. Rational drug therapy is based on the assumption of a causal relationship between exposure and response. Therefore, characterizing the PK of a drug is of utmost importance. Conventionally, non-compartmental analysis (NCA) methods were used for PK analysis, but these are less powerful and informative for typical NTD PK studies, which are sparse and heterogeneous of nature. NCA has a low power to identify true covariate effects and does not allow for simulations of alternative dosing regimens. Population-based modeling and simulation techniques are therefore more appropriate to describe and predict the relationship between exposure (PK), response (pharmacodynamics [PD]), individual patient characteristics and other covariates of interest (e.g., body weight, sex, and concomitant medication). These pharmacometric methods have become standard in drug development worldwide, and have been recommended by FDA and EMA for PK-PD data analysis and clinical trial design, particularly in pediatric and small sized patient populations[10-12]. Nevertheless, these methodologies appear to be systematically underutilized to address NTDs, likely because their advent occurred much later than the time when many of these drugs were developed.

To better understand to what extent clinical PK studies have contributed to optimization of treatment regimens for NTDs, we performed a systematic review of published clinical PK studies on NTD therapeutics. We hypothesize that for many of the NTD therapeutics, proper PK studies and thus a rationale for their dosing are plainly missing, that only few of these studies use modeling and simulation tools. By providing a comprehensive overview of performed PK studies, advantages and drawbacks of different PK methodologies will be illustrated and gaps in PK research for particular NTDs will be identified to indicate the areas where NTD therapeutics can be further improved.

2.   Methods

2.1   Study identification

We performed a systematic literature review following applicable criteria of the most current PRISMA guidelines (Preferred Reporting Items for Systematic Reviews and Meta-Analyses)[13], the PRISMA Checklist is in the Supplemental Data online. The

MEDLINE database was systematically searched through Pubmed for all human clinical pharmacokinetic studies until September 2015 that described the clinical PK of a drug in the treatment of any of the NTDs. For instance, the search term used for studies for Chagas disease was: ((Chagas disease[Title/Abstract] OR American trypanosomiasis[Title/Abstract])) AND (pharmacokinetics[Title/Abstract] OR pharmacokinetic[Title/Abstract]). Reviews were excluded from the search, as well as preclinical research and research concerning animals other than human. The search was limited to publications in English. A full list of all the search terms used is shown in Supplemental Table S.1.1.1.

Secondary literature was identified using bibliography of the primary identified literature and by specifically querying PubMed using the drug name in combination with the disease. Because we were particularly interested in the application of population PK approaches in NTDs, also the abstracts of the Population Approach Group Europe (PAGE) conference[14] were searched using the same search terms. No specific protocol was developed for this systematic review.

2.2 Study selection

Records were initially screened to identify relevant publications based on title and abstract. If the abstract lacked sufficient detail, the full publication was assessed. The aim of this study was the identification of clinical PK studies in the context of the treatment of NTDs, and therefore studies were excluded if the study's subjects were not healthy subjects (phase I studies) or patients diagnosed with one of the NTDs; or if the drug of interest was symptomatic treatment (e.g., suppression of fever) or for treatment of concomitant diseases instead of the NTD itself (primary criteria). Articles with only pharmacodynamic results or only reporting a bioanalytical method were also excluded.

2.3 Assessment of PK data analysis methods

The methods used to analyze the PK data were extracted from the identified records and qualitatively categorized as follows, in order of level of complexity: (I) comparison of average trough/steady-state concentrations, (II) NCA, (III) individual-based compartmental analysis, (IV) population-based compartmental analysis, and (V) the use of simulations and/or extrapolations. In category I, studies were included which basically compared a drug concentration at a single time point between different formulations or different patient groups. In category II we included studies that described concentration-time profiles or PK parameters by using NCA techniques[15]. Analyses in category III used non-linear equations to describe individual concentration-time curves, by using theoretical compartments and inter-compartmental transfer rates, deriving individual PK parameters that can be averaged. In population-based

analysis (category IV) similar techniques are being used, but with simultaneous estimation of both inter-individual and intra-individual variability (nonlinear mixed-effects models). The derived model is descriptive for the entire population and can subsequently be used for predictions and simulations, and potentially for extrapolation to other populations (additional category V).

2.4   Extraction and analysis of data

Besides the PK data analysis method, other data that was extracted from the identified study reports were: administrated compound, measured analytes (parent compound and/or metabolites), route of administration, PK sample matrix, the type and number of subjects, and particularly whether pediatric patients were included in the study. Additionally, the main conclusions were extracted from all studies in a qualitative way, focused on the study recommendations in regard to dose adjustments or other treatment optimizations. The risk of bias in these recommendations, for instance when used analysis methods were insufficient to support these treatment recommendations, was gauged and reported if detected. Given the nature of extracted data, only a simple descriptive analysis was conducted, summarizing individual studies.

3.   Results

3.1   Study characteristics

The primary literature search identified 431 unique publications. After screening, 341 publications were excluded based on the primary criteria. Combined with additional articles through secondary sources, 82 publications were eventually included in this systematic review (Figure 1.1.1). No full texts were available for 6 studies; however, the abstracts of these publications contained all the information to be extracted and they did not need to be excluded. The search and inclusion results stratified per NTD are shown in Supplemental Table S1.1.1. A summary of all identified PK studies together with their main characteristics is shown in Table 1.1.2.
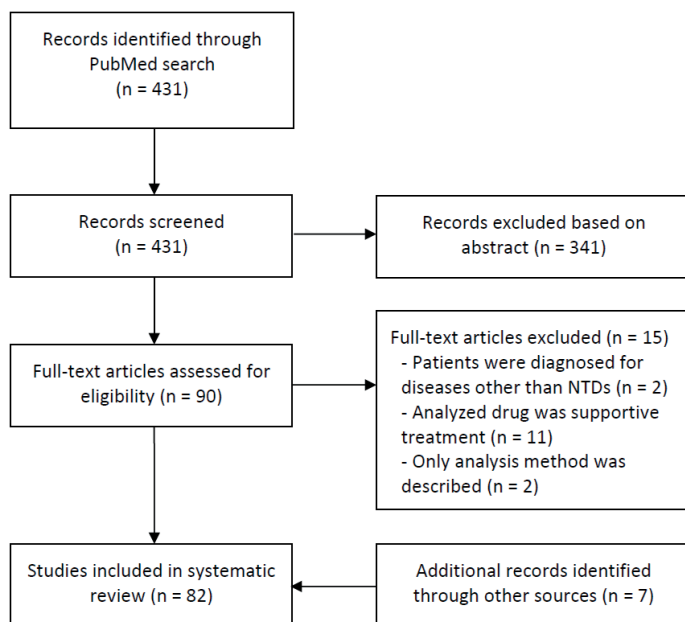
```
┌─────────────────────────┐
│  Records identified     │
│  through PubMed search  │
│      (n = 431)          │
└─────────────────────────┘
            │
            ▼
┌─────────────────────────┐        ┌─────────────────────────┐
│  Records screened       │───────▶│  Records excluded based  │
│     (n = 431)           │        │  on abstract (n = 341)   │
└─────────────────────────┘        └─────────────────────────┘
            │
            ▼
┌─────────────────────────┐        ┌──────────────────────────────┐
│  Full-text articles     │        │ Full-text articles excluded  │
│  assessed for           │───────▶│ (n = 15)                     │
│  eligibility (n = 90)   │        │ - Patients were diagnosed for│
└─────────────────────────┘        │   diseases other than NTDs   │
            │                      │   (n = 2)                    │
            │                      │ - Analyzed drug was supportive│
            │                      │   treatment (n = 11)         │
            │                      │ - Only analysis method was   │
            │                      │   described (n = 2)          │
            ▼                      └──────────────────────────────┘
┌─────────────────────────┐        ┌──────────────────────────────┐
│  Studies included in    │◀───────│  Additional records          │
│  systematic review      │        │  identified through other    │
│     (n = 82)            │        │  sources (n = 7)             │
└─────────────────────────┘        └──────────────────────────────┘
```

Figure 1.1.1 Study flow diagram. NTDs: neglected tropical diseases.

For 4 out of the 17 (24%) NTDs not a single PK study could be identified, these were yaws, dracunculiasis, dengue/chikungunya/zika and soil-transmitted helminthiases. For 6 (41%) other NTDs, less than 5 PK studies had been reported. Most studies had included small patient numbers, only 5 studies (6.1%) had included >50 subjects (Table 1.1.2). Pediatrics were included in 9 (11%) studies. The majority of these studies were not very recent; 56% of studies were published before 2000; the frequency of studies per year is depicted in Figure 1.1.2. Concerning the used analysis methods, some studies employed multiple analysis methods, e.g., both comparison of steady-state concentrations and NCA (Table 1.1.2). When looking at the most complicated method employed in the study, most studies used NCA methods for PK analysis (62%). Twelve studies (15%) used population-based compartmental analysis of which 8 (10%) additionally performed simulations or extrapolation. Regarding the aim of the studies, 38 studies (46%) focused on describing the PK of a compound without further interpretations. Only 5 studies (6%) evaluated exposure-response relationships. Although some of these studies reported side effects[16-18], none of these attempted to relate drug exposure to observed toxicity. On the other hand, relatively many studies (28%) evaluated drug-drug and food interactions. This is due to the frequent use of combination therapies for the treatment of NTDs, and due to the implementation of overlapping prophylactic mass drug administrations for e.g., onchocerciasis, lymphatic filariasis, and schistosomiasis.

Table 1.1.2   Summary of PK studies

Disease	Study	Drug	Administration route	Analytes (parent and metabolites)	Analyzed matrix	Subjects (n)	Pediatrics included	Comparing concentrations (1)	Non-compartmental (2)	Compartmental (individual-based) (3)	Compartmental (population-based) (4)	Simulation and/or extrapolation (5)	Descriptive (a)	Suggesting alternative dose regimens (b)	Comparing different formulations (c)	Evaluating drug-drug and food interactions (d)	Evaluating exposure-response relationships (e)
Chagas disease																	
	Shapiro et al. 1991	Allopurinol riboside	Oral	Allopurinol, - riboside, oxipurinol	Plasma, urine	Male healthy subjects (32)			✓				✓				
	Were et al. 1993	Allopurinol riboside	Oral	Allopurinol riboside, oxipurinol	Plasma, urine	Male healthy subjects (3)			✓				✓		✓		
	Garcia-Bournissen et al. 2010	Nifurtimox	Oral	Nifurtimox	Plasma	Healthy subjects (7)					✓	✓	✓				
	Richle et al. 1980	Benznidazole	Oral	Benznidazole	Plasma	Chagas disease patients (8)			✓				✓				
	Altcheh et al. 2014	Benznidazole	Oral	Benznidazole	Plasma	Chagas disease patients (40)	✓				✓	✓	✓				
	Soy et al. 2015	Benznidazole	Oral	Benznidazole	Plasma	Chagas disease patients (39)					✓	✓		✓	✓		
Human African trypanosomiasis																	
	Bronner et al. 1991	Pentamidine	IM[1]	Pentamidine	Plasma, whole blood, CSF[2]	T. b. gambiense trypanosomiasis patients (11)			✓				✓				
	Bronner et al. 1995	Pentamidine	IV[3]	Pentamidine	Plasma	T. b. gambiense trypanosomiasis patients (11)			✓				✓				
	Harrison et al. 1997	Melarsoprol	IV	Arsenic	Urine	T. b. rhodesiense trypanosomiasis patients (28)		✓					✓				
	Burri et al. 1993	Melarsoprol	IV	Melarsoprol	Serum, CSF	T. b. gambiense trypanosomiasis patients (19)				✓		✓		✓			
	Burri et al. 2001	Melarsoprol	IV	Melarsoprol	Serum, CSF	T. b. gambiense trypanosomiasis patients (22)				✓			✓				
	Bronner et al. 1998	Melarsoprol	IV	Melarsoprol	Plasma, urine, CSF	T. b. gambiense trypanosomiasis patients (8)		✓					✓				
	Milord et al. 1993	Eflornithine	IV	Eflornithine	Serum, CSF	T. b. gambiense trypanosomiasis patients (63)			✓				✓				
	Na-Bangchang et al. 2004	Eflornithine	Oral	Eflornithine	Plasma, CSF	T. b. gambiense trypanosomiasis patients (25)			✓	✓				✓			

1.1

Table 1.1.2   (continued)

Disease	Study	Drug	Administration route	Analytes (parent and metabolites)	Analyzed matrix	Subjects (n)	Pediatrics included	Comparing concentrations (1)	Non-compartmental (2)	Compartmental (individual-based) (3)	Compartmental (population-based) (4)	Simulation and/or extrapolation (5)	Descriptive	Suggesting alternative dose regimens	Comparing different formulations	Evaluating drug-drug and food interactions	Evaluating exposure-response relationships
	Jansson-Lofmark et al. 2015	Eflornithine	Oral	Eflornithine	Plasma, CSF	T. b. gambiense trypanosomiasis patients (25)					✓						✓
	Tarral et al. 2014, Gualano et al. 2012	Fexinidazole	Oral	Fexinidazole, - sulfoxide, -sulfone	Plasma, urine	Male healthy subjects (154)			✓		✓	✓		✓	✓	✓	
Leishmaniasis								1	2	3	4	5	a	b	c	d	e
	Jaser et al. 1995	Sodium stibogluconate	IM	Antimony	Blood, urine	CL[4] patients (29)							✓				
	Jaser et al. 1995	Sodium stibogluconate	IM	Antimony	Blood, skin biopsies	CL patients (9)			✓				✓				
	Reymond et al. 1998	Sodium stibogluconate	IV	Antimony	Serum	Patient with AIDS and VL[5] (1)							✓				
	Vasquez et al. 2006	Pentavalent antimony	IM	Pentavalent and trivalent antimony	Blood, urine	Healthy subjects (5)			✓				✓				
	Chulay et al. 1988	Sodium stibogluconate, meglumine antimoniate	IM	Antimony	Blood	VL patients (5)				✓			✓				
	Cruz et al. 2007	Meglumine antimoniate	IM	Antimony	Plasma, urine	CL patient (24)	✓		✓				✓				
	Zaghloul et al. 2010	Sodium stibogluconate	IM	Antimony	Plasma, urine	CL patient (12)			✓	✓			✓				
	Shapiro et al. 1991	Allopurinol riboside	Oral	Allopurinol, - riboside, oxipurinol	Plasma, urine	Male healthy subjects (32)			✓				✓				
	Were et al. 1993	Allopurinol riboside	Oral	Allopurinol riboside, oxipurinol	Plasma, urine	Male healthy subjects (3)			✓							✓	
	Musa et al. 2010	Paromomycin sulphate	IM	Paromomycin	Plasma, urine	VL patients (9)	✓	✓									
	Ravis et al. 2013	Paromomycin, WR 279396	Topical	Paromomycin	Plasma	CL patients (60)	✓	✓						✓	✓		
	Sundar et al. 2011	Sitamaquine	Oral	Sitamaquine, desethyl-sitamaquine	Plasma	VL patients (41)			✓							✓	
	Dorlo et al. 2008	Miltefosine	Oral	Miltefosine	Plasma	Old world CL patients (31)	✓			✓			✓				
	Dorlo et al. 2012	Miltefosine	Oral	Miltefosine	Plasma	VL patients (96)				✓			✓				
	Dorlo et al. 2012	Miltefosine	Oral	Miltefosine	Plasma	Simulated female VL patients						✓		✓			
	Dorlo et al. 2014	Miltefosine	Oral	Miltefosine	Plasma	VL patients (81)	✓				✓						✓

Table 1.1.2 (continued)

Disease	Study	Drug	Administration route	Analytes (parent and metabolites)	Analyzed matix	Subjects (n)	Pediatrics included	Analysis method Comparing concentrations (1)	Non-compartmental (2)	Compartmental (individual-based) (3)	Compartmental (population-based) (4)	Simulation and/or extrapolation (5)	Aim of the study Descriptive (a)	Suggesting alternative dose regimens (b)	Comparing different formulations (c)	Evaluating drug-drug and food interactions (d)	Evaluating exposure-response relationships (e)
Buruli ulcer																	
	Aflfenaar et al. 2010	Streptomycin–rifampin, rifampin–clarithromycin	Oral	Rifampin, 25-desacetylrifampicin, clarithromycin, 14OH-clarithromycin	Plasma	Buruli ulcer patients (13)	✓				✓						✓
Leprosy																	
	Mehta et al. 1986	Rifampicin	Oral	Rifampicin	Serum	MB[6] (6) and PB[7] (12) leprosy patients		✓									✓
	Venkatesan et al. 1986	Rifampicin and dapsone	Oral	Rifampicin and dapsone	Plasma, urine	Leprosy patients (15)		✓	✓							✓	
	Pieters et al. 1986	Monoacetyldapsone	IA[8]	Dapsone	Serum	Healthy subjects (22)		✓	✓								
	Pieters et al. 1987	Dapsone	Oral	Dapsone	Serum	Healthy subjects (5)			✓				✓				
	Garg et al. 1988	Dapsone	Oral	Dapsone, monoacetyldapsone	Plasma	Lepromatous leprosy patients (15)			✓				✓				
	Venkatesan et al. 1993	Dapsomine	Oral	Dapsone	Plasma	Lepromatous leprosy patients (14)			✓								
	Pieters et al. 1988	Dapsone	Oral	Dapsone	Plasma	Leprosy patients (23)		✓	✓				✓				
	Moura et al. 2013	Dapsone	Oral	Dapsone	Plasma	MB leprosy patients (33)			✓							✓	
	Nix et al. 2004	Clofazamine	Oral	Clofazamine	Plasma	Healthy subjects (16)			✓	✓						✓	
	Teo et al. 1999	Thalidomide	Oral	Thalidomide	Plasma	Healthy subjects (17)			✓	✓					✓		
	Teo et al. 2001	Thalidomide	Oral	Thalidomide	Plasma	Healthy subjects (15)			✓	✓			✓				
Trachoma																	
	Amsden et al. 2007	Azithromycin, albendazole, ivermectin	Oral	Azithromycin, albendazole, - sulfoxide, ivermectin H2B1a and H2B1b	Plasma	Healthy subjects (18)			✓				✓				
	El-Tahtawy et al. 2008	Ivermectin	Oral	Ivermectin H2B1a and H2B1b	Plasma	Healthy subjects (15)			✓	✓	✓			✓		✓	
Cysticercosis/taeniasis																	
	Jung et al. 1992	Albendazole	Oral	Albendazole sulfoxide	Plasma	Brain cysticercosis patients (8)			✓		✓	✓		✓		✓	
	Sanchez et al. 1993	Albendazole	Oral	Albendazole sulfoxide	Plasma, urine	Parenchymal brain cysticercosis patients (10)			✓					✓	✓		

Table 1.1.2 (continued)

Disease	Study	Drug	Administration route	Analytes (parent and metabolites)	Analyzed matrix	Subjects (n)	Pediatrics included	Comparing concentrations (1)	Non-compartmental (2)	Compartmental (individual-based) (3)	Compartmental (population-based) (4)	Simulation and/or extrapolation (5)	Descriptive (a)	Suggesting alternative dose regimens (b)	Comparing different formulations (c)	Evaluating drug-drug and food interactions (d)	Evaluating exposure-response relationships (e)
	Jung et al. 1997	Albendazole	Oral	Albendazole sulfoxide	Plasma	Brain cysticercosis patients (8)	✓	✓						✓			
	Takayanagui et al. 1997	Albendazole	Oral	Albendazole sulfoxide	Plasma	Parenchymal brain cysticercosis patients (24)				✓							✓	
	Na-Bangchang et al. 1995	Praziquantel	Oral	Praziquantel	Plasma	Neurocysticercosis patients (11)			✓								✓	
	Jung et al. 1997	Praziquantel	Oral	Praziquantel	Plasma	Healthy subjects (8)			✓								✓	✓
	Garcia et al. 2011	Praziquantel, albendazole	Oral	Praziquantel, albendazole sulfoxide	Plasma	Neurocysticercosis patients (32)				✓							✓	✓
Echinococcosis	Cotting et al. 1989	Albendazole	Oral	Albendazole, - sulfoxide	Plasma	Echinococcosis patients (19)			✓				✓	✓			
	Mingjie et al. 2002	Albendazole	Oral	Albendazole sulfoxide	Serum	Male cystic echinococcosis patients (7)				✓					✓		
	Schipper et al. 2000	Albendazole	Oral	Albendazole sulfoxide	Plasma	Male healthy subjects (6)			✓								✓	✓
Foodborne trematodiases	Na Bangchang et al. 1993	Praziquantel	Oral	Praziquantel	?	Opisthorchiasis patients (18)			✓				✓	✓			
	Choi et al. 2006	Praziquantel	Oral	Praziquantel	Plasma	Healthy subjects (12) and clonorchiasis patients (20)			✓						✓		
	Lecaillon et al. 1998	Triclabendazole	Oral	Triclabendazole, -sulphoxide, -sulphone	Plasma	Fascioliasis patients (20)		✓								✓	
	El-Tantawy et al. 2007	Triclabendazole	Oral	Triclabendazole sulphoxide	Plasma	Healthy subjects (12) and fascioliasis patients (12)			✓					✓			

Table 1.1.2 (continued)

Disease	Study	Drug	Administration route	Analytes (parent and metabolites)	Analyzed matix	Subjects (n)	Pediatrics included	Analysis method					Aim of the study				
								Comparing concentrations (1)	Non-compartmental (2)	Compartmental (individual-based) (3)	Compartmental (population-based) (4)	Simulation and/or extrapolation (5)	Descriptive a	Suggesting alternative dose regimens b	Comparing different formulations c	Evaluating drug-drug and food interactions d	Evaluating exposure-response relationships e
Lymphatic filariasis																	
	Shenoy et al. 2002	Diethylcarbamazine, albendazole	Oral	Diethylcarbamazine, albendazole, - sulfoxide sulphone	Plasma	Healthy subjects (42)			✓							✓	
	Sarin et al. 2003	Albendazole sulfoxide	Oral	Albendazole sulfoxide, albendazole sulphone	Plasma	Healthy subjects (10)			✓				✓				
	Abdel-tawab et al. 2009	Albendazole	Oral	Albendazole, - sulfoxide, - sulphone	Serum, breast milk	Lactating women (33)			✓				✓				
Onchocerciasis																	
	Lecaillon et al. 1990	Amocarzine	Oral	Amocarzine, N-oxide metabolite	Plasma, urine	Onchocerciasis patients (41)			✓				✓				
	Lecaillon et al. 1991	Amocarzine	Oral	Amocarzine, N-oxide metabolite	Plasma, urine	Male onchocerciasis patients (20)			✓					✓			
	Awadzi et al. 1994	Albendazole	Oral	Albendazole sulfoxide	Plasma	Onchocerciasis patients (36)			✓							✓	
	Awadzi et al. 2003	Ivermectin, albendazole	Oral	Ivermectin, albendazole sulfoxide	Plasma	Male onchocerciasis patients (42)			✓							✓	
	Okonkwo et al. 1992	Ivermectin	Oral	Ivermectin	Plasma, urine, saliva	Onchocerciasis patients (9)			✓				✓				
	Baraka et al. 1996	Ivermectin	Oral	Ivermectin	Plasma, tissues	Onchocerciasis patients (25), healthy subjects (14)			✓				✓				
	Homeida et al. 2013	Ivermectin	Oral	Ivermectin	Plasma	Male subjects (10)			✓							✓	
	Chijioke et al. 1998	Suramin	IV	Suramin	Plasma	Male onchocerciasis patients (10)				✓			✓				
	Korth-Bradley et al. 2011	Moxidectin	Oral	Moxidectin	Plasma, breast milk	Healthy lactating women (12)			✓				✓				
Schistosomiasis																	
	Nordgren et al. 1980	Metrifonate	Oral	Metrifonate, dichlorvos	Plasma	Male schistosomiasis patients (2)			✓				✓				
	Daneshmend et al. 1987	Oxamniquine	Oral	Oxamniquine	Plasma	Hepatosplenic schistosomiasis patients (9), healthy subjects (5)			✓				✓				
	Pehrson et al. 1983	Praziquantel	Oral	Praziquantel	Serum, urine, dialysis fluid	Patient with uraemia (1)			✓				✓				

Table 1.1.2   (continued)

Analysis method columns: (1) Comparing concentrations, (2) Non-compartmental, (3) Compartmental (individual-based), (4) Compartmental (population-based), (5) Simulation and/or extrapolation.
Aim of the study columns: (a) Descriptive, (b) Suggesting alternative dose regimens, (c) Comparing different formulations, (d) Evaluating drug-drug and food interactions, (e) Evaluating exposure-response relationships.

Disease	Study	Drug	Administration route	Analytes (parent and metabolites)	Analyzed matrix	Subjects (n)	Pediatrics included	1	2	3	4	5	a	b	c	d	e
	Mandour et al. 1990	Praziquantel	Oral	Praziquantel	Serum or plasma	Healthy subjects (20), schistosomiasis patients (9)		✓								✓	
	Valencia et al. 1994	Praziquantel	Oral	Praziquantel	Serum	Schistosoma japonicum patients (4)			✓				✓				
	El Guiniady et al. 1994	Praziquantel	Oral	Praziquantel	Serum	Schistosoma mansoni patients (40)				✓							✓
Rabies	Merigan et al. 1984	Human leukocyte interferon	I-VENTRIC[9], IT[10], IM	Human leukocyte interferon	Serum, CSF	Suspected rabies patients (2), symptomatic rabies patients (5)		✓									
	Lang et al. 1998	Equine rabies immunoglobulin	IM	Anti-rabies antibodies	Serum	Healthy subjects (27)			✓						✓		
	Gogtay et al. 2012	IgG1 monoclonal antibody	IM	Anti-rabies antibodies	Serum	Male healthy subjects (29)			✓								✓

[1] Intramuscular
[2] Cerebrospinal fluid
[3] Intravenous
[4] Cutaneous leishmaniasis
[5] Visceral leishmaniasis
[6] Multibacillary leprosy
[7] Paucibacillary leprosy
[8] Intra-adipose
[9] Intraventricular
[10] Intrathecal

Figure 1.1.2 Number of identified clinical pharmacokinetic publications on neglected tropical diseases stratified per year.

3.2 Pharmacokinetic studies per neglected tropical disease

Based on the cause of the infection, NTDs can be divided in four groups: diseases caused by protozoal parasites, bacteria, helminthes and viruses (an extensive overview is provided in Table 1.1.1). The protozoal NTDs are all caused by kinetoplastid parasites: Chagas disease, human African trypanosomiasis, and leishmaniasis. Bacteria, a large and diverse group of prokaryotic microorganisms, cause Buruli ulcer, leprosy (both caused by Mycobacteria), trachoma and yaws. Helminthes, commonly known as parasitic worms, are large multicellular organisms. The helminth NTDs are cysticercosis/taeniasis, dracunculiasis, echinococcosis, foodborne trematodiases, lymphatic filariasis, onchocerciasis, schistosomiasis, and the soil-transmitted helminthiases. Viral NTDs include the arboviral disease dengue (plus chikungunya and zika) and rabies. A general overview of medicines that are currently in use for NTDs is listed in Table 1.1.3[1,19].

The most salient identified PK studies for NTD therapies will be discussed, focusing on studies that played a role in treatment optimization. A full overview of identified studies can be found in Table 1.1.2.

Table 1.1.3 Currently used drugs for neglected tropical diseases.

Disease	Drug	Route of administration
Chagas disease		
	Benznidazole	Oral
	Nifurtimox	Oral
Human African trypanosomiasis		
Early stage	Pentamidine	IV, IM
	Suramin	IV
Late stage	Melarsoprol	IV
	Nifurtimox and eflornithine	IV and IV
Leishmaniasis		
	Meglumine antimoniate	IL, IV, IM
	Sodium stibogluconate	IL, IV, IM
	Paromomycin (paromomycin ointment or WR 279396 cream)	Topical, IM
	Pentamidine	IV, IM
	Amphotericin B deoxycholate	IV
	Liposomal amphotericin B	IV
	Fluconazole	Oral
	Ketoconazole	Oral
	Miltefosine	Oral
Buruli ulcer		
	Rifampicin and streptomycin	Oral and IM
	Alternative compounds:	
	Clarithromycin	Oral
	Moxifloxacin	Oral
Leprosy		
Multibacillary	Rifampicin and dapsone	Oral and oral
Paucibacillary	Rifampicin, dapsone and clofazimine	Oral, oral and oral
Trachoma		
	Azithromycin	Oral
	Topical tetracycline	Topical
Endemic treponematoses		
	Azithromycin	Oral
	Penicillin G benzathine	IM
Cysticercosis/taeniasis		
	Albendazole	Oral
	Praziquantel	Oral
Dracunculiasis[1]		
Echinococcosis		
	Albendazole	Oral
Foodborne trematodiases		
Clonorchiasis and opisthorchiasis	Praziquantel	Oral
Fascioliasis	Triclabendazole	Oral
Paragonimiasis	Praziqantel or triclabendazole	Oral and oral
Lymphatic filariasis		
	Diethylcarbamazine	Oral
	Additional treatment:	
	Doxycycline	Oral
	Ivermectin	Oral
	Albendazole	Oral

1.1

Table 1.1.3 (continued)

Disease	Drug	Route of administration
Onchocerciasis		
	Microfilaricidal therapy:	
	Ivermectin	Oral
	Macrofilaricidal therapy:	
	Doxycycline followed by ivermectin	Oral and oral
Schistosomiasis		
	Praziquantel	Oral
Soil-transmitted helminthiases		
	Albendazole	Oral
	Mebendazole	Oral
	Pyrantel pamoate	Oral
Dengue and Chikungunya[2]		
Rabies[3]		

[1] For dracunculiasis, treatment involves removing the adult worm; [2] Treatment of dengue and chikungunya consists of relieving symptoms; [3] After exposure by an animal that might have rabies, postexposure anti-rabies vaccination is recommended to prevent rabies infection.

3.2.1 Chagas disease

Around 5.7 million people worldwide are affected by Chagas disease (also known as American trypanosomiasis), which is caused by the Trypanosoma cruzi parasite[20]. The acute phase of the disease is asymptomatic in most patients. During the chronic phase patients can experience cardiac, digestive or neurological symptoms, which complications lead in many patients to fatality in the late chronic stage mostly decades after start of infection. However, Chagas disease can be cured when treatment is initiated at the acute or early chronic stage. Currently, the only two drugs with proven efficacy in Chagas disease are nifurtumox and benznidazole (Table 1.1.3). Clinical PK studies were found for three drugs: allopurinol riboside[21,22], nifurtimox[23] and benznidazole[24-26] (Table 1.1.2).

Allopurinol was not further evaluated for the treatment of Chagas disease after demonstrating suboptimal exposure[21], which could not be sufficiently increased by probenecid co-administration decreasing the drug's renal excretion[22].

A population PK modelling and simulation approach was used to estimate the exposure of infants to nifurtimox via breastmilk of patients[23]. Transfer of nifurtimox into breastmilk appeared limited and unlikely to lead to significant exposure in infants, yielding nifurtimox safe to use for breastfeeding patients.

The first PK study on benznidazole was published in 1980[24]. Very recently, population-based analyses were performed in children[25] and in adults[26]. Model-based simulations

in these studies suggested that the adult daily dose intervals in chronic Chagas patients could be prolonged, while benznidazole concentrations were kept within the target range, potentially simplifying the treatment regimen.

3.2.2 Human African trypanosomiasis

Human African trypanosomiasis, also known as sleeping sickness, is transmitted by the tsetse fly and caused by T.b. rhodesiense, resulting in an acute infection, and T.b. gambiense, leading to a more chronic infection (Table 1.1.1). Without treatment, the infection of the central nervous system is ultimately fatal[27]. There are currently four treatments in use for the two different stages of human African trypanosomiasis (Table 1.1.3), all of which exhibit substantial toxicities: pentamidine, suramin, melarsoprol and nifurtimox plus eflornithine. Clinical PK studies were identified for three of these treatments: pentamidine[28,29], melarsoprol[30-33], and eflornithine[34-36]. Additionally, PK studies were found for fexinidazole, a drug currently still in late-phase clinical development[37,38].

PK played an important role in the optimization of eflornithine therapy. Based on cerebrospinal fluid (CSF) and plasma PK data from late-stage T. b. gambiense trypanosomiasis, a new dosing regimen was proposed for eflornithine, including different infusion intervals, and increased doses in children, based on body surface area instead of body weight[34]. Later it was shown that the current dosing of oral eflornithine did not result in adequate therapeutic plasma and CSF concentrations in adult patients[35]. Recently, a population-based PK-PD model for the different stereoisomers of eflornithine was developed reanalyzing previous PK data and showed the importance of stereoselective exposure, which provided an explanation why oral eflornithine had failed so far for late-stage human African trypanosomiasis patients[36].

Melarsoprol PK in plasma and CSF were assessed using compartmental methods in 19 trypanosomiasis patients, after which the typical exposure for safer alternative dose regimens could be simulated[31]. However, the PK-PD relationships for melarsoprol remain unclear: melarsoprol PK parameters and CSF/plasma exposure were not significantly different in refractory compared to cured patients[32] and arsenic urinary excretion was not predictive of either toxicity or efficacy of melarsoprol[30].

Fexinidazole, a nitroimidazole-compound currently under clinical development for human African trypanosomiasis, and its active metabolites were studied in healthy volunteers, showing the need for concomitant food intake which increases the bioavailability of this compound substantially and identifying a target dose for the first in-patient studies[37,38].

1.1

3.2.3   Leishmaniasis

Leishmaniasis is caused by various species of *Leishmania* parasites that are transmitted by sandflies, with different and widespread geographical regions of distribution, leading to distinctly different clinical presentations. Cutaneous leishmaniasis is most prevalent and has the potential to progress into mucocutaneous leishmaniasis. Visceral leishmaniasis (VL) is the most severe clinical form and is inevitably fatal if left untreated. Treatment of leishmaniasis depends on the type of disease, parasite species, and on the availability of treatment depending on the geographical location. Local chemotherapeutic treatment with intralesional pentavalent antimonials or paromomycin cream can be an option for cutaneous leishmaniasis, although some species or severe/diffuse disease are rather treated systemically with either parenteral antimonials, liposomal amphotericin B, pentamidine or oral miltefosine, ketoconazole and fluconazole[39]. Recommended treatments for VL are, depending on species and geographical location, either parenteral (liposomal) amphotericin B, the antimonial sodium stibogluconate, paromomycin, oral miltefosine or combinations of sodium stibogluconate with paromomycin (East Africa) or liposomal amphotericin B plus paromomycin/miltefosine (India). Several clinical PK studies were conducted in leishmaniasis, and have helped most notably to optimize dose regimens for miltefosine for VL[40-43], for antimonials for cutaneous leishmaniasis[44-46] and for VL[47,48], to quantify exposure to paromomycin in VL[49], and to assess systemic penetration of topical paromomycin formulations[50]. Few studies have been performed in the context of leishmaniasis on allopurinol[21,22] and sitamaquine[51] which both are not in clinical use at the moment.

Comparing the two pentavalent antimonial compounds in use for leishmaniasis, meglumine antimoniate and sodium stibogluconate, equivalent systemic exposure was shown for the active component pentavalent antimony, possibly indicating that they can be used interchangeably[48]. In cutaneous leishmaniasis, PK studies on parenteral sodium stibogluconate demonstrated wide variability in drug exposure[44], but also penetration of the active component antimony in the skin, with no differences between normal skin and lesions[52]. The first pediatric study of meglumine antimoniate showed that drug exposure is significantly lower in children than in adults treated with the same linear weight-adjusted (mg/kg) regimen, possibly indicating that children are currently undertreated[53]. Only a descriptive analysis of the PK was performed, which did not suggest or evaluate alternative dose regimens for children.

Systemic penetration of paromomycin and gentamycin after application of two different topical formulations in cutaneous leishmaniasis patients was assessed using compartmental methods[50]. While gentamycin remained largely undetectable in plasma, paromomycin accumulated to 5-9% of typical trough concentrations achieved after a

standard intramuscular administration of 15 mg/kg paromomycin, indicating little concern for systemic drug toxicity of the topical formulations.

Most PK studies in leishmaniasis were conducted on the oral drug miltefosine. In 2008 the first population PK model for this drug was developed on data from Dutch military personnel who contracted L. major cutaneous leishmaniasis in Afghanistan[40]. This analysis showed that miltefosine is eliminated at a much slower rate than expected, which has potential implications for emerging drug resistance and the required contraception period due to miltefosine's teratogeniticity. A subsequent simulation study focused on the translation of the reproductive safety limit in animal studies to Indian female VL patients. New recommendations for the duration of contraceptive cover after miltefosine treatment were provided based on these findings[41]. In a model-based study, miltefosine exposure appeared to be lower in children than in adults treated with the same mg/kg dose, possibly explaining increased failure rates observed in pediatric VL patients. A new dosing algorithm based on allometric scaling was proposed and was evaluated by Monte Carlo simulations[42]. Recently, a PKPD model of miltefosine in Nepalese VL patients indeed identified a PK-PD relationship between miltefosine exposure and long-term treatment relapse[43]. The confirmed underexposure in children, reinforces the need for implementing the earlier proposed allometric miltefosine dosing regimen for VL[42,43].

3.2.4 Buruli ulcer

Buruli ulcer is an ulcerating infection caused by Mycobacterium ulcerans, leading to long-term functional disability, loss of productivity and stigmatization. Antimicrobial treatment is particularly effective in small lesions and at an early stage of infection, it reduces healing time, recurrence rate and the need for surgical intervention[54]. Different combinations of antimicrobials are used, depending on available resources and the stage of the disease. The most widely accepted combination is oral rifampin with intramuscular streptomycin, the oral combination of rifampin with clarithromycin is still under clinical evaluation. Only a single PK study could be identified for Buruli ulcer, which studied systemic PK of rifampin and clarithromycin in patients using population compartmental methods[55].

In this study the counteracting interaction effects (both cytochrome P450 3A4 and P-glycoprotein) of clarithromycin and rifampin on each other's PK were investigated. Eventually it was suggested that a doubled dose of clarithromycin should be evaluated in future clinical studies to ensure an increased time above MIC[55].

3.2.5 Leprosy

Leprosy can be divided into paucibacillary and multibacillary disease. If not treated in an early phase, it results in lifelong neuropathy and disability. A combination of drugs is needed due to the emergence of drug resistance. In 1995 WHO supplied free multi-drug therapy to leprosy patients in all endemic countries, which led to a dramatic decrease in prevalence. For paucibacillary treatment the recommended all oral treatment combination is rifampicin plus dapsone, for multibacillary this combination should be extended with clofazimine (Table 1.1.3). Various PK studies have been conducted on dapsone[56-59], clofazimine[60] and specific drug-drug interaction studies focusing on the interactions between dapsone, clofazimine and rifampicine using various formulations[61-64]. A few studies focused on thalidomide PK[65,66], which is currently largely considered obsolete due to its teratogenicity. PK studies for leprosy were mainly performed in the 1980/90s and generally using NCA methods (Table 1.1.2).

A study on dapsone and its main active metabolite monoacetyldapsone in leprosy patients concluded that the standard 100 mg/day dose was sufficient to maintain therapeutic plasma concentrations in relation to in vitro susceptibility values[58]. Nevertheless, dose adjustments might be needed for obese patients treated with this regimen[59]. Various drug-drug interaction studies did not reveal clinically significant interactions, although little is known about the required minimal effective exposure in leprosy[61-64].

PK of clofazimine has been analyzed using compartmental methods after various fed and fasting conditions to determine food effects and the relative bioavailability[60]. A high-fat meal increased bioavailability significantly and was therefore considered preferable, although exposure-effect relationships for clofazimine in leprosy have not been properly established.

3.2.6 Trachoma

Trachoma is the leading infectious cause of blindness worldwide. The infection of the eye by Chlamydia trachomatis can be divided into two clinical stages: initial active trachoma (inflammation) and cicatricial disease (eyelid scarring). Active trachoma is mostly seen in young children and cicatricial disease and eventual blindness is typically seen in adults. Treatment and prevention of trachoma consists of surgery and mass drug administration of antibiotic treatment. The WHO recommends either single dose oral azithromycin or topical tetracycline. Since trachoma commonly geographically overlaps with other NTDs such as onchocerciasis and lymphatic filariasis, regional elimination initiatives for these diseases in terms of mass drug administrations are often aimed to be combined. PK studies have therefore focused on drug-drug

interactions between azithromycin and drugs used in mass drug administration for these other NTDs (ivermectin and albendazole)[67,68].

Ivermectin exposure appeared to be increased in healthy volunteers in combination with azithromycin and the authors recommended subsequent modeling and simulation to predict and evaluate an optimal dosing regimen for this drug combination[67]. A subsequent population PK analysis of the same data showed the benefit of modelling and simulation by pinpointing that the mechanism of this interaction was an increase in bioavailability and demonstrating that maximum expected ivermectin exposures after concomitant administration of azithromycin were still within a well-tolerated range, meaning that combining these drugs in mass drug administrations should be feasible[68].

3.2.7 Endemic treponematoses

Endemic treponematoses are a group of chronic bacterial infections, related to venereal syphilis, caused by treponemes that mainly affect the bones and/or skin causing localized lesions. The spectrum of diseases includes yaws, endemic syphilis (bejel), and pinta. Yaws is the most prevalent form of nonvenereal treponematosis, and while rarely fatal, it can lead to chronic disfigurement and disability. Treatment consists of a single dose of long-acting penicillin or oral azithromycin. No PK studies could be identified for drugs used to treat endemic treponematoses.

3.2.8 Cysticercosis/taeniasis

Cysticercosis and taeniasis are both caused by species of the Taenia tapeworm. Taeniasis is the intestinal infection with adult tapeworms. This mild disease is an important cause for transmission of cysticercosis, an infection with the larval stage of the pork tapeworm Taenia solium that can cause life-threatening clinical manifestations. The most severe form is neurocysticercosis in which the larval cysts are located in the central nervous system and cause severe neurological symptoms. The treatment of (neuro-)cysticercosis is not fully established. Besides symptomatic treatment (antiepileptics) it remains debated whether, and if so in which cases, antiparasitic and concomitant anti-inflammatory treatment to reduce inflammation associated with the dying organism are indicated. The main antiparasitic agents used in cysticercosis are albendazole and praziquantel, while the supportive anti-inflammatory therapy can be corticosteroids or methotrexate. PK studies are available for both albendazole[69-71] and praziquantel[72-74], and have focused on drug-drug interactions[71-74].

Albendazole sulfoxide, the main metabolite of albendazole, has been studied in several clinical trials on neurocysticercosis. Despite the absence of an established PKPD relationship, these studies suggested based on the area under the concentration-time curve and steady-state trough concentrations that albendazole administration could be

changed from the current clinical practice of thrice daily, to twice daily[70,75]. Conversely, a small descriptive study in children advised an opposite dose adjustment, given the increased clearance in children[69]. Drug-drug interaction studies indicated that there were no interactions with antiepileptic drugs and that dexamethasone even decreased the elimination rate of albendazole[71]. Co-administration of the antiparasitic praziquantel increased albendazole sulfoxide exposure possibly synergizing the efficacy of both drugs when administered together[74].

Drug-drug interaction studies with praziquantel demonstrated that exposure was decreased in combination with dexamethasone and anti-epileptics possibly related to induction of cytochrome P450-mediated hepatic metabolism[72]. Conversely, co-administration of the H2-receptor antagonist cimetidine was demonstrated to prolong exposure of praziquantel, suggesting the possibility for further improvement of efficacy of this single-day therapy[73].

3.2.9   Dracunculiasis

Dracunculiasis is also known as guinea-worm disease. The infection is transmitted by drinking unfiltered water containing the larvae of Dracunculus medinensis. Treatment consists of slow extraction of the worm combined with wound care and pain management. There is no specific chemotherapy indicated to treat dracunculiasis and no PK studies were found.

3.2.10   Echinococcosis

There are four species of Echinococcus tapeworms that can cause infection in humans. Humans are an incidental host; with transmission through e.g., contaminated environmental water. The two main types of disease are cystic echinococcosis and alveolar echinococcosis, both characterized by the slow growth of cyst-like larvae, usually in the liver. Development of active disease can take multiple years. Oral albendazole is the chemotherapy of choice for both disease types, sometimes combined with surgery or percutaneous drainage of the cysts. Albendazole is poorly absorbed from the gastro-intestinal tract and most PK studies have focused on improving the bioavailability of the compound[76-78].

The PK of albendazole and its main metabolite, albendazole sulphoxide, have been studied in patients with echinococcosis[76]. It was shown that extrahepatic cholestasis, a common symptom of echinococcosis, delayed the absorption and decreased the elimination rate of albendazole. Another study looked at bioequivalence between a novel emulsified formulation of albendazole compared to a standard oral tablet formulation[77]. To improve the low bioavailability of albendazole, co-administration with cimetidine was studied[78]. The high inter-individual variability in PK and the various

possible contradictory effects of cimetidine on both absorption (increased) by decreasing the gastro-intestinal pH and metabolism by cytochrome P450 enzyme inhibition for both albendazole and its sulfoxide metabolite complicated the descriptive interpretation of the results from this study[78].

3.2.11 Foodborne trematodiases

Foodborne trematodiases are zoonotic infections caused by parasitic flatworms, so called 'liver flukes' which can result in clonorchiasis, opisthorchiasis, fascioliasis, and paragonimiasis. Transmission cycles differ widely, but generally involve ingestion of food contaminated with the parasite larvae. The worms are mainly located in the liver and gall bladder or in the lung (paragonimiasis). Different antihelminthic compounds are used, depending on the infecting worm (Table 1.1.3), but praziquantel and triclabendazole are two of the main drugs in use for this group of diseases. PK studies were found for both these drugs[79-82], although no studies were found in the context of paragonimiasis (lung fluke). Given the liver damage caused by the flukes, many PK studies focused on a disease-effect on cytochrome P450 enzyme-mediated metabolism of the compounds, which appeared most prominent for cytochrome P450 3A4-substrate praziquantel[79].

The bioavailability of triclabendazole, the drug of choice for fascioliasis, and total exposure to active metabolites was shown to be greatly increased by concomitant food-intake[81]. Descriptive PK parameters were not different between fascioliasis patients and healthy subjects, indicating the absence of a disease-effect on triclabendazole metablism despite obvious liver damage[82].

Praziquantel, the antihelminth drug of choice for both opisthorchiasis and clonorchiasis, appeared to have a reduced clearance rate in advanced opisthorchiasis infection, compared to early-stage disease and post-recovery, presumably due to liver impairment[79]. In clonorchiasis patients, a sustained-release formulation was tested to allow for a single-dose treatment with praziquantel. Despite a similar area under the concentration-time curve, the sustained-release formulation with lower maximal concentration and peak time showed unsatisfactory efficacy compared to a single-dose normal-release praziquantel[80].

3.2.12 Lymphatic filariasis

Lymphatic filariasis, also known as elephantiasis, is a disfiguring disease caused by filarial nematodes (roundworms) and is a major cause of disability and social stigma in endemic areas. The filarial worms are transmitted by mosquito's and cause an infection of the lymphatic system and skin, leading to massive edema formation in e.g., extremities and genitalia. Current treatment is generally through mass drug

administration with the aim to stop transmission of the disease by killing the microfilarial stage of the parasite, using albendazole plus either ivermectin in regions with onchocerciasis (i.e., African countries) or albendazole plus diethylcarbamazine in all other regions. PK studies in the context of lymphatic filariasis were found for both these combinations[83-85]. Doxycycline has been proposed as treatment to kill also adult worms, but no PK studies could be identified for this drug in this context.

Co-administration of diethylcarbamazine and albendazole was investigated in healthy volunteers from areas where lymphatic filariasis is endemic[83]. Whereas large inter-individual variability in exposure of all drugs was observed, no significant interaction was detected. To assess the safety of albendazole mass drug administration during breast feeding, the PK of albendazole and metabolites was studied in the breast milk of treated women. Albendazole and albendazole sulphoxide achieved low penetration into breast milk and was not considered to be harmful for breastfed infants[85].

3.2.13 Onchocerciasis

Onchocerciasis, also known as river blindness, is caused by the filarial nematode Onchocerca vulvus, which is transmitted through the bites of blackfly that breed near rivers. It results in various clinical manifestations, such as pruritus, subcutaneous nodules, onchocercal skin disease, and blindness. The therapeutic targets are the young microfilariae located e.g., in the skin, as well as the adult worms (macrofilariae) located generally in the subcutaneous nodules. The clinical approach to treatment is mainly focused on interrupting transmission through mass drug administration programmes with ivermectin (focused on killing the microfilariae) at 6- to 12-monthly intervals, sometimes in combination with albendazole due to overlap with lymphatic filariasis co-infection. For individual treatment doxycycline is used in combination with ivermectin. Various studies have investigated the PK of albendazole and ivermectin in onchocerciasis patients, focusing on dose-finding, food-effect, compliance, disease-effect, tissue distribution and drug-drug interactions[86-90]. No PK studies were found for doxycycline. Other less established treatments include: suramin (too toxic and costly[91]), moxidectin (under development[92]), amocarzine (insufficient efficacy[93,94]).

Combining albendazole and ivermectin appeared to be safe and not to result in any PK interactions, albendazole co-administration offered no advantage over ivermectin alone in terms of efficacy against onchocerciasis[86,87]. A fatty meal increased the bioavailability of albendazole four-fold and concomitant food-intake should thus be recommended[86]. On the other hand, ivermectin PK was shown to be not affected by either food- or alcohol intake[90].

Ivermectin PK parameters were similar between healthy volunteers and onchocerciasis patients and the drug was shown to penetrate in fat, skin, infected nodules and even isolated parasites from these patients[89]. Compliance to non-observed ivermectin

therapy in mass drug administration programmes could be assessed through plasma concentration monitoring[88].

PK of moxidectin, a veterinary antiparasitic, was studied in healthy lactating women, including excretion into breast milk[92]. Moxidectin exposure in infants via breast milk was estimated to be 8.37% of the maternal dose, but PK information from young children is necessary to fully understand the implications of this indirect exposure.

The bioavailability of amocarzine, an experimental drug for onchocerciasis, appeared to be poor in fasting conditions. Additionally, the dosing interval was suggested to be shortened to twice-daily administration to increase exposure[93]. A subsequent study showed improved bioavailability of amocarzine and exposure to its N-oxide metabolite with food intake[94].

3.2.14 Schistosomiasis

Schistosomiasis is caused by Schistosoma blood flukes, whose lifecycle is dependent on fresh water snails. Humans get infected through skin contact with contaminated water. The localization of the infection can vary depending on the infective Schistosoma species and can develop in the intestines, liver, spleen, lungs, and bladder or urinary tract. The acute phase is characterized by a transient hypersensitivity reaction associated with tissue migration of the larvae. Chronic infection can result in many different clinical manifestations such as haematuria (urogenital) or blood in the stool (intestinal), depending on the infected organs. Control of schistosomiasis is based on large-scale treatment mainly using praziquantel, which was the topic of most PK studies in schistosomiasis[95-97,16]. The hepatic and renal dysfunction associated with chronic infection have been the focus of various praziquantel PK studies, which is hepatically metabolized and renally cleared. We also found descriptive PK studies for the experimental drugs metrifonate[98] and oxamniquine[99].

In one schistosomiasis case with chronic kidney failure, praziquantel plasma PK seemed not to be affected. This could indicate that advanced schistosomiasis can be treated with the regular praziquantel dose[95]. In patients infected by Schistosomiasis mansoni with various degrees of hepatic dysfunction, both the time to maximal concentrations as well as the area under the concentration-time curve increased proportional with the degree of hepatic insufficiency[16]. In spite of these pharmacokinetic differences, efficacy appeared not to be affected and dose adjustments based on hepatic function were not advised[16]. Pharmacokinetic parameters of two formulations of praziquantel were compared, to investigate a slower release formulation[96].

1.1

3.2.15 Soil-transmitted helminthiases

Soil-transmitted helminthiases are a diverse set of diseases caused by intestinal worms and often affect the most poor and rural communities. The main species that infect people through contact with contaminated soil are the roundworm (Ascaris), the whipworm (Trichuris), and the hookworms (Necator and Ancylostoma). Treatment for these infections is mainly through administration of antihelminths such as albendazole and mebendazole. Preventive treatment to reduce transmission to endemic populations is also widely used. No PK studies were identified.

3.2.16 Dengue, chikungunya, and zika

Dengue is the most prevalent arthropod-borne viral disease. The Flavivirus infection can cause a wide range of clinical manifestations of which severe hemorrhagic dengue is potentially fatal. Chikungunya and zika, two other flaviviruses that are also transmitted by mosquitos, both cause acute febrile polyarthralgia and arthritis. There are no specific therapeutic treatments available for dengue, chikungunya, or zika, although a few vaccines are currently in development. However, no PK studies were identified for these viral infections.

3.2.17 Rabies

Rabies is caused by a range of lyssaviruses and usually starts with non-specific symptoms during the prodromal phase, but once a patient is symptomatic the infection usually leads to progressive encephalopathy and is virtually always fatal. There are no established antiviral treatment regimens for rabies, although various post-exposure prophylaxis schedules based on vaccine therapy with or without rabies-specific immunoglobulins are being used to prevent development of symptomatic disease. Some PK studies have been performed on the kinetics of administered anti-rabies antibodies[17,18] and administered human interferon to support an early immune response[100].

PK of human leukocyte interferon in cerebrospinal fluid was compared between systemic and local intraventricular direct administration[100]. This study demonstrated that interferon levels in the cerebrospinal fluid could be maintained at potentially therapeutically active levels, also by systemic administration. Two other studies looked at immunoglobulin antibody administrations to increase rabies antibody titers. In one study, two sources of equine rabies immunoglobulin were compared in terms of antigen-binding fragments, which showed similar time-profiles, but no bioequivalence[17]. A phase I study with a recombinant human IgG1 anti-rabies monoclonal antibody determined the required dose to use in future post-exposure prophylaxis studies based on antibody PK[18].

4.   Discussion

This is the first comprehensive and systematic review of clinical PK studies undertaken in the field of NTDs. Our study highlights the paucity of PK data available for the treatments used against NTDs and the lack of application of modelling and simulation techniques in this particular clinical area. For various NTDs (endemic treponematoses, dracunculiasis, dengue/chikungunya, and soil-transmitted helminthiasis) no PK studies could be identified at all, while for others only very few studies (<5) were found (buruli ulcer, trachoma, echinococcosis, lymphatic filariasis, food-borne trematodiases, and rabies). For diseases such as e.g., the soil-transmitted helminthiases and rabies this lack of PK studies is in stark contrast to their massive global burden of disease (2700 and 26400 deaths per year and 5.19 and 1.46 million DALYs, respectively). Whereas for some of these diseases dedicated chemotherapeutic options have never been available (e.g., dracunculiasis and dengue), for other NTDs multiple drugs have been in clinical use for decades as part of established treatment guidelines, but information on PK studies is lacking. Due to the consistent lack of research and development funding for treatment of NTDs, very little innovation has been witnessed in the past century for the management of NTDs. For example, suramin, pentamidine, and melarsoprol, which were discovered in 1920, 1940, and 1949, respectively, are still being used for human African trypanosomiasis and leishmaniasis management. For all of these drugs no or very little PK studies have been performed since their introduction (we identified 1, 2 and 5 studies, respectively), while their live-threatening toxicities and the continuous threat of emerging drug resistance requires continued optimization of these dose regimens. The gap of knowledge on PK and PK-PD relationships limiting treatment optimization and adaptation has been pointed out before e.g., for praziquantel[101] and schistosomiasis[102], but has largely been neglected for other NTDs previously.

4.1   Limitations

Since our systematic review focused on clinical PK studies, the term 'pharmacokinetics' was the most central search term in our analysis. However, this term itself has only been introduced in the field of pharmacology in 1953 by Dost and has been popularized in the two decades afterwards[103]. Given that several current drugs against NTDs have been in use for a few decades already, it could be that various older publications for these particular NTD drugs were not identified, since they potentially did not make mention of the term 'pharmacokinetics'. This might also explain that our two oldest identified studies date from 1980[24,98], which might thus be a biased observation. While drug development activities in the field of NTDs have substantially increased during the past 15 years, mainly through increased political awareness and novel innovation mechanisms such as the product development partnership Drugs for Neglected Diseases initiative (http://www.dndi.org), this appeared not to be reflected in the

number of PK studies conducted. There is no particular increasing trend in the number of clinical PK reports for NTDs since 2000 (Figure 1.1.2). On the contrary, more than half of all identified PK studies were published prior to 2000, with a peak of publications in the mid-1990s (7 studies in 1993). This might indicate that, despite innovative breakthroughs and increased clinical trial activities in the field of NTDs, pharmacokinetic studies are still being neglected; an observation which is corroborated by a recent review that found only 4/382 active clinical trials on NTDs directed at pharmacokinetic studies[9]. Regarding the type of PK analysis, there was an increasing trend of using a population approach to analyze the PK data over the past decade (Figure 1.1.2).

A limitation in our search strategy was the English language restriction, potentially missing papers e.g., in French from African journals or Chinese from Asian journals. Additionally, (national) journals from countries/regions where NTDs are endemic are not particularly well covered by Pubmed/MEDLINE. Theoretically this might have precluded our access to some literature, but given the topic of our literature analysis this potential bias is probably in reality very small or even non-existent and more relevant for clinical publications than PK publications.

While the list of NTDs used can be variable, the word 'neglected' in that term generally refers to the lack of interest from pharmaceutical industry and the overall lack of funding and innovation in terms of therapeutic research and development for these diseases, but also to neglect by health ministries in countries where infected people live, by the World Bank, or relative to HIV/AIDS, tuberculosis and malaria. Typically, NTDs are infectious diseases closely interrelated to poverty and social-ecological systems promoting close contact between affected populations, vectors and animal reservoirs. Malaria, tuberculosis and HIV/AIDS are not considered as NTDs. The list of NTDs has since the turn of the century often been expanded to more than 30 diseases and disease complexes[104]. We adhered to the list of NTDs put forward by WHO[1], which contains 17 items of which various are disease 'complexes', such as 'soil-transmitted helminthiases', comprising multiple clinical infectious disorders.

4.2 Challenges in clinical pharmacokinetic studies in patients with NTDs

In the rural settings in which NTD clinical trials take place, collecting samples, maintaining cold chains and generally performing large clinical trials is logistically challenging. Obtaining useful blood samples from patients can be practically difficult due to a lack of laboratory infrastructure and restrictive clinical characteristics such as anemia. NTDs typically affect the poorest of the poor and disadvantaged populations, inherently constituting ethical difficulties, while language barriers and illiteracy make it

1.1

difficult to acquire informed consent from patients. Additionally, following up patients after their treatment, e.g., to sample the elimination phase of a drug or identify long-term outcome, is often practically impossible, e.g., in nomadic populations. Moreover, there is limited research and development funding available for the clinical development of drugs for NTDs[9]. For all these reasons, clinical trials on NTDs therefore typically result in small and heterogeneous datasets. This is illustrated by our systematic review, as 94% of the identified studies included small patient numbers (n<50). Patients in PK studies on NTDs are highly heterogeneous due to variability in clinical characteristics such as degree of liver impairment, malnourishment, or concomitant underlying infections, which subsequently can lead to large inter-individual variability in PK parameters. Many studies in this review, e.g., almost all studies on cysticercosis and taeniasis[69,70,72-75], reported large inter-individual variabilities in PK profiles and parameters. That large unexplained inter-individual variability can limit conclusions of trials is also exemplified in our review. For instance, in one study on Buruli ulcer, no significant differences in PK parameters could be found between two treatment groups because of the small population size and high degree of inter-patient variability[55]. In another study on albendazole in echinococcosis, a dose-dependent increase of the active metabolite's C_{max} could not be identified due to high intra- and inter-individual variability in bioavailability[78]. Furthermore, in the found PK studies some attention has been paid to drug-drug and food interactions (28% of studies), but only few studies (11%) made suggestions for optimizing dosing. Also, little attention has been paid to exposure-response relationships (6% of studies), which is of high importance to make proper decisions regarding dosing schemes.

4.3 Advantages of pharmacometric techniques

To optimize treatment regimens and to design efficient and cost-effective clinical trials, the use of population-based analyses can provide substantial advantages. FDA and EMA recommend the use of pharmacometrics in data analysis and clinical trial designs, especially in pediatrics or small patient groups[10-12]. Modelling and simulation techniques are pivotal in designing and simulating dosing regimens and trials and are a useful tool to extrapolate proposed regimens e.g., from healthy to diseased populations. Particularly for pediatrics, the application of quantitative pharmacometric methods has been considered essential to increase the success rates of clinical trials[105]. Not only in a priori pediatric trial design, but particularly also in the a posteriori analysis of collected PK (and PD) data, pharmacometric methods are needed to deal with the typical pediatric challenges of small study populations and low number of measurements[106]. For many NTDs, e.g., human African trypanosomiasis, leishmaniasis, soil-transmitted helminthiases, schistosomiasis, and dengue, more than 50% of the burden of disease is occurring in children[4].

The use of population-based approaches can aid in understanding and explaining the heterogeneity in PK and dealing with sparse sampling and smaller sample sizes, which are all so typical for studies in NTDs (see above). Physiological covariates could be identified to understand factors that contribute to variability among patients, even with a smaller sample size, unstructured sampling time points and sparse data per individual[107]. More information could be gained from studies with high intra- and inter-individual variability when part of the variability can be explained. Therefore, more emphasis on identification of appropriate covariate and error models could be particularly helpful, which requires the application of pharmacometrics[108].

An additional complication with infectious diseases is the need for combination therapy, either due to the fear of emerging (or already existing) drug resistance of the causative pathogen, but also because of the presence of co-infections. Identifying and understanding drug-drug interactions is therefore important for NTDs, that often appear in conjunction with malaria, HIV or tuberculosis, and also here the use of pharmacometrics has been recommended[108-110].

4.4   Extrapolations and simulation-based studies

Only 11% of the PK studies in our review included pediatric populations, which is in dire contrast to the actual burden of disease of most NTDs, as mentioned above. Again, population PK studies offer many advantages in this context. PK models derived from the adult population can be extrapolated to pediatric populations based on appropriately identified physiological covariate models[111]. Nevertheless, no studies were identified in this review that actually employed such extrapolation. Similar applications could be useful to extrapolate between ethnic groups or between patients from different geographical regions, all of which are relevant due to the wide geographical distribution of many NTDs (Table 1.1.1). Models could also be used to bridge PK results between different diseases, as some NTD drugs are (primarily) used for other diseases. For example, rifampin (or rifampicin) is used for tuberculosis, with various published population PK models available, which could be extrapolated to assess PK-PD relationships for its use in leprosy and Buruli ulcer patients.

Once PK and PK-PD models are developed and exposure-response relationships are established, optimal dosing schemes can be designed to reach the desired drug effect in all patients. This can be done in a cost-effective way by PK or PK-PD simulations of various dose regimens, taking into account the actual variability in patient characteristics in the target population. In our review we identified only four studies that actually made recommendations for alternative dose regimens. These four studies performed population PK analyses and subsequent simulations with the developed models to define optimal doses[25,26,38,42]. Other PK studies, mainly employing non-compartmental or individual compartmental analyses (together 78%), typically made

simple non-specific suggestions to lower or increase the dose, or conclude that more research was needed to suggest alternative doses. Additionally, for at least four studies we identified, a re-analysis performed using population PK methods provided more details about the PK-PD relationship or optimal dose regimens, compared to previous reports of the same PK datasets using conventional analyses[26,36,38,42].

Simulation-based studies can also help to limit and assess potential toxicity of dose regimens. For example, one study investigated the PK of benznidazole in Chagas Disease patients[26], and simulations revealed that the studied dose might lead to overexposure in most patients. In another study simulations showed that the maximum ivermectin exposure used in combination with azithromycin was in accordance with the safe exposure that was observed previously[68]. Furthermore, we identified two studies that assessed the toxicity of a drug to infants exposed by breast feeding[23,41]. In the first study, the drug exposure in breast milk was simulated by only using data from literature, and consequently the exposure of the drug to the infant was predicted. This gave insight in potential exposure and toxicity in infants without exposing actual infants to the drug. Another example was the use of population-based simulations and data from animal reproductive studies to define human contraceptive cover periods for the potentially teratogenic drug miltefosine for leishmaniasis[41]. Often there is a lack of women included in clinical trials, but still insight can be gained in drug exposure to women by the use of simulation and extrapolation techniques. All these examples highlight the opportunities of applying pharmacometric methods over more conventional analysis methods in assessing therapeutics for NTDs.

5.   Conclusion

In conclusion, this review provides an overview of the current status and gaps in pharmacokinetic research for NTDs, as well as the lack of population-based modeling in the performed clinical trials. Simulation and extrapolation tools have been minimally applied. For many NTDs no registered therapy is available, and more clinical PK trials are needed to establish evidence-based treatments and define PK-PD relationships. To make future clinical trials feasible and affordable, population PK modeling should be used to optimally analyze the often sparse data available and simulation-based studies should be used to inform trial design. This would minimize risks and maximize success rates of clinical trials, and optimally use the limited funding available in this neglected clinical area.

Acknowledgments

References

1. World Health Organization. Neglected tropical diseases [Internet]. 2015 [cited 2015 Jan 14]. Available from: http://www.who.int/neglected_diseases/diseases/en/
2. The END fund; Ending Neglected Diseases. NTD Overview [Internet]. 2015 [cited 2015 Jan 14]. Available from: http://www.end.org/whatwedo/ntdoverview
3. Hotez PJ, Alvarado M, Basáñez M-G, Bolliger I, Bourne R, Boussinesq M, et al. The Global Burden of Disease Study 2010: Interpretation and Implications for the Neglected Tropical Diseases. de Silva N, editor. PLoS Negl. Trop. Dis. 2014;8:e2865.
4. Murray CJL, Vos T, Lozano R, Naghavi M, Flaxman AD, Michaud C, et al. Disability-adjusted life years (DALYs) for 291 diseases and injuries in 21 regions, 1990-2010: a systematic analysis for the Global Burden of Disease Study 2010. Lancet. 2012;380:2197–223.
5. Hotez P, Ottesen E, Fenwick A, Molyneux D. The neglected tropical diseases: the ancient afflictions of stigma and poverty and the prospects for their control and elimination. Adv. Exp. Med. Biol. 2006;582:23–33.
6. Kennedy PG. Clinical features, diagnosis, and treatment of human African trypanosomiasis (sleeping sickness). Lancet Neurol. 2013;12:186–94.
7. Sabbaga V, Francisco F, Amato V, Carlos A. Mucosal leishmaniasis Current scenario and prospects for treatment. 2008;105:1–9.
8. Sundar S, Sinha PR, Agrawal NK, Srivastava R, Rainey PM. A cluster of cases of severe cardiotoxicity among kala-azar patients treated with a high-osmolarity lot of sodium antimony gluconate. 1998;59:139–43.
9. Pedrique B, Strub-Wourgaft N, Some C, Olliaro P, Trouiller P, Ford N, et al. The drug and vaccine landscape for neglected diseases (2000–11): a systematic assessment. Lancet Glob. Heal. 2013;1: e371-9.
10. European Medicines Agency. Guideline on the role of pharmacokinetics in the development of medicinal products in the paediatric population [Internet]. 2006 [cited 2015 Jan 14]. Available from: http://www.ema.europa.eu/ema/index.jsp?curl=pages/regulation/document_listing/document_listing _000087.jsp
11. Food and Drug Administration. Guidance for Industry Population Pharmacokinetics [Internet]. 1999 [cited 2015 Jan 14]. Available from: http://www.fda.gov/downloads/ScienceResearch/SpecialTopics/ WomensHealthResearch/UCM133184.pdf
12. Food and Drug Administration. Guidance for Industry: Exposure-Response Relationships - Study Design, Data Analysis and Regulatory Applications [Internet]. 2003 [cited 2015 Jan 14]. Available from: http://www.fda.gov/downloads/drugs/guidancecomplianceregulatoryinformation/guidances/ucm0721 09.pdf
13. Moher D, Shamseer L, Clarke M, Ghersi D, Liberati A, Petticrew M, et al. Preferred reporting items for systematic review and meta-analysis protocols (PRISMA-P) 2015 statement. Syst. Rev. 2015;4:1–9.
14. PAGE-meeting. Population Approach Group Europe [Internet]. 2015. Available from: http://www.page-meeting.org/default.asp?keuze=search&orderby=&keywordNumber=&keywordAuthor=&keywordTitle =&keywordContent=&meeting=
15. Gabrielsson J, Weiner D. Pharmacokinetic and Pharmacodynamic Data Analysis: Concepts and Applications. 4th ed. Gabriellson & Weiner, editor. Stockholm: Taylor & Francis; 2007.
16. El Guiniady M a, el Touny M a, Abdel-Bary M a, Abdel-Fatah S a, Metwally A. Clinical and pharmacokinetic study of praziquantel in Egyptian schistosomiasis patients with and without liver cell failure. Am. J. Trop. Med. Hyg. 1994;51:809–18.
17. Lang J, Attanath P, Quiambao B, Singhasivanon V, Chanthavanich P, Montalban C, et al. Evaluation of the safety, immunogenicity, and pharmacokinetic profile of a new, highly purified, heat-treated equine rabies immunoglobulin, administered either alone or in association with a purified, Vero-cell rabies vaccine. Acta Trop. 1998;70:317–33.
18. Gogtay N, Thatte U, Kshirsagar N, Leav B, Molrine D, Cheslock P, et al. Safety and pharmacokinetics of a human monoclonal antibody to rabies virus: A randomized, dose-escalation phase 1 study in adults. Vaccine. 2012;30:7315–20.

1.1

19. Post T, editor. UpToDate. Waltham, MA: UpToDate; 2015.
20. Bern C. Chagas' Disease. N. Engl. J. Med. 2015;373:456–66.
21. Shapiro TA, Were JB, Danso K, Nelson DJ, Desjardins RE, Pamplin CL. Pharmacokinetics and metabolism of allopurinol riboside. Clin. Pharmacol. Ther. 1991;49:506–14.
22. Were JBO, Shapiro TA. Effects of probenecid on the pharmacokinetics of allopurinol riboside. Antimicrob. Agents Chemother. 1993;37:1193–6.
23. Garcia-Bournissen F, Altcheh J, Panchaud A, Ito S. Is use of nifurtimox for the treatment of Chagas disease compatible with breast feeding? A population pharmacokinetics analysis. Arch. Dis. Child. 2010;95:224–8.
24. Richle RW, Raaflaub J. Difference of effective antitrypanosomal dosages of benznidazole in mice and man. Chemotherapeutic and pharmacokinetic results. Acta Trop. 1980;37:257–61.
25. Altcheh J, Moscatelli G, Mastrantonio G, Moroni S, Giglio N, Marson ME, et al. Population Pharmacokinetic Study of Benznidazole in Pediatric Chagas Disease Suggests Efficacy despite Lower Plasma Concentrations than in Adults. PLoS Negl. Trop. Dis. 2014;8:1–9.
26. Soy D, Aldasoro E, Guerrero L, Posada E, Serret N, Mejía T, et al. Population Pharmacokinetics of Benznidazole in Adult Patients with Chagas Disease. Antimicrob. Agents Chemother. 2015;59:3342–9.
27. World Health Organization. Human African trypanosomiasis [Internet]. 2015 [cited 2015 Jan 14]. Available from: http://www.who.int/trypanosomiasis_african/en/
28. Bronner U, Doua F, Ericsson O, Gustafsson LL, Miézan TW, Rais M, et al. Pentamidine concentrations in plasma, whole blood and cerebrospinal fluid during treatment of Trypanosoma gambiense infection in Côte d'Ivoire. Trans. R. Soc. Trop. Med. Hyg. 1991;85:608–11.
29. Bronner U, Gustafsson LL, Doua F, Ericsson O, Miézan T, Rais M, et al. Pharmacokinetics and adverse reactions after a single dose of pentamidine in patients with Trypanosoma gambiense sleeping sickness. Br. J. Clin. Pharmacol. 1995;39:289–95.
30. Harrison SM, Harris RW, Bales Jr JD. Attempt to correlate urine arsenic excretion with clinical course during melarsoprol therapy of patients with Rhodesian trypanosomiasis. Am. J. Trop. Med. Hyg. 1997; 56:632–6.
31. Burri C, Baltz T, Giroud C, Doua F, Welker HA, Brun R. Pharmacokinetic properties of the trypanocidal drug melarsoprol. Chemotherapy. 1993;39:225–34.
32. Burri C, Keiser J. Pharmacokinetic investigations in patients from northern Angola refractory to melarsoprol treatment. Trop. Med. Int. Heal. 2001;6:412–20.
33. Bronner U, Brun R, Doua F, Ericsson O, Burri C, Keiser J, et al. Discrepancy in plasma melarsoprol concentrations between HPLC and bioassay methods in patients with T. gambiense sleeping sickness indicates that melarsoprol is metabolized. Trop. Med. Int. Heal. 1998;3:913–7.
34. Milord F, Loko L, Ethier L, Mpia B, Pepin J. Eflornithine concentrations in serum and cerebrospinal fluid of 63 patients treated for Trypanosoma brucei gambiense sleeping sickness. Trans. R. Soc. Trop. Med. Hyg. 1993;87:473–7.
35. Na-Bangchang K, Doua F, Konsil J, Hanpitakpong W, Kamanikom B, Kuzoe F. The pharmacokinetics of eflornithine (alpha-difluoromethylornithine) in patients with late-stage T.b. gambiense sleeping sickness. Eur. J. Clin. Pharmacol. 2004;60:269–78.
36. Jansson-Löfmark R, Na-Bangchang K, Björkman S, Doua F, Ashton M. Enantiospecific Reassessment of the Pharmacokinetics and Pharmacodynamics of Oral Eflornithine against Late-Stage Trypanosoma brucei gambiense Sleeping Sickness. Antimicrob. Agents Chemother. 2015;59:1299–307.
37. Tarral A, Blesson S, Mordt OV, Torreele E, Sassella D, Bray M a., et al. Determination of an optimal dosing regimen for fexinidazole, a novel oral drug for the treatment of human African trypanosomiasis: First-in-human studies. Clin. Pharmacokinet. 2014;53:565–80.
38. Gualano V, Felices M, Evene E, Blesson S, Tarral A. Dose Regimen Assessement for Oral fexinidazole, a new antimicrobial agent of the treatment of HAT: Population Pharmacokinetic Analysis of fexinidazole and 2 metabolites. Presented at the 21th Population Approach Group in Europe Meeting, Venice, Italy. 2012.
39. Blum J, Buffet P, Visser L, Harms G, Bailey MS, Caumes E, et al. LeishMan recommendations for treatment of cutaneous and mucosal leishmaniasis in travelers, 2014. J. Travel Med. 21:116–29.

40. Dorlo TPC, Van Thiel PP a M, Huitema ADR, Keizer RJ, De Vries HJC, Beijnen JH, et al. Pharmacokinetics of miltefosine in old world cutaneous leishmaniasis patients. Antimicrob. Agents Chemother. 2008;52:2855–60.

41. Dorlo TPC, Balasegaram M, Lima MA, De Vries PJ, Beijnen JH, Huitema ADR. Translational pharmacokinetic modelling and simulation for the assessment of duration of contraceptive use after treatment with miltefosine. J. Antimicrob. Chemother. 2012;67:1996–2004.

42. Dorlo TPC, Huitema ADR, Beijnen JH, De Vries PJ. Optimal dosing of miltefosine in children and adults with visceral leishmaniasis. Antimicrob. Agents Chemother. 2012;56:3864–72.

43. Dorlo TPC, Rijal S, Ostyn B, De Vries PJ, Singh R, Bhattarai N, et al. Failure of miltefosine in visceral leishmaniasis is associated with low drug exposure. J. Infect. Dis. 2014;210:146–53.

44. Jaser M Al, El-Yazigi A, Croft SL. Pharmacokinetics of Antimony in Patients Treated with Sodium Stibogluconate for Cutaneous Leishmaniasis. Pharm. Res. 1995;12:113–6.

45. Vásquez L, Scorza Dagert J V., Scorza J V., Vicuña-Fernández N, de Peña YP, López S, et al. Pharmacokinetics of experimental pentavalent antimony after intramuscular administration in adult volunteers. Curr. Ther. Res. - Clin. Exp. 2006;67:193–203.

46. Zaghloul IY, Radwan MA, Jaser MH Al. Clinical Efficacy and Pharmacokinetics of Antimony in Cutaneous Leishmaniasis Patients Treated With Sodium Stibogluconate. J. Clin. Pharmacol. 2010;50:1230–7.

47. Reymond J-M, Desmeules J. Sodium Stibogluconate (Pentostan) Overdose in a Patient With Acquired Immunodeficiency Syndrome. Ther. Drug Monit. 1998;20:714–6.

48. Chulay JD, Fleckenstein L, Smith DH. Pharmacokinetics of antimony during treatment of visceral leishmaniasis with sodium stibogluconate or meglumine antimoniate. Trans. R. Soc. Trop. Med. Hyg. 1988;82:69–72.

49. Musa AM, Younis B, Fadlalla A, Royce C, Balasegaram M, Wasunna M, et al. Paromomycin for the treatment of visceral leishmaniasis in Sudan: A randomized, open-label, dose-finding study. PLoS Negl. Trop. Dis. 2010;4:4–10.

50. Ravis WR, Llanos-Cuentas a., Sosa N, Kreishman-Deitrick M, Kopydlowski KM, Nielsen C, et al. Pharmacokinetics and Absorption of Paromomycin and Gentamicin from Topical Creams Used To Treat Cutaneous Leishmaniasis. Antimicrob. Agents Chemother. 2013;57:4809–15.

51. Sundar S, Sinha PK, Dixon S a., Buckley R, Miller AK, Mohamed K, et al. Pharmacokinetics of oral sitamaquine taken with or without food and safety and efficacy for treatment of visceral leishmaniais: A randomized study in Bihar, India. Am. J. Trop. Med. Hyg. 2011;84:892–900.

52. Jaser M a Y a L, El-yazigi A, Kojan M, Croft SL. Skin Uptake , Distribution , and Elimination of Antimony following Administration of Sodium Stibogluconate to Patients with Cutaneous Leishmaniasis. Microbiology. 1995;39:516–9.

53. Cruz A, Rainey PM, Herwaldt BL, Stagni G, Palacios R, Trujillo R, et al. Pharmacokinetics of antimony in children treated for leishmaniasis with meglumine antimoniate. J. Infect. Dis. 2007;195:602–8.

54. Nienhuis WA, Stienstra Y, Thompson WA, Awuah PC, Abass KM, Tuah W, et al. Antimicrobial treatment for early, limited Mycobacterium ulcerans infection: a randomised controlled trial. Lancet. 2010;375:664–72.

55. Alffenaar JWC, Nienhuis W a., De Velde F, Zuur a. T, Wessels a. M a, Almeida D, et al. Pharmacokinetics of rifampin and clarithromycin in patients treated for Mycobacterium ulcerans infection. Antimicrob. Agents Chemother. 2010;54:3878–83.

56. Pieters FA, Zuidema J. Intra-adipose administration of monoacetyldapsone to healthy volunteers. Int J Lepr Other Mycobact Dis. 1986;54:510–6.

57. Pieters FA, Zuidema J. The absolute oral bioavailability of dapsone in dogs and humans. Int J Clin Pharmacol Ther Toxicol. 1987;25:396–400.

58. Garg SK, Kumar B, Bakaya V, Lal R, Shukla VK, Kaur S. Plasma dapsone and its metabolite monoacetyldapsone levels in leprotic patients. Int J Clin Pharmacol Ther Toxicol. 1988;26:552–4.

59. Moura FM, Dias RM, Araujo EC, Brasil LM, Ferreira M V, Vieira JL. Dapsone and Body Mass Index in Subjects With Multibacillary Leprosy. Ther. Drug Monit. 2013;36:261–3.

60. Nix DE, Adam RD, Auclair B, Krueger TS, Godo PG, Peloquin C a. Pharmacokinetics and relative bioavailability of clofazimine in relation to food, orange juice and antacid. Tuberculosis. 2004;84:365-73.

61. Venkatesan K, Mathur A, Girdhar BK, Bharadwaj VP. The effect of clofazimine on the pharmacokinetics of rifampicin and dapsone in leprosy. J. Antimicrob. Chemother. 1986;18:715–8.
62. Venkatesan K, Chauhan SL, Girdhar A, Girdhar BK. Bioavailability of dapsone on oral administration of Dapsomine--a comparative evaluation. Indian J Lepr. 1993;65:157–61.
63. Mehta J, Gandhi I, Sane S, Wamburkar M. Effect of clofazimine and dapsone on rifampicin (Lositril) pharmacokinetics in multibacillary and paucibacillary leprosy cases. Lepr. Rev. 1986;57:67–76.
64. Pieters F a, Woonink F, Zuidema J. Influence of once-monthly rifampicin and daily clofazimine on the pharmacokinetics of dapsone in leprosy patients in Nigeria. Eur. J. Clin. Pharmacol. 1988;34:73–6.
65. Teo SK, Scheffler MR, Kook K a, Tracewell WG, Colburn W a, Stirling DI, et al. Thalidomide dose proportionality assessment following single doses to healthy subjects. J. Clin. Pharmacol. 2001;41: 662-7.
66. Teo SK, Colburn W a, Thomas SD. Single-dose oral pharmacokinetics of three formulations of thalidomide in healthy male volunteers. J. Clin. Pharmacol. 1999;39:1162–8.
67. Amsden GW, Gregory TB, Michalak C a., Glue P, Knirsch C a. Pharmacokinetics of azithromycin and the combination of ivermectin and albendazole when administered alone and concurrently in healthy volunteers. Am. J. Trop. Med. Hyg. 2007;76:1153–7.
68. El-Tahtawy A, Glue P, Andrews EN, Mardekian J, Amsden GW, Knirsch C a. The effect of azithromycin on ivermectin pharmacokinetics - A population pharmacokinetic model analysis. PLoS Negl. Trop. Dis. 2008;2.
69. Jung H, Sanchez M, Gonzalez-Astiazaran A, Martiner JM, Suastegui R, Gonzalez-Esquivel D. Clinical Pharmacokinetics of Albendazole in Children with Neurocysticercosis. Am. J. Ther. 1997;4:23–6.
70. Sanchez M, Suastegui R, Gonzalez-Esquivel D, Sotelo J, Jung H. Pharmacokinetic Comparison of Two Albendazole Dosage Regimens in Patients with Neurocysticercosis. Clin. Neuropharmacol. 1993;16: 77-82.
71. Takayanagui OM, Lanchote VL, Marques MP, Bonato PS. Therapy for neurocysticercosis: pharmacokinetic interaction of albendazole sulfoxide with dexamethasone. Ther. Drug Monit. 1997;19:51–5.
72. Na-Bangchang, K Vanijanonta S, Karbwang J. Plasma concentrations of praziquantel during the therapy of neurocysticerosis with praziquantel, in the presence of antiepileptics and dexamethasone. Southeast Asian J Trop Med Public Heal. 1995;26:120–3.
73. Jung H, Medina R, Castro N, Corona T, Sotelo J. Pharmacokinetic study of praziquantel administered alone and in combination with cimetidine in a single-day therapeutic regimen. Antimicrob. Agents Chemother. 1997;41:1256–9.
74. Garcia HH, Lescano AG, Lanchote VL, Pretell EJ, Gonzales I, Bustos J a., et al. Pharmacokinetics of combined treatment with praziquantel and albendazole in neurocysticercosis. Br. J. Clin. Pharmacol. 2011;72:77–84.
75. Jung H, Hurtado M, Sanchez M, Medina M, Sotelo J. Clinical Pharmacokinetics of Albendazole in Patients with Brain Cysticercosis. J. Clin. Pharmacol. 1992;32:28–31.
76. Cotting J, Zeugin T, Steiger U, Reichen J. Albendazole kinetics in patients with echinococcosis: Delayed absorption and impaired elimination in cholestasis. Eur. J. Clin. Pharmacol. 1990;38:605–8.
77. Mingjie W, Shuhua X, Junjie C, Bin L, Cheng F, Weixia S, et al. Albendazole-soybean oil emulsion for the treatment of human cystic echinococcosis: Evaluation of bioavailability and bioequivalence. Acta Trop. 2002;83:177–81.
78. Schipper HG, Koopmans RP, Nagy J, Butter JJ, Kager PA, Van Boxtel CJ. Effect of dose increase or cimetidine co-administration on albendazole bioavailability. Am. J. Trop. Med. Hyg. 2000;63:270–3.
79. Na Bangchang K, Karbwang J, Pungpak S, Radomyos B, Bunnag D. Pharmacokinetics of praziquantel in patients with opisthorchiasis. Southeast Asian J. Trop. Med. Public Health. 1993;24:717–23.
80. Choi M-H, Chang B-C, Lee S-J, Jang I-J, Shin S-G, Kho W-G, et al. Therapeutic evaluation of sustained-releasing praziquantel (SRP) for clonorchiasis: Phase 1 and 2 clinical studies. Korean J. Parasitol. 2006;44:361.
81. Lecaillon JB, Godbillon J, Campestrini J, Naquira C, Miranda L, Pacheco R, et al. Effect of food on the bioavailability of triclabendazole in patients with fascioliasis. Br. J. Clin. Pharmacol. 1998;45:601–4.

82. El-Tantawy WH, Salem HF, Mohammed Safwat N a S. Effect of Fascioliasis on the pharmacokinetic parameters of triclabendazole in human subjects. Pharm. World Sci. 2007;29:190–8.

83. Shenoy RK, Suma TK, John a, Arun SR, Kumaraswami V, Fleckenstein LL, et al. The pharmacokinetics, safety and tolerability of the co-administration of diethylcarbamazine and albendazole. Ann. Trop. Med. Parasitol. 2002:603–14.

84. Sarin R, Dash a. P, Dua VK. Albendazole sulphoxide concentrations in plasma of endemic normals from a lymphatic filariasis endemic region using liquid chromatography. J. Chromatogr. B Anal. Technol. Biomed. Life Sci. 2004;799:233–8.

85. Abdel-Tawab AM, Bradley M, Ghazaly E a., Horton J, El-Setouhy M. Albendazole and its metabolites in the breast milk of lactating women following a single oral dose of albendazole. Br. J. Clin. Pharmacol. 2009;68:737–42.

86. Awadzi K, Hero M, Opoku NO, Buttner DW, Coventry PA, Prime MA, et al. The chemotherapy of Onchocerciasis XVII. A clinical evaluation of albendazole in patients with onchocerciasis; effects of food and pretreatment with ivermectin on drug response and pharmacokinetics. Trop. Med. Parasitol. 1994;45:203–8.

87. Awadzi K, Edwards G, Duke BOL, Opoku NO, Attah SK, Addy ET, et al. The co-administration of ivermectin and albendazole - safety, pharmacokinetics and efficacy against Onchocerca volvulus. Ann. Trop. Med. Parasitol. 2003;97:165–78.

88. Okonkwo PO, Ogbuokiri JE, Ofoegbu E, Klotz U. Protein binding and ivermectin estimations in patients with onchocerciasis. Clin. Pharmacol. Ther. 1993;53:426–30.

89. Baraka OZ, Mahmoud BM, Marschke CK, Geary TG, Homeida MM a, Williams JF. Ivermectin distribution in the plasma and tissues of patients infected with Onchocerca volvulus. Eur. J. Clin. Pharmacol. 1996;50:407–10.

90. Homeida MM, Malcolm SB, ElTayeb a. Z, Eversole RR, Elassad AS, Geary TG, et al. The lack of influence of food and local alcoholic brew on the blood level of Mectizan® (ivermectin). Acta Trop. Elsevier B.V.; 2013;127:97–100.

91. Chijioke CP, Umeh RE, Mbah AU, Nwonu P, Fleckenstein LL, Okonkwo PO. Clinical pharmacokinetics of suramin in patients with onchocerciasis. Eur. J. Clin. Pharmacol. 1988;54:249–51.

92. Korth-Bradley JM, Parks V, Chalon S, Gourley I, Matschke K, Gossart S, et al. Excretion of moxidectin into breast milk and pharmacokinetics in healthy lactating women. Antimicrob. Agents Chemother. 2011;55:5200–4.

93. Lecaillon JB, Dubois JP, K A, Poltera a a, Ginger CD. Pharmacokinetics of CGP 6140 (amocarzine) after oral administration of single 100-1600 mg doses to patients with onchocerciasis. Br. J. Clin. Pharmacol. 1990;30:625–8.

94. Lecaillon JB, Poltera AA, Zea-Flores G, de Ramirez I, Nowell de Arevalo A. Influence of food related to dose on the pharmacokinetics of amocarzine and of its N-oxide metabolite, CGP 13 231, after oral administration to 20 onchocerciasis male patients from Guatemala. Trop. Med. Parasitol. 1991;42: 286-90.

95. Pehrson PO, Bengtsson E, Diekmann HW, Groll E. Treatment with praziquantel in a patient with schistosomiasis and chronic renal failure. Trans. R. Soc. Trop. Med. Hyg. 1983;77:687–8.

96. Mandour ME, El Turabi H, Homeida MMA, El Sadig T, Ali HM, Bennett JL, et al. Pharmacokinetics of praziquantel in healthy volunteers and patients with schistosomiasis. Trans. R. Soc. 1990;84:389–93.

97. Valencia CI, Catto BA, Webster LT, Barcelon E, Ofendo-Reyes R. Concentration time course of praziquantel in Filipinos with mild Schistosoma japonicum infection. Southeast Asian J. Trop. Med. Public Health. 1994;25:409–14.

98. Nordgren I, Holmstedt BO, Bengtsson E, Finkel A. Plasma levels of metrofonate and dichlorvos during treatment of schistosomiasis with Bilarcil®. Am. J. Trop. Med. Hyg. 1980;29:426–30.

99. Daneshmend TK, Homeida MA. Oxamniquine pharmacokinetics in hepatosplenic schistosomiasis in the Sudan. J. Antimicrob. Chemother. 1987;19:87–93.

100. Merigan TC, Baer GM, Winkler WG, Bernard KW, Gibert CG, Chany C, et al. Human leukocyte interferon administration to patients with symptomatic and suspected rabies. Ann. Neurol. 1984;16:82–7.

1.1

101. Olliaro P, Delgado-Romero P, Keiser J. The little we know about the pharmacokinetics and pharmacodynamics of praziquantel (racemate and R-enantiomer). J. Antimicrob. Chemother. 2014;69:863–70.
102. Wilby KJ, Gilchrist SE, Ensom MHH. A review of the pharmacokinetic implications of schistosomiasis. Clin. Pharmacokinet. 2013;52:647–56.
103. Wagner JG. History of pharmacokinetics. Pharmacol. Ther. 1981;12:537–62.
104. Hotez PJ, Yamey G. The Evolving Scope of PLoS Neglected Tropical Diseases. PLoS Negl. Trop. Dis. Public Library of Science; 2009;3:e379.
105. Gobburu JVS. Pharmacometrics 2020. J. Clin. Pharmacol. 2010;50:151S-157S.
106. Jadhav PR, Kern SE. The Need for Modeling and Simulation to Design Clinical Investigations in Children. J. Clin. Pharmacol. 2010;50:121S=129S.
107. Mould DR, Upton RN. Basic Concepts in Population Modeling, Simulation, and Model-Based Drug Development—Part 2: Introduction to Pharmacokinetic Modeling Methods. CPT Pharmacometrics Syst. Pharmacol. 2013;2:e38.
108. Pillai G, Davies G, Denti P, Steimer J-L, McIlleron H, Zvada S, et al. Pharmacometrics: Opportunity for Reducing Disease Burden in the Developing World: The Case of Africa. CPT Pharmacometrics Syst. Pharmacol. 2013;2:e69.
109. Davies GR, Hope W, Khoo S. Opinion: The Pharmacometrics of Infectious Disease. CPT Pharmacometrics Syst. Pharmacol. 2013;2:e70.
110. Svensson EM, Acharya C, Clauson B, Dooley KE, Karlsson MO. Pharmacokinetic Interactions for Drugs with a Long Half-Life—Evidence for the Need of Model-Based Analysis. AAPS J. 2016;18:171–9.
111. European Medicines Agency (EMA). Reflection paper on extrapolation of efficacy and safety in paediatric medicine development. 2016.

Supplemental material

Table S1.1.1 Pubmed search protocol and corresponding results.

Disease	Search term	Search results	Studies included	No full text	Additional records
Chagas disease	Chagas disease OR trypanosomiasis OR American trypanosomiasis NOT African trypanosomiasis	67	6	0	0
Human African trypanosomiasis	Trypanosomiasis OR African trypanosomiasis OR sleeping sickness NOT American trypanosomiasis	74	7	1	4
Leishmaniasis	Leishmaniasi OR kala-azar	88	16	0	0
Buruli ulcer	Buruli ulcer OR Bairnsdale ulcer OR Searls ulcer OR Daintree ulcer OR Mycobacterium ulcerans	3	1	0	0
Leprosy	Leprosy OR Hansen disease	45	11	2	0
Trachoma	Trachoma OR granular conjunctivitis OR Egyptian ophthalmia	3	1	0	1
Yaws	Endemic treponematoses OR yaws OR framboesia OR pian OR endemic syphilis OR bejel OR pinta	3	0	0	0
Cysticercosis/Taeniasis	Taeniasis OR cysticercosis	16	7	2	0
Dracunculiasis	Dracunculiasis OR guinea-worm disease	0	0	0	0
Echinococcosis	Echinococcosis	16	2	0	1
Foodborne trematodiases	Food-borne trematod* OR foodborne trematod* OR clonorchiasis OR fascioliasis OR opisthorchiasis OR paragonimiasis	20	4	1	0
Lymphatic filariasis	Lymphatic filariasis OR elephantiasis	9	2	0	1
Onchocerciasis	Onchocerciasis OR river blindness OR Robles disease	16	9	0	0
Schistosomiasis	Schistosomiasis OR bilharzia OR snail fever OR katayama fever	39	6	1	0
Soil-transmitted helminthiases	Soil-transmitted helminth* OR geohelminths OR ascariasis OR hookworm disease OR trichuriasis	6	0	0	0
Dengue, chikungunya, and zika	Dengue OR chikungunya OR zika	21	0	0	0
Rabies	Rabies	5	3	0	0
Total		431	75	6	7

All search terms were used in combination with "pharmacokinetics[Title/Abstract] OR pharmacokinetic[Title/abstract]", and restricted to title and abstract.

Chapter 1.2

Influence of malnutrition on the pharmacokinetics of
drugs used in the treatment of poverty-related diseases:
A systematic review

Luka Verrest, Erica A. Wilthagen, Jos H. Beijnen,
Alwin D. R. Huitema, Thomas P. C. Dorlo

Abstract

Objectives: Patients affected by poverty-related infectious diseases (PRDs) are disproportionally affected by malnutrition. To optimize treatment of patients affected by PRDs, we aimed to assess the influence of malnutrition associated with PRDs on drug pharmacokinetics by a systematic review.

Methods: A systematic review was performed of the effects of malnourishment on the pharmacokinetics of drugs to treat PRDs, including HIV, TB, malaria, and neglected tropical diseases.

Results: In 21/29 of PRD drugs included in this review, pharmacokinetics was affected by malnutrition. Effects were heterogeneous, but trends were observed for specific classes of drugs and different types and degrees of malnutrition. Bioavailability of lumefantrine, sulfadoxine, pyrimethamine, lopinavir, and efavirenz was decreased in severely malnourished patients, but increased for P-glycoprotein substrates abacavir, saquinavir, nevirapine, and ivermectin. Distribution volume was decreased for lipophilic drugs isoniazid, chloroquine, and nevirapine, and for α1-acid glycoprotein-bound drugs quinine, rifabutin, and saquinavir. Distribution volume was increased for the hydrophilic drug streptomycin and albumin-bound drugs rifampicin, lopinavir, and efavirenz. Drug elimination was decreased for isoniazid, chloroquine, quinine, zidovudine, saquinavir, and streptomycin, but increased for the albumin-bound drugs quinine, chloroquine, rifampicin, lopinavir, efavirenz, and ethambutol. Clinically relevant effects were observed mainly in severely malnourished and kwashiorkor patients.

Conclusions: Malnutrition-related effects on pharmacokinetics potentially affect treatment response, particularly for severe malnutrition or kwashiorkor. However, pharmacokinetic knowledge is lacking for specific populations, especially patients with neglected tropical diseases and severe malnutrition. To optimize treatment in these neglected subpopulations, adequate pharmacokinetic studies are needed, including severely malnourished or kwashiorkor patients.

Key points
- Malnutrition leads to physiological alterations which affect drug pharmacokinetics.
- Patients affected by poverty-related diseases are a highly vulnerable population, requiring optimal and individualized drug treatment.
- This systematic review highlights the key findings of pharmacokinetic drug alterations by malnutrition, for specific drug classes and patient populations.
- This overview can be used as a basis to predict the effects of malnutrition on the drug pharmacokinetics of poverty-related infectious diseases.

1. Introduction

Malnutrition, defined here as lack of protein and/or calorie intake, is a major public health problem, especially in low-income countries where malnutrition is associated with about 50% of the 10.8 million deaths per year in children under five[1-4]. Because of poor hygienic conditions and a lack of access to healthcare, a large proportion of this population is affected by poverty-related infectious diseases (PRDs), including HIV, TB, malaria, and neglected tropical diseases (NTDs) as defined by the World Health Organization (WHO)[5]. To illustrate, 42% of African children[6] and 43% of Ethiopian adults[7] with HIV were affected by malnutrition. Similarly, 57% of Ethiopian TB patients[8] and 75% of Sudanese children affected by malaria[9] were malnourished. The association between malnutrition and PRDs is bi-directional, where on the one hand malnutrition increases the susceptibility to infections as a result of secondary immune deficiency, and on the other hand, infections can add to development of malnutrition because of the increased need of anabolic energy by the prolonged activated immune system, and because of complications such as chronic diarrhoea, cachexia, and anaemia[10-12]. An association between NTDs and underweight was found in African children under five[13], and similarly, a negative correlation between malaria parasite density and malnutrition was found in Cameroonian children[14].

Malnutrition can manifest in various forms, depending on the type and severity of protein and calorie deficiency. Kwashiorkor is predominantly characterized by protein deficiency and comes with different clinical signs, including oedema, fatty liver, and anaemia. Marasmus reflects an overall deficiency of energy, mainly characterized by muscular wasting and loss of subcutaneous fat. Although there is still no consensus about the clinical definition of these phenotypes, the differences in biological features have been well described[15]. In children, stunting is usually a result of long-term nutritional deprivation, causing gut mucosal changes and altered levels of drug-metabolizing enzymes, whereas wasting is an acute condition, characterized by insufficient food intake or a high incidence of infectious diseases, and is associated with fatty liver but also an impaired functioning of the immune system[16,17].

The different pathophysiological conditions in malnutrition can alter the pharmacokinetics of drugs. Gastrointestinal changes include hypochlorhydria, delayed gastrointestinal emptying time, increased or decreased intestinal transit time, gastric and mucosal atrophy and dysfunction, gastrointestinal inflammation, and pancreatic insufficiency[18-20]. Besides, in the enterocytes, P-glycoprotein activity is decreased and tight junctions are enlarged, influencing the uptake of nutrients and drugs[21]. Total body water is increased, and adipose mass and lean body mass is reduced especially in children with marasmus and marasmic-kwashiorkor[20], and kwashiorkor is associated with the presence of oedema[22]. Also, hypoproteinaemia is a common feature of

malnutrition[20]. Hypoalbuminemia is more severe in kwashiorkor than marasmus, and is associated with malnutrition combined with infectious or non-infectious inflammation, likely caused by the increased capillary permeability in inflammation, and a higher albumin degradation rate in the liver[23]. The synthesis of acute-phase proteins such as α1-acid glycoprotein is often increased in malnutrition, although this is related to the inflammation caused by infections, which often accompanies malnutrition[24-26]. In the liver, the basal metabolic rate is reduced with impaired synthesis of protein, and fat accumulation occurs, particularly in kwashiorkor[19]. In severe protein energy malnutrition or kwashiorkor, glomerular filtration rate (GFR) and renal blood flow are diminished, particularly in the presence of dehydration[20], and tubular excretion and reabsorption might be impaired[18]. These physiological alterations can alter the pharmacokinetics of drugs in different ways, which can lead to either reduced treatment efficacy in case of sub-therapeutic drug levels, or toxicity in case of overdosing.

An understanding of the effect of different types of malnutrition on pharmacokinetic processes is needed to characterise drug exposure in all patients affected by PRDs, and to improve treatment and dosing guidelines in this vulnerable population. A previous general review found heterogeneous effects of protein-energy malnutrition on pharmacokinetics in children and concluded that studies should take into account the differential effects of different forms of malnutrition on drug pharmacokinetics[27]. To provide a complete and systematic overview of the influence of malnutrition on PRD drug pharmacokinetics, we performed a systematic review of published literature on this topic. We aimed to characterise the effects of different types of malnutrition on different pharmacokinetic processes, if mentioned by the included studies - the potential clinical relevance and whether dose recommendations are necessary for malnourished PRD patients, and to identify gaps of knowledge in specific populations.

2. Methods

2.1 Search strategy

A systematic literature review was performed by a medical information specialist according to the PRISMA guidelines[28]. A full literature search was performed on 19 October 2020 in MEDLINE (PubMed), Embase (OVID), and SCOPUS. Publications were searched on a combination of three following free-text words and related standardized keywords (MeSH and Emtree terms): Malnutrition, PRDs, and pharmacokinetics. Malnutrition is defined as protein-energy malnutrition (PEM), including kwashiorkor and marasmus. PRDs include HIV, TB, malaria, and NTDs as defined by WHO [5]. NTDs include Buruli ulcer, Chagas disease, Dengue and Chikungunya, Dracunculiasis (guinea-worm disease), Echinococcosis, Foodborne trematodiases, Human African

trypanosomiasis (sleeping sickness), Leishmaniasis, Leprosy (Hansen's disease), Lymphatic filariasis, Mycetoma, chromoblastomycosis and other deep mycoses, Onchocerciasis (river blindness), Rabies, Scabies and other ectoparasites, Schistosomiasis, Soil-transmitted helminthiases, Snakebite envenoming, Taeniasis/Cysticercosis, Trachoma, Yaws (Endemic treponematoses), and Zika. Pharmacokinetics include any parameters describing drug exposure, bioavailability, absorption, distribution, protein binding, clearance, or elimination half-life. No limits were applied for date, study design or language. The full search strategy is shown in table S1.2.1 in the supplemental material. Duplicate articles were removed according to the method of Bramer *et al.*[29].

2.2   Study selection

Studies were screened and included by two independent reviewers (LV and TD) through each phase of the review. Rayyan QCRI[30] was used to screen references on title and abstract. Studies were included when the studied population included malnourished patients at risk for or affected by one or more PRDs as well as non-malnourished patients or healthy volunteers. Although the scope of this review is to compare pharmacokinetics between malnourished and well-nourished infected patients, studies including non-infected patients or healthy individuals as controls were also included here due to overall scarcity of studies with infected patients as controls. Secondly, studies were included when the pharmacokinetics of drugs intended to treat PRDs in both populations was reported. Studies were excluded when one or more of these criteria were not met. Other exclusion criteria were missing abstract or full-text, non-clinical research, and wrong publication type (i.e., case reports, reviews or any article not reporting original research). The reviewers resolved discrepancies by consensus. Secondary sources were identified through the reference lists of the included studies.

2.3   Data extraction

Information from the included studies was extracted and summarized, including PRDs, PRD drugs used for pharmacokinetic analysis, route of administration of these drugs, number of patients, type of malnourished patients, classification of malnutrition as defined by the original study, definition of the control group, patient age range, and country. The methodology of pharmacokinetic analysis was reported, including 1) non-compartmental analysis when concentration time points were compared, C_{max} and T_{max} were derived by visual inspection of the data, AUC was calculated by the trapezoidal rule, and/or $T_{1/2}$ was derived by linear regression of the last data points, and 2) compartmental analysis, including a standard two-stage approach or population approach. Collected pharmacokinetic parameters for exposure included AUC, concentration on different time points after treatment (C_t), C_{max}, and C_{trough}; drug absorption was characterized by bioavailability; drug absorption rate by T_{max},

absorption rate constant, and absorption lag time; drug distribution by apparent central or peripheral volume of distribution and apparent inter-compartmental clearance; drug clearance by apparent clearance , elimination half-life, and elimination rate constant; drug metabolism by drug/metabolite ratio; and protein binding by free fraction in plasma, maximum enzyme binding rate, and drug concentration where enzyme achieves half Vmax. Results were summarized as the change in any of the pharmacokinetic parameters in the malnourished population compared to those of a non-malnourished control population.

2.4   Summary and interpretation of the results

In order to summarize the findings and interpret the results of the heterogeneous studies, a selection of the main findings was summarized by the reviewers according to the different pharmacokinetic processes (absorption, distribution, metabolism, and elimination). The main findings were summarized per studied drug, and the effects on pharmacokinetics were attempted to relate to mechanistic explanations based on explanations by the original studies or based on other relevant literature. This includes the type and severity of malnutrition, as well as specific drug characteristics (e.g., lipophilicity, P-glycoprotein binding, plasma protein binding, route of elimination). Malnutrition was considered severe when the original study defined patients as severely malnourished or severely wasted, or when patients had a Z-score for any of the used body size/mass descriptors of ≤-3. Other definitions of malnutrition were considered as moderate malnutrition. The different pathophysiological processes in malnutrition associated with pharmacokinetic changes observed for specific drugs were summarized, and when observed for a specific type of malnutrition, this was specified. In the summarizing figure, the effects on pharmacokinetics were categorized as weak or strong by the reviewers, based on the level of evidence. The evidence for the effect was considered strong when identified by multiple studies, or when the quality of the results of the original study was high (i.e., when the difference between patients and controls was adequately assessed, when pharmacokinetic parameters were adequately and precisely identified). The evidence for the effect was considered weak when the study design to identify an effect was considered poor, when the definition of the malnourished patient and control group was unclear, when the effect was statistically nonsignificant, when contradicting effects were found by different studies, or when other studies could not replicate the results.

3.   Results and discussion

3.1   Publications

The systematic search yielded 1929 abstracts after deduplication (Figure 1.2.1). Screening of the abstracts left 44 publications for inclusion. Five additional publications

—

were identified through reference screening of the included publications. In total, 49 publications were included in this review. The studies were mainly conducted in TB patients (24), HIV patients (12), and malaria patients (11). Only two studies were conducted in patients with a NTD, which were helminthiasis caused by Trichuris trichiura and visceral leishmaniasis.

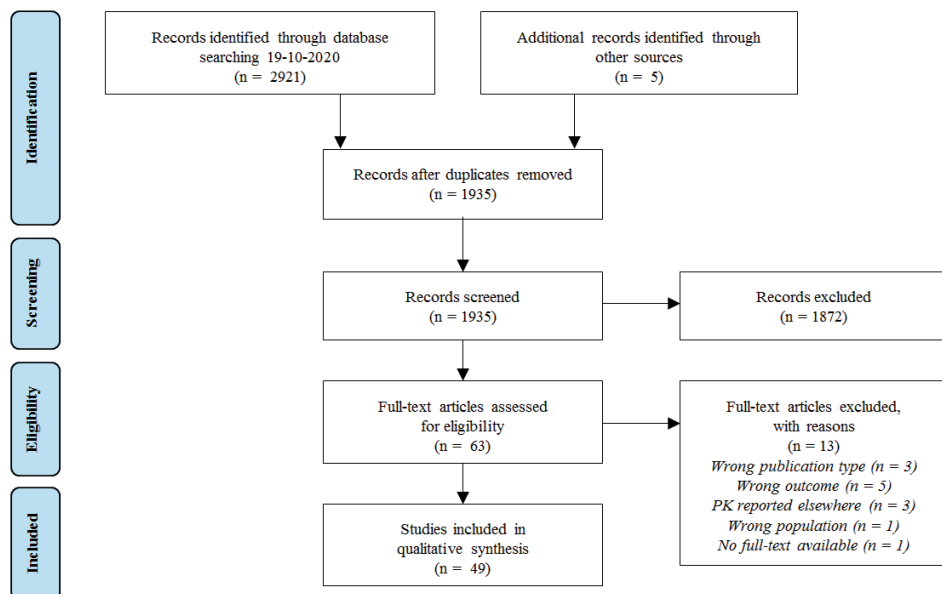**Figure 1.2.1** PRISMA Flow Diagram.

3.2   Study population and methodology

Overall, the majority of studies was conducted in children (19/24 in TB, 8/12 in HIV, 9/11 in malaria, and 2/2 in NTDs) (Table 1.2.1). All studies were performed in malnourished patients with well-nourished patients or well-nourished noninfected volunteers as control subjects. In 2/24 TB studies[31,32] and 2/12 HIV studies[33,34], the same patients served as control after nutritional rehabilitation. Malnourished patients had different degrees and forms of malnutrition (moderately or severely malnourished, underweight, wasted, stunted, marasmus, or kwashiorkor), measured by different metrics (see Section 3.3). Pharmacokinetic analysis was mostly performed by non-compartmental analysis (20/24 studies in TB, 6/12 in HIV, 7/11 in malaria, and 1/2 in NTDs) (Table 1.2.2)

Table 1.2.1a Overview of included studies in TB patients.

Author (year) (ref)	Drug	Route of administration	Total number of patients	Malnourished patients (n)	Control group (n)[a]	Classification malnutrition	Age (years)[b]	Country
Buchanan et al. (1979)[31]	Isoniazid	i.v.	7	Kwashiorkor (7)	Same patients after 21 days (7)	Wellcome classification	1.53±0.79	Pakistan
Polasa et al. (1984)[59]	Rifampicin	p.o.	28	Uninfected volunteers (8)	Well-nourished uninfected volunteers (10)	AI <0.18	49	India
	Rifampicin	p.o.		Patients on rifampicin therapy (10)				
Prasad et al. (1978)[75]	Streptomycin	i.m.	34	(15)	(6)	AI <0.18	(25-35)	India
Bolme et al. (1988)[54]	Streptomycin	i.m.	56	Underweight (6); marasmic (6); kwashiorkor (3)	(4)	Wellcome classification	4.9 (0.5-12)	Ethiopia
	Streptomycin	i.m.		Underweight (11); marasmic (12); kwashiorkor (5)	(9)			
Eriksson et al. (1988)[c67]	Isoniazid	p.o.	41	Underweight (9); marasmic (15); kwashiorkor (6)	(11)	Wellcome classification	(0.5-12)	Ethiopia
Garg et al. (1988)[65]	Isoniazid	p.o.	63	Malnourished (10)	(13)	AI <0.18	45 ± 5.2 (40-50)	India
	Rifampicin	p.o.		Malnourished (10)	(11)			
	Isoniazid and rifampicin	p.o.		Malnourished (10)	(9)			
Seth et al. (1992)[d18]	Rifampicin	p.o.	115	Undernourished (30); malnourished (10)	(15)	Grade I and II: undernourished; grade III and IV: malnourished	Children	India
	Isoniazid	p.o.		Undernourished (30); malnourished (10)	(20)			
Seifart et al. (1995)[32]	Isoniazid	p.o.	13	PEM (no marasmus or kwashiorkor) (13), mean MUAC 135 mm	Same patients after 6 months (13), mean MUAC 150 mm	Weight, weight-for-age, and MUAC scores	2.3 (0.8-7.6)	South Africa

Table 1.2.1a (continued)

Author (year) (ref)	Drug	Route of administration	Total number of patients	Malnourished patients (n)	Control group (n)[a]	Classification malnutrition	Age (years)[b]	Country
Graham et al. (2006)[88]	Pyrazinamide	p.o.	34	Undernourished (12); marasmic (9)	(6)	Wellcome classification	5.6	Malawi
McIlleron et al. (2009)[82]	Ethambutol Isoniazid	p.o. p.o.	56	Undernourished (3); marasmic (1) Kwashiorkor (NA)	(3) (NA)	Clinical diagnosis and presence of edema	3.22 (0.25-13)	South Africa
Roy et al. (2010)[66]	Isoniazid	p.o.	20	Moderately malnourished (NA)	(NA)	WAZ <-2 and >-3	(5-12)	India
Verhagen et al. (2012)[78]	Isoniazid, rifampicin, and pyrazinamide	p.o.	30	Malnourished patients (4)	(26)	<5 years of age: WAZ or HAZ <-2; >5 years of age: BAZ <-2	(1-15)	Venezuela
Ramachandran et al. (2013)[77]	Isoniazid, rifampicin, and pyrazinamide	p.o.	84	Stunting (22); underweight (31); wasting (16)	(NA)	WAZ, HAZ, or WHZ <-2	(1-12)	India
Garcia-Prats et al. (2015)[89]	Ofloxacin	p.o.	85	Underweight (14)	(71)	WAZ <-2	3.4 (IQR 1.9-5.2)	South Africa
Mukherjee et al. (2015)[90]	Isoniazid, rifampicin, pyrazinamide, and ethambutol	p.o.	127	Severely malnourished (32)	(32)	<5 years of age: weight for height <70%; >5 years of age: BMI for age <5th percentile	(0.5-15)	India
	Isoniazid, rifampicin, pyrazinamide, and ethambutol	p.o.		Severely malnourished (26)	(37)			
te Brake et al. (2015)[80]	Rifampicin	p.o.	36	Severely malnourished (7); malnourished (4)	(25)	Severely malnourished: BMI <16.0 kg/m²; malnourished: BMI <18.5 kg/m²	35 (18-55)	Indonesia
Thee et al. (2015)[87]	Moxifloxacin	p.o.	23	Underweight for age (3)	(20)	WAZ <-2	Median 11.1 (7-15)	South Africa
Antwi et al. (2017)[55]	Isoniazid, rifampicin, pyrazinamide, and ethambutol	p.o.	113	HIV co-infected patients (59), median WAZ -2.7, median HAZ -2.8	HIV uninfected patients (54), median WAZ -2.1, median HAZ -1.6	WAZ, HAZ, BAZ, MUAC and head circumference scores	Median 5.0 (IQR 2.2-8.3)	Ghana

1.2

Table 1.2.1a   (continued)

Author (year) (ref)	Drug	Route of administration	Total number of patients	Malnourished patients (n)	Control group (n)[a]	Classification malnutrition	Age (years)[b]	Country
Ramachandran et al. (2016)[83]	Isoniazid, rifampicin, and pyrazinamide	p.o.	161	NA	(NA)	NA[e]	(1-5)	India
Rogers et al. (2016)[79]	Isoniazid	p.o.	30	Underweight (7); stunted (4); wasted (9)	(NA)	WAZ, HAZ, or WHZ <-2	(0-10)	South Africa
Ramachandran et al. (2017)[84]	Isoniazid, rifampicin, and pyrazinamide	p.o.	1912	Patients (961)	(951)	Body weight <48	Median 38 (IQR 27-50)	India
Dayal et al. (2018)[86]	Isoniazid and pyrazinamide	p.o.	37	Severely wasted (11); underweight (19); stunted (15); severely malnourished (14)	(NA)	According WHO growth standards	(1-15)	India
Justine et al. (2018)[76]	Isoniazid, rifampicin, pyrazinamide, and ethambutol	p.o.	51	Malnourished (39)	(12)	WAZ, HAZ, or BAZ <-2	(0.75–14)	Tanzania
Kumar et al. (2018)[91]	Levofloxacin, pyrazinamide, ethionamide, cyclosporine	p.o.	25	Underweight (10); stunted (14)	Not underweight (11); not stunted (7)	WAZ or HAZ <-2	16 (5-18)	India

AI: anthropometric index; BAZ: BMI-for-age Z-score; HAZ: height-for-age Z-score; MUAC: mid-upper arm circumference; WAZ: weight-for-age Z-score; WHZ: weight-for-height Z-score; [a] Well-nourished patients, unless stated otherwise; [b] Mean ± SD (range), unless stated otherwise; [c] Streptomycin results reported by Bolme et al. (1988); [d] Original publication not traceable; [e] HAZ, WAZ, and WHZ scores were tested as factors influencing drug concentration.

1.2

Table 1.2.1b   Overview of included studies in HIV patients.

Author (year) [ref]	Drug	Route of administration	Total number of patients	Malnourished patients (n)	Control group (n)[a]	Classification malnutrition	Age (years)[b]	Country
Gatti et al. (1999)[60]	Rifabutin	p.o.	20	Wasting syndrome (10)	(10)	Weight loss >10% in the last year	Wasting syndrome: 35.3±6.0; controls: 37±7	Italy
Brantley et al. (2003)[44]	Stavudine, zidovudine, didanosine, and/or lamivudine	p.o.	19	Wasting and diarrhea (12)	(7)	Weight loss >10% in the last 2 months	32.8 (21 - 54)	Brazil
Trout et al. (2004)[49]	Saquinavir	p.o.	100	AIDS symptomatic patients with severe body weight loss and/or diarrhea (33)	Asymptomatic patients (30); AIDS symptomatic patients (37)	Weight loss >10% in the last month	40 ± 10	France
Ellis et al. (2007)[50]	Nevirapine	p.o.	127	Stunting and wasting (NA)	(NA)	Stunting based on height-for-age, wasting based on BMI-for-age	(0.67 - 18)	Malawi and Zambia
Pollock et al. (2009)[92]	Nevirapine	p.o.	37	Mild to moderate malnutrition (12)	(25)	Weight-for-height 75%-85% of median	4.4 (0.7-16.0)	Malawi
Swaminathan et al. (2011)[17]	Nevirapine	p.o.	88	Underweight (51), stunted (55)	Not underweight (37), not stunted (33)	Underweight: WAZ <-2; stunting: HAZ <-2	6.5 (0.5-12)	India
Bartelink et al. (2014)[81]	Lopinavir and ritonavir	p.o.	116	Underweight (42)	(160)	BMI<18.5[c]	30.5 (18–49)	Uganda
	Efavirenz	p.o.	105					
Fillekes et al. (2014)[68]	Zidovudine	p.o.	45	Moderate wasting (NA) and stunting (NA)	(NA)	Na[d]	3.4 (IQR 2.6–6.2)	Uganda
Vreeman et al. (2014)[53]	Nevirapine	p.o.	21	Malnourished (NA)	(NA)	Na[e]	5.4 (3-13)	Kenya

Table 1.2.1b (continued)

Author (year) [ref]	Drug	Route of administration	Total number of patients	Malnourished patients (n)	Control group (n)[a]	Classification malnutrition	Age (years)[b]	Country
Bartelink et al. (2015)[48]	Efavirenz	p.o.	163	Ugandan children (32) (44% malnourished)	Dutch children (52) (10% underweight)	WAZ, HAZ, or BAZ <-2	(0.7-7)	Uganda
	Lopinavir	p.o.		Ugandan children (83) (47% malnourished)	French children (56) (14% underweight)			
	Nevirapine	p.o.		Ugandan children (48) (50% malnourished)	American children (96) (14% malnourished)			
Archary et al. (2018)[33]	Lopinavir	p.o.	63	Severe acute malnutrition (34)	Patients after nutritional recovery (29) (WHZ ≥-2, >15% weight gain, or resolution of edema and return of appetite)	WHZ <-3, MUAC <115mm, or peripheral edema	0.9 (0.1-3.9)	South Africa
Archary et al. (2019)[34]	Abacavir and lamivudine	p.o.	75	Severe acute malnutrition (36)	Patients after nutritional recovery (39) (WHZ ≥-2, >15% weight gain, or resolution of edema and return of appetite)	WHZ <-3, MUAC <115mm, or peripheral edema	(0.08-12)	South Africa

BMI: body mass index; BAZ: MBI-for-age Z-score; GWG: gestational weight gain; HAZ: height-for-age Z-score; HFIAS: household food insecurity access scale; HHS: household hunger scale; MUAC: Mid-Upper Arm Circumference; TBW%: total body water percentage; WAZ: weight-for-age Z-score; WHZ: weight-for-height Z-score. [a] Well-nourished patients, unless stated otherwise; [b] Mean ± SD (range), unless stated otherwise; [c] BMI, GWG, MUAC, HFIAS, and HHS scores were tested as factors influencing drug concentration; [d] Weight-for-age and height-for-age scores were tested as factors influencing drug concentration; [e] MUAC, WAZ scores, and TBW% were tested as factors influencing PK parameters.

1.2

Table 1.2.1c Overview of included studies in malaria patients

Author (year) [ref]	Drug	Route of administration	Total number of patients	Malnourished patients (n)	Control group (n)[a]	Classification malnutrition	Age (years)[b]	Country
Wharton et al. (1970)[69]	Chloroquine	p.o.	13	Kwashiorkor uninfected children (10)	Well-nourished uninfected children (3); kwashiorkor children after 2-3 weeks recovery (7)	NA	Children	Uganda
Tulpule et al. (1983)[74]	Chloroquine	p.o.	15	Undernourished uninfected subjects (8)	Well-nourished uninfected subjects (7)	AI <0.18	(25 - 40)	India
Walker et al. (1987)[70]	Chloroquine	p.o.	11	Kwashiorkor uninfected subjects (5)	Well-nourished uninfected subjects (6)	Wellcome classification	2.5 (2 - 3.5)	Nigeria
Salako et al. (1989)[72]	Quinine	p.o.	13	Kwashiorkor uninfected subjects (6)	Well-nourished uninfected subjects (7)	Universally accepted clinical grounds	2.2 ± 0.6 (1.5 - 3)	Nigeria
Treluyer et al. (1996)[26]	Quinine	i.m.	15	Undernourished patients (8)	Well-nourished patients (7)	MUAC/head circumference ratio <0.28	(0.75 - 5)	Gabon
Pussard et al. (1999)[58]	Quinine	i.v.	40	Malnourished uninfected subjects (10); malnourished patients (10)	Well-nourished uninfected subjects (10)	At least 2/3 measures (WAZ, HAZ, and WHZ) <-2	(2 - 6)	Niger
Dua et al. (2002)[71]	Chloroquine	p.o.	22	Malnourished tribal uninfected volunteers (6); Malnourished tribal patients (6)	Healthy volunteers (AI > 0.2) (5); Non-tribal patients (AI > 0.2) (5)	AI <0.18	Mean 29 - 34	India
WWARN (2015)[93]	Artemether-lumefantrine	p.o.	567	Underweight patients <3 yrs (28); Underweight patients 3-4 yrs (48)	Well-nourished patients <3 yrs (262); Well-nourished patients 3-4 yrs (229)	WAZ <-2	3 (1 - 4)	Africa and Asia
Kadam et al. (2016)[52]	Chloroquine	p.o.	25	PEM (13)	(12)	IAP classification	(5 - 12)	India
de Kock et al. (2018) [46]	Sulfadoxine and pyrimethamine	p.o.	383	Malnourished (41)	(326)	-3 ≤ WAZ <-2; WAZ <-3	(0.25 - 4.9)	Africa
Chotsiri et al. (2019)[47]	Artemether-lumefantrine	p.o.	263	Severely malnourished (16); SAM (131)	Non-SAM (160)	WHZ <-3 or MUAC <115 cm	(0.5 - 4.9)	Mali and Niger

AI: anthropometric index; IAP: Indian Academy of Pediatrics; MUAC: mid-upper arm circumference; HAZ: height-for-age Z-score; PEM: protein-energy malnutrition; SAM: severe acute malnutrition; WAZ: weight-for-age Z-score; WHZ: weight-for-height Z-score. [a] Well-nourished patients, unless stated otherwise; [b] Mean ± SD (range), unless stated otherwise.

Table 1.2.1d Overview of included studies in NTD patients

Author (year) (ref)	Disease	Drug	Route of administration	Total number of patients	Malnourished patients (n)	Control group (n)	Classification malnutrition	Age (years)[a]	Country
Schulz et al. (2019)[51]	Helminthiasis	Ivermectin	p.o.	80	(NA)	Well-nourished patients (NA)	NA[b] (Total BMI: mean 15 (range 12 - 24))	(2 - 5)	Ivory Coast
	Helminthiasis	Ivermectin	p.o.	120	(NA)	Well-nourished patients (NA)	NA[b] (Total BMI: mean 16 (range 12 - 25))	(6 - 12)	Ivory Coast
Palić et al. (2020)[94]	Visceral leishmaniasis	Miltefosine	p.o.	51	(NA)	Well-nourished patients (NA)	BAZ, WHZ, or HAZ <-2	(4 – 12)	Kenya, Sudan, Uganda

BAZ: BMI-for-age Z-score; BMI: body mass index; HAZ: height-for-age Z-score; WAZ: weight-for-age Z-score; WHZ: weight-for-age Z-score. [a] Range; [b] The correlation between BMI and PK parameters was investigated.

3.3   Classification of malnutrition

The classification of malnutrition in the included studies was very heterogeneous. In the majority of studies, Z-score was used to classify the degree of malnutrition (Table 1.2.1), i.e., the difference in terms of standard deviations from a median nutritional status reference value as defined e.g. by the NCHS/WHO Growth Standards[35-38]. A Z-score ≤-2 and >-3 was considered as moderate malnutrition, a score ≤ -3 as severe malnutrition. In children, the weight-for-age Z-score (WAZ), height-for-age Z-score (HAZ), and weight-for-height Z-score (WHZ) were used to define the degree of underweight, stunting, or wasting, respectively. In children over 5 years of age, adolescents, and adults, the HAZ, BMI-for-age Z-score (BAZ), and BMI were generally used as a nutritional status metric[37]. Severe malnutrition in children was further categorized as marasmus (absence of oedema) or kwashiorkor (presence of oedema)[39]. Other used metrics for classification in children were 1) the Wellcome Classification[40], based on the percentage of expected weight for age (WFA): >80% WFA was graded as normal, 60 to 80% WFA as undernutrition, <60% WFA as marasmus, and low WFA in combination with oedema and low serum protein as kwashiorkor; or 2) The Indian Academy of Pediatrics classification of PEM based on Khadilkar's growth charts[41]. Measurements included height, weight, head circumference, and penile length (≤3 years of age); weight, height, BMI, penile length, and standard metabolic rate (4-8 years of age); weight, BMI, and standard metabolic rate (9-18 years of age); or 3) the left mid-upper arm circumference (MUAC)[42]. For adults, the anthropometric index (AI)[43] was used, defined as (weight(kg)/height(cm)2)*100, where an AI <0.18 was considered as malnutrition.

3.4   Effect of malnutrition on pharmacokinetics

A complete overview of the effects of malnutrition on the various pharmacokinetic processes is presented in Table 1.2.2. If possible, the effects were related to the type and severity of malnutrition or specific drug characteristics in the subsections below. The main findings with mechanistic explanations are summarized in Figure 1.2.2.

1.2

Table 1.2.2a Pharmacokinetic results of TB studies

Drug	Absorption	Exposure	Distribution	Elimination	PK methodology	Reference
Isoniazid			V_d/F decreased	Cl/F decreased*; $T_{1/2}$ increased*	NCA	Buchanan (1979)[31]
		AUC and C_{max} unchanged		$T_{1/2}$ increased	NCA	Eriksson (1988)[67]
		AUC_{0-inf} unchanged		$T_{1/2}$ increased	NCA	Garg (1988)[65]
	T_{max} unchanged	AUC and C_{max} increased		$T_{1/2}$ increased; k_e decreased	NA	Seth (1992)[18]
		C_{2h} unchanged		$T_{1/2}$ and k_e unchanged	NCA	Seifart (1995)[32]
		C_{max} unchanged			NCA	McIlleron (2009)[82]
	T_{max} unchanged	AUC_{0-24} and AUC increased; C_{max} unchanged	V_d/F unchanged	Cl/F decreased; $T_{1/2}$ and k_e unchanged	CA	Roy (2010)[66]
		AUC_{0-24} unchanged			NCA	Verhagen (2012)[78]
		AUC_{0-8} and C_{max} decreased in stunting*			NCA	Ramachandran (2013)[77]
	T_{max} unchanged	AUC_{0-4}, C_{2h}, and C_{max} unchanged			NCA	Mukherjee (2015)[90]
	T_{max} decreased*	AUC_{0-8} and C_{max} unchanged	Normalized V_d/F unchanged	Normalized Cl/F unchanged	NCA	Antwi (2017)[55]
		AUC_{0-8} decreased with low WAZ; C_{max} decreased with low HAZ			NCA	Ramachandran (2016)[83]
		C_{2h} decreased*	V_{max} and K_m unchanged	k_e unchanged	CA	Rogers (2016)[79]
		AUC_{0-8} and C_{max} unchanged			NCA	Ramachandran (2017)[84]
		C_{2h} decreased*			NCA	Dayal (2018)[86]
					NCA	Justine (2018)[76]
Rifampicin		AUC_{0-inf} and C_{max} decreased*	Plasma protein binding decreased*	Cl/F and Cl_r increased*, $T_{1/2}$ unchanged	NCA	Polasa (1984)[59]
		AUC_{0-inf} increased			NCA	Garg (1988)[65]
	T_{max} unchanged	AUC and C_{max} increased		$T_{1/2}$ unchanged	NA	Seth (1992)[18]
		AUC_{0-24} unchanged		$T_{1/2}$ and k_e unchanged	NCA	Verhagen (2012)[78]
		AUC_{0-8} and C_{max} decreased in stunting* and underweight*			NCA	Ramachandran (2013)[77]
	T_{max} unchanged	AUC_{0-4}, C_{2h}, and C_{max} unchanged	V_d/F and f_{free} unchanged	Cl/F and $T_{1/2}$ unchanged	NCA	Mukherjee (2015)[90]
	T_{max} unchanged	AUC_{0-24} and C_{max} unchanged			NCA	te Brake (2015)[80]
	T_{max} unchanged	AUC_{0-8} and C_{max} decreased*	Normalized V_d/F unchanged	Normalized Cl/F increased*	NCA	Antwi (2017)[55]
		AUC_{0-8} and C_{max} unchanged			NCA	Ramachandran (2016)[83]
		C_{2h} unchanged			NCA	Ramachandran (2017)[84]
		C_{2h} decreased*			NCA	Justine (2018)[76]

1.2

Table 1.2.2a (continued)

Drug	Absorption	Exposure	Distribution	Elimination	PK methodology	Reference
Pyrazinamide	T_{max} unchanged	AUC_{0-24} and C_{max} decreased; $AUC_{0-24}/dose$ and $C_{max}/dose$ unchanged			NCA	Graham (2006)[88]
		AUC_{0-24} decreased			NCA	Verhagen (2012)[78]
		AUC_{0-8} and C_{max} decreased in stunting* and underweight*			NCA	Ramachandran (2013)[77]
	T_{max} unchanged	AUC_{0-4}, C_{2h}, and C_{max} unchanged			NCA	Mukherjee (2015)[90]
	T_{max} decreased*	AUC_{0-8} decreased*; C_{max} unchanged	Normalized V_d/F unchanged	Normalized Cl/F increased*	NCA	Antwi (2017)[55]
		AUC_{0-8} and C_{max} unchanged			NCA	Ramachandran (2016)[83]
		C_{2h} decreased*			NCA	Ramachandran (2017)[84]
		AUC_{0-8} decreased in severe wasting*, stunting*, and severe malnutrition*; C_{max} decreased in severe malnutrition*			NCA	Dayal (2018)[86]
		C_{2h} unchanged			NCA	Justine (2018)[76]
		AUC_{0-8} unchanged; C_{max} decreased in underweight*			NCA	Kumar (2018)[91]
Ethambutol	T_{max} decreased	AUC_{0-24} and $AUC_{0-24}/dose$ unchanged; C_{max} and $C_{max}/dose$ increased			NCA	Graham (2006)[88]
	T_{max} unchanged	AUC_{0-4}, C_{2h}, and C_{max} unchanged			NCA	Mukherjee (2015)[90]
	T_{max} unchanged	AUC_{0-8} and C_{max} decreased*	Normalized V_d/F increased*	Normalized Cl/F increased*	NCA	Antwi (2017)[55]
		C_{2h} unchanged			NCA	Justine (2018)[76]
Streptomycin	$T_{1/2,abs}$ unchanged		V_d/F increased in kwashiorkor*	Cl/F unchanged; $T_{1/2,el}$ increased in kwashiorkor*	CA	Bolme (1988)[54]
	T_{max} increased	Concentrations unchanged	V_d/F and plasma protein binding unchanged	$T_{1/2}$ unchanged	NCA	Prasad et al. (1978)[75]
Ofloxacin	T_{max} unchanged	AUC_{0-8}, AUC_{0-24}, and C_{max} unchanged	V_d/F unchanged	Cl/F and $T_{1/2}$ unchanged	NCA	Garcia-Prats (2015)[89]
Moxifloxacin	T_{max} unchanged	AUC_{0-8} decreased*; C_{max} unchanged			NCA	Thee (2015)[87]
Levofloxacin		AUC_{0-8} and C_{max} unchanged			NCA	Kumar (2018)[91]
Ethionamide		AUC_{0-8} and C_{max} unchanged			NCA	Kumar (2018)[91]
Cyclosporine		AUC_{0-8} and C_{max} unchanged			NCA	Kumar (2018)[91]

AUC: area under the curve; C_{2h}: concentration at 2 hrs; CA: compartmental analysis; Cl/F: apparent oral clearance; Cl_r: renal clearance; C_{max}: peak concentration; f_{free}: unbound fraction; HAZ: height-for-age Z-score; k_e: elimination rate constant; K_m: drug concentration where enzyme achieves half V_{max}; NA: not available; NCA: non-compartmental analysis; $T_{1/2,abs}$: absorption half-life; $T_{1/2,el}$: elimination half-life; $T_{1/2}$: terminal half-life; T_{max}: time to maximum plasma concentration; V_d/F: apparent volume of distribution; V_{max}: maximum enzyme binding rate; WAZ: weight-for-age Z-score. * significant difference.

Table 1.2.2b   Pharmacokinetic results of HIV studies

Drug	Absorption	Exposure	Distribution	Elimination	PK methodology	Reference
Rifabutin	T_{max} decreased	AUC unchanged; C_{max} increased*, C_{24h} increased*	V_d/F decreased; V_d/F/kg decreased	Cl/F unchanged; Cl/F/kg unchanged; $T_{1/2}$ decreased	NCA	Gatti et al. (1999)[60]
Stavudine		C_{max} decreased*			NCA	Brantley et al. (2003)[44]
Didanosine		C_{max} decreased			NCA	Brantley et al. (2003)[44]
Lamivudine		C_{max} unchanged			NCA	Brantley et al. (2003)[44]
	k_a unchanged		V_d/F unchanged	Cl/F unchanged	CA	Archary et al. (2019)[34]
Abacavir	k_a unchanged, F increased*		V_d/F unchanged; Q/F unchanged; V_p/F unchanged	Cl/F unchanged	CA	Archary et al. (2019)[34]
Saquinavir	T_{lag} decreased*; k_a decreased*; T_{max} unchanged	AUC increased*; C_{max} increased*	V/F decreased*	Cl/F decreased*; ke decreased*	CA	Trout et al. (2004)[49]
Nevirapine		C_{max} increased in wasting*, C_{max} decreased in stunting*			NCA	Ellis et al. (2007)[50]
		AUC_{0-12}, C_{max} and C_{trough} unchanged			NCA	Pollock et al. (2009)[92]
		C_{2h} decreased in stunting*; C_{trough} unchanged			NCA	Swaminathan et al. (2011)[17]
	k_a unchanged		V_d/F decreased with increasing TBW%	Cl/F unchanged	CA	Vreeman et al. (2014)[53]
	F increased*		V_d/F decreased*	Cl/F decreased*	CA	Bartelink et al. (2015)[48]
Lopinavir	F unchanged			Cl/F unchanged	CA	Bartelink et al. (2014)[81]
	F decreased*		V_d/F increased*	Cl/F increased*	CA	Bartelink et al. (2015)[48]
	k_a unchanged	C_{max} decreased	V_d/F unchanged	Cl/F unchanged	CA	Archary et al. (2018)[33]
Efavirenz	F unchanged			Cl/F unchanged	CA	Bartelink et al. (2014)[81]
	F decreased*		V_d/F increased*	Cl/F increased*	CA	Bartelink et al. (2015)[48]
Ritonavir	F unchanged			Cl/F unchanged	CA	Bartelink et al. (2014)[81]
Zidovudine		C_{max} unchanged			NCA	Brantley et al. (2003)[44]
		AUC_{0-12} increased in wasting*, C_{max} and C_{12h} unchanged		Cl/F decreased in wasting*, $T_{1/2}$ unchanged	NCA	Fillekes et al. (2014)[68]

AUC: area under the curve; C_{12h}: concentration at 12 hrs; C_{24h}: concentration at 24 hrs; CA: compartmental analysis; Cl_r: renal clearance; C_{max}: peak concentration; Cl/F: apparent oral clearance; F: apparent bioavailability; k_e: elimination rate constant; NCA: non-compartmental analysis; Q/F: apparent intercompartmental clearance; $T_{1/2}$: terminal half-life; T_{lag}: absorption lag time; V_d/F: central volume of distribution; V_d/F: volume of distribution; V_p/F: peripheral volume of distribution. * significant difference.

Table 1.2.2c Pharmacokinetic results of malaria studies.

Drug	Absorption	Exposure	Distribution	Metabolism	Elimination	PK methodology	Reference
Chloroquine				Drug/metabolite ratio increased*		NCA	Wharton et al. (1970)[69]
		AUC unchanged			Cl/F increased*, $T_{1/2}$ unchanged	NCA	Tulpule et al. (1983)[74]
	T_{max} increased	AUC decreased*		Drug/metabolite ratio increased	$T_{1/2}$ unchanged	NCA	Walker et al. (1987)[70]
		AUC_{0-168h}, AUC_{0-inf}, and C_{max} unchanged		Drug/metabolite ratio increased	Cl/F unchanged; $T_{1/2}$ unchanged	NCA	Dua et al. (2002)[71]
		AUC_{0-inf} increased; C_{max} unchanged	V_d/F decreased	Drug/metabolite ratio unchanged	Cl/F decreased; $T_{1/2}$ unchanged	NCA	Kadam et al. (2016)[52]
Quinine	$T_{1/2,abs}$ increased*	AUC increased*; C_{max} decreased*			Cl/F decreased*, $T_{1/2}$ increased*	CA	Salako et al. (1989)[72]
	T_{max} decreased*	C_{max} unchanged; C_{12h} decreased	V_d/F and plasma protein binding unchanged	Drug/metabolite ratio decreased*	Cl/F increased*, $T_{1/2}$ decreased*	NCA	Treluyer et al. (1996)[26]
		AUC_{0-8} and C_{max} increased*	V_d/F decreased*, plasma protein binding increased*, erythrocyte binding unchanged		Cl/F decreased*, $T_{1/2}$ increased*	CA	Pussard et al. (1999)[58]
Lumefantrine		C^a decreased in children <3 years of age				NCA	WWARN (2015)[93]
Sulfadoxine	F decreased*					CA	Chotsiri et al. (2019)[47]
	F decreased*					CA	de Kock et al. (2018)[46]
Pyrimethamine	F decreased*					CA	de Kock et al. (2018)[46]

AUC: area under the curve; C_{12h}: concentration at 12 hrs; CA: compartmental analysis; Cl/F: apparent oral clearance; C_{max}: peak concentration; F: apparent bioavailability; k_e: elimination rate constant; NCA: non-compartmental analysis; $T_{1/2,abs}$: apparent absorption half-life; $T_{1/2}$: terminal half-life; V_d/F: volume of distribution. a Day 7 concentrations at different time points; * significant difference.

Table 1.2.2d Pharmacokinetic results of NTD studies.

Drug	Absorption	Exposure	Distribution	Excretion	PK methodology	Reference
Ivermectin		AUC increased*			NCA	Schulz et al. (2019)[51]
Miltefosine	F and k_a unchanged		V_c/F, Q/F, and V_p/F unchanged	Cl/F unchanged	CA	Palić et al. (2020)[94]

AUC: area under the curve; Cl/F: apparent oral clearance; F: apparent bioavailability; k_a: absorption rate constant; NCA: non-compartmental analysis; Q/F: apparent intercompartmental clearance; V_c/F: apparent central volume of distribution; V_d/F: apparent volume of distribution; V_p/F: apparent peripheral volume of distribution.

1.2

Absorption
↓ severe malnutrition
  lumefantrine, sulfadoxine, pyrimethamine
↓ moderate malnutrition
  lopinavir, efavirenz
↑ P-glycoprotein substrates, severe malnutrition
  (abacavir), (saquinavir), (ivermectin), (nevirapine)

- Loss of mucosal surface area
- Inflammation of the GI tract

- ↓ P-glycoprotein activity

- Impaired hepatic functioning

Hepatic elimination
↓ severe malnutrition
  (isoniazid), (chloroquine), zidovudine
↓ α1-acid glycoprotein-bound drugs,
  severe malnutrition
  (quinine), saquinavir
↑ albumin-bound drugs, marasmus
  and moderate malnutrition
  (quinine), (chloroquine), (rifampicin),
  lopinavir, efavirenz

Volume of distribution
↑ hydrophilic drugs, kwashiorkor
  streptomycin
↓ lipophilic drugs
  (isoniazid in kwashiorkor),
  (chloroquine), nevirapine

↑ albumin-bound drugs
  (rifampicin), lopinavir, efavirenz
↓ α1-acid glycoprotein-bound drugs
  quinine, (rifabutin), saquinavir

- Increased extracellular body water
- Decreased lean body mass

- ↓ albumin plasma levels
- ↑ α1-acid glycoprotein levels with infectious inflammation

- ↓ glomerular filtration rate

Renal elimination
↓ kwashiorkor
  streptomycin
↑ albumin-bound drugs
  (ethambutol)

Figure 1.2.2 Alterations in drug pharmacokinetics by malnutrition. Figure summarizes the main pathophysiological changes (left) and the associated effects on drug pharmacokinetics in different pharmacokinetic stages, illustrated by effects found for drugs against poverty-related infectious diseases (right). Drug names are mentioned when the evidence for the effect was considered strong, or mentioned in brackets when the evidence for the effect was considered weak.

3.4.1 Absorption

Drug absorption might be impaired because of loss of mucosal surface area and inflammation of the gastro-intestinal tract, often observed in patients with severe wasting and diarrhoea (Figure 1.2.2)[20,44,45]. Whereas a change in absorption rate might not be clinically relevant, an altered extent of absorption (bioavailability) might impact drug exposure and consequently drug effect. According to the studies included in this review, apparent bioavailability of lumefantrine, sulfadoxine, pyrimethamine, lopinavir, and efavirenz was decreased in severely malnourished patients[46-48]. On the other hand, apparent bioavailability of abacavir was increased in severe acute malnutrition[34], and increased exposure for saquinavir[49], nevirapine[50], and ivermectin[51] in severely wasted[49,50]/malnourished[51] patients was potentially caused by an increased absorption. As suggested by literature, the increased absorption of these drugs is likely due to decreased P-glycoprotein activity in the enterocytes or the enlargement of their tight junctions, enhancing paracellular passive uptake of the drug[21,49].

3.4.2 Distribution and protein binding

Severe malnutrition is associated with changes in body composition such as increased extracellular body water and decreased lean body mass, and presence of oedema in kwashiorkor, leading to decreased drug distribution of lipophilic drugs and increased distribution of hydrophilic drugs (Figure 1.2.2)[19,20]. This was demonstrated by various identified studies: volume of distribution was decreased for the lipophilic drugs isoniazid in kwashiorkor[31], and for chloroquine[52] and nevirapine[48,53] in malnutrition. Volume of distribution was increased for the hydrophilic drug streptomycin in kwashiorkor[54]. These effects seem to exhibit mainly in kwashiorkor, as the effects could not be demonstrated for isoniazid and streptomycin in moderate malnutrition[19,52,55].

Besides, distribution of highly protein-bound drugs with a high extraction ratio may be changed because of altered plasma protein levels (Figure 1.2.2)[19,20,56]. Basic drugs mainly bind to albumin, whereas acidic drugs mainly bind to α1-acid glycoprotein. Binding of drugs to α1-acid glycoprotein becomes pharmacologically relevant when the dissociation constant for α1-acid glycoprotein is <0.1 times lower compared to albumin[25]. Malnutrition in combination with infectious inflammation is associated with low serum albumin levels[23], but with increased inflammatory proteins such as α1-acid glycoprotein[57,58]. This was supported by some of the studies: protein binding for rifampicin was decreased[59], and volume of distribution for lopinavir and efavirenz was increased in malnourished patients[48], potentially causing increased drug elimination and resulting decreased drug exposure. The increased levels of α1-acid glycoprotein in malnutrition resulted in higher quinine plasma protein binding and increased exposure in malnourished patients[58]. For the weak bases rifabutin[60] and saquinavir[49], the decreased volume of distribution and resulting increased C_{max} in wasting[49,60] might also be a result of elevated α1-acid glycoprotein binding[61]. However, it should be noted that the increased levels of α1-acid glycoprotein in malnourished patients are a result of infections, often accompanied by malnutrition. The effect of malnutrition itself on α1-acid glycoprotein levels is not well investigated. Although it is believed that the humoral immune response is well preserved in malnourished patients during infection, some studies demonstrated an impaired acute-phase protein response in children with severe protein-energy malnutrition, especially in kwashiorkor[62]. This complicates the evaluation of α1-acid glycoprotein binding in relation to malnutrition.

3.4.3 Metabolism and excretion

Metabolism of hepatically cleared drugs may be altered in severe malnutrition, due to impaired hepatic functioning by fat infiltration of the liver and decreased synthesis and activity of certain phase I and II metabolizing enzymes[19,20,45,63,64]. Impaired glomerular filtration rate in severe malnutrition may impact the excretion of renally cleared drugs (Figure 1.2.2)[19,20]. Decreased elimination was observed for the hepatically cleared drugs isoniazid in kwashiorkor or different degrees of malnutrition[18,31,65-67], for saquinavir and

zidovudine in wasting[49,68], for chloroquine in kwashiorkor[69,70] and malnutrition[52,71], and for quinine in kwashiorkor[72] and severely malnourished patients[58]. An increased AUC and slower clearance of isoniazid in malnutrition is likely caused by reduced metabolism by acetylation, although the effect of malnutrition on the process of acetylation could not be clearly determined[73]. Saquinavir, zidovudine, chloroquine, and quinine metabolism is mainly driven by cytochrome P450 enzymes, whose activity is reduced in malnutrition[64]. Another reason for the decreased metabolism of e.g., quinine and saquinavir could be the increase of α1-acid glycoprotein levels in kwashiorkor and severe malnutrition, leading to a decrease of the unbound fraction and consequently lower hepatic uptake[26,58]. Likewise, the increased excretion of chloroquine[74], quinine[26], ethambutol[55], rifampicin[55,59], lopinavir[48], and efavirenz[48] in (moderate) malnutrition might be caused by the increased free fraction of these highly albumin-bound drugs. For the renally cleared drug streptomycin, excretion was decreased in kwashiorkor[54], but unchanged in malnutrition[75].

3.5   Type of malnutrition

The alterations in drug exposure likely depend on the patient population, as for some drugs relationships could be identified between the type or severity of malnutrition and the effect on drug exposure in these studies. For example, isoniazid and rifampicin exposure was decreased in moderately malnourished patients[59,76,77], potentially due to either reduced absorption or decreased protein binding and consequently an increased volume of distribution or elevated drug clearance[59]. On the other hand, isoniazid and rifampicin exposure was increased in severe malnutrition[18,65,66], potentially caused by a more pronounced suppression of enzyme activity in severe malnutrition[65]. On the other hand, chloroquine exposure was decreased in kwashiorkor, potentially caused by decreased bioavailability[70]. Nevirapine concentrations were decreased in stunted children but increased in wasted children[50]. This might be explained by the different pathophysiological conditions: the decreased absorption and enhanced clearance of protein-bound drugs associated with stunting might lead to decreased serum concentrations, whereas reduced metabolism in wasting might cause an increase in plasma concentration[17].

3.6   Study design and data analysis

The effects of malnutrition on PRD drug pharmacokinetics were not always replicable, which might be due to the underpowered study designs. The sample size was small (<50 participants) in the majority of studies, which can be the reason that a potentially expected effect could not be demonstrated in some of the studies[32,67,78-81]. The effect might not be traceable because of the small difference in malnutrition status between patient groups[32,55,76,78,79,81]. In other studies, the number of malnourished patients was unknown[82,83] or malnutrition was poorly diagnosed[84].

The studies included in this review include a heterogeneous patient population with a wide variety in source and severity of malnutrition, as well as different metrics used to define and score malnourished patients. In order to identify effects of malnutrition on pharmacokinetics, a standard and generic definition of the different types of malnutrition is needed to compare different studies. Moreover, the studied populations included patients of different age ranges and patients infected by different PRDs, different severity of disease, as well as non-infected subjects. Disease activity with increased inflammatory cytokine levels, local disease activity in the GI tract, and co-medications can all impact pharmacokinetics. Malnutrition may impact physiological processes differently in patients of different ages. All these sources of heterogeneity complicate the extraction of the effects of malnutrition on pharmacokinetics. Besides, the dosing guidelines might impact drug exposure in the different populations. When fixed dosing is applied, the dose per kg body weight will be higher in malnourished patients after fixed dosing, but even when using a linear weight-based dosing, exposure differences might be expected.

1.2

3.7   Conclusions and recommendations

Forty-nine studies were included in this review, with most of the studies conducted in TB, HIV, and malaria patients. For most of the NTDs, no studies were identified at all. In 21/29 of the PRD drugs included in this review, pharmacokinetics was affected by malnutrition. A complete overview of the literature is summarized in Table 1.2.1 and Table 1.2.2. The included studies were relatively small and heterogeneous. However, trends were observed for specific classes of drugs and types of malnutrition. An interpretation of the results by the reviewers is summarized in Figure 1.2.2, where the effects are categorized as strong or weak effects based on the level of evidence. Bioavailability of lumefantrine, sulfadoxine, pyrimethamine, lopinavir, and efavirenz was decreased in severely malnourished patients, but increased for the P-glycoprotein substrates abacavir, saquinavir, nevirapine, and ivermectin. Volume of distribution was decreased for the lipophilic drugs isoniazid, chloroquine, and nevirapine, and for the α1-acid glycoprotein-bound drugs quinine, rifabutin, and saquinavir. Volume of distribution was increased for the hydrophilic drug streptomycin, and for the albumin-bound drugs rifampicin, lopinavir, and efavirenz. Drug elimination was decreased in severe malnutrition for the hepatically cleared drugs isoniazid, chloroquine, quinine, zidovudine, and saquinavir, and for the renally cleared drug streptomycin. On the other hand, elimination was increased for the albumin-bound drugs quinine, chloroquine, rifampicin, lopinavir, efavirenz, and ethambutol.

The alterations in pharmacokinetics in malnourished patients might impact clinical efficacy and/or toxicity, and therefore may require dose adjustments in the malnourished population. A systematic review on antibiotics suggested that normal doses of penicillins, cotrimoxazole and gentamicin are safe in malnourished children,

while the dose or frequency of chloramphenicol requires adjustment, although evidence was not sufficiently strong to establish dosing recommendations[85]. These studies suggested a clinically relevant impact of malnutrition on the pharmacokinetics of certain PRD drugs. Various studies included in this systematic review addressed the need for dose adjustments in the malnourished population for isoniazid[18,67,76,77,83,84], rifampicin[55,76,77], pyrazinamide[55,77,84,86], ethionamide[55], moxifloxacin[87], stavudine[44], nevirapine[17], chloramphenicol[70], and ivermectin[51]. A specifically adapted treatment regimen in malnourished patients was only suggested for nevirapine[50] and quinine[26]. Other studies concluded that the identified effect on pharmacokinetics was of no clinical relevance, and no dose adjustment might be needed for rifampicin[59,65], rifabutin[60], chloramphenicol[52], quinine[58], and pyrimethamine[46]. These results imply a trend between the degree of malnutrition and the pharmacokinetic effect size: a clinically relevant effect was observed in severe malnutrition and kwashiorkor[18,50,67,70,86], except for quinine[58], whereas no dose adjustment was needed in mainly moderately malnourished patients. The clinical impact of these pharmacokinetic effects in severely malnourished patients is highly relevant as these patients are mostly excluded in clinical trials, whereas in reality these patients constitute a sizeable proportion of the PRD patient populations. This highlights the importance to include severely malnourished patients in pharmacokinetic studies for PRD drugs.

This systematic review summarizes the main effects of malnutrition on PRD drug pharmacokinetics, with potentially clinically relevant effects on treatment response. This overview can be used as a basis to predict the effects of malnutrition on PRD drug pharmacokinetics. This might be relevant for the study design of clinical studies, to account for possible clinically relevant effects of malnutrition on pharmacokinetics, based on the drug characteristics and types of malnutrition in the studied population.

Funding

References

1. Rice AL, Sacco L, Hyder A, Black RE. Malnutrition as an underlying cause of childhood deaths associated with infectious diseases in developing countries. Bull World Health Organ. 2000;78:1207–21.
2. Pelletier DL, Frongillo EA. Changes in child survival are strongly associated with changes in malnutrition in developing countries. J Nutr. 2003;133:107–19.
3. Black RE, Victora CG, Walker SP, Bhutta ZA, Christian P, De Onis M, et al. Maternal and child undernutrition and overweight in low-income and middle-income countries. Lancet. 2013;382:427–51.
4. Bryce J, Boschi-Pinto C, Shibuya K, Black RE. WHO estimates of the causes of death in children. Lancet. 2005;365:1147–52.
5. World Health Organisation. Neglected Tropical Diseases [Internet]. 2020 [cited 2020 Mar 25]. Available from: https://www.who.int/neglected_diseases/diseases/en/
6. Jesson J, Masson D, Adonon A, Tran C, Habarugira C, Zio R, et al. Prevalence of malnutrition among HIV-infected children in Central and West-African HIV-care programmes supported by the Growing Up Programme in 2011: A cross-sectional study. BMC Infect Dis. ???; 2015;15:1–12.
7. Gizaw A, Eshetu A, Birhanu D. Malnutrition and associated factors among adult people living with HIV/AIDS receiving antiretroviral therapy at Organization for Social Service Health Development in Jimma Town Oromia Region South West Ethiopia. Gen Med Open Access. 2018;06:4–11.
8. Feleke BE, Feleke TE, Biadglegne F. Nutritional status of tuberculosis patients, a comparative cross-sectional study. BMC Pulm Med. 2019;19:1–9.
9. Charchuk R, Houston S, Hawkes MT. Elevated prevalence of malnutrition and malaria among school-aged children and adolescents in war-ravaged South Sudan. Pathog Glob Health. 2015;109:395–400.
10. Schaible UE, Kaufmann SHE. Malnutrition and infection: Complex mechanisms and global impacts. PLoS Med. 2007;4:0806–12.
11. Walson JL, Berkley JA. The impact of malnutrition on childhood infections. Curr Opin Infect Dis. 2018;31:231–6.
12. Katona P, Katona-Apte J. The interaction between nutrition and infection. Clin Infect Dis. 2008;46:1582–8.
13. Hall A, Zhang Y, MacArthur C, Baker S. The role of nutrition in integrated programs to control neglected tropical diseases. BMC Med. BioMed Central Ltd; 2012;10:41.
14. Nkuo- Akenji T, Sumbele I, Mankah E, Njunda A, Samje M, Kamga L. The burden of malaria and malnutrition among children less than 14 years of age in a rural village of Cameroon. African J Food, Agric Nutr Dev. 2008;8:252–64.
15. Pham TPT, Alou MT, Golden MH, Million M, Raoult D. Difference between kwashiorkor and marasmus: Comparative meta-analysis of pathogenic characteristics and implications for treatment. Microb Pathog. Elsevier Ltd; 2021;150:104702.
16. World Health Organisation. Nutrition Landscape Information System (NLIS) country profile indicators: interpretation guide [Internet]. 2010. p. 1–51. Available from: https://apps.who.int/iris/bitstream/handle/10665/44397/9789241599955_eng.pdf?sequence=1&isAllowed=y
17. Swaminathan S, Ramachandran G, Kupparam HKA, Mahalingam V, Soundararajan L, Kannabiran BP, et al. Factors influencing plasma nevirapine levels: A study in HIV-infected children on generic antiretroviral treatment in India. J Antimicrob Chemother. 2011;66:1354–9.
18. Seth V, Beotra A, Bagga A, Seth S. Drug therapy in malnutrition. Indian Pediatr. 1992;29:1341–6.
19. Krishnaswamy K. Drug Metabolism and Pharmacokinetics in Malnourished Children. Clin Pharmacokinet. 1989;17:68–88.
20. Oshikoya KA, Senbanjo IO. Pathophysiological changes that affect drug disposition in protein-energy malnourished children. Nutr Metab. 2009;6:1–7.
21. Washington CB, Duran GE, Man MC, Sikic BI, Blaschke TF. Interaction of anti-HIV protease inhibitors with the multidrug transporter P-glycoprotein (P-gp) in human cultured cells. J Acquir immune Defic Syndr Hum retrovirology. United States; 1998;19:203–9.
22. Coulthard MG. Oedema in kwashiorkor is caused by hypoalbuminaemia. Paediatr Int Child Health. 2015;35:83–9.

23. Soeters PB, Wolfe RR, Shenkin A. Hypoalbuminemia: Pathogenesis and Clinical Significance. J Parenter Enter Nutr. 2019;43:181–93.

24. Morlese JF, Forrester T, Jahoor F. Acute-phase protein response to infection in severe malnutrition. Am J Physiol - Endocrinol Metab. 1998;275:3–8.

25. Smith SA, Waters NJ. Pharmacokinetic and Pharmacodynamic Considerations for Drugs Binding to Alpha-1-Acid Glycoprotein. Pharm Res. Pharmaceutical Research; 2019;36.

26. Treluyer J, Roux A, Mugnier C, Flouvat B, Lagardere B. Metabolism of Quinine in Children with Global Malnutrition. Pediatr Res. 1996;40:558–63.

27. Oshikoya KA, Sammons HM, Choonara I. A systematic review of pharmacokinetics studies in children with protein-energy malnutrition. Eur J Clin Pharmacol. 2010;66:1025–35.

28. Moher D, Shamseer L, Clarke M, Ghersi D, Liberati A, Petticrew M, et al. Preferred reporting items for systematic review and meta-analysis protocols (PRISMA-P) 2015 statement. Syst Rev. 2015;4:1–9.

29. Bramer WM, Giustini D, Jonge GB De, Holland L, Bekhuis T. De-duplication of database search results for systematic reviews in EndNote. J Med Libr Assoc. 2016;104:240–3.

30. Ouzzani M, Hammady H, Fedorowicz Z, Elmagarmid A. Rayyan-a web and mobile app for systematic reviews. Syst Rev. Systematic Reviews; 2016;5:1–10.

31. Buchanan N, Eyberg C, Davis MD. Isoniazid pharmacokinetics in kwashiorkor. South African Med J. 1979;56:299–300.

32. Seifart HI, Donald PR, De Villiers JN, Parkin DP, Jaarsveld PP, H.I. S, et al. Isoniazid elimination kinetics in children with protein-energy malnutrition treated for tuberculous meningitis with a four-component antimicrobial regimen. Ann Trop Paediatr. H.I. Seifart, Dept of Pharmacology, Faculty of Medicine, University of Stellenbosch, PO Box 19063, 7505 Tygerberg, South Africa; 1995;15:249–54.

33. Archary M, McLlleron H, Bobat R, Russa P La, Sibaya T, Wiesner L, et al. Population Pharmacokinetics of Lopinavir in Severely Malnourished HIV-infected Children and the Effect on Treatment Outcomes. Pediatr Infect Dis J. M. Archary, Department of Paediatrics and Children Health, King Edward VIII Hospital, Nelson R Mandela School of Medicine, 719 Umbilo Road, Durban, South Africa; 2018;37: 349-55.

34. Archary M, Mcllleron H, Bobat R, LaRussa P, Sibaya T, Wiesner L, et al. Population pharmacokinetics of abacavir and lamivudine in severely malnourished human immunodeficiency virus-infected children in relation to treatment outcomes. Br J Clin Pharmacol. 2019;85:2066–75.

35. World Health Organization. Management of severe malnutrition: a manual for physicians and other senior health workers [Internet]. 1999. Available from: https://apps.who.int/iris/bitstream/handle/10665/41999/a57361.pdf?sequence=1&isAllowed=y

36. World Health Organization. Department of Nutrition for Health and Development. WHO Child Growth Standards [Internet]. 2006. Available from: https://www.who.int/childgrowth/standards/Technical_report.pdf

37. de Onis M, Onyango AW, Borghi E, Siyam A, Nishida C, Siekmann J. Development of a WHO growth reference for school-aged children and adolescents. Bull World Health Organ. 2007;85:660–7.

38. Centers for Disease Control and Prevention. Growth Charts - 2000 CDC Growth Charts. CDC.gov. 2017 [Internet]. Available from: https://www.cdc.gov/growthcharts/clinical_charts.htm

39. Gernaat HBPE, Voorhoeve HWA. A new classification of acute protein-energy malnutrition. J Trop Pediatr. 2000;46:97–106.

40. Wellcome Trust Working Party. Classification of infantile malnutrition. Lancet. 1970;2:302–3.

41. Khadilkar V, Khadilkar A, Choudhury P, Agarwal K, Ugra D, Shah NK. IAP growth monitoring guidelines for children from birth to 18 years. Indian Pediatr. 2007;44:187–97.

42. Voorhoeve H. A new reference for the mid-upper arm circumference? J Trop Pediatr. 1990;36:256–62.

43. Rao KS, Mukherjee NR, Rao K V. A survey of diabetes mellitus in a rural population of India. Diabetes. 1972;21:1192–6.

44. Brantley RK, Williams KR, Silva TMJ, Sistrom M, Thielman NM, Ward H, et al. AIDS-associated diarrhea and wasting in Northeast Brazil is associated with subtherapeutic plasma levels of antiretroviral medications and with both bovine and human subtypes of Cryptosporidium parvum. Brazilian J Infect Dis. R.K. Brantley, Division of Geographic and International Medicine, Department of Internal Medicine, University of Virginia School of Medicine, Virginia 22908, USA.; 2003;7:16–22.

45. Mehta S. Malnutrition and drugs: Clinical implications. Dev Pharmacol Ther. 1990;15:159–65.

46. de Kock M, Tarning J, Workman L, Allen EN, Tekete MM, Djimde AA, et al. Population pharmacokinetic properties of sulfadoxine and pyrimethamine: A pooled analysis to inform optimal dosing in african children with uncomplicated malaria. Antimicrob Agents Chemother. P. Dentia, Worldwide Antimalarial Resistance Network (WWARN), Oxford, United Kingdom; 2018;62:1–16.

47. Chotsiri P, Denoeud-Ndam L, Baudin E, Guindo O, Diawara H, Attaher O, et al. Severe acute malnutrition results in lower lumefantrine exposure in children treated with artemether-lumefantrine for uncomplicated malaria. Clin Pharmacol Ther. 2019;106:1299–309.

48. Bartelink IH, Savic RM, Dorsey G, Ruel T, Gingrich D, Scherpbier HJ, et al. The effect of malnutrition on the pharmacokinetics and virologic outcomes of lopinavir, efavirenz and nevirapine in food insecure HIV-infected children in Tororo, Uganda. Pediatr Infect Dis J. 2015;34:e63–70.

49. Trout H, Mentré F, Panhard X, Kodjo A, Escaut L, Pernet P, et al. Enhanced saquinavir exposure in human immunodeficiency virus type 1-infected patients with diarrhea and/or wasting syndrome. Antimicrob Agents Chemother. 2004;48:538–45.

50. Ellis JC, L'homme RFA, Ewings FM, Mulenga V, Bell F, Chileshe R, et al. Nevirapine concentrations in HIV-infected children treated with divided fixed-dose combination antiretroviral tablets in Malawi and Zambia. Antivir Ther. 2007;12:253–60.

51. Schulz JD, Coulibaly JT, Schindler C, Wimmersberger D, Keiser J. Pharmacokinetics of ascending doses of ivermectin in Trichuris trichiura-infected children aged 2-12 years. J Antimicrob Chemother. 2019;74:1642–7.

52. Kadam P, Gogtay N, Karande S, Shah V, Thatte U. Evaluation of pharmacokinetics of single-dose chloroquine in malnourished children with malaria- a comparative study with normally nourished children. Indian J Pharmacol. N. Gogtay, Department of Clinical Pharmacology, Seth GS Medical College, KEM Hospital, Mumbai, Maharashtra, India; 2016;48:498–502.

53. Vreeman RC, Nyandiko WM, Liechty EA, Busakhala N, Bartelink IH, Savic RM, et al. Impact of adherence and anthropometric characteristics on nevirapine pharmacokinetics and exposure among HIV-infected Kenyan children. J Acquir Immune Defic Syndr. 2014;67:277–86.

54. Bolme R, Eriksson M, Habte D, Paalzow L. Pharmacokinetics of streptomycin in Ethiopian children with tuberculosis and of different nutritional status. J Clin Pharmacol. 1988;33:647–9.

55. Antwi S, Yang H, Enimil A, Sarfo AM, Gillani FS, Ansong D, et al. Pharmacokinetics of the first-line antituberculosis drugs in Ghanaian children with tuberculosis with or without HIV coinfection. Antimicrob Agents Chemother. 2017;61:1–8.

56. Heuberger J, Schmidt S, Derendorf H. When is protein binding important? J Pharm Sci. 2013;102: 3458-67.

57. Jagadeesan V, Krishnaswamy K. Drug binding in the undernourished: A study of the binding of propranolol to α1-acid glycoprotein. Eur J Clin Pharmacol. Food and Drug Toxicology Research Centre, National Institute of Nutrition, Indian Council of Medical Research, Jamai-Osmania, Hyderabad 500 007; 1985;27:657–9.

58. Pussard E, Barennes H, Daouda H, Clavier F, Sani AM, Osse M, et al. Quinine disposition in globally malnourished children with cerebral malaria. Clin Pharmacol Ther. 1999;65:500–10.

59. Polasa K, Murthy K, Krishnaswamy K. Rifampicin kinetics in undernutrition. Br J Clin Pharmacol. 1984;17:481–4.

60. Gatti G, Di Biagio A, De Pascalis CR, Guerra M, Bassetti M, Bassetti D. Pharmacokinetics of rifabutin in HIV-infected patients with or without wasting syndrome. Br J Clin Pharmacol. 1999;48:704–11.

61. Holladay JW, Dewey MJ, Michniak BB, Wiltshire H, Halberg DL, Weigl P, et al. Elevated alpha-1-acid glycoprotein reduces the volume of distribution and systemic clearance of saquinavir. Drug Metab Dispos. 2001;29:299–303.

62. Bresnahan KA, Tanumihardjo SA. Undernutrition, the Acute Phase Response to Infection, and Its Effects on Micronutrient Status Indicators. Adv Nutr. 2014;5:702–11.

63. Oshikoya KA, Senbanjo IO. Caution when treating tuberculosis in malnourished children. Arch Dis Child. 2018;103:1101–3.

64. Zhang W, Parentau H, Greenly RL, Metz CA, Aggarwal S, Wainer IW, et al. Effect of protein-calorie malnutrition on cytochromes P450 and glutathione S-transferase. Eur J Drug Metab Pharmacokinet. 1999;24:141–7.

1.2

65. Garg S, Dhand R, Malik S, Kalra S, Gupta P, Jha V, et al. Single dose kinetics of rifampicin and isoniazid in well-nourished and malnourished patients of tuberculosis. J Clin Pharmacol Ther Toxicol. 1988;26:417-20.

66. Roy V, Gupta D, Gupta P, Sethi GR, Mishra TK, V. R, et al. Pharmacokinetics of isoniazid in moderately malnourished children with tuberculosis. Int J Tuberc Lung Dis. V. Roy, Department of Pharmacology, Maulana Azad Medical College and Associated Hospitals, New Delhi 110002, India; 2010;14:374–6.

67. Eriksson M, Bolme P, Habte D, Paalzow L. INH and streptomycin in Ethiopian children with tuberculosis and different nutritional status. Acta Paediatr Scand. 1988;77:890–4.

68. Fillekes Q, Kendall L, Kitaka S, Mugyenyi P, Musoke P, Ndigendawani M, et al. Pharmacokinetics of zidovudine dosed twice daily according to world health organization weight bands in Ugandan HIV-infected children. Pediatr Infect Dis J. 2014;33:495–8.

69. Wharton BA, McChesney EW. Chloroquine metabolism in kwashiorkor. J Trop Pediatr. 1970;130–2.

70. Walker O, Dawodu A, Salako L, Alvan G, Johnson A. Single dose disposition of chloroquine in kwashiorkor and normal children-evidence for decreased absorption in kwashiorkor. Br J Clin Pharmacol. 1987;23:467–72.

71. Dua VK, Gupta NC, Kar PK, Edwards G, Singh N, Sharma VP. Pharmacokinetics of chloroquine in Indian tribal and non-tribal healthy volunteers and patients with Plasmodium falciparum malaria. Curr Sci. 2002;83:1128–31.

72. Salako L, Sowunmi A, Akinbami F. Pharmacokinetics of quinine in African children suffering from kwashiorkor. Br J Clin Pharmacol. 1989;28:197–201.

73. Mehta S. Drug Metabolism in the Malnourished Child. Malnourished Child. Nestle Nutr. Work. Ser. 1990. p. 329–38.

74. Tulpule A, Krishnaswamy K. Chloroquine Kinetics in the Undernourished. Eur J Clin Pharmacol. 1983;24:273–6.

75. Prasad J, Krishnaswamy K. Streptomycin pharmacokinetics in malnutrition. Chemotherapy. Nat. Inst. Nutrit., Indian Council Med. Res., Jamai-Osmania, Hyderabad; 1978;24:333–7.

76. Justine M, Yeconia A, Nicodemu I, Augustino D, Gratz J, Mduma E, et al. Pharmacokinetics of First-Line Drugs Among Children With Tuberculosis in Rural Tanzania. J Pediatric Infect Dis Soc. 2018;7–9.

77. Ramachandran G, Hemanth Kumar AK, Bhavani PK, Poorana Gangadevi N, Sekar L, Vijayasekaran D, et al. Age, nutritional status and INH acetylator status affect pharmacokinetics of anti-tuberculosis drugs in children. Int J Tuberc Lung Dis. 2013;17:800–6.

78. Verhagen LM, López D, Hermans PWM, Warris A, de Groot R, García JF, et al. Pharmacokinetics of anti-tuberculosis drugs in Venezuelan children younger than 16 years of age: Supportive evidence for the implementation of revised WHO dosing recommendations. Trop Med Int Heal. 2012;17:1449–56.

79. Rogers Z, Hiruy H, Pasipanodya JG, Mbowane C, Adamson J, Ngotho L, et al. The Non-Linear Child: Ontogeny, Isoniazid Concentration, and NAT2 Genotype Modulate Enzyme Reaction Kinetics and Metabolism. EBioMedicine. Forschungsgesellschaft für Arbeitsphysiologie und Arbeitschutz e.V.; 2016;11:118–26.

80. Te Brake LHM, Ruslami R, Later-Nijland H, Mooren F, Teulen M, Apriani L, et al. Exposure to total and protein-unbound rifampin is not affected by malnutrition in Indonesian tuberculosis patients. Antimicrob Agents Chemother. 2015;59:3233–9.

81. Bartelink IH, Savic RM, Mwesigwa J, Achan J, Clark T, Plenty A, et al. Pharmacokinetics of lopinavir/ritonavir and efavirenz in food insecure HIV-infected pregnant and breastfeeding women in Tororo, Uganda. J Clin Pharmacol. 2014;54:121–32.

82. McIlleron H, Willemse M, Werely CJ, Hussey GD, Schaaf HS, Smith PJ, et al. Isoniazid Plasma Concentrations in a Cohort of South African Children with Tuberculosis: Implications for International Pediatric Dosing Guidelines. Clin Infect Dis. 2009;48:1547–53.

83. Ramachandran G, Kumar AKH, Kannan T, Bhavani PK, Kumar SR, Gangadevi NP, et al. Low Serum Concentrations of Rifampicin and Pyrazinamide Associated with Poor Treatment Outcomes in Children with Tuberculosis Related to HIV Status. Pediatr Infect Dis J. 2016;35:530–4.

84. Ramachandran G, Kupparam HKA, Vedhachalam C, Thiruvengadam K, Rajagandhi V, Dusthackeer A, et al. Factors influencing tuberculosis treatment outcome in adult patients treated with thrice-weekly regimens in India. Antimicrob Agents Chemother. 2017;61:1–12.

85. Williams PCM, Berkley JA. Guidelines for the treatment of severe acute malnutrition: a systematic review of the evidence for antimicrobial therapy. Paediatr Int Child Health. P.C.M. Williams, Nuffield Department of Clinical Medicine, University of Oxford, Oxford, United Kingdom: Taylor & Francis; 2018;38:S32–49.

86. Dayal R, Singh Y, Agarwal D, Kumar M, Swaminathan S, Ramachandran G, et al. Pharmacokinetic study of isoniazid and pyrazinamide in children: Impact of age and nutritional status. Arch Dis Child. 2018;103:1150–4.

87. Thee S, Garcia-Prats AJ, Draper HR, McIlleron HM, Wiesner L, Castel S, et al. Pharmacokinetics and safety of moxifloxacin in children with multidrug-resistant tuberculosis. Clin Infect Dis. 2015;60:549–56.

88. Graham SM, Bell DJ, Nyirongo S, Hartkoorn R, Ward SA, Molyneux EM. Low levels of pyrazinamide and ethambutol in children with tuberculosis and impact of age, nutritional status, and human immunodeficiency virus infection. Antimicrob Agents Chemother. S.M. Graham, Malawi-Liverpool-Wellcome Trust Clinical Research Programme, P.O. Box 30096, Blantyre 3, Malawi; 2006;50:407–13.

89. Garcia-Prats AJ, Draper HR, Thee S, Dooley KE, McIlleron HM, Seddon JA, et al. Pharmacokinetics and safety of ofloxacin in children with drug-resistant tuberculosis. Antimicrob Agents Chemother. 2015;59:6073–9.

90. Mukherjee A, Velpandian T, Singla M, Kanhiya K, Kabra SK, Lodha R. Pharmacokinetics of isoniazid, rifampicin, pyrazinamide and ethambutol in Indian children. BMC Infect Dis. 2015;15:1–11.

91. Kumar AKH, Kumar A, Kannan T, Bhatia R, Agarwal D, Kumar S, et al. Pharmacokinetics of Second-Line Antituberculosis Drugs in Children with Multidrug-Resistant Tuberculosis in India. Antimicrob Agents Chemother. 2018;62:1–9.

92. Pollock L, Else L, Poerksen G, Molyneux E, Moons P, Walker S, et al. Pharmacokinetics of nevirapine in HIV-infected children with and without malnutrition receiving divided adult fixed-dose combination tablets. J Antimicrob Chemother. 2009;64:1251–9.

93. Worldwide Antimalarial Resistance Network (WWARN) Lumefantrine PK/PD Study Group. Artemether-lumefantrine treatment of uncomplicated Plasmodium falciparum malaria: a systematic review and meta-analysis of day 7 lumefantrine concentrations and therapeutic response using individual patient data. BMC Med. 2015;13:227.

94. alic S, Kip AE, Beijnen JH, Mbui J, Musa A, Solomos A, et al. Characterizing the non-linear pharmacokinetics of miltefosine in paediatric visceral leishmaniasis patients from Eastern Africa. J Antimicrob Chemother. 2020;75:3260–8.

1.2

Supplemental material

Table S1.2.1 PubMed search protocol

Search	Query	Items found
#4	Search #1 AND #2 AND #3	895
#3	Search "Pharmacokinetics"[Mesh] OR "pharmacokinetics"[Subheading] OR pharmacokinetic*[tiab] OR drug kinetic*[tiab] OR "volume of distribution"[tiab] OR Cmax[tiab] OR peak concentration*[tiab] OR peak time*[tiab] OR Tmax[tiab] OR AUC[tiab] OR "area under the curve"[tiab] OR T1/2[tiab] OR half life*[tiab] OR kinetic profile*[tiab] OR bioavailabilit*[tiab] OR biological availabilit*[tiab] OR biologic availabilit*[tiab] OR tissue distribution*[tiab] OR "protein binding"[tiab] OR "Absorption, Physiological"[Mesh] OR absorption[tiab] OR "Metabolic Clearance Rate"[Mesh] OR clearance[tiab] OR elimination[tiab] OR excretion[tiab] OR PK[tiab]	1214578
#2	Search "Chagas Disease"[Mesh] OR "Trypanosomiasis, African"[Mesh] OR chagas[tiab] OR trypanosomias*[tiab] OR ((trypanosoma[tiab] OR trypanosome[tiab]) AND (infection*[tiab] OR infected[tiab])) OR sleeping sickness*[tiab] OR "Leishmaniasis"[Mesh] OR leishmanias*[tiab] OR leishmanios*[tiab] OR "kala-azar"[tiab] OR (leishmania[tiab] AND (infection*[tiab] OR infected[tiab])) OR "Buruli Ulcer"[Mesh] OR buruli ulcer*[tiab] OR mycobacterium ulcer*[tiab] OR bairnsdale ulcer*[tiab] OR "buruli disease"[tiab] OR searls ulcer*[tiab] OR daintree ulcer*[tiab] OR mycoburuli ulcer*[tiab] OR "Leprosy"[Mesh] OR lepros*[tiab] OR Hansen disease*[tiab] OR hansens disease*[tiab] OR hansen's disease*[tiab] OR ((leprae[tiab] OR lepromatos*[tiab]) AND (infection*[tiab] OR infected[tiab])) OR "Trachoma"[Mesh] OR trachoma*[tiab] OR "egyptian opthalmia"[tiab] OR "granular conjunctivitis"[tiab] OR "chlamydia conjunctivitis"[tiab] OR "chlamydial conjunctivitis"[tiab] OR trachomatous trichias*[tiab] OR ("chlamydia trachomatis" [tiab] AND (infection*[tiab] OR infected[tiab])) OR "Yaws"[Mesh] OR yaws[tiab] OR frambesia*[tiab] OR framboesia*[tiab] OR parangi[tiab] OR pian[tiab] OR "treponema pertenue infection"[tiab] OR thymosis[tiab] OR "polypapilloma tropicum"[tiab] OR bouba[tiab] OR frambosie[tiab] OR "endemic treponematoses"[tiab] OR "endemic treponematosis"[tiab] OR "endemic syphilis"[tiab] OR bejel[tiab] OR "nonvenereal syphilis"[tiab] OR pinta[tiab] OR (("treponema pallidum pertenue" [tiab] OR "Treponema pallidum endemicum" [tiab] OR "Treponema carateum" [tiab]) AND (infection*[tiab] OR infected[tiab])) OR "Taeniasis"[Mesh] OR Taenias*[tiab] OR taenia infection*[tiab] OR Cysticercosis[tiab] OR Cysticercoses[tiab] OR neurocysticercosis[tiab] OR neurocysticercoses[tiab] OR (("Taenia solium" [tiab] OR "Taenia siginata"[tiab] OR "Taenia asiatica"[tiab]) AND (infection*[tiab] OR infected[tiab])) OR "Dracunculiasis"[Mesh] OR Dracunculias*[tiab] OR dracanculias*[tiab] OR drancunculias*[tiab] OR Guinea Worm Disease*[tiab] OR (("Guinea worm"[tiab] OR guineaworm[tiab]) AND (infection*[tiab] OR infected[tiab])) OR "Echinococcosis"[Mesh] OR Echinococcos*[tiab] OR echinococcis[tiab] OR echinococces[tiab] OR Hydatidos*[tiab] OR Hydatid[tiab] OR echinococcal[tiab] OR (echinococcus[tiab] AND (infection*[tiab] OR infected[tiab])) OR (("Foodborne Diseases"[Mesh] OR foodborne[tiab] OR food-borne[tiab] OR food poison*[tiab]) AND ("Trematode Infections"[Mesh:NoExp] OR trematode*[tiab] OR trematodo* OR Fasciolopsias*[tiab] OR Metagonimias*[tiab])) OR "Clonorchiasis"[Mesh] OR clonorchias*[tiab] OR (("clonorchis sinensis"[tiab]) AND (infection*[tiab] OR infected[tiab])) OR "Fascioliasis"[Mesh] OR fasciolias*[tiab] OR fasciolos*[tiab] OR fasciolas*[tiab] OR distomatos*[tiab] OR "liver rot"[tiab] OR (fasciola[tiab] AND (infection*[tiab] OR infected[tiab])) OR "Opisthorchiasis"[Mesh] OR opisthorchias*[tiab] OR (opisthorchis[tiab] OR (infection*[tiab] OR infected[tiab])) OR "Paragonimiasis"[Mesh] OR paragonimias*[tiab] OR ((paragonimus[tiab] OR "P. westermani"[tiab]) AND (infection*[tiab] OR infected[tiab])) OR "Elephantiasis, Filarial"[Mesh] OR lymphatic filarias*[tiab] OR (elephantias*[tiab] AND (filaria	2346136

Search	Query	Items found
	bancroft*[tiab])) OR filarial lymph*[tiab] OR "Bancroftian filarial"[tiab] OR wuchererias*[tiab] OR timor filaria*[tiab] OR malayan filaria*[tiab] OR brugias*[tiab] OR ((Brugia[tiab] OR Wuchereria[tiab] OR "W. bancrofti"[tiab]) AND (infection*[tiab] OR infected[tiab] OR elephantias*[tiab])) OR "Onchocerciasis"[Mesh] OR onchocercias*[tiab] OR onchocercos*[tiab] OR onchoceros*[tiab] OR "river blindness"[tiab] OR filarial blinding disease*[tiab] OR robles disease*[tiab] OR ((onchocerca[tiab] OR "O. volvulus"[tiab]) AND (infection*[tiab] OR infected[tiab])) OR "Schistosomiasis"[Mesh] OR schistosomias*[tiab] OR schistosomatos*[tiab] OR schistosomal[tiab] OR schistosomatic[tiab] OR "katayama fever"[tiab] OR bilharzia[tiab] OR neuroschistosomia*[tiab] OR "snail fever" [tiab] OR ((schistosome*[tiab] OR schistoma*[tiab] OR "blood fluke"[tiab] OR "blood flukes"[tiab]) AND (infection*[tiab] OR infected[tiab])) OR (("Helminthiasis"[Mesh] OR helminthias*[tiab]) AND ("Soil"[Mesh] OR STH[tiab] OR STHs[tiab] OR "soil transmitted"[tiab])) OR soil transmitted helminth*[tiab] OR geohelminth*[tiab] OR ascarias*[tiab] OR ascarios*[tiab] OR trichurias*[tiab] OR anchylostomias*[tiab] OR ancylostomias*[tiab] OR ankylostomias*[tiab] OR necatorias*[tiab] OR hookworm disease*[tiab] OR strongyloidias*[tiab] OR ((ascaris[tiab] OR "A. lumbricoides" [tiab] OR hookworm[tiab] OR "necator americanus"[tiab] OR "ancylostoma duodenale"[tiab] OR whipworm[tiab] OR trichuris[tiab] OR trichiura[tiab] OR trichiuris[tiab] OR trichocephal*[tiab] OR "strongyloides stercoralis" [tiab] OR "S. fulleborni"[tiab]) AND (infection*[tiab] OR infected[tiab])) OR "Dengue"[Mesh] OR dengue[tiab] OR dengues[tiab] OR breakbone fever*[tiab] OR break bone fever*[tiab] OR "Chikungunya Fever"[Mesh] OR chikungunya[tiab] OR "Zika Virus Infection"[Mesh] OR zika[tiab] OR ZikV[tiab] OR "Rabies"[Mesh] OR rabies[tiab] OR lyssa[tiab] OR lyssas[tiab] OR hydrophobia[tiab] OR hubert disease*[tiab] OR rabbia[tiab] OR neglected tropical disease*[tiab] OR "HIV Infections"[Mesh] OR HIV[tiab] OR "human immunodeficiency virus"[tiab] OR HTLV-III infection*[tiab] OR T-lymphotropic virus type III infection*[tiab] OR AIDS[tiab] OR "acquired immune deficiency syndrome"[tiab] OR "Tuberculosis"[Mesh] OR tuberculosis[tiab] OR tuberculoses[tiab] OR koch disease*[tiab] OR kochs disease*[tiab] OR koch's disease*[tiab] OR phthisis[tiab] OR "Malaria"[Mesh] OR malaria[tiab] OR "remittent fever"[tiab] OR paludism[tiab] OR "marsh fever"[tiab] OR "swamp fever"[tiab]) OR (plasmodium[tiab] AND (infection*[tiab] OR infected[tiab])) OR "Mycetoma"[Mesh] OR mycetoma*[tiab] OR eumycetoma*[tiab] OR maduromycos*[tiab] OR actinomycetoma*[tiab] OR "Chromoblastomycosis"[Mesh] OR chromoblastomycos*[tiab] OR chromomycos*[tiab] OR dermatitis verrucosa[tiab] OR verrucous dermatitis[tiab] OR cladosporios*[tiab] OR phaeosporotrichos*[tiab] OR (("fonsecaea pedrosoi"[tiab] OR "phialophora verrucosa"[tiab] OR "cladophialophora carrionii"[tiab] OR "fonsecaea compacta"[tiab]) AND (infection*[tiab] OR infected[tiab])) OR "Scabies"[Mesh] OR scabies[tiab] OR "sarcoptic manage"[tiab] OR ("sarcoptes scabiei"[tiab] AND (infection*[tiab] OR infected[tiab])) OR "Ectoparasitic Infestations"[Mesh] OR ectoparasitic infestation*[tiab] OR "Snake Bites"[Mesh] OR snake bite*[tiab] OR snakebite*[tiab] OR snake envenomation*[tiab]	
#1	Search "Malnutrition"[Mesh:NoExp] OR "Severe Acute Malnutrition"[Mesh] OR "Starvation"[Mesh] OR "Protein-Energy Malnutrition"[Mesh] OR malnutrition*[tiab] OR undernutrition*[tiab] OR "deficient nutrition"[tiab] OR malnourishment*[tiab] OR undernourishment*[tiab] OR underfeeding*[tiab] OR nutritional deficien*[tiab] OR marasmus[tiab] OR kwashiorkor[tiab] OR starvation*[tiab] OR famine*[tiab] OR stunting[tiab] OR wasting[tiab] OR underweight[tiab]	117061

1.2

Chapter 2

Pharmacokinetics of
paromomycin and miltefosine

Chapter 2.1

Geographical variability in paromomycin pharmacokinetics does not explain efficacy differences between Eastern African and Indian visceral leishmaniasis patients

Luka Verrest, Monique Wasunna, Gilbert Kokwaro, Rashid Aman, Ahmed M. Musa, Eltahir A. G. Khalil, Mahmoud Mudawi, Brima M. Younis, Asrat Hailu, Zewdu Hurissa, Workagegnehu Hailu, Samson Tesfaye, Eyasu Makonnen, Yalemtsehay Mekonnen, Alwin D. R. Huitema, Jos H. Beijnen, Smita A. Kshirsagar, Jaya Chakravarty, Madhukar Rai, Shyam Sundar, Fabiana Alves, Thomas P. C. Dorlo

Abstract

Introduction: Intramuscular paromomycin monotherapy to treat visceral leishmaniasis (VL) has been shown effective for Indian patients, while a similar regimen resulted in lower efficacy in Eastern Africa, which could be related to differences in paromomycin pharmacokinetics.

Methods: Pharmacokinetic data were available from two randomized controlled trials in VL patients from Eastern Africa and India. African patients received intramuscular paromomycin monotherapy (20 mg/kg for 21 days) or in a combination therapy (15 mg/kg for 17 days) with sodium stibogluconate. Indian patients received paromomycin monotherapy (15 mg/kg for 21 days). A population pharmacokinetic model was developed for paromomycin in Eastern African and Indian VL patients.

Results: 74 African patients (388 observations) and 528 Indian patients (1321 observations) were included in this pharmacokinetic analysis. A one-compartment model with first-order kinetics of absorption and elimination best described paromomycin in plasma. Bioavailability (RSE) was 1.17 (5.18%) times higher in Kenyan and Sudanese patients, and 2.46 (24.5%) times higher in Ethiopian patients, compared to Indian patients. Ethiopian patients had a ~4 times slower absorption rate constant of 0.446 h^{-1} (18.2%). $AUC_{0\text{-tau,SS}}$ for 15 mg/kg/day (median [IQR]) was higher in Kenya and Sudan (172.7 µg·h/mL [145.9-214.3]), and in Ethiopia (230.1 µg·h/mL [146.3-591.2]), compared to India (97.26 µg·h/mL [80.83-123.4]).

Conclusion: The developed model provides detailed insight in the pharmacokinetic differences among Eastern African countries and India, however the resulting differences in paromomycin exposure does not seem to explain the geographical differences in paromomycin efficacy in the treatment of VL patients.

Key points
- Intramuscular paromomycin is one of the recommended treatment options in regions where VL is endemic, although efficacy has been shown to be highly variable between geographical regions.
- To explore if the geographical differences in efficacy might be caused by variability in pharmacokinetics, the pharmacokinetics of paromomycin was investigated in Eastern African and Indian patients.
- Although paromomycin pharmacokinetics can most probably not explain the efficacy differences, remarkable differences in exposure were observed between VL patient populations, demonstrating the relevance of pharmacokinetic analysis in VL clinical trials globally.

1. Introduction

Over the past decades, substantial progress has been made in the treatment of visceral leishmaniasis (VL). Geographical differences in treatment efficacy have led to variable treatment recommendations for VL, with intramuscular paromomycin being one of the recommended treatment options in regions where VL is endemic. In South Asia, a 10 day combination of paromomycin and miltefosine is recommended as second-line treatment, while in Eastern Africa, a 17 day combination of paromomycin and sodium stibogluconate (SSG) is recommended by the WHO[1].

While paromomycin is affordable and has a reasonable safety profile compared to the conventional treatment of VL with antimonial compounds, efficacy of paromomycin monotherapy has been shown to be highly variable between geographical regions where VL is endemic. Intramuscular paromomycin sulfate ("paromomycin") as monotherapy in a dose of 15 mg/kg for 21 days was highly effective in Indian VL patients (final cure rate 94.6%), assessed 6 months after the end of treatment[2], but failed to show a similar efficacy in Eastern Africa. Within Eastern Africa, large geographical variability in efficacy of this treatment regimen has been observed with lowest efficacy in sites in Sudan (14.3% and 46.7%) compared to Kenya (80.0%), Northern Ethiopia (75.0%), and Southern Ethiopia (96.6%)[3]. A dose increase (20 mg/kg for 21 days) or longer treatment duration (15 mg/kg for 28 days) resulted in an improved but still insufficient paromomycin monotherapy efficacy in Sudan of 80% and 81%, respectively[4]. A combination therapy of 15 mg/kg paromomycin for 17 days plus SSG showed an adequate efficacy of 91.4% in Eastern Africa[5].

As variability in drug exposure might explain the geographical and regional differences in clinical efficacy of paromomycin monotherapy between India and Eastern Africa, but also within Eastern Africa, paromomycin pharmacokinetics should be investigated. In general, pharmacokinetic studies to optimize treatment of VL are lacking[6,7]. Likewise, little is known about the pharmacokinetics of paromomycin after intramuscular injection; a pharmacokinetic study in 15 healthy volunteers has been conducted[8], two clinical studies reported paromomycin plasma concentrations in 9 Sudanese[4] and 453 Indian VL patients[2]. Paromomycin is poorly absorbed after oral administration[9,10], however after intramuscular administration, absorption is fast with peak concentrations typically between one and two hours after administration[2,4,8], and bioavailability is expected to be nearly 100%[10]. Paromomycin is a hydrophilic compound with moderate plasma protein binding capacity of 33%[9] and limited distribution to tissues (~40% of body weight)[8,10], and is mainly excreted unchanged by glomerular filtration[9,10]. However, only 60.1% urine recovery has been reported after a 15 mg/kg paromomycin dose[8], suggesting that absorption might not be complete. Elimination of paromomycin is characterized by short half-life of 2-3 hours and no dose accumulation

has been observed with daily paromomycin dosing[8-10]. Whether there is variability in exposure between VL patients from different geographical regions following intramuscular paromomycin therapy is currently unknown.

To explore if the geographical differences in efficacy might be caused by variability in pharmacokinetics, the pharmacokinetics of paromomycin among Eastern African countries and India was investigated. To allow for analysis of sparse and heterogeneous data, a population approach was applied for pharmacokinetic modelling of paromomycin in Eastern African and Indian VL patients. A covariate analysis was performed to identify variables explaining the heterogeneity, including demographic differences and patient characteristics reflecting the patient's health status and renal function.

2. Methods

2.1 Study design and patients

Pharmacokinetic data were available from a subset of patients from two open label, multi-centre randomized controlled trials in VL patients in Eastern Africa[5] (NCT00255567) and India[2] (NCT00216346). Eastern African patients were enrolled at four clinical trial sites in Kassab, Sudan; Gondar, Northern Ethiopia; Arba Minch, Southern Ethiopia; Nairobi, Kenya. Indian patients were enrolled at four clinical trial sites in Bihar, India. Patients aged 4-60 years (Africa) or 5-55 years (India) with parasitologically confirmed VL were included. Patients with severe VL or co-morbidities, including HIV co-infection were excluded from the trials. In addition, patients less than 30 kg (Kenya and Sudan) or less than 7 years (Ethiopia) were excluded from the pharmacokinetic sub-study. Other inclusion and exclusion criteria have been described previously[2,3].

2.2 Study medication

Paromomycin solution, containing 375 mg paromomycin base (500 mg paromomycin sulfate) per milliliter, produced at Pharmamed Parenterals Ltd (PPL), Malta (Indian trial) or Gland Pharma, India (African trial), was administered intramuscularly into the gluteus muscle. A salt correction factor 0.7554 (India) or 0.733 (Africa) was used to convert the paromomycin sulfate dose to paromomycin base. Indian patients received paromomycin monotherapy (15 mg/kg paromomycin sulfate for 21 days). African patients received paromomycin monotherapy (20 mg/kg paromomycin sulfate for 21 days), or paromomycin plus SSG combination therapy (15 mg/kg paromomycin sulfate and 20 mg/kg SSG for 17 days).

2.3 Sample collection

Blood samples were drawn from patients in Sudan and Kenya according to an intensive schedule, with samples drawn before and 0.5, 1, 3, 6, 10, and 24 hours after treatment administration on the first and last day of treatment (day 21 in monotherapy arm, day 17 in combination arm). In Ethiopia, blood samples (3 per patients) were drawn according to a sparse schedule on days 7, 14, or 21 for the monotherapy arm and on days 7, 14, or 17 for the combination arm. In India, blood samples (3 per patient) were collected at pre-specified times over the course of the 21-day study for purposes of population modelling.

2.4 Bioanalysis

2.1

Plasma samples were analysed by high performance liquid chromatography coupled to UV detection (HPLC-UV) upon pre-column derivatization of paromomycin (Africa) or by liquid chromatography tandem mass spectrometry (LC/MS/MS) (India). A description of the assay and assay validation can be found in Supplementary Material 2.1.1.

2.5 Population pharmacokinetic analysis

To allow for analysis of sparse and heterogeneous data, a population approach was applied for pharmacokinetic modelling of paromomycin plasma concentrations. The population pharmacokinetic model was developed using a nonlinear mixed effects modelling approach (NONMEM, version 7.3, ICON Development Solutions, Ellicott City, MD, USA), using the first-order conditional estimation method with interaction (FOCE-I) and ADVAN13. Tools used to evaluate the model and visualize the data and model output were R (version 3.6.2), RStudio (version 1.2.5033; Boston, MA, USA), PsN (version 4.7.0), and the graphical interface Pirana (version 2.9.9). Model development and evaluation was performed in three steps: (1) selection of a structural and stochastic model; (2) selection of the covariate model; (3) internal model evaluation.

2.6 Structural and stochastic model development

During development of the structural pharmacokinetic model, one- and two-compartment models with first-order absorption and elimination were tested to fit paromomycin plasma concentration–time data. Different methods for handling below the limit of quantification (BLQ) were investigated: BLQ observations set to half the limit of quantitation, the M3 method, or excluding BLQ observations[11]. In the stochastic model, between-subject variability was modelled assuming a log-normal distribution (eq. 1). Residual variability was modelled using a proportional error model (eq. 2).

$$P_i = P_{pop} * e^{\eta_i} \qquad \text{Eq. 1}$$
$$Y_{i,j} = C_{i,j} * (1 + \varepsilon) \qquad \text{Eq. 2}$$

where P_{pop} is the population estimate for a parameter, P_i the individual (post-hoc) value for that parameter, and η_i the between-subject variability of the ith individual with mean zero and variance ω^2. $Y_{i,j}$ is the observed concentration and $C_{i,j}$ is the predicted concentration for the jth observation of the ith individual, and ε is the residual error with mean zero and variance σ^2. A separate residual variability was estimated for the two studies, as pharmacokinetic samples were processed and analysed differently.

2.7   Covariate model development

In the covariate model, time-varying body weight was included *a priori* with fixed allometric exponents of 0.75 for clearance, and 1.00 for volume of distribution[12]. Other covariates were tested on absorption rate constant, bioavailability, volume of distribution, and clearance. SSG comedication was evaluated as binary covariate to check for potential drug-drug interactions. Paromomycin dose level (15 versus 20 mg/kg/day) was evaluated as binary covariate to check for dose proportionality. Evaluated patient characteristics included baseline age, and time-varying serum creatinine, standardized glomerular filtration rate (GFR) for a typical body surface area (BSA) of 1.73 m^2, absolute GFR unadjusted to typical BSA (GRF$_{abs}$), and serum albumin. GFR was calculated according to the Modification of Diet in Renal Disease (MDRD) formula[13] (eq. 3).

$$GFR = 32788 * serum\ creatinine^{-1.154} * age^{-0.203} * (0.742\ if\ female) \quad \text{Eq. 3}$$

where GFR is expressed in mL/min/1.73 m^2, age in years, and serum creatinine in μmol/L. GFR$_{abs}$ was calculated by multiplying the original GFR with the individual BSA[14] (eq. 4–5).

$$GFR_{abs} = \frac{GFR}{1.73} * BSA \qquad \text{Eq. 4}$$

$$BSA = 0.20247 * height^{0.725} * weight^{0.425} \qquad \text{Eq. 5}$$

where BSA is expressed in m^2, height in m, and weight in kg. Serum creatinine and GFR may reflect renal function, which may impact clearance of the renally cleared drug paromomycin. VL patients are haematologically depleted[15] and the majority of the patients is malnourished. Serum albumin, which is usually decreased in VL patients, may be influenced by both processes and may represent the overall health status of the patient, possibly impacting paromomycin absorption, distribution, or clearance. Besides, time after start of treatment was tested as a covariate to assess whether pharmacokinetic parameters changed during treatment, *e.g.,* due to overall clinical improvement of the patient. To investigate geographical differences which were not explained by plausible physiological covariates, country and study sites were evaluated as covariates, *e.g.,* representing other unaccounted demographical differences or

study-specific procedures. Missing baseline covariates were handled by implementing the median value in the study population, or in case of time-varying covariates, using the last observation measured in that subject carried forward.

To assess covariate relations, post-hoc values and between-subject variability were plotted against covariates. Continuous covariates were tested in a linear, exponential, and power function (eq. 6–8):

$$P_{TV} = P_{pop} * (1 + (Cov_{i,t} - Cov_{med}) * l)$$ Eq. 6

$$P_{TV} = P_{pop} * e^{(Cov_{i,t} - Cov_{med}) * h}$$ Eq. 7

$$P_{TV} = P_{pop} * \left(\frac{Cov_{i,t}}{Cov_{med}}\right)^k$$ Eq. 8

2.1

where P_{pop} represents the population estimate of this parameter, P_{TV} the typical parameter value at covariate value $Cov_{i,t}$, $Cov_{i,t}$ the covariate value for the ith individual at time t, and Cov_{med} the median covariate value in the population. Cov_{med} was set to 0 for time. In the linear function (eq. 6), l represents the slope factor, and h and k represent the scaling factors in the exponential (eq. 7) an d power function (eq. 8). Clearance was also evaluated as fraction of GFR_{abs}, where renal clearance is assumed to be the only route of elimination. Categorical covariates were tested as proportional changes relative to the reference category.

2.8   Model selection and evaluation

The model selection was based on scientific plausibility, minimum objective function value (OFV), goodness-of-fit plots, and precision of parameter estimates. A decrease in OFV over 6.63 points between nested models was considered statistically significant, corresponding to P <0.01 following a chi-square distribution with 1 degree of freedom. The final population pharmacokinetic model was evaluated by goodness-of-fit (GoF) plots[16], a prediction-corrected visual predictive check (VPC)[17], and sampling-importance-resampling (SIR)[18]. SIR was used to derive the 95% confidence interval (CI) of the model parameters. Paromomycin exposure for the different countries was derived using the final individual pharmacokinetic model estimates, expressed by the area under the plasma concentration-time curve for 24 hours at steady-state ($AUC_{0-tau,ss}$) determined on the last day concentrations were measured.

3.   Results

3.1   Patients and data

Data from 74 African patients (388 observations) and 448 Indian patients (933 observations) were used for the pharmacokinetic analysis (Figure S2.1.1B in Supplementary Material 2.1.2, Table 2.1.1 and Table 2.1.2). Reliable serum creatinine levels were only available from patients in Kenya and Ethiopia, with baseline creatinine levels almost all within the normal range of 50-130 μmol/L (observed range 44.2-134 μmol/L, Table 2.1.1). As expected for VL patients, baseline albumin levels, which were available for all Kenyan, Ethiopian and Sudanese patients, were low (observed range 7-40 g/L, Table 2.1.1), but levels increased during treatment and follow-up (Figure S2.1.2 in ESM 2). Six observations from 3 subjects were excluded from this analysis because paromomycin concentrations were extremely high (*n*=3) or sampling time was missing (*n*=3). In both the African and Indian data, observations 24 hours after the last administered dose, right before the next dose, were highly variable and in some cases physiologically implausible, whereas observations at time of dosing were always BLQ (Figure S2.1.1A in Supplementary Material 2.1.2). Therefore, it was likely that these samples were collected after dosing and, therefore, all observations around time of dosing (time after dose (TAD) = 0 or 24 hours) were excluded from the analysis. In the final dataset, only 9 (2.3%) African and 34 (3.5%) Indian BLQ observations were present. Exclusion of BLQ observations did not lead to changes in model fit, and therefore, these observations were excluded from the pharmacokinetic analysis.
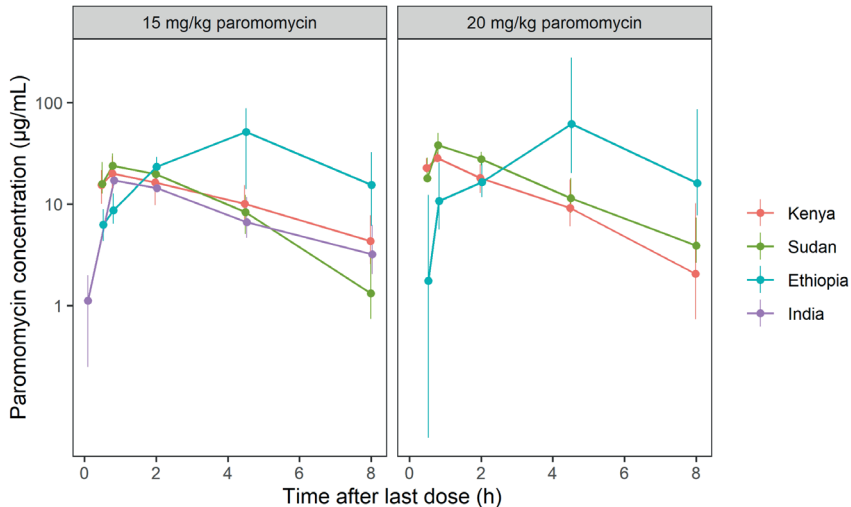
Figure 2.1.1 Paromomycin plasma concentrations (median and inter-quartile range) of all sampling days included in the pharmacokinetic analysis, stratified by country and paromomycin dose.

Table 2.1.1 Patient characteristics.

	Kenya	Sudan	Ethiopia	India	Total
Subjects (n)	16	16	42	454	528
Male (n (%))	13 (81)	13 (81)	34 (81)	296 (65)	356 (67)
Age (years)[a]	23.1 (15-45)	25.4 (12-40)	19.9 (8-60)	22.5 (5-54)	22.4 (5-60)
Paediatric patients[c] (n (%))	3 (19)	3 (19)	18 (43)	190 (42)	214 (41)
Body weight (kg)[b]	47.3 (37-56)	49.1 (34-73)	39.4 (15-62)	35.8 (11-68)	36.8 (11-73)
Creatinine[b] (μmol/L)	95.3 (79.6-134)	NA	79.5 (44.2-115)	NA	83.8 (44.2-134)
eGFR[b] (mL/min/1.73 m^2)	110 (62-147)	NA	143 (72.6-288)	NA	134.2 (62-288)
Albumin[b] (g/L)	23.8 (7-33)	27.4 (21-40)	28.0 (13-40)	NA	27.0 (7-40)

eGFR: estimated glomerular filtration rate. [a] Mean (range); [b] Mean (range) at baseline; [c] Patients <18 years old.

Table 2.1.2 Available pharmacokinetic observations.

	Kenya		Sudan		Ethiopia		India	
	PM	PM+SSG	PM	PM+SSG	PM	PM+SSG	PM	Total
Subjects (n)[a]	4	12	10	6	22	20	454	528
Observations (n)[a]	47	153	137	77	65	60	1333	1872
Observations BLQ (n (%))	14 (30)	32 (21)	32 (23)	23 (30)	6 (9)	4 (7)	277 (21)	388 (21)
Observations analysed (n (%))[b]	32 (68)	109 (71)	95 (69)	54 (70)	51 (78)	47 (78)	933 (70)	1321 (71)
Treatment duration	21	17	21	17	21	17	21	
Sampling days	1, 21	1, 17	1, 21	1, 17	7, 14, 21	7, 14, 17	1, 8, 15, 21	

PM: paromomycin; SSG: sodium stibogluconate; BLQ: below limit of quantification. [a] Subjects and observations after exclusion of unreliable data (6 observations from 5 subjects); [b] Observations after exclusion of T=0h and T=24h observations and BLQ observations.

3.2   Population pharmacokinetic model

A one-compartment model with first-order kinetics of absorption and elimination described the available paromomycin observations in plasma adequately. The typical values (RSE) for clearance and volume of distribution of paromomycin were estimated at 4.38 L/h (2.36%) and 15.6 L (2.02%), respectively (Table 2.1.3). Between-subject variability (CV% [RSE%]) could be identified for clearance (33.2% [10.4%]) for all subjects, and for volume of distribution only for the African populations (31.5% [29.0%]). Absorption from the intramuscular site of injection was fast with a rate constant of 1.99 h^{-1} (6.52%). Exposure in Eastern African patients was higher compared to Indian patients, which was best characterized by 1.17 (5.18%) times higher bioavailability in Kenya and Sudan, and 2.46 (24.5%) times higher bioavailability in Ethiopia. To describe the higher variability among Ethiopian concentration-time profiles, between-subject variability was applied to F1 for the Ethiopian population (150% [24.0%]). Additionally, the deviating concentration-time profiles in Ethiopia were characterized by a ~4 times slower absorption rate constant of 0.446 h^{-1} (18.2%). On top of allometric scaling of clearance and volume of distribution for body weight, a linear relationship between age and clearance improved the model significantly (-57.6 OFV), resulting in a decline of clearance by 1.25% (10.6%) per year increase in

age. Only for Eastern African patients, a significant and clinically relevant exponential relationship between time and clearance was identified (-31.3 OFV), amounting to -32.6% (15.2%) decrease in clearance between start and end of treatment (day 21). A separate residual error for both studies improved the model significantly, with residual variabilities of 56.1% (2.96%) and 64.6% (4.54%) for the Indian and Eastern African data, respectively. No drug-drug interaction between paromomycin and SSG could be identified and paromomycin pharmacokinetics was dose-proportional for the studied dose range. At the end of treatment, $AUC_{0-tau,SS}$ for 15 mg/kg/day (median [IQR]) was higher in Kenya and Sudan (172.7 µg·h/mL [145.9-214.3]), and in Ethiopia (230.1 µg·h/mL [146.3-591.2]), compared to India (97.26 µg·h/mL [80.83-123.4]).

Table 2.1.3 Parameter estimates of the final population pharmacokinetic model.

	Estimate	95% CI[a]	Shrinkage (%)
Population parameters			
Cl_{pop} (L/h)	4.38	4.17 - 4.59	
$V_{d,pop}$ (L)	15.6	15.0 - 16.2	
$k_{a,pop}$ (h^{-1})	1.99	1.76 - 2.27	
$F1_{pop}$	1.00 (fixed)		
$COV_{Cl,time}$ (h^{-1})	-0.000782	-0.00101 - -0.000561	
$COV_{Cl,age}$ (year^{-1})	-0.0125	-0.0151 - -0.0100	
$k_{a,Ethiopia}$ (fold change $k_{a,pop}$)	0.224	0.151 - 0.305	
$F1_{Ethiopia}$ (fold change $F1_{pop}$)	2.46	1.59 - 4.01	
$F1_{Kenya,Sudan}$ (fold change $F1_{pop}$)	1.17	1.06 - 1.30	
Between-subject variability			
Cl (CV%)	33.2	30.1 - 36.5	29
$V_{d,Eastern-Africa}$ (CV%)	31.5	23.3 - 41.0	40
$F1_{Ethiopia}$ (CV%)	150	120.3 - 189.1	8
Residual variability			
Proportional error India (CV%)	56.1	54.6 - 57.9	10
Proportional error Eastern Africa (CV%)	64.6	62.1 - 67.7	10

$$Cl_{TV} = Cl_{pop} * \left(\frac{WT_{i,t}}{WT_{med}}\right)^{0.75} * e^{TIME*COV_{Cl,time}} * \left(1 + (AGE_t - AGE_{med}) * COV_{Cl,age}\right)$$

$$V_{d,TV} = V_{d,pop} * \left(\frac{WT_{i,t}}{WT_{med}}\right)^{1.00}$$

AGE: age (years); AGE_{med}: median population age (20 years); CI: confidence interval; Cl: apparent oral clearance; COV: covariate; CV: coefficient of variation; F1: bioavailability; k_a: absorption rate constant; SIR: sampling importance resampling; V_d: central volume of distribution; WT: body weight (kg); WT_{med}: median population body weight (39 kg). [a] Obtained by SIR.

Table 2.1.4   Paromomycin exposure by dose and country.

Dose	Country	$AUC_{0-tau,SS}$ (μg·h/mL)[a]
15 mg/kg	Kenya	188.4 (151.4-233.5)
	Sudan	149.4 (137.6-170.8)
	Ethiopia	230.1 (146.3-591.2)
	India	97.26 (80.83-123.4)
20 mg/kg	Kenya	215.0 (142.8-337.0)
	Sudan	287.8 (244.5-341.6)
	Ethiopia	235.9 (117.7-391.2)

$AUC_{0-tau,SS}$: Area under the plasma concentration-time curve for 24 hours at steady-state, determined on the last day concentrations were measured. [a] Median (IQR).

2.1

3.3   Model evaluation

The final parameters of the population PK model were adequately estimated (Table 2.1.3), with acceptable parameter precisions based on SIR (<30% RSE), shrinkages of between-subject variabilities (<40%), correlations between parameters (≤0.6), and a low condition number (13.59). Population and individual model predictions were adequately describing the observations, with no major trends visible in the GoF plots (Figure 2.1.2). Simulation based diagnostics indicated overall a good predictive performance of the model, although the plasma concentrations in the absorption phase in the Ethiopian population are slightly over-predicted, illustrated by the VPC (Figure 2.1.3). The different variability in plasma concentrations between the countries was well described by the model.
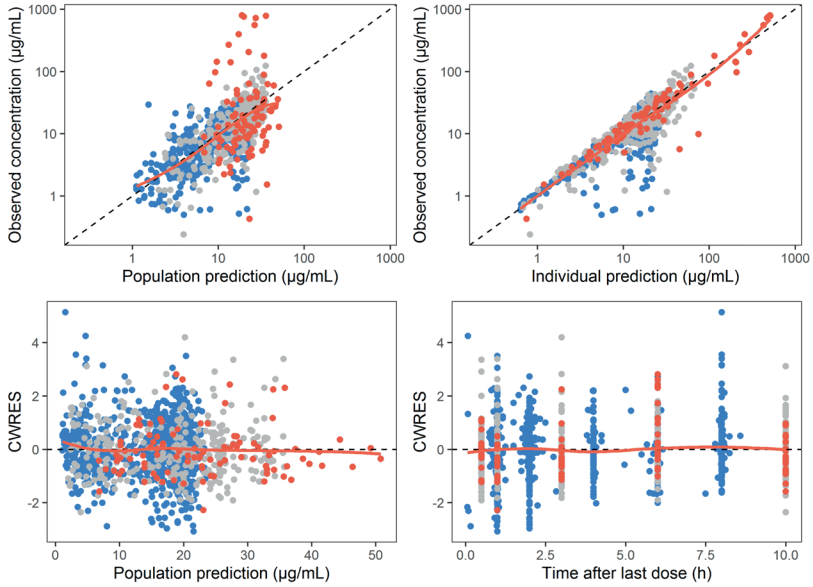
Figure 2.1.2 Goodness-of-fit plots for the final population pharmacokinetic model coloured by country. Model predicted population and individual paromomycin concentrations versus observed concentrations, and conditional weighted residuals (CWRES) versus time after last dose and population predictions; for Kenya and Sudan (grey), Ethiopia (red) and India (blue).
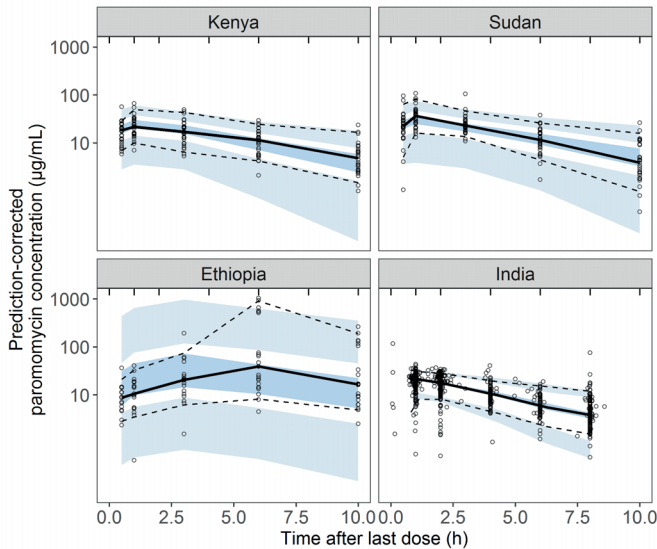
Figure 2.1.3 Prediction-corrected visual predictive check of the final paromomycin pharmacokinetic model stratified by country. Solid and dashed lines represent the 50th, 5th and 95th percentiles of the observed values, respectively, whereas the dark and light blue areas indicate the 90% confidence intervals of the simulated 50th, 5th and 95th percentiles, based on 1000 simulations.

4   Discussion

The population pharmacokinetic model adequately described paromomycin pharmacokinetics in VL patients from different Eastern African countries and India. A decline in clearance during treatment was observed, as well as a decline in clearance with age. There was no drug-drug interaction observed with SSG, and paromomycin pharmacokinetics was dose-proportional for the studied dose range.

The shape and variability of the concentration-time profiles in Ethiopian patients differed greatly from the other Eastern African and Indian patient populations. The differences were best characterized by a slower absorption rate (4-fold slower) and a higher typical intramuscular bioavailability (2.46-fold), but with a very high between-subject variability of this bioavailability (150%). The sparse sampling scheme used in Ethiopia cannot be responsible for the observed pharmacokinetic differences, as the population pharmacokinetic approach accounts for sparse and heterogeneous data. The fast absorption rate of 1.99 h^{-1} observed in Kenya, Sudan, and India is more in line with the absorption rate of 2.65 h^{-1} shown earlier in 7 healthy volunteers receiving the same paromomycin dose regimen[8]. Variable absorption rates and bioavailability have been observed for other aminoglycosides such as amikacin and gentamicin[19,20], although not as extreme as we observed in this study. Possible explanations were considered. The same paromomycin product and batch was used in all sites in Eastern Africa, but differences in e.g. storage conditions (altering product stability and/or solubility), different conditions during sample transport and analysis (altering analyte stability in the samples), or exact site of injections (e.g. subdermal instead of intramuscular) between study sites and/or trials cannot be fully excluded. Notable in this respect is that Ethiopian patients had been included at two distinct sites in North and South Ethiopia, but no differences in pharmacokinetics could be identified between those two sites (data not shown). Alterations in body composition and physiological changes are associated with malnutrition and/or clinical manifestations of VL[21,22], which might also impact pharmacokinetics. However, we could not identify any correlations between age or factors related to malnutrition or disease severity (body weight, serum albumin) and exposure, clearance or drug absorption.

A priori we expected a correlation between serum creatinine or GFR and paromomycin clearance, as paromomycin is mainly cleared renally. However, inclusion of these covariates did not significantly improve the model fit, probably because all Eastern African patients in this study had relatively normal serum creatinine levels (range 44.2-134 µmol/L). Secondly, to find a mechanistic explanation for the decline in clearance, the effect of time-varying serum albumin was evaluated on volume of distribution and clearance. Patients had hypoalbuminemia at the start of treatment (range 7-40 g/L), which increased during and after treatment (range 20-57 g/L at 2-month follow-up

2.1

after end of treatment). In treatment with other aminoglycosides, decreased albumin has been correlated with increased volume of distribution[23–26], which can in turn cause a decrease in C_{max}[24,26] and possibly a lower renal clearance. The increase in serum albumin over time corresponds to the decrease in clearance over time. However, we did not find any significant effect of time-varying albumin levels on any pharmacokinetic parameter.

In this pooled pharmacokinetic analysis, data were retrieved from different trials with different treatment regimens (different paromomycin mg/kg dose, with and without companion drug) and sampling schemes were different. To optimally analyse the heterogenic data, a population approach was used, allowing to adequately characterize paromomycin pharmacokinetics, to link geographical differences to certain pharmacokinetic parameters, and to describe part of the variability by explanatory covariates. Moreover, the population approach allows adequate analysis of different sampling schemes, e.g. the sparse sampling scheme used in Ethiopian sites. However, the retrospective design of the study brings limitations. Serum creatinine and albumin data were missing in the Indian population, and therefore these covariates could only be evaluated in a subset of patients. Secondly, 27.2% of data of paromomycin plasma levels at dosing time points (TAD=0 and TAD=24 hours) were excluded because the data were highly variable and physiologically implausible. However, exclusion of these data did not lead to any substantial changes in identification and parameter estimates of the structural pharmacokinetic model, implying a negligible effect on subsequent model development.

Surprisingly, the substantial geographical differences in exposure that we identified here were not in line with the observed geographical variability in efficacy. Efficacy rates after a lower paromomycin dose (15 mg/kg paromomycin for 21 days)[3] were in line with exposure differences among Eastern African countries in the current study, which was lowest in Sudan (14.3% and 46.7%) and highest in Southern (96.6%) Ethiopia[3]. Contrarily, exposure in Sudanese patients was higher compared to Kenyan and Ethiopian patients when receiving 20 mg/kg paromomycin. For this dose level, geographical efficacy differences within Eastern Africa were not observed, although the current clinical trial was not powered to perform a by-site analysis[5]. Moreover, high efficacy in Indian patients (94.6%)[2] was observed (15 mg/kg for 21 days), while exposure was significantly lower compared to all Eastern African countries. Therefore, the reported differences in efficacy were most probably not related to the pharmacokinetics. While the pharmacokinetic sub-studies included e.g. less children than the total clinical trial populations on which the efficacy figures were based, there are no indications that there are significant efficacy differences between children and adults at the evaluated dose levels[2,5]. The lower efficacy in Sudan compared to India might be related to the virulence of the *Leishmania* parasite or related to

immunological and pathophysiological differences between populations, while parasite susceptibility differences have not been documented up till date *in vitro*. Moreover, this trend of lowered efficacy in Eastern Africa is not only observed for paromomycin treatment but also for other VL treatment regimens[27].

In summary, this pooled population pharmacokinetic model provides detailed insight in the geographical pharmacokinetic differences among Eastern African countries and India, however, the resulting differences in paromomycin pharmacokinetics most probably do not explain the geographical differences in efficacy of paromomycin monotherapy in the treatment of VL patients. Potential explanations for these efficacy differences might be host-related, *e.g.,* immunological or genetic differences, or parasite-related *e.g.,* parasite virulence differences. Moreover, this analysis demonstrates the relevance of pharmacokinetic analysis in these populations, as remarkable differences in exposure were observed between geographic populations, despite the use of a body weight-guided dosing regimen.

2.1

Acknowledgments

Funding

Ethical approval and informed consent

All procedures were conducted in accordance with the Declaration of Helsinki (2002 version) relating to the conduct of research on human subjects and followed the International Committee on Harmonization guidelines for the conduct of clinical trials. The relevant ethics committees from each country approved the clinical studies. Patients or their legal guardians (if they were minors) provided signed informed consent prior to being randomized to the different treatment arms. In India, patients were randomly assigned in the pharmacokinetic sub-study, while in Eastern Africa patients were asked to participate in the pharmacokinetic sub-study using a separate informed consent.

References

1. World Health Organization. Recommended treatment regimens for visceral leishmaniasis [Internet]. Available from: https://www.who.int/leishmaniasis/research/978924129496_pp67_71.pdf?ua=1
2. Sundar S, Jha TK, Thakur CP, Sinha PK, Bhattacharya SK. Injectable Paromomycin for Visceral Leishmaniasis in India. N Engl J Med. 2007;356:2571–81.
3. Hailu A, Musa A, Wasunna M, Balasegaram M, Yifru S, Mengistu G, et al. Geographical variation in the response of visceral leishmaniasis to paromomycin in East Africa: A multicentre, open-label, randomized trial. PLoS Negl Trop Dis. 2010;4:e709.
4. Musa AM, Younis B, Fadlalla A, Royce C, Balasegaram M, Wasunna M, et al. Paromomycin for the treatment of visceral leishmaniasis in Sudan: A randomized, open-label, dose-finding study. PLoS Negl Trop Dis. 2010;4:4–10.
5. Musa A, Khalil E, Hailu A, Olobo J, Balasegaram M, Omollo R, et al. Sodium stibogluconate (SSG) & paromomycin combination compared to SSG for visceral leishmaniasis in East Africa: A randomised controlled trial. PLoS Negl Trop Dis. 2012;6:e1674.
6. Verrest L, Dorlo TPC. Lack of Clinical Pharmacokinetic Studies to Optimize the Treatment of Neglected Tropical Diseases: A Systematic Review. Clin Pharmacokinet. 2017;56:583–606.
7. Kip AE, Schellens JHM, Beijnen JH, Dorlo TPC. Clinical Pharmacokinetics of Systemically Administered Antileishmanial Drugs. Clin Pharmacokinet. 2018;57:151–76.
8. Kanyok TP, Killian AD, Rodvold KA, Danziger LH. Pharmacokinetics of intramuscularly administered aminosidine in healthy subjects. Antimicrob Agents Chemother. 1997;41:982–6.
9. Seyffart G. Drug dosage in renal insufficiency. Springser Science Business Media; 1991.
10. Institute for OneWorld Health. Application for inclusion of paromomycin in the WHO Model List of Essential Medicines [Internet]. 2006. Available from: http://archives.who.int/eml/expcom/expcom15/applications/newmed/paromomycin/paromomycin.pdf
11. Beal SL. Ways to fit a PK model with some data below the quantification limit. J Pharmacokinet Pharmacodyn. 2001;28:481–504.
12. Anderson BJ, Holford NHG. Mechanism-Based Concepts of Size and Maturity in Pharmacokinetics. Annu Rev Pharmacol Toxicol. 2008;48:303–32.
13. Stevens LA, Coresh J, Feldman HI, Greene T, Lash JP, Nelson RG, et al. Evaluation of the modification of diet in renal disease study equation in a large diverse population. J Am Soc Nephrol. 2007;18:2749–57.
14. Du Bois D, Du Bois EF. A formula to estimate the approximate surface area if height and weight be known. 1916. Nutrition. 1989;5:303.
15. Varma N, Naseem S. Hematologic changes in visceral Leishmaniasis/Kala Azar. Indian J Hematol Blood Transfus. 2010;26:78–82.
16. Karlsson MO, Savic RM. Diagnosing model diagnostics. Clin Pharmacol Ther. 2007;82:17–20.
17. Bergstrand M, Hooker AC, Wallin JE, Karlsson MO. Prediction-corrected visual predictive checks for diagnosing nonlinear mixed-effects models. AAPS J. 2011;13:143–51.
18. Dosne AG, Bergstrand M, Karlsson MO. An automated sampling importance resampling procedure for estimating parameter uncertainty. J Pharmacokinet Pharmacodyn. 2017;44:509–20.
19. Thomson AH, Kokwaro GO, Muchohi SN, English M, Mohammed S, Edwards G. Population pharmacokinetics of intramuscular gentamicin administered to young infants with suspected severe sepsis in Kenya. Br J Clin Pharmacol. 2003;56:25–31.
20. Pfeffer M, van Harken DR. Effect of Dosing Volume on Intramuscular Absorption Rate of Aminoglycosides. J. Pharm. Sci. Wiley; 1981.
21. Feleke BE. Nutritional status of visceral leishmaniasis patients: A comparative cross-sectional study. Clin Nutr ESPEN. Elsevier Ltd; 2019;33:139–42.
22. Mengesha B, Endris M, Takele Y, Mekonnen K, Tadesse T, Feleke A, et al. Prevalence of malnutrition and associated risk factors among adult visceral leishmaniasis patients in Northwest Ethiopia: A cross sectional study. BMC Res Notes. 2014;7:1–6.
23. Davis RL, Lehmann D, Stidley CA, Neidhart J. Amikacin Pharmacokinetics in Patients Receiving High-Dose Cancer Chemotherapy. Antimicrob Agents Chemother. 1991;35:944–7.

2.1

24. Etzel J V., Nafziger AN, Bertino JS. Variation in the pharmacokinetics of gentamicin and tobramycin in patients with pleural effusions and hypoalbuminemia. Antimicrob Agents Chemother. 1992;36:679–81.

25. Romano S, Fdez de Gatta MM, Calvo M V, Caballero D, Dominquez-Gil A, Lanao JM. Population pharmacokinetics of amikacin in patients with haematological malignancies. J Antimicrob Chemother. 1999;44:235–42.

26. Hodiamont CJ, Juffermans NP, Bouman CSC, Jong MD De, Mathôt RAA, Hest RM Van. Determinants of gentamicin concentrations in critically ill patients: a population pharmacokinetic analysis. Int J Antimicrob Agents. 2017;49:204–11.

27. Alves F, Bilbe G, Blesson S, Goyal V, Monnerat S, Mowbray C, et al. Recent Development of Visceral Leishmaniasis Treatments: Successes, Pitfalls, and Perspectives. Clin Microbiol Rev. 2018;31:1–30.

Supplementary Material 2.1.1. Bioanalysis

African plasma samples were assayed for paromomycin concentrations using HPLC-UV , based on a previously reported method[1], which was further validated at the Clinical Pharmacology Section, African Centre for Clinical Trials, Nairobi, Kenya. Aliquots (50-300 µl) of plasma samples from study subjects were processed up to a final step involving pre-column derivatization to convert paromomycin, an aminoglycoside that does not absorb UV light into a derivative that absorbs UV light, thus allowing quantification by high performance liquid chromatography (HPLC). Paromomycin and internal standard (kanamycin) were derivatized with 2, 4 – dinitrofluorobenzene at 65°C, followed by extraction with tert-butyl methyl ether (TBME). The organic phase (TBME) was then evaporated in a water bath (37°C) under a gentle flow of white spot nitrogen. The resulting residue was reconstituted in a mixture of acetonitrile and water, and injected into the chromatography system. Separation was performed on a Thermohypersil reverse phase C18 column (4.6 x 150 mm) coupled to a guard column. The mobile phase was a mixture of water/acetonitrile /methanol, adjusted to pH 3.0 with phosphoric acid. The mobile phase was degassed for 20 minutes in an ultra-sonic water bath before use, and delivered in isocratic mode at a flow rate of 1.2 ml/min. Column effluent was monitored at 350 nm. Calibration curves were prepared in duplicate by spiking blank plasma with varying known amounts of paromomycin sulphate (0.2-25 µg of base equivalents) and a fixed amount (5 µg) of kanamycin sulphate, followed by derivatization and extraction as described above. Quantification of paromomycin in samples from patients was done with reference to the linear portion of the calibration curve. Quality control (QC) samples representing high, medium and low concentrations of paromomycin were analyzed simultaneously with the patient samples, demonstrating good assay precision with intra- and inter-day coefficient of variation below 10%. Accuracy as determined from assay of QC samples was within acceptable ranges for low, medium and high QC values for both urine and plasma samples. The % recovery was over 80% for all QC concentrations. The limit of detection of paromomycin was 0.05 µg/mL and the lower limit of quantification 0.1 µg/mL.

In Indian plasma samples, paromomycin concentrations were determined by the use of a sensitive and specific liquid chromatography coupled to tandem mass spectrometry (LC/MS/MS) method, performed at the Analytical Division of the Drug Studies Unit (DSU) at the University of California, San Francisco, CA, USA. Human plasma samples (200 µl) were analyzed for paromomycin with a LC/MS/MS procedure on a Micromass Quattro Ultima LC system equipped with an Allure PFP propyl column (4.6 x 50 mm, 5 µm particle size), a methanol/water (v/v) containing 20 mM ammonium acetate and 0.14% trifluoroacetic acid, pH 3.3 mobile phase, and mass spectrometric detection with positive ionization by electrospray and mass scanning by MRM (Multiple Reaction

2.1

Monitoring) analysis. Sample preparation consisted of the addition of internal standard into 200 µl of plasma samples, precipitation of the samples with 30% trifluoroacetic acid, centrifugation, transfer of the supernatant and addition of 50% methanol to each sample prior to separation by LC/MS/MS. Calibration standards and QC samples were generated by spiking blank (interference-free) human plasma with paromomycin. Calibration standards at ten concentrations, excluding blanks, and QC samples at three concentrations within the calibration range of the assay were analyzed routinely with study samples. The QC samples were used to monitor the performance of the assay. All human plasma concentrations were calculated from a paromomycin human plasma calibration curve. The range for the assay was 0.5 to 240 µg/ml with inter-day precision of 2.93 to 5.04% and intra-day precision of 1.09 to 2.53%. Plasma concentrations of paromomycin less than 0.5 µg/ml were reported as below the limit of quantitation (BLQ). Assay validation procedures and criteria were in accordance with the US Food and Drug Administration (FDA) "Guidance for Industry: Bioanalytical Method Validation" (May, 2001).

Reference

1. Kanyok TP, Killian AD, Rodvold KA, Danziger LH. Pharmacokinetics of intramuscularly administered aminosidine in healthy subjects. Antimicrob Agents Chemother. 1997;41:982–6.

Supplementary Material 2.1.2. Observations

A

B
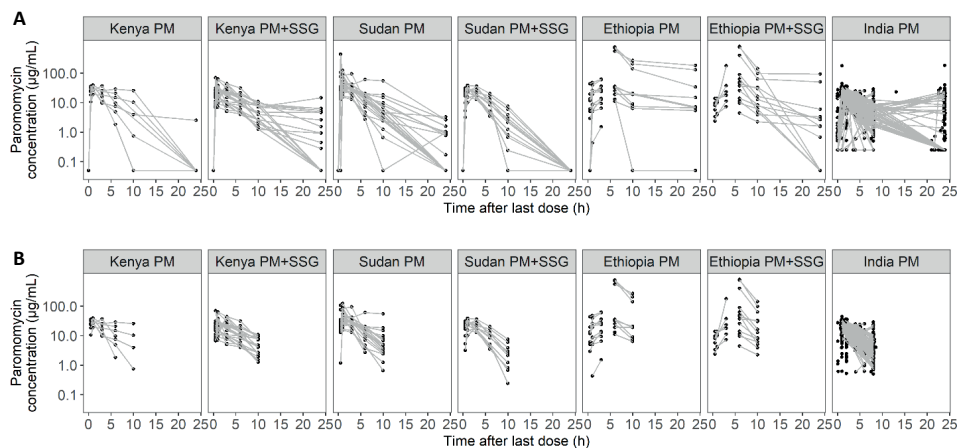
Figure S2.1.1 Paromomycin observations stratified by country and treatment group. Panel **A**: All observations; Panel **B**: Observations included in pharmacokinetic analysis. BLQ observations are fixed to half BLQ (0.05 µg/mL for Eastern Africa, 0.25 µg/mL for India).

2.1
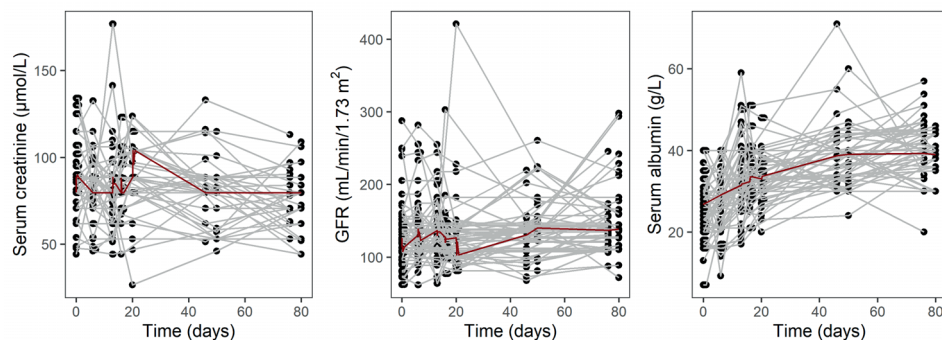
Figure S2.1.2 Serum creatinine levels and glomerular filtration rate in patients from Kenya and Sudan; serum albumin in patients from Kenya, Sudan, and Ethiopia.

Supplementary Material 2.1.3. NONMEM control stream

; Description: Final pooled paromomycin PK model Eastern Africa and India
; Author: L. Verrest
$PROBLEM PK
$INPUT ID DOSE DOSEBASE DV TIME CMT AMT II ADDL WTB AGE CNTRY FLAG EVID
MDV BLQ
;;;; Dataset description ;;;;
; ID   = Original subject ID
; DOSE   = Daily PM sulfate dose (mg)
; DOSEBASE = PM base (mg): PM sulfate * 0.7554
; DV   = PM plasma concentration (ug/mL)
; TIME   = Time after first dose (h)
; CMT   = Compartment. 1 = dose, 2 = PM plasma concentration
; AMT   = PM base dose amount (mg)
; II   = Inter-dose interval
; ADDL   = Additional doses
; WTB   = Body weight at baseline (kg)
; AGE   = Age (years)
; CNTRY   = Country. 1 = Kenya, 2 = Sudan, 3 = Ethiopia, 4 = India
; FLAG   = Samples to be excluded. 0= include, 1 = exclude
; EVID   = Event ID. 0 = DV, 1 = dose, 2 = no dose or DV. EVID = 2 for DVs at T=0
              and T=24.
; MDV   = Missing DV. = DV, 1 = dose. MDV = 1 for DVs at T=0 and T=24.
; BLQ   = DV below limit of quantification (0.1 ug/mL for East-Africa, 0.5 ug/mL for
              India). 0 = no, 1 = yes.
$DATA nm.paromomycinPooled.final.csv IGNORE=@
IGNORE(BLQ.EQ.1) ; no BLQ samples
IGNORE(FLAG.EQ.1) ; remove excluded samples
$SUBROUTINE ADVAN13 TOL=6

$MODEL
COMP = (DEPOT)
COMP = (CENTRAL)
COMP = (AUC)
$ABB COMRES=2
$PK
TVCL = THETA(1)
TVV2 = THETA(2)
TVKA = THETA(3)
TVF1 = THETA(4)
;; Covariates

```
CLAGE = ( 1 + THETA(5)*(AGE - 20)) ; 20 = median population age
CLTIME = EXP(THETA(6)*TIME)
CL = TVCL *(WTB/39)**0.75 * EXP(ETA(1)) * CLAGE * CLTIME  ; 39 = median population
baseline body weight
IF(CNTRY.EQ.4) CL = TVCL *(WTB/39)**0.75 * EXP(ETA(1)) * CLAGE
V2  = TVV2 *(WTB/39)**1.00* EXP(ETA(2))
IF(CNTRY.EQ.4) V2  = TVV2 *(WTB/39)**1.00
KA = TVKA
IF(CNTRY.EQ.3) KA = THETA(3) * THETA(7)
F1 = TVF1
IF(CNTRY.EQ.3) F1 =  1 * THETA(8) * EXP(ETA(3))  ; Ethiopia
IF(CNTRY.LT.3) F1 =  1 * THETA(9)                 ; Kenya and Sudan
K20   = CL/V2
S2    = V2
AUCtau = F1*DOSEBASE/CL
IF(NEWIND.LE.1) THEN
COM(1)=0
COM(2)=0
ENDIF
$DES
;; Derive paromomycin Cmax, Tmax, and AUC
CONC = A(2)/V2
IF(CONC.GT.COM(1)) THEN
COM(1)=CONC
COM(2)=T
ENDIF
CC = A(2)/V2
DADT(1)= -KA*A(1
DADT(2)=  KA*A(1)-K20*A(2)
DADT(3)=  CC
AUC = A(3)
$ERROR
CMAX=COM(1)
TMAX=COM(2)
IPRED = F
IF(IPRED.LT.1E-6) IPRED=1E-6
IF(CNTRY.LT.4) W = SQRT(THETA(10)**2*IPRED**2 + THETA(12)**2) ; Eastern Africa
IF(CNTRY.EQ.4) W = SQRT(THETA(11)**2*IPRED**2 + THETA(13)**2) ; India
Y = IPRED + W*EPS(1)
IRES = DV-IPRED
IWRES = IRES/W
```

2.1

$THETA
```
(0, 4.38)    ; 1 CL
(0, 15.6)    ; 2 V2
(0, 1.99)    ; 3 KA
(1 FIX)      ; 4 F1
(-0.000782)  ; 5 COV(Cl,time)
(-0.0125)    ; 6 COV(Cl,age)
(0, 0.224)   ; 7 ka(Ethiopia)
(0, 2.46)    ; 8 F1(Ethiopia)
(0, 1.17)    ; 9 F1(Kenya,Sudan)
(0, 0.418)   ; 10 Prop. RE Eastern Africa
(0, 0.315)   ; 11 Prop. RE India
(0 FIX)      ; 12 Add. RE Eastern Africa
(0 FIX)      ; 13 Add. RE India
```
$OMEGA
```
0.216843     ; 1 CL
0.2          ; 2 V2
0.8          ; 3 F1(Ethiopia)
```
$SIGMA
```
(1 FIX)
```
$ESTIMATION METHOD=1 INTER MAXEVAL=2000 NOABORT PRINT=10 POSTHOC
ATOL=6 SIGL=6 NSIG=2 ETASTYPE=1
$COV PRINT=E
$TABLE ID DOSE DOSEBASE DV TIME CMT AMT II ADDL WTB AGE CNTRY FLAG BLQ EVID
IPRED CWRES CL V2 KA F1 ETA1 ETA2 ETA3 CMAX TMAX AUCtau AUC CC
ONEHEADER NOPRINT FILE=sdtab0017

Chapter 2.2

Paromomycin and miltefosine combination as
an alternative to treat patients with visceral
leishmaniasis in Eastern Africa:
A randomized, controlled, multicountry trial

Ahmed M. Musa, Jane Mbui, Rezika Mohammed, Joseph Olobo,
Koert Ritmeijer, Gabriel Alcoba, Gina Muthoni Ouattara,
Thaddaeus Egondi, Prossy Nakanwagi, Truphosa Omollo,
Monique Wasunna, Luka Verrest, Thomas P. C. Dorlo,
Brima Musa Younis, Ali Nour, Elmukashfi Taha Ahmed Elmukashfi,
Ahmed Ismail Omer Haroun, Eltahir A. G. Khalil, Simon Njenga,
Helina Fikre, Tigist Mekonnen, Dagnew Mersha, Kasaye Sisay,
Patrick Sagaki, Jorge Alvar, Alexandra Solomos, Fabiana Alves

Abstract

Background: To determine whether paromomycin plus miltefosine (PM/MF) is non-inferior to sodium stibogluconate plus paromomycin (SSG/PM) for treatment of primary visceral leishmaniasis in Eastern Africa.

Methods: An open-label, Phase III, randomized, controlled, trial was conducted in adult and paediatric patients at 7 sites in Eastern Africa. Patients were randomly assigned to either 20 mg/kg paromomycin plus an allometric dose of miltefosine (14 days), or 20 mg/kg sodium stibogluconate plus 15 mg/kg paromomycin (17 days). Primary endpoint was definitive cure at 6 months follow-up.

Results: Of the 439 patients randomized, 424 completed the trial. Ninety-eight were randomized to a subsequently discontinued 28-day MF/14-day PM arm. Definitive cure at 6 months was 91.2% (155/170) and 91.8% (156/170) in the PM/MF and SSG/PM arms in the primary efficacy mITT analysis (difference: 0.6% [97.5%CI: - 6.2; 7.4]), narrowly missing the non-inferiority margin of 7%. In the PP analysis, efficacy was 92% (149/162) and 91.7% (155/169) in the PM/MF and SSG/PM arms (difference: -0.3% [97.5%CI: -7.0; 6.5]), demonstrating non-inferiority. Treatments were well tolerated. Four of the 18 serious adverse events were study drug-related and one death was related to SSG. Allometric dosing of MF ensured similar exposure in children <12 years and adults.

Conclusions: Efficacies of PM/MF and SSG/PM were similar, ADRs were as expected given the safety profiles of the drugs. With one less injection each day, reduced treatment duration, and no risk of SSG-associated life-threatening cardiotoxicity, PM/MF is a more patient-friendly alternative for children and adults with primary VL in Eastern Africa.

1. Introduction

The number of cases of visceral leishmaniasis (VL), a potentially fatal parasitic disease caused by *Leishmania*, is decreasing, mainly due to VL elimination efforts in South Asia. Eastern Africa has the highest burden of VL globally, mainly affecting children, with numbers stagnating in recent years[1,2]. Since 2010, sodium stibogluconate (SSG) and paromomycin (PM) combination has been the standard of care treatment for VL in Africa[3]. It was an improvement on 30-day SSG monotherapy but entails hospitalization with painful twice-daily injections for 17 days and potentially life-threatening antimony-associated toxicities such as cardiotoxicity, hepatotoxicity, and pancreatitis. Liposomal amphotericin B (AmBisome®) is a second-line drug for rescue treatment and specific target populations; the need for a cold chain, sterile two-step dilution process, well-trained personnel, and (rare) anaphylactic reactions limit its use in Eastern Africa. Alternative efficacious, safe, ideally short-course treatments suitable for use in remote areas are needed.

Miltefosine (MF), the only oral treatment for VL, has been extensively used in Asia as a 28-day monotherapy. It is well tolerated, with mainly mild to moderate gastro-intestinal side effects, and transient increases in liver enzymes and creatinine. Female patients of childbearing potential are required to use contraception during treatment and for ≥5 months afterwards, due to potential teratogenicity. In a Phase II clinical trial in Kenya and Sudan[4,5], MF (2.5mg/kg/day) used as monotherapy or in combination with AmBisome® did not reach the predefined satisfactory efficacy level of >90%. Treatment failure was associated with poor MF exposure in children (59% efficacy)[5,6]. Allometric MF dosing in 30 children (4-12 years old) for 28 days in Kenya achieved increased and less-variable exposure, with a cure rate of 90.0% (95% CI: 73.5-97.9%) at 6 months follow-up[7,8]. MF may, therefore, be an option for Africa, ideally in combination to reduce treatment duration and improve efficacy.

PM treatment of 15mg/kg/day for 21 days showed satisfactory efficacy in Asia, but only 63.8% efficacy in Africa[9] with high variability. A higher daily dose of 20mg/kg/day for 21 days was well tolerated and resulted in a more homogeneous response, with overall efficacy of 84.3% at 6 months follow-up[10]. Side effects included reversible kidney and liver toxicity, and ototoxicity.

In Asia, a 10-day combination of MF (2.5mg/kg/day) with PM (15mg/kg/day) has been very successful with definitive cure rates at 6 months ranging from 96.9% to 98.7%[11]. An adapted PM/MF treatment regimen is expected to achieve satisfactory efficacy in Africa. PM/MF combination therapy could be an alternative to SSG/PM, minimizing the number of injections and removing antimonial-related toxicity. It could be an attractive option for children, a high proportion of the population at risk, and the elderly, the

2.2

most at risk of SSG-related toxicity. We investigated whether a 14-day PM/MF combination treatment is non-inferior to SSG/PM in Eastern African patients with primary VL.

2.   Methods

2.1   Trial design

This open label, Phase III, randomized, controlled multicentre noninferiority trial was conducted in hospitals at seven sites in Kenya, Uganda, Sudan, and Ethiopia. The trial started with two investigational arms: PM/MF for 14 days (arm 1) and PM for 14 days/MF for 28 days (arm 2), and a third study arm, the standard of care SSG/PM (arm 3). Since initial enrolment was considerably slower than anticipated, two additional sites were included, exclusion criteria were revised to allow for recruitment of a more representative VL population (see Supplementary Text 2.2.1), and recruitment in arm 2 was discontinued. Therefore, comparative analysis was performed between PM/MF arm 1 and SSG/PM arm 3, whereas results for arm 2 were descriptive. The choice to prematurely discontinue arm 2 was due to practical advantages of the arm 1 regimen, i.e., shorter duration, complete administration during hospitalization, and lower cost. No efficacy or safety concerns required early termination of arm 2.

2.2   Participants

Patients aged 4 to ≤50 years with VL symptoms and parasitological diagnosis were included unless they had relapse, severe malnutrition, severe VL, positive HIV diagnosis or a concomitant severe infection, or were women of childbearing potential unwilling to use contraception until 5 months after end of treatment (Supplementary Text 2.2.1 lists all criteria). Approval was obtained from independent ethics committees in Sudan, Kenya, Uganda, and Ethiopia and from Médecins Sans Frontières' Ethics Review Board. Informed consent and assent (when applicable) were obtained as per regulatory requirements in each country.

2.3   Interventions

Arm 1 comprised a once-daily IM injection of 20 mg/kg/day PM for 14 days and oral MF (Impavido®) BID for 14 days. Children <30kg received MF allometric dosing based on sex, weight, and height[12] (Supplementary Figure S2.2.1), patients ≥30kg to <45kg received 100mg/day, and patients ≥45kg received 150mg/day. The arm 2 (discontinued) regimen was as arm 1, but with MF for 28 days. Arm 3 was SSG 20 mg/kg/day IM/intravenous (IV) with PM 15 mg/kg/day IM for 17 days. Arm 1 and 3 patients were hospitalized during treatment, arm 2 patients were hospitalized for the

first 14 days of treatment followed by 14 days as outpatients. Rescue treatment was indicated in case of initial treatment failure, relapse, or intolerability (Supplementary Text 1). End-of-treatment (EOT) assessments were conducted on D28. Patients were followed up for 6 months until D210. Compliance was measured as described in Supplementary Text 2.2.1.

2.4 Pharmacokinetics

Pharmacokinetics measurements of MF were made in all patients in arm 1 at D14 and in arms 1 and 2 at D28 and D56. Intensive pharmacokinetics sampling for both PM and MF was performed in a subset of patients at D1 and D14 (Supplementary Text 2.2.1).

2.5 Outcomes

The primary efficacy endpoint was definitive cure at 6 months follow-up, defined as absence of clinical signs and symptoms of VL at D210 and no rescue treatment during the trial. Safety endpoints were the frequency and severity of adverse events (AE) from treatment start to D210 and the frequency of serious AEs and AEs requiring treatment discontinuation. A secondary efficacy endpoint was initial cure at EOT (resolution of clinical signs and symptoms, negative microscopy (spleen or bone marrow) and no rescue treatment).

The pharmacokinetics endpoint was total and partial blood plasma exposure to PM and MF defined as the area under the concentration-time curve for PM and the maximal concentrations (C_{max}) for MF, during treatment and until end of follow-up for MF and based on full curves both on D1 and D14 for PM.

2.2

2.6 Sample size

The sample size of 153 patients per arm was based on an expected efficacy at 6 months follow-up of 93% for arm 1 and 91% for arm 3, a non-inferiority margin of 7%, power of 80% and alpha of 0.025 (one-sided, no adjustment for multiplicity). A 10% provision for loss to follow-up brought the sample size to 170 per arm (arms 1 and 3).

2.7 Randomization

Patients were originally randomized centrally to treatment in a 1:1:1 allocation ratio using varying block sizes of 6, 9, or 12 subjects in random order. Following discontinuation of arm 2, a 1:1 allocation ratio was used with varying block sizes of 4, 6 or 8 to assign patients to study arms 1 and 3. Randomization codes were generated through an online system.

2.8   Statistical methods

Efficacy analysis was performed comparing treatment arm 1 with arm 3. Data for the discontinued arm 2 were described. Estimates of the proportion with initial (EOT)/ definitive (D210) cure were reported. The difference in proportions between treatment arms was presented in the mITT (all randomized patients receiving at least one dose of treatment) and in the PP (patients in mITT with no major protocol deviations) sets. The Blackwelder test was used to test for non-inferiority. For sensitivity analysis for imputation of missing data and the set of completers see Supplementary Table S2.2.1. Multivariate logistic regression analysis was conducted to assess the difference in odds of failure between treatment arms adjusting for country, age group, and sex.

Safety analysis was performed in the mITT set, based on treatment emergent adverse events (TEAEs). The proportion of patients with at least one adverse drug reaction (ADR) was compared for each treatment arm. All AEs were categorized by system organ class (SOC) and preferred term (PT) according to the Medical Dictionary for Regulatory Activities (MedDRA) Versions 20.1 to 24.0.

3.   Results

3.1   Participants

A total of 439 patients were recruited between 23 January 2018 and 17 May 2020; 171, 170, and 98 patients were assigned to arms 1, 3, and 2, respectively. 424/439 (96.6%) of patients reached EOT and 408/439 (92.9%) reached the end of the study (D210), with only 8 (1.8%) lost to follow-up (Figure 2.2.1). Apart from 1 patient in Arm 1 who died before starting treatment, all patients were included in the mITT set and 416/439 (94.8%) of patients in the PP set. Demographic and baseline characteristics were generally comparable between treatment arms. The median age was 11 years (IQR 8.0-19.0y) and 59.7% of the trial patients were ≤12 years. There was a higher proportion of male patients (79.7%), consistent with the overall VL population in the region (Table 2.2.1). 95.5% of female patients recruited were ≤12 years. Nearly all patients (99.3%) presented with fever at baseline and most (80.6%) had weight loss (Supplementary Table S2.2.2).
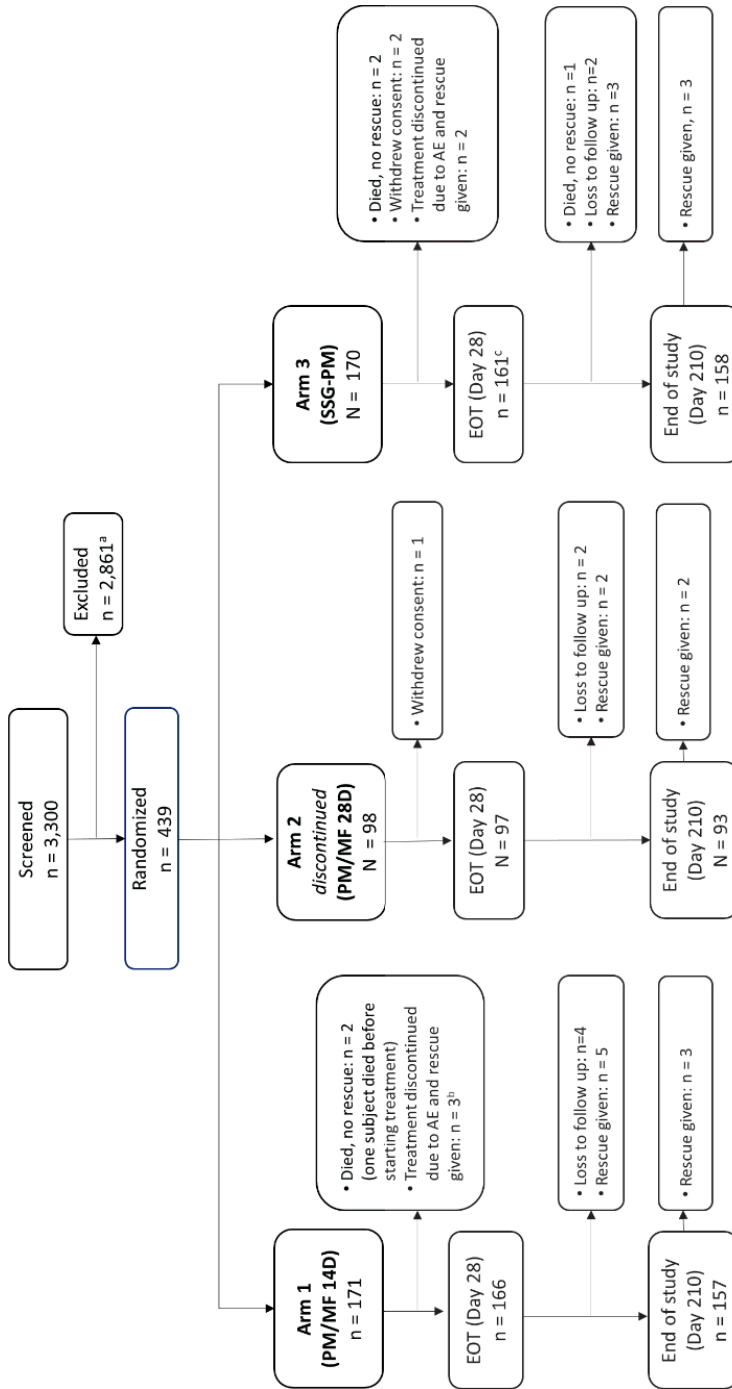
Figure 2.2.1 Patient disposition. [a]The most common reasons for screening failure were negative parasitology (746 patients, 22.6%), laboratory abnormalities (338 patients, 13%), age <4 years or >50 years (329 patients, 12.7%), severe malnourishment (230 patients, 8.9%), or other reasons (245 patients, 9.4%). One patient died during screening. [b]One additional patient discontinued the study treatment due to AEs but did not receive rescue medication and completed the study. [c]Three patients missed the EOT (day 28) visit but were included at later visits. Abbreviations: AE, adverse event; D, day; EOT, end of treatment; MF, miltefosine; PM, paromomycin; SSG, sodium stibogluconate.

2.2

Table 2.2.1 Baseline characteristics by treatment arm and overall – ITT set.

Parameter	Statistics	Arm 1 PM/MF 14D (n=171)	Arm 2[a] PM/MF 28D (n=98)	Arm 3 SSG/PM (n=170)	Overall (n=439)
Age (years)	Mean (SD)	13.5 (7.9)	13.9 (8.0)	13.0 (7.1)	13.4 (7.6)
	Median (Q1-Q3)	10.0 (8.0-19.0)	12.0 (8.0-20.0)	10.0 (8.0-18.0)	11.0 (8.0-19.0)
Age category	4 to ≤12 years, n (%)	103 (60.2)	54 (55.1)	105 (61.8)	262 (59.7)
	>12 to 50 years, n (%)	68 (39.8)	44 (44.9)	65 (38.2)	177 (40.3)
Sex	Female, n (%)	34 (19.9)	17 (17.3)	38 (22.4)	89 (20.3)
	Male, n (%)	137 (80.1)	81 (82.7)	132 (77.6)	350 (79.7)
Weight (kg)	Range (Min-Max)	11.0-71.0	14.0-61.0	11.0-60.0	11.0-71.0
	Mean (SD)	32.7 (14.4)	33.4 (13.7)	31.4 (13.4)	32.4 (13.9)
	Median (Q1-Q3)	28.0 (21.0-46.0)	32.0 (20.5-47.0)	27.3 (19.5-43.0)	28.0 (20.0-45.0)
Height (cm)	Range (Min-Max)	93.0-190.0	102.0-182.0	92.0-190.0	92.0-190.0
	Mean (SD)	141.0 (23.8)	143.9 (22.8)	139.9 (23.3)	141.2 (23.4)
	Median (Q1-Q3)	137.0 (124.0-165.0)	141.5 (123.0-166.0)	138.0 (121.0-163.0)	139.0 (122.0-164.0)
Nutritional status a/c WHO reference curves and BMI		N=145	N=79	N=145	N=369
	Moderate underweight, n (%)	43 (29.7)	35 (44.3)	49 (33.8)	127 (34.4)
	Normal, n (%)	101 (69.7)	42 (53.2)	95 (65.5)	238 (64.5)
	Overweight, n (%)	1 (0.7)	2 (2.5)	1 (0.7)	4 (1.1)
Nutritional status, MUAC (mm)		N=26	N=19	N=25	N=70
	Range (min-max)	160.0-260.0	165.0-240.0	168.0-255.0	160.0-260.0
	Mean (SD)	217.0 (23.1)	200.1 (18.8)	208.2 (23.3)	209.3 (22.8)
	Median (Q1-Q3)	220.0 (200.0-230.0)	200.0 (184.0-220.0)	205.0 (190.0-225.0)	210.0 (190.0-223.0)
Haemoglobin (g/dL)	Range (Min-Max)	5.0-12.3	5.1-19.7	5.1-13.8	5.0-19.7
	Mean (SD)	8.0 (1.4)	8.5 (2.2)	8.1 (1.7)	8.2 (1.7)
	Median (Q1-Q3)	8.0 (6.9-8.9)	8.1 (7.0-9.6)	8.0 (6.7-9.2)	8.0 (6.9-9.1)
WBCs (×10³/µL)	Range (Min-Max)	0.9-9.1	1.0-8.5	0.5-6.4	0.5-9.1
	Mean (SD)	2.8 (1.3)	2.4 (1.0)	2.8 (1.2)	2.7 (1.2)
	Median (Q1-Q3)	2.6 (2.0-3.4)	2.3 (1.6-3.0)	2.6 (1.9-3.5)	2.5 (1.9-3.3)
Platelets (×10³/µL)	Range (Min-Max)	19.0-338.0	45.0-342.0	26.0-446.0	19.0-446.0
	Mean (SD)	118.8 (56.5)	113.9 (50.8)	120.8 (61.7)	118.5 (57.3)
	Median (Q1-Q3)	108.0 (73.0-154.0)	108.5 (83.0-134.0)	105.0 (80.0-147.0)	107.0 (79.0-146.0)
AST (U/L)	Range (Min-Max)	6.0-592.0	13.0-118.0	10.0-621.0	6.0-621.0
	Mean (SD)	79.9 (85.3)	51.9 (26.0)	89.8 (94.8)	77.5 (81.6)
	Median (Q1-Q3)	58.0 (40.0-83.0)	45.5 (31.0-68.0)	62.5 (38.0-99.0)	56.0 (36.0-87.0)
ALT (U/L)	Range (Min-Max)	0.8-473.0	2.0-105.0	6.0-397.0	0.8-473.0
	Mean (SD)	40.1 (50.0)	27.0 (18.9)	46.7 (58.9)	39.7 (49.4)
	Median (Q1-Q3)	27.0 (18.0-44.0)	22.0 (14.0-40.0)	30.0 (18.0-48.0)	27.0 (16.0-45.0)

Table 2.2.1 (continued)

Parameter	Statistics	Arm 1 PM/MF 14D (n=171)	Arm 2[a] PM/MF 28D (n=98)	Arm 3 SSG/PM (n=170)	Overall (n=439)
Creatinine (mg/dL)	Range (Min-Max)	0.1-1.5	0.3-1.3	0.1-1.4	0.1-1.5
	Mean (SD)	0.8 (0.3)	0.9 (0.2)	0.7 (0.3)	0.8 (0.3)
	Median (Q1-Q3)	0.8 (0.6-1.0)	0.8 (0.7-1.0)	0.7 (0.6-0.9)	0.8 (0.6-1.0)
Albumin (g/L)	Range (Min-Max)	1.5-54.61	4.0-53.2	9.0-48.6	1.5-54.6
	Mean (SD)	27.4 (7.8)	29.9 (9.5)	26.8 (7.1)	27.7 (8.0)
	Median (Q1-Q3)	27.0 (23.0-31.0)	28.4 (23.6-35.4)	26.4 (22.2-31.0)	27.0 (23.0-31.8)
Spleen size (cm)	Range (Min-Max)	0.0-22.0	0.0-20.0	0.0-24.0	0.0-24.0
	Mean (SD)	7.6 (4.1)	8.8 (3.9)	7.8 (4.5)	7.9 (4.2)
	Median (Q1-Q3)	7.0 (4.0-10.0)	8.0 (6.0-11.5)	7.0 (4.0-11.0)	8.0 (5.0-11.0)
Liver size (cm)	Range (Min-Max)	0.0-7.0	0.0-8.0	0.0-10.0	0.0-10.0
	Mean (SD)	1.6 (2.0)	1.0 (1.8)	1.5 (2.1)	1.4 (2.0)
	Median (Q1-Q3)	0.0 (0.0-4.0)	0.0 (0.0-2.0)	0.0 (0.0-3.0)	0.0 (0.0-2.0)

D = Day(s); ITT = Intention-to-treat; MF = Miltefosine; PM = Paromomycin; Q = Quartile; SD = Standard deviation; SSG = Sodium stibogluconate; Max = Maximum; Min = Minimum. [a]Recruitment into arm 2 was discontinued.

2.2

Table 2.2.2 Primary efficacy outcome of definite cure with primary imputation by treatment arm.

Analysis set	Statistics	Arm 1 PM/MF 14D	Arm 3 SSG/PM
mITT[a]	n	170	170
	Number cured	155	156
	Efficacy, %	91.2	91.8
	Difference in efficacy[b] (97.5% CI)	0.6 (-6.2; 7.4)	
PP[c]	n	162	169
	Number cured	149	155
	Efficacy, %	92.0	91.7
	Difference in efficacy[b] (97.5% CI)	-0.3 (-7.0; 6.5)	

CI=Confidence interval; D=Day(s); MF=Miltefosine; mITT=Modified intention-to-treat; PM=Paromomycin; PP=Per-protocol; SSG=Sodium stibogluconate. [a]Primary analysis. [b]Difference in efficacy from SSG/PM, i.e., efficacy of SSG/PM minus efficacy of PM/MF14D. [c]Sensitivity analysis.

3.2   Compliance

Full (90-110%) compliance to all treatments was >95% during hospitalization, and 90% (to MF) during home treatment in arm 2.

3.3   Efficacy

Definitive cure at 6 months follow-up was achieved in 155/170 (91.2%) patients in arm 1 and 156/170 (91.8%) in arm 3 in the mITT set. The resulting difference in efficacy was 0.6% (97.5% CI: -6.2; 7.4). Non-inferiority was not demonstrated for a pre-defined margin of 7%, as the upper limit of the 97.5% CI of 7.4% exceeded slightly the non-inferiority margin of 7%. In the PP set, 149/162 (92.0%) patients in arm 1 and 155/169

(91.7%) in arm 3 achieved definitive cure at 6 months follow-up and PM/MF was non-inferior to SSG/PM (difference in efficacy = -0.3% [97.5% CI: -7.0; 6.5]) (Table 2.2.2).

Efficacy was similar between the two arms by age group, although the study was not powered for subgroup analysis. Definitive cure was achieved more often in patients 4 to ≤12 years (94.1% and 95.2% in arms 1 and 3, respectively) than in patients >12 to 50 years (86.8% and 86.2% in arms 1 and 3, respectively).

Logistic regression analysis showed no statistically significant difference in the odds of treatment failure between arms 1 and 3 after adjusting for age, sex, and country (odds ratio of 1.04 [95%CI: 0.5; 2.3], p=0.926). Reasons for treatment failure requiring rescue medication were relapse (3.6%), AE leading to treatment discontinuation (1.1%), one case of initial failure and one case of PKDL with mucosal involvement.

In arm 2, 92/98 (93.9%) of patients (97.5% CI: 86.1; 98.1) in the mITT set achieved definite cure. Initial cure at EOT was achieved in 164/170 (96.5%) of patients in arm 1 and 159/166 (95.8%) in arm 3 in the mITT set. The resulting difference in efficacy was -0.7% (97.5% CI: -5.4; 4.0); similar results were obtained in the PP set.

3.4   PKDL

28 patients presented PKDL after treatment, 5/170 (2.9%) in arm 1 and 23/170 (13.5%) in arm 3. All PKDL cases were reported in Sudan and Ethiopia, where the frequency of PKDL in VL patients was significantly lower in arm 1 than in arm 3 (5/114 (4.4%) and 23/110 (20.9%), respectively, p=0.0002).

3.5   Safety

At least one TEAE occurred in in 54.6% of patients, mostly during the treatment period, with 52.4%, 64.3%, and 51.2% in arms 1, 2, and 3, respectively (Table 2.2.3). The most common severe or life-threatening AEs were anaemia (3.7%) and aspartate aminotransferase increased (2.5%). At least one ADR was reported in 30.6% of patients, the most common being MF-related vomiting (13.5%), injection site pain (10.3%), and PM-related hypoacusis (5.0%) (Table 2.2.4). Although the frequency of ADRs was higher in the PM/MF arms, most of the ADRs were mild and moderate vomiting events associated with MF, and only one patient discontinued treatment due to severe vomiting. ADRs suggesting SSG-related cardiac toxicity were reported in 6.5% of patients in the SSG/PM arm. CTCAE Grade ≥3 ADRs were reported in 6.4% of patients, with 4.1% in arm 2, and 7.1% in both arms 1 and 3, the most common being increases in aspartate (2.5%) and alanine aminotransferases (0.7%), and electrocardiogram QT prolonged (0.7%) (Table 2.2.5). Non-serious ADRs leading to treatment discontinuation were reported in 6 patients (1.4%). SAE occurred in 11 patients (2.5%), with 2.9%, 3.1%,

and 1.8% in arms 1, 2, and 3, respectively. These included one ADR of SSG-related cardiotoxicity and 3 cases of infections that led to death in 4 patients (0.9%). Two patients not included in the mITT population died of internal abdominal bleeding possibly due to complications from splenic aspiration before study drug administration. Serious ADRs of acute kidney injury were reported in one patient in arm 1 and one in arm 2, related to PM and MF, and MF, respectively; the patient in arm 1 also had a serious ADR of bilateral deafness related to PM that was ongoing at the end of the study (Table 2.2.4).

Table 2.2.3 Summary of treatment emergent adverse events – mITT set.

Description	Arm 1 PM/MF 14D (n=170)	Arm 2 PM/MF 28D[a] (n=98)	Arm 3 SSG/PM (n=170)	Overall (n=438)
Any treatment emergent AE	89 (52.4)	63 (64.3)	87 (51.2)	239 (54.6)
Any at least severe TEAE[b]	26 (15.3)	14 (14.3)	18 (10.6)	58 (13.2)
Any treatment emergent SAE	5 (2.9)	3 (3.1)	3 (1.8)	11 (2.5)
Any TEAE leading to death	1 (0.6)	0 (0.0)	3 (1.8)	4 (0.9)
Any TEAE leading to treatment discontinuation	4 (2.4)	0 (0.0)	2 (1.2)	6 (1.4)
Any treatment emergent ADR	59 (34.7)	44 (44.9)	31 (18.2)	134 (30.6)
Any at least severe treatment emergent ADR[b]	12 (7.1)	4 (4.1)	12 (7.1)	28 (6.4)
Any treatment emergent serious ADR	1 (0.6)	1 (1.0)	1 (0.6)	3 (0.7)
Any treatment emergent ADR leading to death	0 (0.0)	0 (0.0)	1 (0.6)	1 (0.2)
Any treatment emergent ADR leading to treatment discontinuation	4 (2.4)	0 (0.0)	2 (1.2)	6 (1.4)

ADR = Adverse drug reaction; CTCAE = Common Terminology Criteria for Adverse Events; D = Day(s); MF = Miltefosine; mITT = Modified intention-to-treat; PM = Paromomycin; SAE = Serious adverse event; SSG = Sodium stibogluconate; AE = adverse event. [a]Recruitment into Arm 2 was discontinued. [b]Events with a severity classification as severe (CTCAE Grade 3), life-threatening (CTCAE Grade 4), or death (CTCAE Grade 5). Data are presented as n (%) of patients with at least one event.

Table 2.2.4 Summary of treatment emergent ADRs by treatment arm, by SOC and PT – mITT set.

System Organ Class	Preferred Term	Treatment Arm			
		PM/MF (14D) n=170	PM/MF (28D)[a] n=98	SSG/PM n=170	Total n=438
Any treatment emergent ADR		59 (34.7) [108]	44 (44.9) [77]	31 (18.2) [46]	134 (30.6) [231]
Blood and lymphatic system disorders	Neutropenia	0 (0.0) [0]	0 (0.0) [0]	1 (0.6) [1]	1 (0.2) [1]
		0 (0.0) [0]	0 (0.0) [0]	1 (0.6) [1]	1 (0.2) [1]
Cardiac disorders		0 (0.0) [0]	0 (0.0) [0]	4 (2.4) [4]	4 (0.9) [4]
	Arrhythmia	0 (0.0) [0]	0 (0.0) [0]	3 (1.8) [3]	3 (0.7) [3]
	Sinus arrhythmia	0 (0.0) [0]	0 (0.0) [0]	1 (0.6) [1]	1 (0.2) [1]
Ear and labyrinth disorders		9 (5.3) [15]	11 (11.2) [17]	3 (1.8) [4]	23 (5.3) [36]
	Hypoacusis	8 (4.7) [14]	11 (11.2) [17]	3 (1.8) [4]	22 (5.0) [35]
	Deafness bilateral	1 (0.6) [1]	0 (0.0) [0]	0 (0.0) [0]	1 (0.2) [1]

2.2

Table 2.2.4   (continued)

System Organ Class	Preferred Term	Treatment Arm		SSG/PM	Total
		PM/MF (14D)	PM/MF (28D)[a]		
		n=170	n=98	n=170	n=438
Gastrointestinal disorders		40 (23.5) [59]	26 (26.5) [37]	1 (0.6) [1]	67 (15.3) [97]
	Vomiting	34 (20.0) [48]	25 (25.5) [35]	0 (0.0) [0]	59 (13.5) [83]
	Gastritis	4 (2.4) [4]	1 (1.0) [1]	0 (0.0) [0]	5 (1.1) [5]
	Abdominal pain	2 (1.2) [2]	1 (1.0) [1]	0 (0.0) [0]	3 (0.7) [3]
	Dyspepsia	2 (1.2) [2]	0 (0.0) [0]	0 (0.0) [0]	2 (0.5) [2]
	Nausea	1 (0.6) [1]	0 (0.0) [0]	0 (0.0) [0]	1 (0.2) [1]
	Abdominal pain upper	1 (0.6) [1]	0 (0.0) [0]	0 (0.0) [0]	1 (0.2) [1]
	Gastrointestinal inflammation	1 (0.6) [1]	0 (0.0) [0]	0 (0.0) [0]	1 (0.2) [1]
	Pancreatitis	0 (0.0) [0]	0 (0.0) [0]	1 (0.6) [1]	1 (0.2) [1]
General disorders and administration site conditions		17 (10.0) [17]	14 (14.3) [14]	14 (8.2) [14]	45 (10.3) [45]
	Injection site pain	17 (10.0) [17]	14 (14.3) [14]	14 (8.2) [14]	45 (10.3) [45]
Hepatobiliary disorders		2 (1.2) [2]	0 (0.0) [0]	0 (0.0) [0]	2 (0.5) [2]
	Hepatitis	1 (0.6) [1]	0 (0.0) [0]	0 (0.0) [0]	1 (0.2) [1]
	Drug-induced liver injury	1 (0.6) [1]	0 (0.0) [0]	0 (0.0) [0]	1 (0.2) [1]
Injury, poisoning and procedural complications	Cardiotoxicity	0 (0.0) [0]	0 (0.0) [0]	1 (0.6) [1]	1 (0.2) [1]
		0 (0.0) [0]	0 (0.0) [0]	1 (0.6) [1]	1 (0.2) [1]
Investigations		11 (6.5) [12]	6 (6.1) [7]	16 (9.4) [20]	33 (7.5) [39]
	Aspartate aminotransferase increased	6 (3.5) [6]	1 (1.0) [1]	6 (3.5) [6]	13 (3.0) [13]
	Blood creatinine increased	4 (2.4) [4]	3 (3.1) [3]	3 (1.8) [3]	10 (2.3) [10]
	Electrocardiogram QT prolonged	0 (0.0) [0]	0 (0.0) [0]	6 (3.5) [7]	6 (1.4) [7]
	Alanine aminotransferase increased	0 (0.0) [0]	2 (2.0) [2]	2 (1.2) [2]	4 (0.9) [4]
	Blood bilirubin increased	1 (0.6) [1]	1 (1.0) [1]	1 (0.6) [1]	3 (0.7) [3]
	Liver function test increased	1 (0.6) [1]	0 (0.0) [0]	1 (0.6) [1]	2 (0.5) [2]
Musculoskeletal and connective tissue disorders		0 (0.0) [0]	1 (1.0) [1]	0 (0.0) [0]	1 (0.2) [1]
	Myalgia	0 (0.0) [0]	1 (1.0) [1]	0 (0.0) [0]	1 (0.2) [1]
Renal and urinary disorders		3 (1.8) [3]	1 (1.0) [1]	1 (0.6) [1]	5 (1.1) [5]
	Acute kidney injury	3 (1.8) [3]	1 (1.0) [1]	1 (0.6) [1]	5 (1.1) [5]

ADR = Adverse drug reaction; D = Day(s); MF = Miltefosine; mITT = Modified intention-to-treat; PM = Paromomycin; PT = Preferred term; SOC = System organ class; SSG = Sodium stibogluconate. [a]Recruitment into Arm 2 was discontinued. Note: data are presented as n (%) of patients with at least one event and number [n] of events.

Table 2.2.5   Treatment emergent ADRs > CTCAE Grade 3 by SOC and PT– mITT set.

System Organ Class Preferred Term	Arm 1 PM/MF 14D (n=170)	Arm 2 PM/MF 28D[b] (n=98)	Arm 3 SSG/PM (n=170)	Overall (n=438)
Any at least severe[a] treatment emergent ADR	12 (7.1) [13]	4 (4.1) [6]	12 (7.1) [13]	28 (6.4) [32]
Investigations	8 (4.7) [8]	3 (3.1) [4]	10 (5.9) [10]	21 (4.8) [22]
Aspartate aminotransferase increased	6 (3.5) [6]	1 (1.0) [1]	4 (2.4) [4]	11 (2.5) [11]
Alanine aminotransferase increased	0 (0.0) [0]	2 (2.0) [2]	1 (0.6) [1]	3 (0.7) [3]
Electrocardiogram QT prolonged	0 (0.0) [0]	0 (0.0) [0]	3 (1.8) [3]	3 (0.7) [3]
Blood bilirubin increased	1 (0.6) [1]	0 (0.0) [0]	1 (0.6) [1]	2 (0.5) [2]
Liver function test increased	1 (0.6) [1]	0 (0.0) [0]	1 (0.6) [1]	2 (0.5) [2]
Blood creatinine increased	0 (0.0) [0]	1 (1.0) [1]	0 (0.0) [0]	1 (0.2) [1]
Ear and labyrinth disorders	1 (0.6) [1]	1 (1.0) [1]	1 (0.6) [1]	3 (0.7) [3]
Hypoacusis	0 (0.0) [0]	1 (1.0) [1]	1 (0.6) [1]	2 (0.5) [2]
Deafness bilateral	1 (0.6) [1]	0 (0.0) [0]	0 (0.0) [0]	1 (0.2) [1]
Hepatobiliary disorders	2 (1.2) [2]	0 (0.0) [0]	0 (0.0) [0]	2 (0.5) [2]
Hepatitis	1 (0.6) [1]	0 (0.0) [0]	0 (0.0) [0]	1 (0.2) [1]
Drug-induced liver injury	1 (0.6) [1]	0 (0.0) [0]	0 (0.0) [0]	1 (0.2) [1]
Renal and urinary disorders	1 (0.6) [1]	1 (1.0) [1]	0 (0.0) [0]	2 (0.5) [2]
Acute kidney injury	1 (0.6) [1]	1 (1.0) [1]	0 (0.0) [0]	2 (0.5) [2]
Blood and lymphatic system disorders	0 (0.0) [0]	0 (0.0) [0]	1 (0.6) [1]	1 (0.2) [1]
Neutropenia	0 (0.0) [0]	0 (0.0) [0]	1 (0.6) [1]	1 (0.2) [1]
Gastrointestinal disorders	1 (0.6) [1]	0 (0.0) [0]	0 (0.0) [0]	1 (0.2) [1]
Vomiting	1 (0.6) [1]	0 (0.0) [0]	0 (0.0) [0]	1 (0.2) [1]
Injury, poisoning and procedural complications	0 (0.0) [0]	0 (0.0) [0]	1 (0.6) [1]	1 (0.2) [1]
Cardiotoxicity	0 (0.0) [0]	0 (0.0) [0]	1 (0.6) [1]	1 (0.2) [1]

2.2

ADR = Adverse drug reaction; CTCAE = Common Terminology Criteria for Adverse Events; D = Day(s); MF = Miltefosine; mITT = Modified intention-to-treat; PM = Paromomycin; PT = Preferred term; SOC = System organ class; SSG = Sodium stibogluconate. [a]Events with a severity classification as severe (CTCAE Grade 3), life-threatening (CTCAE Grade 4), or death (CTCAE Grade 5); [b]Recruitment into Arm 2 was discontinued. Data are presented as n (%) of patients with at least one event and number [n] of events.

3.6   Pharmacokinetics

PM exposure increased from D1 to D14, possibly due to decreased PM clearance over time[13]. PM AUC_{0-24} appeared higher in adolescents/adults (aged >12 years) than in children (≤12 years of age), while C_{max} was similar. One patient had a 10-fold higher PM exposure on D14, probably due to renal failure resulting from acute kidney injury, which led to ototoxicity and bilateral deafness. Allometric miltefosine dosing gave relatively similar MF exposures in children and adolescents/adults. Median D28 MF concentrations in arm 2 and achievement of the pharmacokinetic target in children

were higher than previously reported[12]. Detailed results of PK analysis and modelling will be presented separately.

4.   Discussion

In this study, we showed that a PM/MF combination achieved similar cure rates at 6 months follow-up as the standard of care SSG/PM in adult and paediatric patients with VL in Eastern Africa. Non-inferiority was demonstrated in the per protocol set but was narrowly missed in the mITT population. This is the first time a new combination treatment has achieved a cure rate of 91% in Eastern Africa, exceeding that of MF monotherapy (72%), AmBisome® and SSG (87%), and AmBisome® and MF (77%) combination therapies in the LEAP 0208 trial[14]. As expected, definitive cure rates as high as 99%, as for PM/MF in India[11,15], were not achieved, probably due to differences in parasite susceptibility and higher genetic diversity of the African parasite population, or host factors such as immunological response[16], since drug exposure appeared adequate.

In our study, MF exposure in children ≤12 years was similar to that in adults, confirming the LEAP 0714 trial conclusion that allometric MF dosing is more suitable for children, and leads to a satisfactorily high cure rate[7,8].

Changes made to allow inclusion of a population more representative of VL patients in Eastern Africa (exclusion criterion modified from BMI to MUAC for Ethiopia, change in the laboratory abnormalities criterion) proved appropriate, as there was no apparent difference in efficacy before and after the protocol amendment.

The higher proportion of ADR in arms 1 and 2 can mostly be attributed to MF intolerability, however, 6.5% of patients receiving SSG/PM experienced SSG-related cardiotoxicity, including 1 patient with a fatal cardiac TESAE. PM/MF was generally well tolerated, with ADRs as expected given the drug safety profiles[17]. MF-related vomiting was usually a single episode, with only one patient discontinuing treatment. A patient with a TESAE of acute kidney injury had considerably increased PM plasma levels, hypothesized to have contributed to a subsequent serious ADR of bilateral deafness. This exceptional and unfortunate case shows the importance of monitoring renal function during treatment with PM.

PM/MF is more patient-friendly than SSG/PM with one less injection per day and a three days shorter treatment and hospitalization duration. This is particularly important since most VL patients are children. Additionally, this alternative treatment removes the risk of SSG-associated life-threatening cardiotoxicity.

The frequency of PKDL in patients from Ethiopia and Sudan was significantly lower in the PM/MF arm (4.4%) than the SSG/PM arm (20.9%); PM/MF would thus support VL control programs by reducing potential transmission reservoirs.

SSG/PM efficacy in this trial was 91.8%, similar to that previously described[10]. Nevertheless, a retrospective analysis of SSG/PM efficacy in MSF routine treatment in South Sudan (2001-2018) indicates a trend of increased relapse rates, not explained by changes in patient characteristics, compliance to treatment or other factors [Naylor-Leyland et al, 2022, submitted]. A prospective study will be performed to better characterize response to treatment in South Sudan. A potential reduction in SSG/PM treatment effectiveness is another reason to bring alternative combination treatments to Eastern Africa.

The preponderance of male patients in this trial is consistent with the particularly low proportion of women of childbearing potential (10% to 19%) amongst VL patients in Eastern Africa[2]. The requirement for a pregnancy test and contraception during treatment and for 5 months afterwards probably contributed to the very low number of adolescent and adult female patients participating in the study, and is an access barrier for this population, especially in Sudan and the West Pokot region. Possible strategies to minimize this barrier should be sought through qualitative research in reproductive health. In addition, access plans in endemic countries may include collection of effectiveness and safety information within routine VL care for this population and the elderly.

Life-threatening haemorrhage is a well-known complication of splenic aspiration, occurring in about 0.1% of individuals [3]. The two deaths associated to this procedure during screening highlights the need to validate and replace current methods with non-invasive parasitological diagnostics and tests of cure for VL.

In conclusion, our results demonstrate that a 14-day PM/MF regimen for VL has a similar efficacy to the standard of care for patients in Eastern Africa. This alternative treatment regimen is associated with a lower frequency of PKDL, has no risk of SSG-associated life-threating cardiotoxicity, and is more patient-friendly. For the longer term, a pipeline of new chemical entities aims to deliver oral treatments that will respond to patients' needs as highlighted in the WHO NTD Roadmap[18].

2.2

Acknowledgments

Doka, Umelkher and Tabarakallah (MSF) in Sudan; and Gondar and Abdurafi (MSF) in Ethiopia. We are thankful to the DND*i* clinical team members Samuel Tesema, Ayub Mpoya, Bonface Kaunyangi Mwarama, Millicent Aketch and Lilian Were, and the Data Management and Biostatistics department, as well as the local consultant clinical monitors in Sudan and Ethiopia; we also thank the Data and Safety Monitoring Board's members. Louise Burrows (DND*i*) drafted the manuscript.

Funding

References

1.   World Health Organization. Global leishmaniasis surveillance: 2019–2020, a baseline for the 2030 roadmap. Wkly Epidemiol Rec 2021;35:401–420. Available at: https://www.who.int/news-room/fact-sheets/detail/. Accessed 22 February 2022.

2.   Harhay MO, Olliaro PL, Vaillant M, et al. Who Is a Typical Patient with Visceral Leishmaniasis? Characterizing the Demographic and Nutritional Profile of Patients in Brazil, East Africa, and South Asia. Am J Trop Med Hyg 2011;84:543–550.

3.   World Health Organization. Control of the leishmaniases. Report of a meeting of the WHO Expert Committee on the Control of Leishmaniases, Geneva, 22–26 March 2010:1–186.

4.   Omollo R, Alexander N, Edwards T, et al. Safety and Efficacy of miltefosine alone and in combination with sodium stibogluconate and liposomal amphotericin B for the treatment of primary visceral leishmaniasis in East Africa: study protocol for a randomized controlled trial. Trials 2011;12:166.

5.   Wasunna M, Njenga S, Balasegaram M, et al. Efficacy and Safety of AmBisome in Combination with Sodium Stibogluconate or Miltefosine and Miltefosine Monotherapy for African Visceral Leishmaniasis: Phase II Randomized Trial. PLoS Negl Trop Dis 2016;10:e0004880.

6.   Dorlo TPC, Kip AE, Younis BM, et al. Visceral leishmaniasis relapse hazard is linked to reduced miltefosine exposure in patients from Eastern Africa: a population pharmacokinetic/pharmacodynamic study. J Antimicrob Chemother 2017;72:3131–3140.

7.   Mbui J, Olobo J, Omollo R, et al. Pharmacokinetics, Safety, and Efficacy of an Allometric Miltefosine Regimen for the Treatment of Visceral Leishmaniasis in Eastern African Children: An Open-label, Phase II Clinical Trial. Clin Infect Dis 2019;68:1530–8.

8.   Palic S, Kip AE, Beijnen JH, et al. Characterizing the non-linear pharmacokinetics of miltefosine in paediatric visceral leishmaniasis patients from Eastern Africa. J Antimicrob Chemother 2020;75:3260–3268.

9.   Hailu A, Musa A, Wasunna M, et al. Geographical Variation in the Response of Visceral Leishmaniasis to Paromomycin in East Africa: A Multicentre, Open-Label, Randomized Trial. PLoS Negl Trop Dis 2010; 4:e709.

10. Musa A, Khalil E, Hailu A, et al. Sodium Stibogluconate (SSG) & Paromomycin Combination Compared to SSG for Visceral Leishmaniasis in East Africa: A Randomised Controlled Trial. PLoS Negl Trop Dis 2012; 6:e1674.

11. Sundar S, Sinha PK, Rai M, et al. Comparison of short-course multidrug treatment with standard therapy for visceral leishmaniasis in India: an open-label, non-inferiority, randomised controlled trial. Lancet (London, England) 2011;377:477–486.

12. Dorlo TPC, Huitema ADR, Beijnen JH, De Vries PJ. Optimal dosing of miltefosine in children and adults with visceral leishmaniasis. Antimicrob Agents Chemother 2012;56:3864–72.

13. Verrest L, Wasunna M, Kokwaro G, et al. Geographical Variability in Paromomycin Pharmacokinetics Does Not Explain Efficacy Differences between Eastern African and Indian Visceral Leishmaniasis Patients. Clin Pharmacokinet 2021;60:1463–1473.

14. Wasunna M, Njenga S, Balasegaram M, et al. Efficacy and Safety of AmBisome in Combination with Sodium Stibogluconate or Miltefosine and Miltefosine Monotherapy for African Visceral Leishmaniasis: Phase II Randomized Trial. 2016;10: e0004880.

15. Goyal V, Mahajan R, Pandey K, et al. Field safety and effectiveness of new visceral leishmaniasis treatment regimens within public health facilities in Bihar, India. PLoS Negl Trop Dis 2018; 12:e0006830.

16. Alves F, Bilbe G, Blesson S, et al. Recent development of visceral leishmaniasis treatments: Successes, pitfalls, and perspectives. Clin Microbiol Rev 2018;31: e00048-18.

17. Paladin Therapeutics. Highlights of Prescribing Information : Impavido, (revised March 2014). 2014. Available at: https://www.accessdata.fda.gov/drugsatfda_docs/label/2014/204684s000lbl.pdf.

18. World Health Organization. Ending the neglect to attain the Sustainable Development Goals: A road map for neglected tropical diseases 2021–2030. 2020. Available at: https://www.who.int/publications/i/item/9789240010352. Accessed 8 June 2021.

2.2

Supplementary material 2.2

A

FEMALE									
HT (cm)	80-89	90-99	100-109	110-119	120-129	130-139	140-149	150-159	160
WT (kg)									
7									
8	30								
9	30								
10	30	40							
11	40	40	40						
12	40	40	40						
13	40	40	40						
14	40	40	40	50					
15	40	40	50	50					
16	40	50	50	50					
17	40	50	50	50	50				
18	50	50	50	50	60				
19	50	50	50	60	60				
20	50	50	50	60	60	60			
21	50	50	60	60	60	60			
22	50	50	60	60	60	60			
23	50	50	60	60	60	70	70		
24	50	50	60	60	60	70	70		
25	50	60	60	60	70	70	70		
26	50	60	60	60	70	70	70	70	
27	50	60	60	70	70	70	70	80	
28	50	60	60	70	70	70	80	80	
29	50	60	60	70	70	70	80	80	
30	50	60	60	70	70	80	80	80	80

RISK OF SEVERE MALNUTRITION

REFER TO THE WHO REFERENCE CURVES

B

MALE									
HT (cm)	80-89	90-99	100-109	110-119	120-129	130-139	140-149	150-159	160
WT (kg)									
7									
8	40								
9	40								
10	40	40							
11	40	40							
12	40	50							
13	50	50	50						
14	50	50	50						
15	50	50	60	60					
16	50	50	60	60					
17	50	60	60	60					
18	50	60	60	60	70				
19	50	60	60	70	70				
20	50	60	60	70	70				
21	60	60	60	70	70	70			
22	60	60	70	70	70	80			
23	60	60	70	70	80	80			
24	60	60	70	70	80	80	80		
25	60	60	70	70	80	80	80		
26	60	70	70	80	80	80	100		
27	60	70	70	80	80	80	100		
28	60	70	70	80	80	100	100	100	
29	60	70	70	80	80	100	100	100	
30	60	70	80	80	100	100	100	100	

RISK OF SEVERE MALNUTRITION
REFER TO THE WHO REFERENCE CURVES

2.2

Figure S2.2.1 Daily allometric miltefosine dose for female (1A) and male (1B) children based on fat-free mass.

Table S2.2.1 Primary efficacy outcome of definite cure with primary imputation by treatment arm for completers.

Analysis set	Statistics	Arm 1 PM/MF 14D	Arm 3 SSG/PM
Completers[1]	n	168	168
	Number cured	154	155
	Efficacy, %	91.7	92.3
	Difference in efficacy[2] (97.5% CI)	0.6 (-6.1; 7.2)	

CI=Confidence interval; D=Day(s); MF=Miltefosine; mITT=Modified intention-to-treat; PM=Paromomycin; PP=Per-protocol; SSG=Sodium stibogluconate. [1]Sensitivity analysis. [2]Difference in efficacy from SSG/PM, i.e., efficacy of SSG/PM minus efficacy of PM/MF14D.

Table S2.2.2 Clinical symptoms and signs of VL at baseline by treatment arm and overall – ITT set.

	Arm 1 PM/MF 14D (n=171)	Arm 2 PM/MF 28D[a] (n=98)	Arm 3 SSG/PM (n=170)	Overall (n=439)
Clinical symptoms				
Fever, n (%)	170 (99.4)	96 (98.0)	170 (100.0)	436 (99.3)
Weight loss, n (%)	135 (78.9)	91 (92.9)	128 (75.3)	354 (80.6)
Loss of appetite, n (%)	115 (67.3)	67 (68.4)	118 (69.4)	300 (68.3)
Abdominal swelling, n (%)	82 (48.0)	69 (70.4)	91 (53.5)	242 (55.1)
Coughing, n (%)	57 (33.3)	37 (37.8)	70 (41.2)	164 (37.4)
Epistaxis, n (%)	22 (12.9)	22 (22.4)	22 (12.9)	66 (15.0)
Diarrhea, n (%)	7 (4.1)	7 (7.1)	4 (2.4)	18 (4.1)
Other bleeding signs, n (%)	0 (0.0)	0 (0.0)	3 (1.8)	3 (0.7)
Clinical signs				
Mucosal pallor, n (%)	125 (73.1)	66 (67.3)	127 (74.7)	318 (72.4)
Inguinal lymphadenopathy, n (%)	80 (46.8)	31 (31.6)	77 (45.3)	188 (42.8)
Other signs, n (%)	113 (66.1)	63 (64.3)	117 (68.8)	293 (66.7)
Splenomegaly, n (%)	*62 (36.3)*	*45 (45.9)*	*68 (40.0)*	*175 (39.9)*
Hepatosplenomegaly, n (%)	*35 (20.5)*	*11 (11.2)*	*37 (21.8)*	*83 (18.9)*
Hepatomegaly, n (%)	*6 (3.5)*	*3 (3.1)*	*5 (2.9)*	*14 (3.2)*
Muscle wasting, n (%)	3 (1.8)	8 (8.2)	3 (1.8)	14 (3.2)
Edema, n (%)	1 (0.6)	1 (1.0)	2 (1.2)	4 (0.9)
Cervical lymphadenopathy, n (%)	2 (1.2)	1 (1.0)	0 (0.0)	3 (0.7)
Axillary lymphadenopathy, n (%)	1 (0.6)	0 (0.0)	1 (0.6)	2 (0.5)
Jaundice, n (%)	0 (0.0)	0 (0.0)	1 (0.6)	1 (0.2)

D = Day(s); ITT = Intention-to-treat; MF = Miltefosine; PM = Paromomycin; SSG = Sodium stibogluconate.
[a]Recruitment into Arm 2 was discontinued.

Supplementary Text 2.2.1. Additional information

Revision of exclusion criteria

Since 30-40% of patients in Ethiopia were excluded due to severe malnutrition, an Ethiopia-specific amendment was implemented to modify the indicator for severe malnutrition from body mass index to mid-upper arm circumference. Individual laboratory parameters (white blood cells, platelets, ALT/AST, bilirubin and creatinine) in the exclusion criteria were replaced by one criteria involving investigator judgement for liposomal amphotericin B (LAmB) therapy based on the severity of the clinical manifestations of the disease and laboratory parameters.

Exhaustive list of inclusion and exclusion criteria

Patients had to meet all of the following inclusion criteria to be eligible for enrolment into the study:

- Clinical signs and symptoms of visceral leishmaniasis (VL) and confirmatory parasitological microscopic diagnosis
- Aged 4 to ≤50 years and able to comply with the study protocol
- Provided written informed consent (if aged 18 years and over) or signed by parents or legal guardian for patients under 18 years of age. In the case of minors, assent from the children also had to be obtained as per each country's regulatory requirements.

2.2

The presence of any of the following excluded a patient from study enrolment:

- Relapse
- Para-kala-azar dermal leishmaniasis Grade 3
- Any anti-leishmanial drugs in the last 6 months
- Severe malnutrition (for children aged <5 years: weight-for-height WHO reference curves by sex z-score <-3; for patients aged 5 to 18 years: body mass index [BMI]-for-age WHO reference curves by sex z-score <-3; for adults >18 years: BMI <16). For Ethiopia only, patients with severe malnutrition (for patients aged 4 to 18 years: mid-upper arm circumference (MUAC) cut-off based on MUAC-for-height reference table; for patients >18 years: MUAC <170mm)
- Positive HIV diagnosis
- Previous history of hypersensitivity reaction or known drug class allergy to any of the study treatment
- Previous history of cardiac arrhythmia or with a clinically significant abnormal electrocardiogram
- Concomitant severe infection such as tuberculosis, schistosomiasis, or any other serious underlying disease (e.g., cardiac, renal, hepatic) or chronic condition which would preclude evaluation of the patient's response to study medication

- Pregnant or lactating women
- Female patients of childbearing age who do not agree to have a pregnancy test done at screening and/or who do not agree to use contraception from the treatment period until 5 months after the end of treatment (EOT)
- Haemoglobin <5g/dL
- Severe VL according to Investigator's judgement, requiring an indication for liposomal amphotericin B (LAmB) therapy based on the clinical manifestations (such as jaundice, bleeding, oedema) and clinically significant abnormalities in the following laboratory parameters: haemoglobin, white blood cells (WBCs), platelets, liver enzymes (ALT and AST), total bilirubin, and creatinine
- Pre-existing hearing loss based on audiometry at baseline
- Unable to comply with the planned scheduled visits and procedures of the study protocol.

Rescue treatment

If treatment had to be interrupted for >72 hours due to an adverse event (AE) related to miltefosine (MF), or if treatment had to be interrupted permanently due to an AE related to PM or sodium stibogluconate (SSG), rescue treatment had to be considered. In case of treatment failure or intolerability (when treatment had to be permanently interrupted), rescue treatment was provided to the patient at the discretion of the study physician/Investigator and based on the national VL treatment guidelines.

For patients in Arms 1 and 2, rescue treatment was planned to be SSG/PM (SSG 20 mg/kg/day IV/IM QD, PM 15 mg/kg/day IM QD, for 17days) or LAmB at multiple doses (3 to 5mg/kg/day IV QD for 6 to 10 days, up to 30mg/kg total dose) according to national treatment guidelines in each country. In Arm 3, rescue treatment was planned to be LAmB at multiple doses (3 to 5mg/kg/day IV QD for 6 to 10days, up to 30mg/kg total dose).

Patients were to be given rescue treatment if they had:
- Failed to respond to PM/MF treatment or to SSG/PM reference treatment within the treatment period (lack of improvement or worsening of the clinical signs and symptoms of VL)
- Failed to respond to PM/MF treatment or to SSG/PM reference treatment at the EOT assessments (Day 28). This was to be reflected by positive parasitological assessment and/or lack of improvement or worsening of the clinical signs and symptoms of VL
- Failed to tolerate study treatment/occurrence of AE(s) during receipt of study treatment that required permanent treatment interruption, and rescue treatment was indicated by the Investigator

- Relapsed, i.e., experienced recurrence of symptoms, signs, and presence of parasites after EOT (Day 28) during the follow-up
- Developed severe post-kala-azar dermal leishmaniasis (PKDL) that necessitated rescue treatment

Intensive pharmacokinetics sampling

PM pharmacokinetics (PK) assessments was performed only in the intensive cohort (subset of patients in MF/PM combination arms) at Screening, Day 1, and Day 14.

PK samples for PM on D1 and D14 were collected at 0, 1, 2, 4, 8, and 24 hours post-dose.

In order to minimize blood volume collected, each patient was randomly allocated to one of the following sparse PK sampling schedules:

D1: either 1, 2, 4, and 24h or 1, 2, 8, and 24h.

D14 (arm 1 and 2): either 0, 1, 2, 4, and 24h or 0, 1, 2, 8, and 24h.

PK samples for MF on D1 and D14 were collected at the same time points as PK samples for PM at 0, 1, 2, 4, 8 and 24h (according to the sparse sampling scheme to which the patient was allocated).

2.2

Measurement of compliance

For arms 1 and 2, in-patient administration of MF was directly observed; compliance was expected to be 100%, unless the patient vomited and could not tolerate re-administration. SSG and PM were administered by study staff. During the 14 days of outpatient treatment for patients in arm 2, compliance was assessed by collecting the empty blisters at the Day 28 visit and checking for any unused drug.

Compliance was assessed as the relationship between overall administered dose of study drug in relation to the expected overall dose to be administered over the treatment period. Compliance was further assessed through cross-checks with PK data. Full compliance was assumed if 90-110% of the prescribed dose were administered.

Chapter 2.3

Population pharmacokinetics of a combination of miltefosine and paromomycin in Eastern African children and adults with visceral leishmaniasis

Luka Verrest, Ignace C. Roseboom, Monique Wasunna, Jane Mbui, Ahmed Musa, Joseph Olobo, Rezika Mohammed, Koert Ritmeijer, Alwin D.R. Huitema, Alexandra Solomos, Fabiana Alves, Thomas P.C. Dorlo

Abstract

Introduction: To improve visceral leishmaniasis treatment in Eastern Africa, 14- and 28-day combination regimens of paromomycin plus allometrically dosed miltefosine were evaluated. As the majority of patients affected by VL are children, adequate pediatric exposure to miltefosine and paromomycin is key to ensure good treatment response.

Methods: Pharmacokinetic data was collected in a multi-center randomized controlled trial in VL patients from Kenya, Sudan, Ethiopia and Uganda. Patients received paromomycin (20 mg/kg/day for 14 days) plus miltefosine (allometric dose for 14 or 28 days). Population pharmacokinetic models were developed. Adequacy of exposure and target attainment of paromomycin and miltefosine was evaluated in children and adults.

Results: Data from 265 patients (59% ≤12 years) were available for this pharmacokinetic analysis. Paromomycin exposure was lower in pediatrics compared to adults (median (IQR) end-of-treatment AUC_{0-24h} 187 (162-203) and 242 (217-328) µg·h/mL, respectively), but were both within the inter-quartile range of end of treatment exposure in Kenyan and Sudanese adult patients from a previous study. Cumulative miltefosine end-of-treatment exposure in pediatrics and adults (AUC_{d0-28} 517 (464-552) and 524 (456-567) µg·day/mL, respectively) and target attainment (time above the *in vitro* susceptibility value EC_{90} 27 (25-28) and 30 (28-32) days, respectively) was comparable to previously observed values in adults.

Conclusion: Paromomycin and miltefosine exposure in this new combination regimen corresponded to the desirable levels of exposure. Moreover, the lack of a clear exposure-response and exposure-toxicity relationship indicated adequate exposure within the therapeutic range in the studied population, including pediatrics.

1.   Introduction

Visceral leishmaniasis (VL), a potentially fatal disease caused by the *Leishmania* parasite, is endemic in Eastern Africa[1], where effective, safe, and affordable treatments are still lacking. Children are the mainstay of the population affected by VL, particularly in Eastern Africa, a vulnerable and often malnourished population that has higher risk of failure to VL treatment. Paromomycin and miltefosine are favorable treatment options because of their relatively good safety profile and suitability for use in remote areas. However, earlier studies with paromomycin or miltefosine monotherapy, or a combination with other drugs, resulted in unsatisfactory efficacy in Africa, with high geographical variability[2-5]. A combination therapy of miltefosine and paromomycin was shown to be highly effective in Asia (96.9-98.7% cure rate)[6]. In Eastern Africa, an adapted 14-day regimen of paromomycin (20 mg/kg/day) plus miltefosine (BID allometric dose) was recently shown to exhibit a satisfactory cure rate of 91.2%[7]. This regimen is favorable over the current first line therapy (a 17-day combination therapy of sodium stibogluconate plus paromomycin), as it requires 3 days less hospitalization, and reduces one daily painful injection or avoids IV drug administrations. More importantly, this will be the first combination therapy for VL in Eastern Africa without an antimonial drug component, reducing the risk of fatal toxicities such as antimony-associated cardiotoxicity and pancreatitis.

2.3

Pharmacokinetic studies have been performed to evaluate whether the lower treatment response to paromomycin and miltefosine in Africa was caused by underexposure to the drugs and whether dose adaptations would be warranted for Eastern African patients. A previous pharmacokinetic study of paromomycin in Eastern African and Indian VL patients revealed important geographical differences in paromomycin exposure, although drug efficacy could not be linked to differences in drug exposure[8]. While in India a paromomycin dose of 15 mg/kg/day for 21 days is effective, an adapted regimen of 20 mg/kg/day for 21 days in Eastern Africa has been used[7,9], suggesting a different exposure-response relationship between the populations. Miltefosine monotherapy treatment failure using the conventional miltefosine mg/kg dosing regimen for 28 days in Kenya and Sudan has been associated with low drug exposure in pediatrics[3,10]. The time above the *in vitro* intracellular susceptibility of 90% maximal effective concentration of miltefosine (EC_{90}) has been identified as a predictor for VL relapse in Eastern African VL patients[10]. An adapted allometric miltefosine dose for 28 days in pediatrics led to increased and less variable exposure, with adequate exposure, pharmacokinetic target attainment and satisfactory efficacy of 90%, equivalent to adults[11].

Whereas underexposure to the drugs can lead to poor treatment efficacy, overexposure could lead to drug-induced complications, such as liver toxicity (miltefosine), renal toxicity or ototoxicity (paromomycin). For miltefosine, an exposure-

response relationship has clearly been demonstrated[3,10]. An exposure-response relationship of paromomycin has not been demonstrated, however, the initial lack of paromomycin efficacy appears to be exposure-driven, as a dose increase from 15 mg/kg to 20 mg/kg led to improved efficacy[5,12]. Although paromomycin efficacy did not appear to differ between adults and children[5], paromomycin exposure in children and adults has not been compared so far. As the majority of patients affected by VL are children, adequate and similar exposure to miltefosine and paromomycin in children compared to adults is key to ensure good treatment response in the whole VL population. Therefore, we aimed to evaluate target attainment and adequacy of exposure of the adapted miltefosine plus paromomycin combination treatment regimens in Eastern African children and adults with VL using a population pharmacokinetic approach, in addition to exploring exposure-efficacy/toxicity relationships.

2.   Methods

2.1   Study design and patients

Pharmacokinetic data were collected in patients from an open label, Phase III, randomized controlled multicenter non-inferiority trial in VL patients in Eastern Africa[7] (NCT03129646). Patients in the investigational arms received a combination of paromomycin for 14 days plus miltefosine for 14 days (PM+MF14D) or paromomycin for 14 days plus miltefosine for 28 days (PM+MF28D). The study was conducted at seven clinical trial sites, with pharmacokinetic data available from six sites: Kacheliba, Kenya; Amudat, Uganda; Doka and Um El Kher in Sudan; Gondar and Abdurafi in Ethiopia. Patients aged 4 to ≤50 years with VL symptoms and parasitological diagnosis were included. Patients were excluded when they had relapse, severe malnutrition, severe VL, positive HIV diagnosis or concomitant severe infection, or were women with childbearing potential unwilling to use contraception. Other inclusion and exclusion criteria have been described previously[7]. Ethical approval was obtained from independent ethics committees in Sudan, Kenya, Uganda, and Ethiopia and from the Médecins Sans Frontières' Ethics Review Board. Informed consent was obtained per regulatory requirements in each country.

2.2   Study medication

Paromomycin (Gland Pharma, India) and miltefosine (Paladin labs and Knight Therapeutics Inc.) were administered simultaneously, both starting at Day 1. Patients received a once-daily intramuscular injection of 20 mg/kg/day paromomycin sulphate (equivalent to 15 mg/kg/day paromomycin base) for 14 days and oral miltefosine BID for 14 days (PM+MF14D) or 28 days (PM+MF28D). Children <30 kg received an

allometric dosing of miltefosine based on sex, weight and height (Supplementary Figure S2.3.1), patients ≥30 kg to <45 kg received 100 mg/day, and patients ≥45 kg received 150 mg/day. When patients vomited within 30 minutes after miltefosine administration, they received a miltefosine re-dose.

2.3   Sample collection and bioanalysis

Miltefosine plasma concentrations were measured in patients at Day 14 (PM+MF14D arm only), Day 28 and Day 56 (PM+MF14D and PM+MF28D). More intensive pharmacokinetic sampling for both paromomycin and miltefosine was performed in a subset of patients from Kenya and Sudan who consent to participate to the intensive sampling cohort, with EDTA blood plasma samples collected at 0, 1, 2, 4, and 24h, or at 0, 1, 2, 8, and 24h at Day 1 and Day 14. Paromomycin and miltefosine were analyzed using FDA/EMA validated liquid chromatography-tandem mass spectrometry (LC-MS/MS) bioanalytical assays[13,14]. The lower limit of quantification was 5 ng/mL for paromomycin and 4 ng/mL for miltefosine.

2.4   Population pharmacokinetic analysis

A population approach was applied to model paromomycin and miltefosine plasma concentrations, using the nonlinear mixed effects modelling software NONMEM (version 7.5, ICON Development Solutions, USA). Data management, model evaluation and graphical analysis were performed using R (version 4.1.2), Perl-speaks-NONMEM (PsN, version 5.2.6), and the graphical interface Pirana (version 3.0.0). Model development was initiated based on previously published population pharmacokinetic models of paromomycin and miltefosine in (pediatric) Eastern African VL patients[8,15].

Model development was carried out in four consecutive steps: 1) Re-evaluation of the initial structural model, 2) re-evaluation of the initial stochastic model, 3) selected covariate analysis, and 4) model evaluation. In the paromomycin structural model, the presence of a second compartment was evaluated, as well as a decrease in paromomycin clearance after start of treatment, as described previously[8]. In the paromomycin structural model, relative bioavailability was fixed to 1.17, for comparability to previously obtained parameter estimates from Sudanese and Kenyan patients[8]. In the miltefosine structural model, the presence of a lower bioavailability at start of treatment and stagnation in miltefosine accumulation associated with increased cumulative dose was evaluated, as described previously[15]. In the stochastic models, between-subject variability (BSV) on all parameters was evaluated, and was implemented assuming a log-normal distribution (eq. 1). Residual variability was implemented using a proportional error model (eq. 2).

$$P_i = P_{pop} * e^{\eta_i}$$

Eq. 1

$$Y_{i,j} = C_{i,j} * (1 + \varepsilon)$$

Eq. 2

where P_i is the individual parameter estimate for an individual i, P_{pop} is the population estimate for a parameter, and η_i the BSV of the ith individual, assumed to be distributed N $(0, \omega^2)$. $Y_{i,j}$ is the observed concentration and $C_{i,j}$ is the predicted concentration for observation j of individual i, and ε is the residual error, distributed N $(0, \sigma^2)$.

2.5 Covariate analysis

Body weight was maintained as a covariate in the paromomycin and miltefosine models, with fixed allometric exponents of 0.75 for clearance, and 1 for volume of distribution. Selection of other covariates was based on physiological plausibility and graphical inspection of covariate-parameter relationships, and were tested univariately in the model. eGFR unadjusted to typical body surface area (BSA) (16), here referred to as absolute eGFR (eGRF$_{abs}$) (eq.3), was evaluated on paromomycin clearance, as the drug is mainly cleared renally[17].

$$eGFR_{abs} = \frac{eGFR}{1.73} * BSA$$

Eq. 3

Specific formulas to estimate GFR in African or other malnourished populations are lacking[18]. For adults, the Chronic Kidney Disease Epidemiology Collaboration (CKD-EPI) formula[19] without the adjustment for ethnicity was previously suggested for this population[14], which was used here for adults and adolescents >14 years old[20]. For children ≤14 years old, the Schwartz formula was used as previously suggested[21]. Clearance was also evaluated as a fraction of eGFR$_{abs}$, where renal clearance is assumed to be the only route of elimination, or in combination with a nonrenal clearance route. Furthermore, neutropenia has been associated with an increased clearance and sometimes increased volume of distribution of several aminoglycosides[22,23], and therefore an inverse correlation between serum neutrophils and paromomycin clearance and volume of distribution was evaluated. Likewise, an inverse correlation between serum albumin and paromomycin volume of distribution was evaluated, as this has been observed in patients with hematological malignancies treated with other aminoglycosides[24-27]. After the inclusion of the above-mentioned covariates, a potential remaining population difference between countries was evaluated on paromomycin bioavailability, absorption rate, volume of distribution and clearance. Time was evaluated on paromomycin clearance to investigate a change in clearance over time, not explained by the included covariates.

A decrease in miltefosine bioavailability at the start of treatment might be related to disease severity and/or malnutrition, as patients are severely ill, often combined with anemia, leukopenia and malnourishment, when they start VL treatment. Evaluated covariates that might represent disease severity included the number of *Leishmania* parasites in either spleen, bone marrow or lymph nodes (expressed by a microscopy score ranging from 0 to 6) at start of treatment, serum albumin, neutrophil levels and

total white blood cell levels, and covariates representing nutritional status included BMI for patients from 19 years old, and height-for-age and BMI-for-age Z-scores for patients up to 19 years old. Malnutrition Z-scores were derived using the R package "zscorer", based on the WHO Child Growth Standards.

Continuous covariates were normalized to the median value in the population and included using a linear relationship (Eq. 4).

$$P_{TV} = P_{pop} * (1 + (Cov_{i,t} - Cov_{med}) * l)$$

Eq. 4

where P_{TV} is the typical parameter value at covariate value $Cov_{i,t}$, P_{pop} the population estimate of this parameter, $Cov_{i,t}$ the covariate value for individual i at time t, Cov_{med} the median covariate value in the population, and l the slope factor. Exponential and power functions were also evaluated. Categorical covariates were tested as proportional changes relative to the reference category.

2.6   Model selection and evaluation

Model selection was based on scientific plausibility, minimum objective function value (OFV), goodness-of-fit (GoF) plots, and precision of parameter estimates. A significance level of $P<0.01$ in a likelihood ratio test was considered statistically significant. Predictiveness of the final models was evaluated by a visual predictive check (VPC), stratified per treatment arm. Precision in parameter estimates was obtained by sampling importance resampling (SIR)[28].

2.3

2.7   Exposure and target attainment

Paromomycin exposure in children and adults was derived using the final individual maximum a priori Bayesian pharmacokinetic model estimates (obtained by the POSTHOC option in NONMEM), expressed by the area under the plasma concentration-time curve (AUC) for 24 hours determined on Day 1 ($AUC_{0-24,d1}$) and Day 14 ($AUC_{0-24,d14}$). Paromomycin exposure was compared to previously reported AUCs on Day 21 in VL patients from Kenya and Sudan, in which the majority of patients were adults, receiving paromomycin monotherapy (20 mg/kg/day) for 21 days[8]. Miltefosine exposure was represented by the AUC from Day 1 until Day 7, Day 21, and Day 210 (AUC_{d0-7}, AUC_{d0-21}, AUC_{d0-210}, respectively), and the time that the miltefosine concentration was over the *in vitro* susceptibility value EC_{90} (Time >EC_{90}), equivalent to 10.6 µg/mL[10]. Exposure parameters were derived in children and adults and compared to previously reported adult exposure following a conventionally dosed monotherapy dosing regimen[10]. Furthermore, miltefosine exposure and target attainment was compared in relation to clinical efficacy (final cure determined 6 months after the end of treatment versus relapse of disease between end of treatment and 6 months follow-up), and the relationship of paromomycin exposure and occurrence of renal toxicity and ototoxicity was explored.

Table 2.3.1 Patient characteristics.

	Intensive PK sampling			Sparse PK sampling				
	Kenya	Sudan	Total	Kenya	Sudan	Ethiopia	Uganda	Total
Subjects (n)	18	8	26	68	96	59	16	239
Male (n [%])	14 (78)	7 (88)	21 (81)	51 (75)	73 (76)	58 (98)	11 (69)	193 (80)
Age (years)[a]	14.7 (7-35)	11.8 (9-15)	13.8 (7-35)	9.7 (4-30)	10.5 (4-45)	23.4 (14-40)	12.6 (5-35)	13.6 (4-45)
Pediatrics ≤12 yrs (%)	61	63	62	75	81	0	69	59
Body weight (kg)[a]	34.7 (20.5-54)	31.1 (25-52)	33.6 (20.5-54)	26.4 (13.5-53.5)	27.3 (11-70)	49.1 (28.5-61.0)	34.3 (14.5-71.0)	32.9 (11.0-71.0)
BMI[a,b]	17.4 (16.7-18.9)	NA	17.4 (16.7-18.9)	18.3 (17.5-19.4)	19.0 (17.2-21.3)	17.4 (14.6-20.2)	18.9 (17.0-20.8)	17.7 (14.6-21.3)
HAZ[a,c]	-0.07 (-2.3 - 2.7)	-0.9 (-3.1 - 1.7)	-0.4 (-3.1 - 2.7)	-0.3 (-4.2 - 3.3)	-0.8 (-4.1 - 2.8)	-1.7 (-4.2 - 0.3)	0.2 (-3.5 - 3.3)	-0.6 (-4.2 - 3.3)
BAZ[a,c]	-1.6 (-2.6 - 0.9)	-1.5 (-2.7 - -0.8)	-1.6 (-2.7 - 0.9)	-1.6 (-2.9 - 0.8)	-1.3 (-3.1 - 2.3)	-2.0 (-2.8 - -1.2)	-1.6 (-2.9 - 2.0)	-1.5 (-3.1 - 2.3)
Creatinine[a] (mg/dL)	1.0 (0.3-1.4)	0.5 (0.3-0.8)	0.8 (0.3-1.4)	1.0 (0.3-1.3)	0.6 (0.1-1.3)	0.8 (0.5-1.1)	0.9 (0.4-1.5)	0.8 (0.1-1.5)
Absolute eGFR[a] (mL/min)	55.8 (28.8-110.3)	83.7 (41.7-135.0)	64.4 (28.8-135.0)	40.1 (14.9-122.2)	68.8 (18.4-288.1)	107.0 (61.9-151.1)	51.5 (17.9-100.4)	68.9 (14.9-288.1)
Albumin[a] (g/L)	29.9 (20.8-49.7)	26.7 (22.5-32.4)	28.9 (20.8-49.7)	31.4 (12.9-54.6)	28.0 (16.0-54.0)	27.0 (1.5-50.0)	22.2 (14.6-45.8)	28.3 (1.5-54.6)
Neutrophils[a] (cells/µL)	0.92 (0.54-1.64)	1.51 (0.92-3.33)	1.10 (0.54-3.33)	0.92 (0.22-2.9)	1.4 (0.22-2.9)	0.87 (0.17-4.3)	1.2 (0.39-2.1)	1.11 (0.17-4.3)

BAZ: BMI for age Z-score; BMI: body mass index; HAZ: height for age Z-score; NA: not available. [a] Mean (range) at baseline; [b] For patients >19 years old (n=67); [c] For patients ≤ 19 years old (n=198).

3.   Results

3.1   Patients and data

Data from in total 265 patients (232 paromomycin observations and 927 miltefosine observations), of which 59% were pediatric patients ≤12 years old, were available for the pharmacokinetic analysis, with intensive paromomycin and miltefosine pharmacokinetic sampling in 26 patients (Figure S2.3.2 and S2.3.3 in Supplemental Material, Table 2.3.1 and Table 2.3.2). Longitudinal serum creatinine, albumin and neutrophil levels were available for all patients until the end of follow-up (Supplementary Figure S2.3.4 and S2.3.5). Albumin and neutrophil levels were low at start of treatment (IQR 23.4-32.4 g/L and 0.74-1.38 $*10^3$ cells/μL), but levels increased during treatment, as expected. Three paromomycin observations were excluded from the analysis because the quantification was not reliable (n=1), and because trough samples at Day 1 were taken after the next dose was administered (n=2). There were no paromomycin observations below the limit of quantification (BLQ). Seventeen miltefosine observations were excluded from the analysis, including observations that were physiologically implausible and therefore unreliable (n=3), and BLQ observations (n=14, 2.8% of miltefosine observations). In case of vomiting after miltefosine dosing, the dose before vomiting was excluded and the re-dose was included in the dataset (n=20).

2.3

3.2   Population pharmacokinetic models

A two-compartment model with first-order absorption best described paromomycin pharmacokinetics (Table 2.3.3, Figure 2.3.1). A decrease in clearance over time was observed, which was significantly associated with the increase in plasma neutrophils over time (dOFV -19.9), corresponding to a 13% decrease in clearance for each increase in neutrophils of $1*10^3$ cells/μL. A typical VL patient with a neutrophil level of $1.0*10^3$ cells/μL at start of treatment and $2.5*10^3$ cells/μL at the end of treatment would have a corresponding decrease in paromomycin clearance from 2.61 L/h to 2.10 L/h. Age or country of origin could not explain remaining variability in any of the pharmacokinetic parameters on top of the identified covariates, and eGFR$_{abs}$ could not significantly explain variability in clearance. The final paromomycin model including covariates could adequately describe the change in pharmacokinetics over time, shown by the VPC stratified for the first and last day of paromomycin treatment (Figure 2.3.2).

Table 2.3.2 Data summary.

	Intensive PK sampling			Sparse PK sampling		
	PM+MF14D[b]	PM+MF28D[b]	Total	PM+MF14D[b]	PM+MF28D[b]	Total
Subjects (*n*)[a]	23	3	26	145	94	239
Paromomycin observations (*n*)[a]	202	27	229	0	0	0
Paromomycin observations BLQ (*n*)	0	0	0	0	0	0
Miltefosine observations (*n*)[a]	271	38	309	413	188	601
Miltefosine observations BLQ (*n*)	14	0	14	0	0	0

[a] Subjects and observations after exclusion of unreliable data; [b] PM+MF14D: Paromomycin 14 days + miltefosine 14 days, PM+MF28D: Paromomycin 14 days + miltefosine 28 days.

Miltefosine was best described by a two-compartment model with first-order absorption (Table 2.3.4, Figure 2.3.3, Figure 2.3.4), including two non-linearities influencing bioavailability. Similar to the previous study, bioavailability was 65% (95%CI 57%-73%) lower during the first week of treatment (dOFV -196), and this decrease was highly variable between patients (BSV 74.8% [95%CI 62.0-90.3]). As previously described, miltefosine accumulates over time due to the slow absorption and elimination half-life, reaching higher exposure at the end of therapy (Supplementary Figure S2.3.3). A decrease in miltefosine bioavailability was also related to increased miltefosine exposure over time, represented by the total administered miltefosine dose, resulting in stagnation in miltefosine accumulation in plasma in the third week of treatment. For example, when a typical patient of 35 kg received 100 mg/day miltefosine, bioavailability was 21% lower on Day 28. No other covariates could be identified to explain the non-linear effects on bioavailability.

Table 2.3.3 Parameter estimates of the final paromomycin pharmacokinetic model.

	Estimate	95% CI[a]	Shrinkage (%)
Population parameters[b]			
Cl (L/h)	2.62	2.08-3.25	
V_c, (L)	9.17	8.42-9.92	
Q	0.26	0.22-0.31	
V_p (L)	6.55	4.58-9.58	
k_a (h^{-1})	2.05	1.55-2.92	
F1	1.17 (fixed)		
$COV_{Cl,neutr}$[c] (fractional change /10^3 cells/ μL)	-0.13	-0.16 - -0.10	
Between-subject variability			
Cl (CV%)	56.1	44.1-76.6	0.0
Residual variability			
Proportional error (CV%)	53.4	50.9-56.5	4.9

$$Cl_{TV} = Cl_{pop} * \left(\frac{WT_{i,t}}{WT_{med}}\right)^{0.75} * (1 + (NEUTR_i - NEUTR_{med}) * COV_{Cl,neutr})$$

$$V_{d,TV} = V_{d,pop} * \left(\frac{WT_{i,t}}{WT_{med}}\right)^{1.00}$$

CI: confidence interval; Cl: apparent oral clearance; COV: covariate factor; F1: bioavailability; k_a: absorption rate constant; NEUTR: neutrophils (·10^3 cells/μL); NEUTR$_{med}$: median population neutrophils (0.98 ·10^3 cells/μL); Q: intercompartmental clearance; V_c: central volume of distribution; V_p: peripheral volume of distribution; WT: body weight (kg); WT$_{med}$: median population body weight (27.5 kg). [a] Obtained by SIR; [b] Parameter values relative to a bioavailability of 1.17; [c] Cl decreases by 13% per 1·10^3 cells/μL increase of neutrophils.
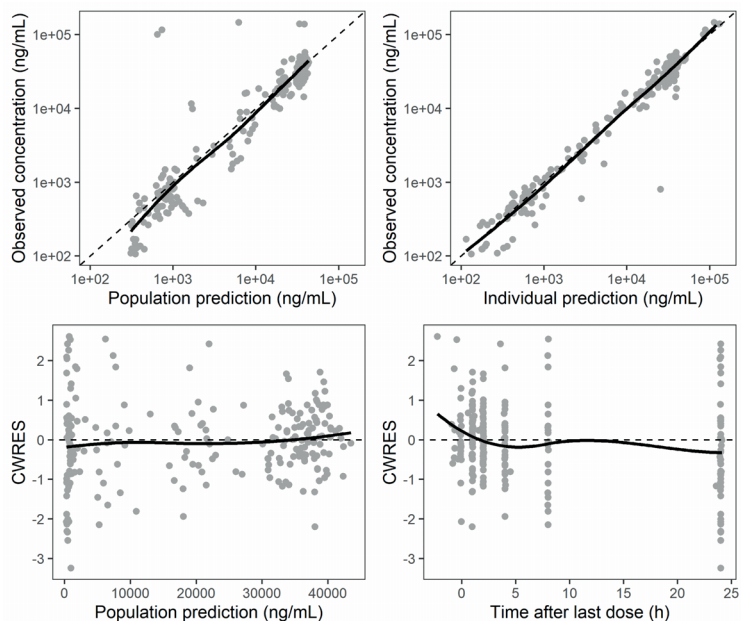
Figure 2.3.1 Goodness-of-fit plots for the final paromomycin pharmacokinetic model. (a) Observed versus population predicted paromomycin concentrations, (b) observed versus individually predicted paromomycin concentrations, (c) conditional weighted residuals (CWRES) versus population predicted concentrations, and (d) CWRES versus time after last dose.

2.3
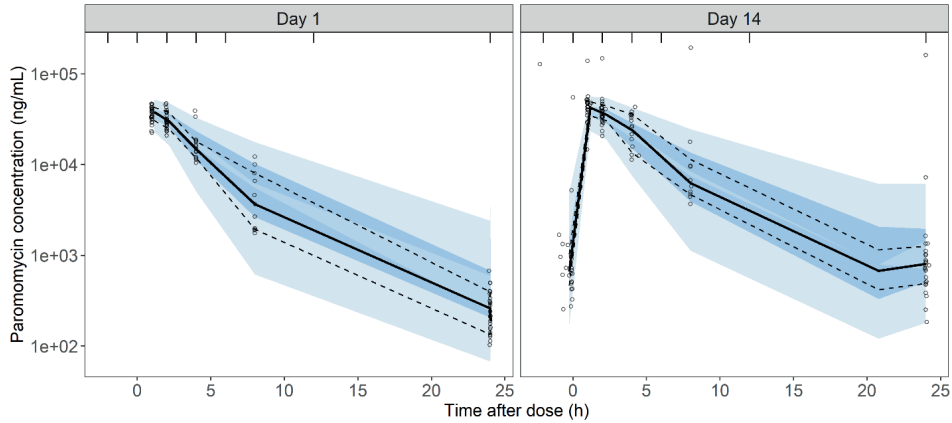
Figure 2.3.2 Prediction corrected visual predictive checks of the final paromomycin pharmacokinetic model. The solid lines represent the median of the observed values, the dashed lines the 20th and 80th percentiles of the observed values. The dark and light blue areas indicate the 90% confidence intervals of the simulated median and percentiles, based on 1000 simulations.

Table 2.3.4 Parameter estimates of the final miltefosine pharmacokinetic model.

	Estimate	95% CI[a]	Shrinkage (%)
Population parameters			
Cl (L/day)	1.85	1.75-1.94	
V_c (L)	13.6	12.8-14.4	
Q (L/day)	0.17	0.13-0.21	
V_p (L)	2.22	1.96-2.59	
k_a (day^{-1})	0.037	0.86-0.91	
F1	1 (fixed)		
COV $_{F,W1}$[b] (fractional change)	-0.65	-0.57 - -0.73	
COV $_{F,CD}$[c] (exponent of power relationship)	-2.40	-3.79 - -1.21	
Between-subject variability			
Cl (CV%)	16.3	14.3-18.5	14
COV $_{F,W1}$ (CV%)	74.8	62.0-90.3	48
Residual variability			
Proportional error (CV%)	31.5	29.7-33.6	14

$$Cl_{TV} = Cl_{pop} * \left(\frac{FFM_{i,t}}{FFM_{med}} \right)^{0.75}$$

$$V_{TV} = V_{pop} * \left(\frac{FFM_{i,t}}{FFM_{med}} \right)^{1.00}$$

$$F_{TV} = F_{pop} * (1 - COV_{F,W1}) * \left(\frac{CD_{i,t}}{CD_{med}} \right)^{COVF,CD}$$

[a] Obtained by SIR; [b] Fractional change in F. Applies during the first week; [c] Exponent of power relationship between cumulative dose and F. Applies after a cumulative dose of 60 mg/kg is reached. CI: confidence interval; Cl: apparent oral clearance; CD: cumulative miltefosine dose (mg/kg); COV: covariate factor; F1: bioavailability; FFM: fat-free mass; ka: absorption rate constant; Q: intercompartmental clearance; RSE: relative standard error; V_c: central volume of distribution; V_p: peripheral volume of distribution.
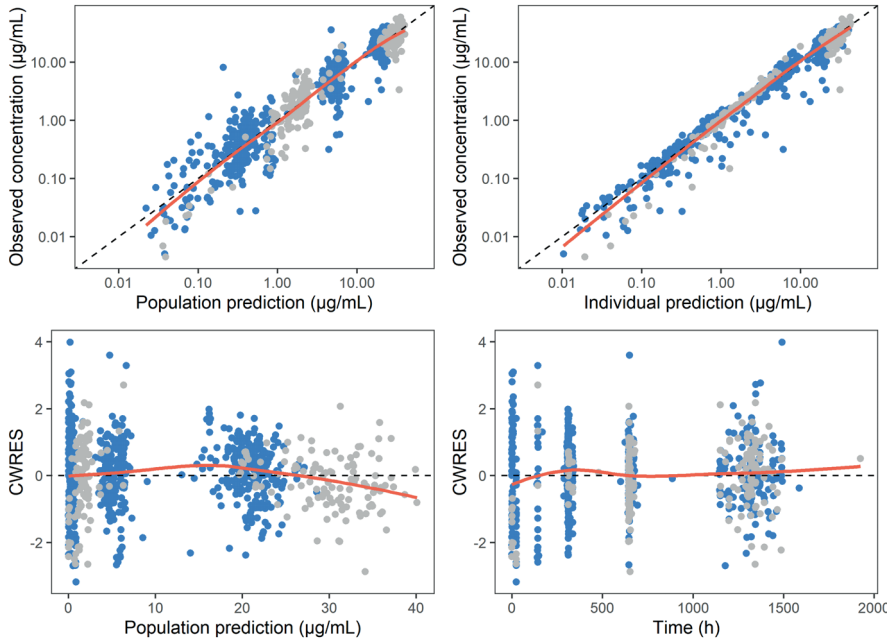
Figure 2.3.3 Goodness-of-fit plots for the final miltefosine pharmacokinetic model, colored by treatment arm. (a) Observed versus population predicted paromomycin concentrations, (b) observed versus individually predicted paromomycin concentrations, (c) conditional weighted residuals (CWRES) versus population predicted concentrations, and (d) CWRES versus time after last dose. Blue dots: Treatment arm 1 (miltefosine dosing for 14 days); grey dots: treatment arm 2 (miltefosine dosing for 28 days).

2.3
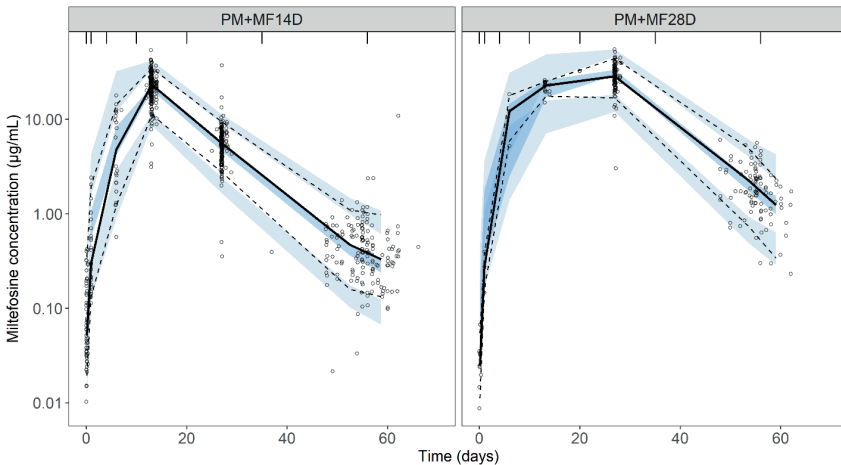
Figure 2.3.4 Prediction corrected visual predictive checks of the final miltefosine pharmacokinetic model. The solid lines represent the median of the observed values, the dashed lines the 5th and 95th percentiles of the observed values. The dark and light blue areas indicate the 90% confidence intervals of the simulated median and percentiles, based on 500 simulations.

3.3 Paromomycin and miltefosine exposure and exposure-response relationships

At the end of treatment, paromomycin exposure ($AUC_{0-24,d14}$) was lower in children compared to adults (Table 2.3.5). However, paromomycin exposure of all individuals, including pediatrics, was within the inter-quartile range (IQR) of end of treatment exposure in Kenyan and Sudanese patients of the previous study[8], in which the majority of patients were adults (Figure 2.3.5). Miltefosine exposure during treatment was comparable between children and adults, although AUC_{d0-210} and Time > EC_{90} were slightly higher in adults (Table 2.3.6). Miltefosine exposure (AUC_{d0-28}) in both adults and pediatrics was within the IQR of adult patients of the previous study[10], when receiving 28 days miltefosine (Figure 2.3.6). Miltefosine target attainment (Time > EC_{90}) in adults (IQR 28-32 days) was within the previously observed IQR in adults (IQR 27-34 days), and numerically lower in pediatrics (IQR 25-28) (Figure 2.3.7).

There were only 12 patients in the investigational regimen arms (PM+MF14D and PM+MF28D), with relapses happening between Day 68 and Day 228. Only pharmacokinetic data of miltefosine was available for these patients. There was no obvious correlation between miltefosine exposure at Day 7, Day 28 or Day 210 or target attainment (Time > EC_{90}) and clinical outcome (Supplementary Figure S2.3.6).

Twenty patients treated with paromomycin experienced ototoxicity. Paromomycin pharmacokinetic data was available for only two of these patients. One of these patients had extremely high paromomycin exposure on Day 14 due to renal failure ($AUC_{0-24,d14}$ 2388 µg·h/mL compared to a median $AUC_{0-24,d14}$ of 202 µg·h/mL), which explains the occurrence of severe ototoxicity. The other patient had a regular $AUC_{0-24,d14}$ of 297 µg·h/mL, presenting mild hypoacusis (left and right hear) at Day 28 visit, which resolved completely at Day 56.

Table 2.3.5 Paromomycin exposure at the first and last day of treatment.

	Paromomycin exposure (AUC_{0-24}[a])		
Treatment day	Children[b] (n=16)	Adults[b] (n=10)	Total (n=26)
1	145 (136-167)	219 (199-252)	171 (144-199)
14	187 (162-203)	242 (217-328)	202 (185-240)

[a] AUC_{0-24} (µg·h/mL) (median [IQR]): Area under the plasma concentration-time curve for 0 till 24 hours after dosing; [b] Children: ≤12 yrs; Adults: >12 yrs.

Table 2.3.6 Miltefosine exposure and target attainment.

| | Miltefosine exposure (median [IQR]) | | | |
| | PM+MF14D[a] | | PM+MF28D[a] | |
	Children[b] (n=102)	Adults[b] (n=66)	Children[b] (n=54)	Adults[b] (n=43)
AUC_{d0-7} (µg·day/mL)	20 (17-25)	22 (15-27)	20 (18-22)	18 (16-20)
AUC_{d0-EOT}^{c} (µg·day/mL)	114 (98-130)	111 (94-136)	517 (464-552)	524 (456-567)
AUC_{d0-210} (µg·day/mL)	336 (293-384)	379 (329 - 440)	790 (687-824)	898 (784-961)
Time > EC_{90}^{d} (days)	12 (11-14)	14 (12-16)	27 (25-28)	30 (28-32)

AUC: Area under the plasma concentration-time curve; EC_{90}: 90% effective miltefosine concentration. [a] PM+MF14D: Paromomycin 14 days + miltefosine 14 days, PM+MF28D: Paromomycin 14 days + miltefosine 28 days; [b] Children: ≤12 yrs; adults: >12 yrs; [c] AUC from Day 1 until end of treatment (Day 14 for PM+MF14D, Day 28 for PM+MF28D); [d] Time that the miltefosine concentration was over the *in vitro* susceptibility value EC_{90}, equivalent to 10.6 µg/mL

2.3
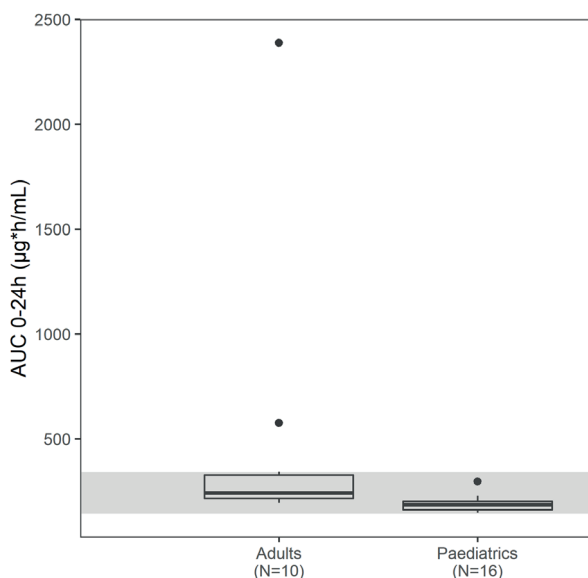
Figure 2.3.5 Paromomycin exposure (AUC_{0-24}) at last day of treatment (Day 14) in pediatrics (≤12 yrs) and adults (>12 yrs), compared to previously observed paromomycin exposure (Day 21) in adult Sudanese and Kenyan patients receiving 20 mg/kg/day paromomycin for 21 days (grey area represents the inter-quartile range) (8). The outlier patient with an extremely high AUC_{0-24} of 2388 µg*h/mL developed ototoxicity due to renal failure.
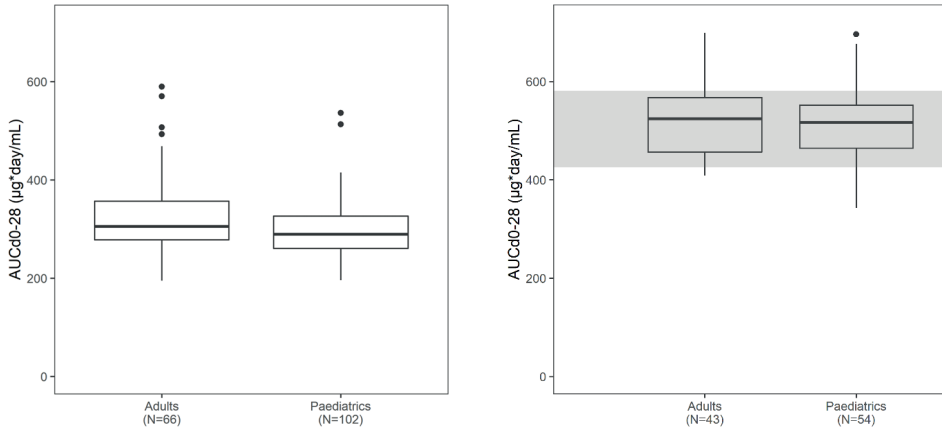
Figure 2.3.6 Cumulative miltefosine exposure until Day 28 (AUC$_{d0-28}$) in pediatrics (≤12 yrs) and adults (>12 yrs), receiving 14 days miltefosine (PM+MF14D, left panel) and 28 days miltefosine (PM+MF28D, right panel), compared to previously observed Day 28 miltefosine exposure in adult Eastern African patients receiving miltefosine allometric dosing for 28 days (grey area represents the inter-quartile range)[10]. One outlier patient with an AUC$_{d0-28}$ of 2106 µg*day/mL (PM+MF14D, 10 years old) is not shown in this figure.
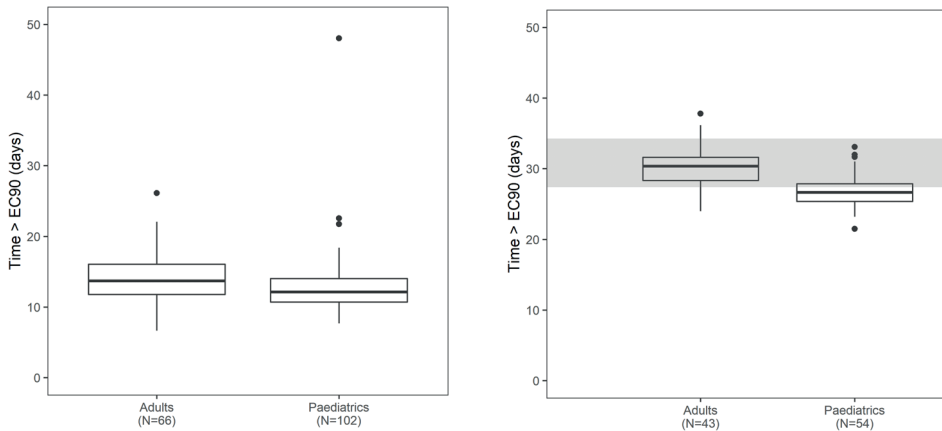
Figure 2.3.7 Miltefosine Time >EC in pediatrics (≤12 yrs) and adults (>12 yrs), receiving 14 days miltefosine (PM+MF14D, left panel) and 28 days miltefosine (PM+MF28D, right panel), compared to previously observed Time >EC$_{90}$ in adult Eastern African patients receiving miltefosine conventional dosing for 28 days (grey area represents the inter-quartile range)[10].

4.   Discussion

This pharmacokinetic study characterized the pharmacokinetics of paromomycin and miltefosine in both pediatric and adult Eastern African VL patients, receiving a new shortened combination regimen. The new treatment corresponded to the desirable levels of exposure, i.e., comparable to exposure in adults that had been associated with cure. Paromomycin exposure in adults was comparable to previously reported exposure in Kenyan and Sudanese VL patients. Children were lower exposed to paromomycin compared to adults, however, they seem nevertheless adequately exposed in combination with allometric miltefosine, given that there was similar efficacy between adults and pediatrics, i.e., in the PM+MF14D regimen, final cure was 94.1% in pediatrics aged ≤12 years and 86.8% in patients aged >12 years[7]. Total miltefosine exposure was also numerically higher in adults compared to children, but exposure in both children and adults was comparable to a previous study in Eastern African VL patients. The comparable exposure of paromomycin and miltefosine to previous monotherapy studies suggests the absence of any obvious drug-drug interaction between paromomycin and miltefosine. Moreover, the absence of clear exposure-response and exposure-toxicity relationships for both paromomycin and miltefosine indicates that the currently used doses in this new combination regimen led to adequate as well as safe exposure ranges of paromomycin and miltefosine. There was one exceptional patient who presumably developed renal failure (serum creatinine increased from 0.4 mg/dL on Day 1 to 10.8 mg/dL on Day 14), leading to extremely high paromomycin exposure at the end of treatment and causing bilateral deafness, explained in the clinical paper in more detail[7]. Renal impairment can lead to prolonged exposure to aminoglycosides, which is a risk factor for ototoxicity. Although the occurrence of renal failure seems rare in this study (2 out of 268 patients developed acute kidney injury)[7], this observation highlights the importance of monitoring renal function during treatment with this combination regimen or, preferably, therapeutic drug monitoring if logistically feasible within the clinical setting and context.

2.3

The developed paromomycin and miltefosine population pharmacokinetic models could adequately describe the pharmacokinetic data, including changes in paromomycin clearance and miltefosine bioavailability over time. Previously, the increase in paromomycin exposure has been described by an empirical decrease in clearance over time[8], while in this study, we could link this decrease in clearance to recovery of disease, more specifically recovery of depleted neutrophil levels over time. An increased clearance of other aminoglycosides in neutropenic patients has been described before[22,23], potentially caused by augmented renal clearance[29,30]. In this study, patients were neutropenic at start of treatment and therefore paromomycin clearance might be increased at start. However, eGFR$_{abs}$ as calculated in this study did not indicate glomerular hyperfiltration, which is present when the eGFR exceeds 160 ml/min/1.73m^2 in men and 150 ml/min/1.73m^2 in women[29]. The decrease in paromomycin clearance over the treatment period might also be explained by the nephrotoxic effect of paromomycin[31,32]. It was expected that eGFR$_{abs}$ decreases during

paromomycin treatment due to drug-induced nephrotoxicity resulting in increasing creatinine levels, but this was not observed in this population and eGFR$_{abs}$ was not associated with paromomycin clearance, despite the fact that this is the main route of excretion of paromomycin[17]. This might indicate that serum creatinine and eGFR$_{abs}$ might not be adequately reflecting the actual renal function in this malnourished African VL population, which is in line with earlier studies that demonstrated that eGFR based on serum creatinine is overestimated in malnourished patients with low muscle mass and low creatinine production[33,34]. In the final paromomycin model, no significant pharmacokinetic differences between countries were identified, indicating no geographical differences that are not explained by the included covariates and demographic differences between populations.

The same effects on miltefosine bioavailability were identified as described previously: a decreased bioavailability during the first week of treatment, and a decreased bioavailability with increased cumulative miltefosine dose. The lower bioavailability might be caused by initial malnourishment and malabsorption, although variables associated with malnutrition, such as height-for-age or BMI-for-age, could not be identified as explanatory covariates on the initially decreased bioavailability. The lower than dose proportional increase in miltefosine exposure was related to a decrease in bioavailability with increasing cumulative dose. A possible explanation could be the slow and saturable transport of miltefosine over the gastrointestinal membrane, resulting in a saturated absorption route after extended exposure to miltefosine[35].

With the developed population pharmacokinetic models we identified different disease-associated factors, such as neutropenia and renal failure, that influence the pharmacokinetics of antileishmanial drugs. Nevertheless, the high efficacy rates in this study, the few cases of toxicity, and the lack of clear exposure-response and exposure-toxicity relationships indicate adequate exposure within the therapeutic range in the studied population, including pediatrics, which can be demonstrated also by the satisfactory cure rates observed in the trial, both in children and adults[7]. This confirms once again that the allometric miltefosine dosing regimen is better suitable for East African pediatric patients with VL than the conventional regimen, also in a 14-day combination regimen with paromomycin. The achieved paromomycin and miltefosine exposure levels could serve as pharmacokinetic targets when monitoring treatment efficacy over time in the endemic regions. The development of this combination therapy also shows the importance to adapt the treatment regimen for children, who comprise approximately 50% of the VL cases globally, to achieve satisfactory efficacy.

Acknowledgments

Funding

2.3

References

1. Ruiz-Postigo JA, Jain S, Mikhailov A, Valadas S, Warusavithana S, Osman M, et al. Global leishmaniasis suveillance: 2019-2020, a baseline for the 2030 roadmap. Wkly Epidemiol Rec. 2021;35:19.
2. Omollo R, Alexander N, Edwards T, Khalil EAG, Younis BM, Abuzaid AA, et al. Safety and Efficacy of miltefosine alone and in combination with sodium stibogluconate and liposomal amphotericin B for the treatment of primary visceral leishmaniasis in East Africa: study protocol for a randomized controlled trial. Trials. 2011;12(1):66.
3. Wasunna M, Njenga S, Balasegaram M, Alexander N, Omollo R, Edwards T, et al. Efficacy and Safety of AmBisome in Combination with Sodium Stibogluconate or Miltefosine and Miltefosine Monotherapy for African Visceral Leishmaniasis: Phase II Randomized Trial. PLoS Negl Trop Dis. 2016;10(9):e0004880.
4. Hailu A, Musa A, Wasunna M, Balasegaram M, Yifru S, Mengistu G, et al. Geographical variation in the response of visceral leishmaniasis to paromomycin in East Africa: A multicentre, open-label, randomized trial. PLoS Negl Trop Dis. 2010;4(10):e709.
5. Musa A, Khalil E, Hailu A, Olobo J, Balasegaram M, Omollo R, et al. Sodium stibogluconate (SSG) & paromomycin combination compared to SSG for visceral leishmaniasis in East Africa: A randomised controlled trial. PLoS Negl Trop Dis. 2012;6(6):e1674.
6. Sundar S, Sinha PK, Rai M, Verma DK, Nawin K, Alam S, et al. Comparison of short-course multidrug treatment with standard therapy for visceral leishmaniasis in India: An open-label, non-inferiority, randomised controlled trial. The Lancet. 2011;377(9764):477–86.
7. Musa AM, Mbui J, Mohammed R, Olobo J, Ritmeijer K, Alcoba G, et al. Paromomycin and Miltefosine Combination as an Alternative to Treat Patients with Visceral Leishmaniasis in Eastern Africa: A Randomized, Controlled, Multicountry Trial. Clinical Infectious Diseases. 2022 Sep 27;
8. Verrest L, Wasunna M, Kokwaro G, Aman R, Musa AM, Khalil EAG, et al. Geographical Variability in Paromomycin Pharmacokinetics Does Not Explain Efficacy Differences between Eastern African and Indian Visceral Leishmaniasis Patients. Clin Pharmacokinet. 2021;60(11):1463–72.
9. Sundar S, Jha TK, Thakur CP, Sinha PK, Bhattacharya SK. Injectable Paromomycin for Visceral Leishmaniasis in India. N Engl J Med. 2007;356(25):2571–81.
10. Dorlo TPC, Kip AE, Younis BM, Ellis SJ, Alves F, Beijnen JH, et al. Visceral leishmaniasis relapse hazard is linked to reduced miltefosine exposure in patients from Eastern Africa: A population pharmacokinetic/pharmacodynamic study. Journal of Antimicrobial Chemotherapy. 2017;72(11): 3131-40.
11. Mbui J, Olobo J, Omollo R, Solomos A, Kip AE, Kirigi G, et al. Pharmacokinetics, Safety, and Efficacy of an Allometric Miltefosine Regimen for the Treatment of Visceral Leishmaniasis in Eastern African Children : An Open-label , Phase II Clinical Trial. Clinical Infectious Diseases. 2019;68(9).
12. Musa AM, Younis B, Fadlalla A, Royce C, Balasegaram M, Wasunna M, et al. Paromomycin for the treatment of visceral leishmaniasis in Sudan: A randomized, open-label, dose-finding study. PLoS Negl Trop Dis. 2010;4(10):4–10.
13. Dorlo TPC, Hillebrand MJX, Rosing H, Eggelte TA, de Vries PJ, Beijnen JH. Development and validation of a quantitative assay for the measurement of miltefosine in human plasma by liquid chromatography-tandem mass spectrometry. J Chromatogr B Analyt Technol Biomed Life Sci. 2008 Apr;865(1–2):55–62.
14. Roseboom IC, Thijssen B, Rosing H, Mbui J, Beijnen JH, Dorlo TPC. Highly sensitive UPLC-MS/MS method for the quantification of paromomycin in human plasma. J Pharm Biomed Anal. 2020;185:113245.
15. Palic S, Kip AE, Beijnen JH, Mbui J, Musa A, Solomos A, et al. Characterizing the non-linear pharmacokinetics of miltefosine in paediatric visceral leishmaniasis patients from Eastern Africa. J Antimicrob Chemother. 2020;75:3260–8.
16. du Bois D, du Bois EF. A formula to estimate the approximate surface area if height and weight be known. 1916. Nutrition. 1989;5(5):303.
17. Seyffart G. Drug dosage in renal insufficiency. 1991.
18. Eastwood JB, Kerry SM, Plange-Rhule J, Micah FB, Antwi S, Boa FG, et al. Assessment of GFR by four methods in adults in Ashanti, Ghana: The need for an eGFR equation for lean African populations. Nephrology Dialysis Transplantation. 2010;25(7):2178–87.

19. Levey AS, Stevens LA, Schmid CH, Zhang Y, Castro III AF, Feldman HI, et al. A New Equation to Estimate Glomerular Filtration Rate. Ann Intern Med. 2009;150(9):604–12.
20. Azzi A, Cachat F, Faouzi M, Mosig D, Ramseyer P, Girardin E, et al. Is there an age cutoff to apply adult formulas for GFR estimation in children? J Nephrol. 2015 Feb 1;28(1):59–66.
21. Schwartz GJ, Muñoz A, Schneider MF, Mak RH, Kaskel F, Warady BA, et al. New equations to estimate GFR in children with CKD. Journal of the American Society of Nephrology. 2009 Mar;20(3):629–37.
22. Lortholary O, Lefort A, Tod M, Chomat AM, Darras-Joly C, Cordonnier C. Pharmacodynamics and pharmacokinetics of antibacterial drugs in the management of febrile neutropenia. Lancet Infect Dis. 2008 Oct 1;8(10):612–20.
23. Bury D, ter Heine R, van de Garde EMW, Nijziel MR, Grouls RJ, Deenen MJ. The effect of neutropenia on the clinical pharmacokinetics of vancomycin in adults. Eur J Clin Pharmacol. 2019;75:921–8.
24. Davis RL, Lehmann D, Stidley CA, Neidhart J. Amikacin Pharmacokinetics in Patients Receiving High-Dose Cancer Chemotherapy. Antimicrob Agents Chemother. 1991;35(5):944–7.
25. Etzel J v, Nafziger AN, Bertino JS. Variation in the pharmacokinetics of gentamicin and tobramycin in patients with pleural effusions and hypoalbuminemia. Antimicrob Agents Chemother. 1992;36(3):679-81.
26. Romano S, Fdez de Gatta MM, Calvo M v, Caballero D, Dominquez-Gil A, Lanao JM. Population pharmacokinetics of amikacin in patients with haematological malignancies. Journal of Antimicrobial Chemotherapy. 1999;44:235–42.
27. Hodiamont CJ, Juffermans NP, Bouman CSC, Jong MD de, Mathôt RAA, Hest RM van. Determinants of gentamicin concentrations in critically ill patients: a population pharmacokinetic analysis. Int J Antimicrob Agents. 2017;49(2):204–11.
28. Dosne AG, Bergstrand M, Karlsson MO. An automated sampling importance resampling procedure for estimating parameter uncertainty. J Pharmacokinet Pharmacodyn. 2017;44(6):509–20.
29. de Lange DW. Glomerular hyperfiltration of antibiotics. Netherlands Journal of Critical Care. 2013;17(5):10–4.
30. Campassi ML, Gonzalez MC, Masevicius FD, Vazquez AR, Moseinco M, Navarro NC, et al. Augmented renal clearance in critically ill patients: incidence, associated factors and effects on vancomycin treatment. Rev Bras Ter Intensiva. 2014;26(1):13–20.
31. Lopez-Novoa JM, Quiros Y, Vicente L, Morales AI, Lopez-Hernandez FJ. New insights into the mechanism of aminoglycoside nephrotoxicity: An integrative point of view. Kidney Int. 2011;79(1):33-45.
32. Rougier F, Claude D, Maurin M, Maire P. Aminoglycoside nephrotoxicity. Curr Drug Targets Infect Disord. 2004;4(2):153–62.
33. Beddhu S, Samore MH, Roberts MS, Stoddard GJ, Pappas LM, Cheung AK. Creatinine production, nutrition, and glomerular filtration rate estimation. Journal of the American Society of Nephrology. 2003;14(4):1000–5.
34. Hari P, Bagga A, Mahajan P, Lakshmy R. Effect of malnutrition on serum creatinine and cystatin C levels. Pediatric Nephrology. 2007;22(10):1757–61.
35. Ménez C, Buyse M, Farinotti R, Barratt G. Inward translocation of the phospholipid analogue miltefosine across caco-2 cell membranes exhibits characteristics of a carrier-mediated process. Lipids. 2007;42(3):229–40.

2.3

Supplementary material 2.3

A

FEMALE									
HT (cm)	80-89	90-99	100-109	110-119	120-129	130-139	140-149	150-159	160
WT (kg)									
7									
8	30								
9	30								
10	30	40							
11	40	40	40						
12	40	40	40						
13	40	40	40						
14	40	40	40	50					
15	40	40	50	50					
16	40	50	50	50					
17	40	50	50	50	50				
18	50	50	50	50	60				
19	50	50	50	60	60				
20	50	50	50	60	60	60			
21	50	50	60	60	60	60			
22	50	50	60	60	60	60			
23	50	50	60	60	60	70	70		
24	50	50	60	60	60	70	70		
25	50	60	60	60	70	70	70		
26	50	60	60	60	70	70	70	70	
27	50	60	60	70	70	70	70	80	
28	50	60	60	70	70	70	80	80	
29	50	60	60	70	70	70	80	80	
30	50	60	60	70	70	80	80	80	80

RISK OF SEVERE MALNUTRITION

REFER TO THE WHO REFERENCE CURVES

Figure S2.3.1A Daily allometric miltefosine dose for female children based on fat-free mass

B

MALE									
HT (cm)	80-89	90-99	100-109	110-119	120-129	130-139	140-149	150-159	160
WT (kg)									
7									
8	40								
9	40								
10	40	40							
11	40	40							
12	40	50							
13	50	50	50						
14	50	50	50						
15	50	50	60	60					
16	50	50	60	60					
17	50	60	60	60					
18	50	60	60	60	70				
19	50	60	60	70	70				
20	50	60	60	70	70				
21	60	60	60	70	70	70			
22	60	60	70	70	70	80			
23	60	60	70	70	80	80			
24	60	60	70	70	80	80	80		
25	60	60	70	70	80	80	80		
26	60	70	70	80	80	80	100		
27	60	70	70	80	80	80	100		
28	60	70	70	80	80	100	100	100	
29	60	70	70	80	80	100	100	100	
30	60	70	80	80	100	100	100	100	

RISK OF SEVERE MALNUTRITION

REFER TO THE WHO REFERENCE CURVES

2.3

Figure S2.3.1B   Daily allometric miltefosine dose for male children based on fat-free mass.
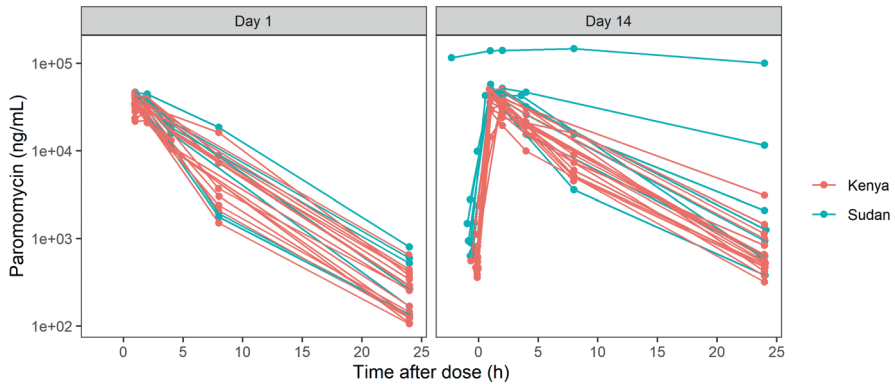
Figure S2.3.2   Paromomycin plasma concentrations included in the PK analysis, stratified by sampling day.
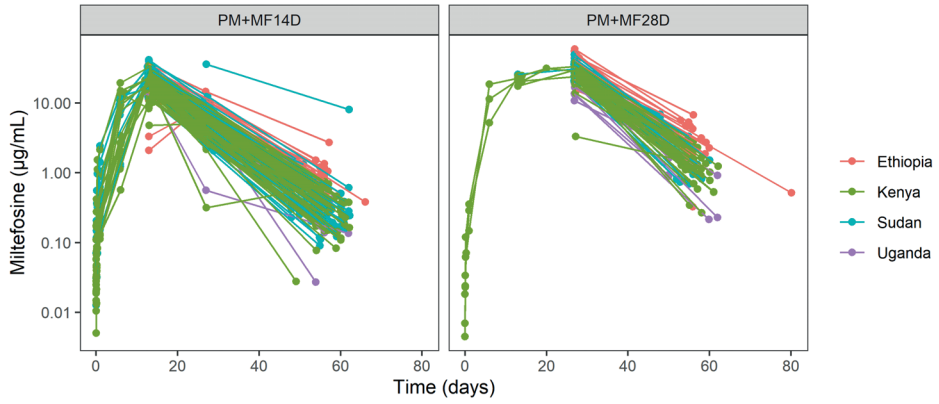
Figure S2.3.3 Miltefosine plasma concentrations included in the PK analysis, stratified by treatment arm. PM+MF14D: Paromomycin 14 days + miltefosine 14 days, PM+MF28D: Paromomycin 14 days + miltefosine 28 days.
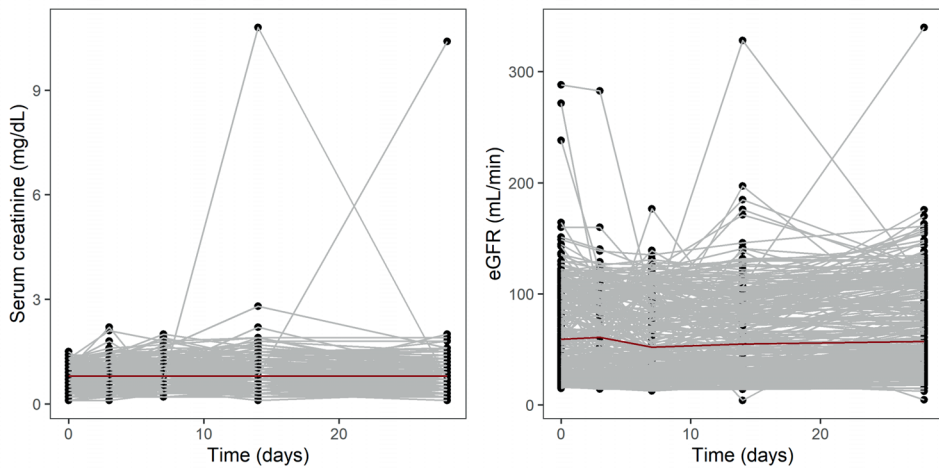
Figure S2.3.4   Serum creatinine levels and calculated absolute eGFR.
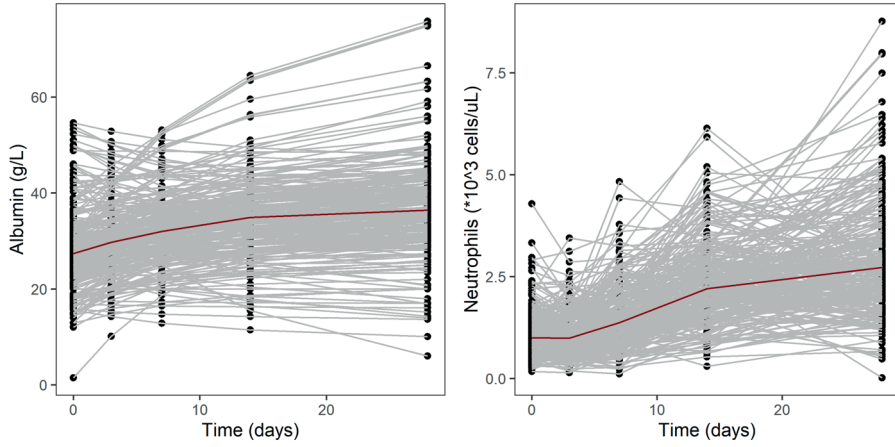
Figure S2.3.5 Serum albumin and neutrophil levels. Albumin levels are interpolated between Day 0 and Day 28 using the function "na.approx{zoo}" in R.
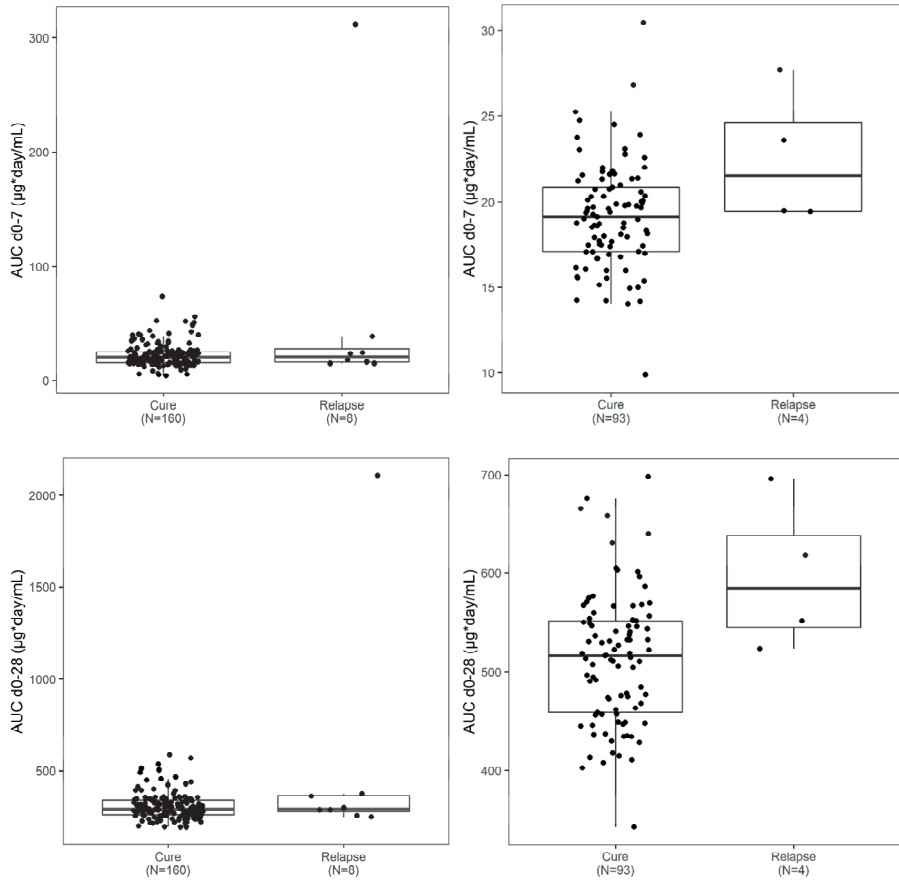
2.3
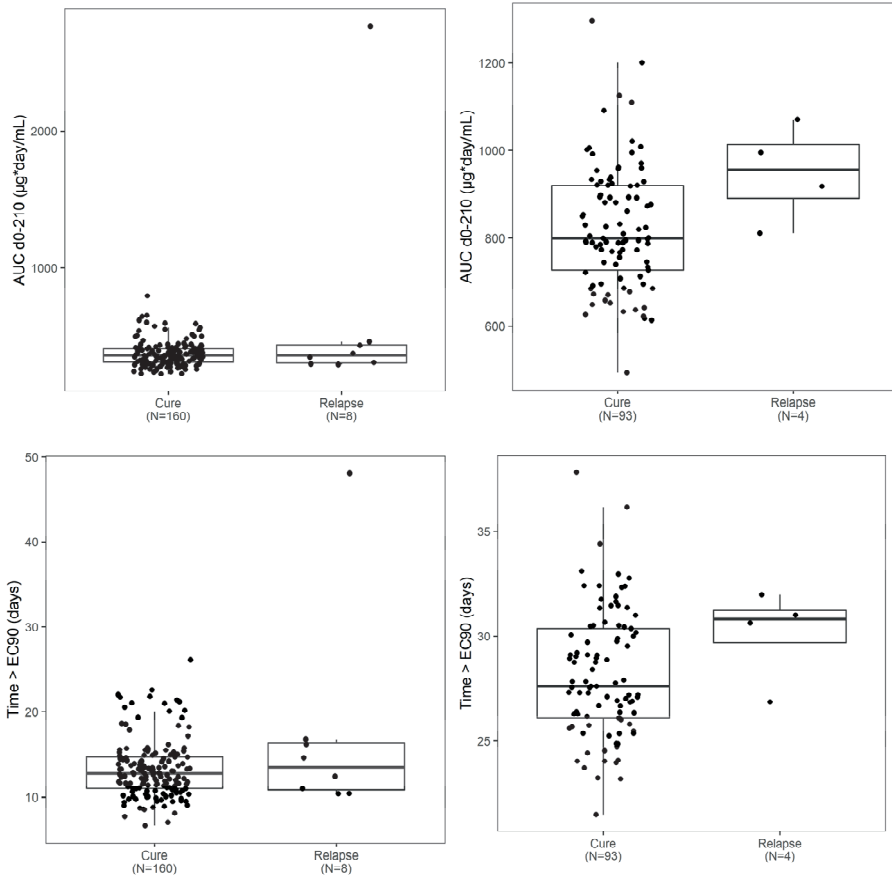
Figure S2.3.6 Miltefosine exposure at Day 7, Day 28 and Day 210 and target attainment (Time > EC90) versus clinical outcome determined at 6 months follow-up. Left panels: PM+MF14D; right panels: PM+MF28D.

NONMEM control stream - paromomycin model

; Description: Final paromomycin PK model
; Author: L. Verrest

$PROBLEM PK

$INPUT ID SITE ARM TIME TIMED DAY TALD TALD2 STIME SDAY CMT MF PM DOSE AMT
AMTT DDOS DV MDV EVID FLAG FLAG2 MFPK PMPK BLQ INT REL RDAY MICR TISSUE
CNTRY SEX AGE HT WT BWT BMI FFM CREAT EGFR EGFRA BSA ALB NEUTR HAZ BAZ

;;;; Dataset description ;;;;
; ID: unique subject number
; SITE: 11 = Gondar (Ethiopia), 13 = Abdurafi (Ethiopia), 29 = Kacheliba (Kenya), 32 =
Tabarak-Allah
; (Sudan), 34 = Um El Kher (Sudan), 38 = Doka (Sudan), 46 = Amudat (Uganda)
; ARM: 1 = PM & MF for 14 days, 2 = PM for 14 days, MF for 28 days
; TIME: time after first dose (hr)
; TIMED: time (days)
; DAY: actual day
; TALD: time after last dose (hr)
; TALD2: time after last dose for plotting Day 1 and Day 14
; STIME: nominal scheduled time (hr)
; SDAY: nominal scheduled day
; CMT: 1 = MF dose / PM dose, 2 = MF PK cent / PM PK cent, 3 = MF PK periph
; MF: MF dosing or DV 0 = no, 1 = yes
; PM: PM dosing or DV 0 = no, 1 = yes
; DOSE: MF: mg, PM: mL (=375 mg/mL PM base)
; AMT: MF: mg, PM: mg PM base (DOSE*375 mg/ml)
; AMTT: total MF dose
; DDOS: AMTT/body weight
; DV: ng/mL (both for MF and PM)
; MDV: missing DV (0 for DV record, 1 for other record)
; EVID: event ID (0 = PK observation, 1 = dosing, 2 = other)
; FLAG: Vomited after dose. 0 = No, 1 = Vomited after this dose, 2 = Redose
; FLAG2: Unreliable PK samples. 2: empty tube, 3: quantification not reliable, 4: Samples
with the same
; Day/Time, 5: Pre-dose sample taken after next dose, 7: Unreliable BLQ samples
; PMPK: PM PK measured for this subject. 0=no, 1=yes
; MFPK: MF PK measured for this subject. 0=no, 1=yes
; BLQ: Below limit of quantification (MF: 4 ng/mL, PM: 5 ng/mL)
; INT: intensive cohort. 0=no, 1=yes
; REL: 0 = no relapse, 1 = relapse
; RDAY: day of rescue treatment
; MICR: microscopy score

2.3

; TISSUE: Tissue where parasite assessment by microscopy is performed. 1 = Spleen, 2 = Bone marrow, ;3 = Lymph Node
; CNTRY: 1 = Ethiopia, 2 = Kenya, 3 = Sudan, 4 = Uganda
; SEX: 1 = male, 2 = female
; AGE
; HT: height (cm)
; WT: body weight (kg)
; BWT: baseline body weight (kg)
; BMI: WT/((HT/100)**2)
; FFM: Fat free mass (kg) according Maturation Model Al-Sallami 2015
; CREAT: creatinine (mg/dL)
; EGFR: eGFR by CKD-EPI, children <=14 Schwartz (mL/min/1.73m2)
; EGFRABS: absolute eGFR (mL/min)
; BSA: Body surface area (m2) according DuBois: 0.20247 x height (m)^0.725 x weight (kg)^0.425
; ALB: albumin (g/L) (interpolated between D0 and D28)
; NEUTR: neutrophils (*10^3 cells/uL)
; HAZ: height for age z-score
; BAZ: BMI for age z-score

$DATA   MILT-PM-01-VL.D.v5.csv
IGNORE=@
IGNORE(PM.EQ.0) ; MF dose or DV
IGNORE(PMPK.EQ.0) ; Subjects without PM PK observations
IGNORE(FLAG2.GT.0) ; unreliable PK samples
IGNORE(SDAY.EQ.0) ; Baseline samples

$SUBROUTINE ADVAN13 TOL=6

$MODEL
COMP = (DEPOT) ; PM dose
COMP = (CENTRAL) ; PM PK
COMP = (PERIPH)
COMP = (AUC)

$ABB COMRES=2

$PK
TVCL = THETA(1)
TVV2 = THETA(2)
TVKA = THETA(3)
TVF1 = THETA(4)
TVQ = THETA(5)
TVV3 = THETA(6)

;; Covariates
CLNEUTR = (1 + THETA(7) * (NEUTR-0.98)) ; 0.98 *10^3 cells/uL = median population baseline neutrophils

;; Parameters
CL = TVCL *(BWT/27.5)**0.75 * EXP(ETA(1)) * CLAGE * CLTIME * CLNEUTR ; 27.5 = median population baseline body weight
V2 = TVV2 *(BWT/27.5)**1.00* EXP(ETA(2))
KA = TVKA * EXP(ETA(3))
F1 = TVF1
Q = TVQ *(BWT/27.5)**0.75
V3 = TVV3 *(BWT/27.5)**1.00

K20   = CL/V2
K23   = Q/V2
K32   = Q/V3
S2   = V2/1000
S3   = V3
AUCtau = F1*AMT/CL

$DES
CC = A(2)/V2
DADT(1)= -KA*A(1)
DADT(2)= KA*A(1) -K23*A(2) +K32*A(3) -K20*A(2)
DADT(3)= K23*A(2) -K32*A(3)

$ERROR
IPRED = F
IF(IPRED.LT.1E-6) IPRED=1E-6
W = SQRT(THETA(8)**2*IPRED**2 + THETA(9)**2)
Y = IPRED + W*EPS(1)
IRES = DV-IPRED
IWRES = IRES/W

$THETA
(0, 2.62) ; 1 CL
(0, 9.17) ; 2 V2
(0, 2.05) ; 3 KA
(1.17) FIX ; 4 F1
(0, 0.262) ; 5 Q
(0, 16.55 ; 6 V3
(-0.1)3 ; 7 COV(Cl,neutr)
(0, 0.285) ; 8 Prop.RE
(0) FIX ; 9 Add.RE

2.3

$OMEGA
 0.276 ; 1 CL
 0 FIX ; 2 V2
 0 FIX ; 3 Ka

$SIGMA
 1 FIX

$ESTIMATION METHOD=1 INTER MAXEVAL=2000 NOABORT PRINT=10 POSTHOC
ATOL=6 SIGL=6 NSIG=2 ETASTYPE=1
$COV PRINT=E
$TABLE ID SITE ARM DOSE DV TIME TALD TALD2 DAY STIME SDAY CMT AMT BWT AGE
CNTRY FLAG2 BLQ EVID IPRED CWRES CL V2 Q V3 KA F1 ETA1 ETA2 ETA3 AUCtau CC
CREAT ALB NEUTR
ONEHEADER NOPRINT FILE=sdtab0026

NONMEM control stream – miltefosine model

; Description: Final miltefosine PK model
; Author: L. Verrest

$PROBLEM   PK

$INPUT ID SITE ARM TIME TIMED DAY TALD TALD2 STIME SDAY CMT MF PM DOSE AMT
AMTT DDOS DV MDV EVID FLAG FLAG2 MFPK PMPK BLQ INT REL RDAY MICR TISSUE
CNTRY SEX AGE HT WT BWT BMI FFM CREAT EGFR EGFRA BSA ALB NEUTR HAZ BAZ

; Dataset description – see paromomycin model

$DATA   MILT-PM-01-VL.D.v5.csv
 IGNORE=@
 IGNORE(PM.EQ.1)   ; MF observations
 IGNORE(FLAG.EQ.1) ; vomited after this dose. Redose is included (FLAG2=2)
 IGNORE(FLAG2.GT.0) ; unreliable PK samples
 IGNORE(SDAY.EQ.0) ; screening samples
 IGNORE(BLQ.EQ.1)   ; BLQ observations

$SUBROUTINE ADVAN13 TOL=3

$MODEL   NCOMP=5
      COMP=(DEPOT,DEFDOSE) ; Dosing compartment
      COMP=(CENTRAL) ; central compartment
      COMP=(PERI1) ; peripheral compartment
      COMP=(AUC) ; MF AUC central compartment

    COMP=(TAT) ; Time Above Threshold $PK

$PK
TVCL = THETA(1)
TVV2 = THETA(2)
TVKA = THETA(3)
TVQ = THETA(4)
TVV3 = THETA(5)
TVF1=THETA(6)

;; Covariates
ALLOCL = (FFM/18)**0.75
ALLOV = (FFM/18)**1
IF(TIME.LE.168) COVF = (1 - THETA(7))*EXP(ETA(4)) ; decreased F first week
IF(TIME.GT.168) COVF = 1
IF(DDOS.LT.60) COVF2 = 1
IF(DDOS.GE.60) COVF2= ((DDOS/70)**THETA(8)) ; decreased F after a cumulative dose
of 60 mg/kg/day

;;Parameters
CL = TVCL * ALLOCL * EXP(ETA(1))
V2 = TVV2 * ALLOV * EXP(ETA(2))
KA = TVKA * EXP(ETA(3))
Q = TVQ
V3 = TVV3 * ALLOV
F1 = TVF1 * COVF * COVF2

ke = CL/V2
k23 = Q/V2
k32 = Q/V3
S2 = V2
S3 = V3

$DES
TCON = 10.6 ; Threshold Concentration
CC = A(2)/V2
TAT = 0 ; Time Above Threshold
IF(CC.GT.TCON) TAT = 1

DADT(1) = -KA*A(1)
DADT(2) = KA*A(1) - k23*A(2) + k32*A(3) - ke*A(2)
DADT(3) = k23*A(2) - k32*A(3)
DADT(4) = CC
DADT(5) = TAT

2.3

AUC = A(4)
TT = A(5)

$ERROR
IPRED = F
Y = IPRED * (1 + EPS(1))
IRES = DV-IPRED
IWRES = IRES/IPRED

$THETA
(0, 0.0768) ; CL
(0, 13.6) ; V
(0, 0.0368) ; KA
(0, 0.007) ; Q
(0, 2.22) ; V3
(1) FIX ; F fix
(0, 0.649,1) ; COV(F,W1)
(-2.4) ; COV(F,DDOS)

$OMEGA
 0.0267 ;   IIV CL
 0 FIX ;   IIV V2
 0 FIX ;   IIV Ka
 0.56 ;   IIV F

$SIGMA
 0.0991 ;prop error

$ESTIMATION METHOD=1 INTER MAXEVAL=2000 NOABORT SIG=3 SIGL=9 PRINT=1
POSTHOC

$COVARIANCE

$TABLE ID TIME TIMED DV MDV EVID CMT CL Q V2 V3 KA AGE WT HT BMI F1 ARM INT
DAY SDAY STIME REL FFM SEX DDOS AMTT IPRED CWRES ETA(1) ETA(4) CC AUC TT
MICR NEUTR ALB HAZ BAZ IWRES
ONEHEADER NOPRINT FILE=sdtab20

Chapter 2.4

Disease-specific differences in pharmacokinetics of paromomycin and miltefosine between post-kala-azar dermal leishmaniasis and visceral leishmaniasis patients in Eastern Africa

Wan-Yu Chu, Luka Verrest, Brima M. Younis, Ahmed M. Musa, Jane Mbui, Rezika Mohammed, Joseph Olobo, Koert Ritmeijer, Séverine Monnerat, Monique Wasunna, Ignace C. Roseboom, Alexandra Solomos, Alwin D.R. Huitema, Fabiana Alves, Thomas P.C. Dorlo

Abstract

Introduction: Post-kala-azar dermal leishmaniasis (PKDL) is a skin complication following primary visceral leishmaniasis (VL) infection. Treatment and dosing regimens for PKDL are usually extrapolated from VL. However, the pharmacokinetics (PK) of drugs may be different between VL and PKDL patients due to disease-specific differences in absorption, distribution and elimination. This study aimed to characterize the PK of paromomycin and miltefosine in PKDL patients and compare them with VL patients in Eastern Africa.

Methods: Pharmacokinetic data were collected from a PKDL (NCT03399955) and a VL study (NCT03129646) in Eastern Africa. In the PKDL study, patients were given a combination of paromomycin for 14 days plus miltefosine for 42 days, or liposomal amphotericin B for 7 days plus miltefosine for 28 days. In the VL study, patients were given paromomycin for 14 days plus miltefosine for 14 days or 28 days. Plasma concentrations of paromomycin and miltefosine were quantified using LC-MS/MS and were used for population PK analysis performed by nonlinear mixed effects modeling.

Results: Data from 109 PKDL patients and 264 VL patients were included in this population PK analysis. The PK of paromomycin was best described by a three-compartment model, with one saturable compartment resembling paromomycin accumulation in tissues, in which PKDL patients had a 1.7-fold (95%CI: 1.21-2.45) higher capacity for accumulation compared to VL patients. The PK of miltefosine was best described by a two-compartment model with first-order absorption and elimination. Only in VL patients, the bioavailability was decreased by 69% (62-76) at the treatment start. The rates of absorption in PKDL and VL patients were 5.43 1/day (4.54-6.26) and 0.99 1/day (0.84-1.17), respectively. PKDL patients given the same regimen as VL patients presented 26% lower paromomycin plasma exposure ($AUC_{0-24 \text{ hours, } D14}$) and 38% higher miltefosine exposure (AUC_{0-28D}) at the end of the treatment. Co-administration with liposomal amphotericin B decreased miltefosine bioavailability by 8.6% (2-15), suggesting a drug-drug interaction.

Conclusion: Pronounced differences in the PK of paromomycin and miltefosine between PKDL and VL patients were identified and characterized, potentially explaining observed toxicity differences and affecting the extrapolation of dosing regimens between these two clinical presentations of leishmaniasis.

1.   Introduction

Visceral leishmaniasis (VL), also known as kala-azar, is the most severe form of the neglected tropical parasitic diseases leishmaniasis and is fatal if left untreated. VL is usually characterized by fever, weight loss, hepatosplenomegaly, lymphadenopathy, anemia, leucopenia, and thrombocytopenia[1]. Post-kala-azar dermal leishmaniasis (PKDL) is a complication of VL that appears as skin lesions months or even years after successful treatment of a primary VL infection[2]. In Eastern Africa, where VL is caused by *Leishmania donovani*, up to 50-60% of VL cases develop PKDL within 6 months after successful treatment, with most cases of PKDL in Sudan[3]. Although PKDL is not life-threatening, symptoms can be severely disfiguring and stigmatizing. Moreover, PKDL is thought to play an important role in VL transmission by parasites in the infected skin. The treatment of PKDL patients is, therefore, considered an important component in elimination efforts for VL.

The current WHO-recommended treatment for VL in Eastern Africa is a 17-day combination therapy of sodium stibogluconate (SSG) and paromomycin[4,5]. A novel 14-day combination treatment of paromomycin and miltefosine without any toxic antimonial component was recently positively evaluated in Eastern African, which is expected to replace the more toxic regimen[6,7]. There is currently no consensus on the best treatment for PKDL[2]. Up to now, the dosing regimens for PKDL patients have been directly extrapolated from VL patients, often with an extended treatment duration due to the slow clearance of skin lesions. Current practice in Sudan is treatment with SSG for over 60 days, which is associated with life-threatening toxicities such as cardiotoxicity and pancreatitis, and requires long hospitalization[8]. There is an urgent need for a safe and efficacious alternative of shorter treatment duration for treatment of PKDL.

Miltefosine is the only oral treatment available for leishmaniasis that can be administered on an outpatient basis and is, therefore, a favorable treatment option. In a recent clinical study in Sudanese PKDL patients (NCT03399955)[9], a longer treatment regimen with miltefosine was combined with a parenteral drug for a short treatment period (liposomal amphotericin B or paromomycin), with the aim to minimize the hospitalization period but still achieve appropriate drug exposure and satisfactory efficacy levels by longer miltefosine treatment. The dosing rationale in PKDL patients is based on doses used in VL patients, with an extended treatment period to reach satisfactory exposure levels in the skin. However, exposure-response relationships in PKDL patients might be considerably different compared to VL patients. First of all, the drug target site is different between VL and PKDL. Whereas in VL, parasites manifest mainly in macrophages in the internal organs, in PKDL the parasites reside in the lesions of the infected skin. Moreover, the pharmacokinetics (PK) of antileishmanial drugs may

2.4

be different between VL and PKDL patients. VL patients are ill and usually suffer from fever, weight loss and hematological depletions, while PKDL patients generally have a better condition except for their skin. These physiological differences might impact drug PK, which could potentially lead to under- or overexposure to the drugs, and might therefore require dose regimen adaptations in PKDL patients.

The PK of paromomycin and miltefosine in VL patients has been studied, but unfortunately, no PK data is available in PKDL patients. Paromomycin, a highly hydrophilic aminoglycoside, is rapidly and almost completely absorbed after intramuscular (IM) injection, and predominantly excreted unchanged via glomerular filtration[10-12]. Typically, PKDL patients have a better renal function than VL patients, which might lead to differences in the elimination of paromomycin. The PK of miltefosine is characterized by slow absorption and elimination[13]. Previous population PK studies in VL patients demonstrated changes in miltefosine bioavailability over the four weeks treatment period. In the first week of treatment, relative bioavailability was decreased by 69-74%, potentially caused by malabsorption due to the systemic infection and/or malnourishment of the patient[14,15]. This effect might be rather disease-specific for VL patients and might not be present in PKDL patients with only a dermal clinical presentation of leishmaniasis.

To properly dose paromomycin and miltefosine in PKDL patients, PK differences between VL and PKDL patients need to be characterized and exposure-response relationships in the PKDL population need to be established. This study aimed to characterize the PK of paromomycin and miltefosine in PKDL patients compared to VL patients from Eastern Africa and to identify disease-specific covariates affecting the PK and exposure to these antileishmanial drugs. Furthermore, drug-drug interactions of combination regimens of miltefosine with paromomycin and liposomal amphotericin B were explored.

2.   Methods

2.1   Clinical trials and patients

Pharmacokinetic data were collected in a PKDL (NCT03399955)[9] and a VL study (NCT03129646)[7] in Eastern Africa. The PKDL study was a phase II, open label, randomized, parallel arm trial, which assessed the safety and efficacy of the combination of paromomycin and miltefosine (PM-MF) and the combination of liposomal amphotericin B and miltefosine (LAmB-MF) for the treatment of PKDL in Sudan. The VL study was a phase III, open label, randomized controlled, multicenter non-inferiority trial, which compared the efficacy of two combination regimens of

paromomycin for 14 days and miltefosine for 14 days or 28 days (PM-MF 14D and PM-MF 28D) with the standard 17-day SSG and paromomycin combination (SSG-PM) for the treatment of VL in Eastern Africa[7]. In both studies, sparse PK sampling for miltefosine was performed in all patients, and a subset of patients was allocated to the intensive sampling cohort for paromomycin and mitlefosine PK analysis. VL patients in the intensive cohort were all from Kenya and Sudan, and sparse samples were available from patients from Ethiopia and Uganda. Informed consent to participate in the trial, including PK assessments, was obtained per regulatory requirements in each country.

In the PKDL study, patients in the PM-MF arm were given paromomycin 20 mg/kg/day intramuscularly for 14 days and oral miltefosine (allometric dosing) for 42 days; patients in the LAmB-MF arm were given liposomal amphotericin B (AmBisome®) 5 mg/kg/day intravenously at day 1, 3, 5, and 7 and oral miltefosine (allometric dosing) for 28 days. In the VL study, patients were given paromomycin 20 mg/kg/day intramuscularly for 14 days combined with oral miltefosine (allometric dosing) for 14 days or 28 days. In both studies, patients were admitted for the whole duration of liposomal amphotericin B or paromomycin administration, after which miltefosine administration was continued on an outpatient basis.

Miltefosine allometric dosing was calculated according to patient's weight, height and sex, and was applied for patients weighing <30 kg[16]. For patients weighing ≥30 kg, the allometric dose corresponded to the conventional dose of 2.5 mg/kg/day, with maximum 150 mg/day. Therefore, patients weighing ≥ 30 to 44 kg received 100 mg/day and patients ≥45 kg received 150 mg/day.

2.4

2.2   Sampling schedule and bioanalysis method

In both studies, blood samples for paromomycin PK were collected at 4 time points on day 1 and day 14 following two different schedules. On day 1, blood samples were collected either at 1, 2, 4, and 24 hours or at 1, 2, 8, and 24 hours after paromomycin administration. On day 14, blood samples were collected before the last paromomycin administration and at 1, 4, and 24 hours or at 2, 8, and 24 hours after the last paromomycin administration. Paromomycin concentrations in plasma were quantified using a previously validated UPLC-MS/MS method, with a lower limit of quantification of 5 ng/mL[17].

In the PKDL study, miltefosine blood samples were collected at day 1, 4-8 hours after the first administration, and at day 7, 14, 28, and 42 and 3-months for all patients. In the VL study, miltefosine concentration was measured in all patients at day 28 and day 56. For patients in the intensive cohort, miltefosine plasma samples were collected on day 1, 7, 14, 28 and 56 in both treatment arms and an additional sample was taken on day 21 for the 28-day treatment arm. Miltefosine samples taken on day 1 and day

14 followed the same schedules as paromomycin PK sampling. Miltefosine plasma concentrations were quantified using a previously validated LC-MS/MS method, with a lower limit of quantification of 4 ng/mL[18].

For all patients, hematology and biochemistry examinations, including serum creatinine concentrations, were available at screening (0-20 days before the start of treatment), on day 3, 7, 14 and 28. Albumin was measured at screening only.

2.3   Population pharmacokinetic analysis

2.3.1   Paromomycin population PK model

Previous population PK studies in VL patients in India and Eastern Africa demonstrated a decrease in paromomycin clearance (CL/F) over time, suggesting potential non-linear kinetics[19,20]. Two possible hypotheses that may explain the nonlinearity in paromomycin PK were evaluated. Firstly, after glomerular filtration, a portion of administered aminoglycosides (≈5%) is accumulated in proximal tubules, which could lead to tubular necrosis[21-23]. This action is mediated by megalin, a large glycoprotein functioning as an endocytic receptor that is abundantly expressed in specific epithelial cells (e.g., renal tubule and inner ear)[24,25]. The uptake of aminoglycosides by megalin-expressing cells is a saturable process and could cause functional alternations in kidney, which might also explain the previously observed time-related change in paromomycin exposure[26-28]. Therefore, in addition to one to three-compartment models with first-order absorption and elimination, a model that included saturable distribution towards the peripheral compartment (representing saturable megalin binding) was tested as a structural model. The saturable distribution was described by a maximal binding capacity (B_{max}) function shown in equation 1[29].

$$\frac{dA_{Peripheral}}{dt} = k_{in} * A_{Central} * \left(1 - \frac{A_{Peripheral}}{B_{max}}\right) - k_{out} * A_{Peripheral} \quad \text{Eq. 1}$$

In this function, B_{max} represents the maximal drug accumulation in the saturable peripheral compartment[28]. k_{in} represents the uptake rate when the saturable peripheral compartment is empty and k_{out} describes the first-order drug release from this compartment.

Secondly, as paromomycin is predominately cleared by glomerular filtration, the change in CL/F is likely a reflection of the change in renal function. Therefore, absolute estimated glomerular filtration rate ($eGFR_{abs}$) and creatinine level at baseline and on day 14 were evaluated as covariates on CL/F to describe potential time-dependent variation. $eGFR_{abs}$ was calculated based on eGFR derived from CKD-EPI creatinine

equation for age ≥18 years[30] and Bedside Schwartz Formula for age <18 years[31], while unadjusted to the typical body surface area (BSA) of 1.73 m^2 but to the individual BSA. Parameters related to CL/F and volume of distribution (Vd/F) were modeled with body weight based allometric scaling, using fixed power exponents of 0.75 and 1, respectively[32]. To quantify the potential PK differences between PKDL and VL patients, disease (PKDL or VL) was tested as a binary covariate on all PK parameters. Besides, since B_{max} describes the maximal paromomycin accumulation in megalin-expressing tissues, factors that might affect receptor amount and drug-receptor interaction, including body weight, age, and albumin, were evaluated as covariates on B_{max}[27,33,34].

2.3.2 Miltefosine population PK model

Population PK of miltefosine in VL patients has been relatively well studied, and the present model was developed using previously developed models as starting point[14,15,35]. A two-compartment disposition model with first order absorption and elimination to and from the central compartment was used as the base structural model. Fat-free mass (FFM) was used as descriptor for body size, and were related to CL/F and Vd/F using allometric scaling with power exponents of 0.75 and 1, respectively. Two effects on relative oral bioavailability (F) found in previous developed models were evaluated sequentially. Firstly, the effect of disease on the reduced F during the first week (EFF $_{Disease}$) was tested on PKDL and VL populations separately. As no intravenous data was available, only the relative bioavailability could be estimated.

In pediatric VL patients, a decrease in F was found when cumulative dose of miltefosine exceeded a threshold of 70 mg/kg[14]. This dose-dependent effect was likely related to saturation in membrane translocation of miltefosine in the gut[36-38]. Therefore, the effect of cumulative miltefosine dose on F over the treatment period (EFF $_{Cumulative\ dose}$) was examined using a previously defined model as described in equation 2.

2.4

$$EFF_{\ Cumulative\ dose}\ \left(\text{if}\ cumulative\ dose\ < 70\frac{mg}{kg}\right) = 1$$

$$EFF_{\ Cumulative\ dose}\ \left(if\ cumulative\ dose\ \geq 70\frac{mg}{kg}\right) = \left(\frac{cumulative\ dose}{70}\right)^{\theta_{cumulative\ dose}}$$

Eq. 2

Lastly, since miltefosine is prone to interact with lipids, forms micelles and is known to be easily incorporated in liposomes, the potential interaction of LAmB on miltefosine was evaluated by adding a binary covariate on all PK parameters[39,40].

2.3.3 Exposure and target attainment

Secondary PK parameters for paromomycin and miltefosine were calculated using the individual estimates of the final PK models. The area under the plasma concentration-time curve (AUC) for 24 hours was used to determine paromomycin exposure on day 1 (AUC$_{0-24,\ D1}$) and day 14 (AUC$_{0-24,\ D14}$). Miltefosine exposure was expressed by the AUC

from start until day 7, 14, 28, and 60, denoted as AUC_{0-D7}, AUC_{0-D14}, AUC_{0-D28}, AUC_{0-D60}, respectively. The time that miltefosine concentration was above the *in vitro* susceptibility value EC_{90} (Time > EC_{90}) during the first 60 days and the time point that the miltefosine concentration reached the EC_{90} (TEC_{90}) were calculated. The EC_{90} value of 10.6 mg/L was selected based on intracellular amastigote *in vitro* susceptibility testing of Leishmania *donovani*[15].

2.3.4 Software

Population PK analysis was performed using the nonlinear mixed-effects modelling program NONMEM (version 7.5; ICON Development Solutions, Ellicott City, MD), aided by Perl-speaks-NONMEM (PsN, version 5.0) and Pirana (version 2.9.9) for run deployment[41,42]. Model parameters were estimated using the first-order conditional estimation with interaction (FOCE-I) method. Inter-individual variability (IIV) in PK parameters was estimated with an exponential variance model and residual unexplained variability was estimated with a proportional error model. Individual PK parameters were obtained by maximum a posterior Bayesian estimation using POSTHOC option of NONMEM.

2.3.5 Model evaluation

Model adequacy was guided by physiological plausibility, statistical significance and graphical evaluation. The change in objective function value (OFV), which equals minus two times the log-likelihood, was used to define statistical significance between hierarchical models following a Chi-square distribution with 1 degree of freedom. A decrease in OFV of ≥3.84, representing a p-value of <0.05, was considered statistically significant. Goodness-of-fit plots were used to assist graphical evaluation using R (version 4.0) and Xpose (version 4). A visual predictive check (VPC) and sampling importance resampling (SIR) were performed to assess the predictive performance and the parameter precision with 95% confidence intervals (CI) for the final model[43,44].

3.   Results

3.1   Patients and data

A total of 328 paromomycin observations and 1516 miltefosine observations were collected in 109 PKDL and 264 VL patients. Plasma concentration-time profiles of paromomycin and miltefosine are depicted in Figure 2.4.1 and Figure 2.4.2, respectively. Demographic characteristics of the included patients are presented in Table 2.4.1A. The majority of the patients were children aged ≤18, accounting for 96% and 72% of included PKDL and VL patients, respectively. The distribution of body weight and BMI were similar between PKDL and VL patients, indicating comparable body size

(Table 2.4.1B). BMI was not considered an indicator of the health status, since both populations were from extremely poor areas and are to a large extent malnourished. The median albumin level and neutrophil count at baseline were 0.71-, 0.34-fold lower, respectively, in VL versus PKDL patients, while the creatinine level was 2-fold higher (Table 2.4.1C), confirming expected disease-specific differences in these hematological and biochemical variables.
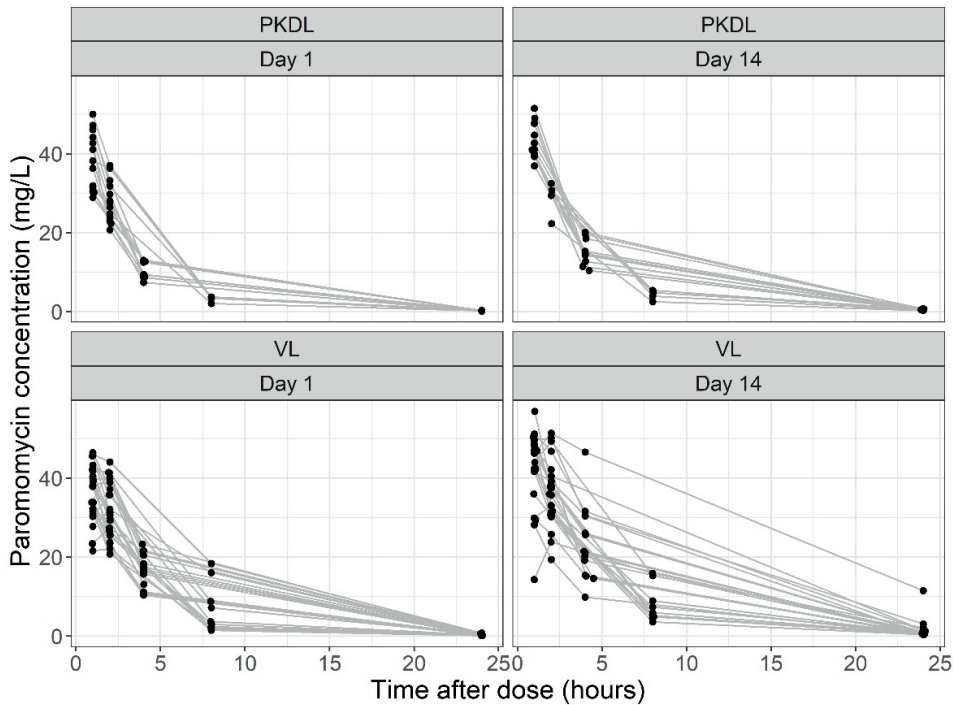
Figure 2.4.1   Paromomycin concentration-time profiles.

2.4
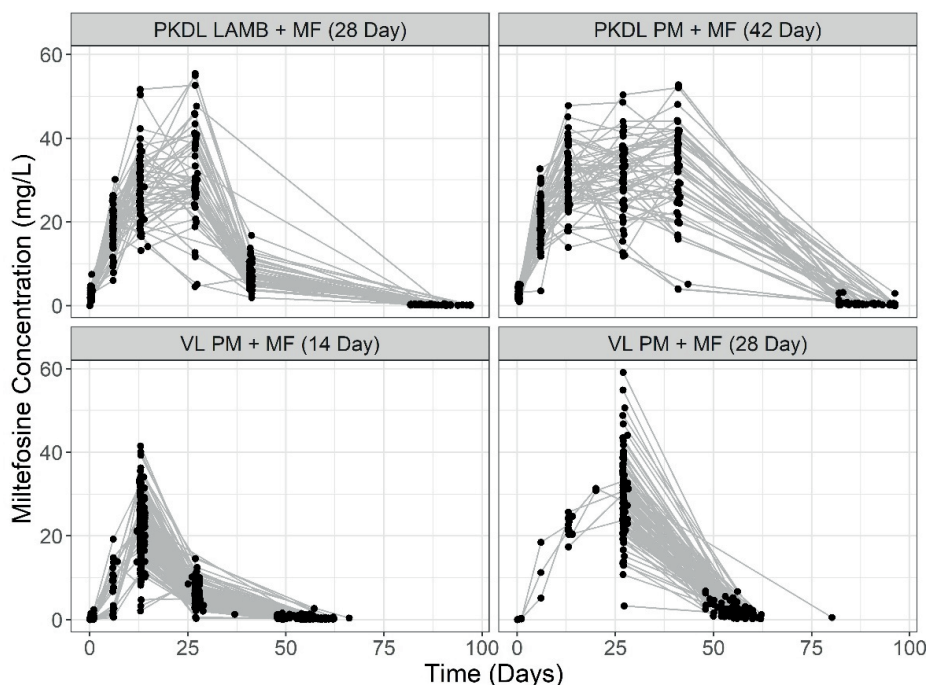
Figure 2.4.2 Miltefosine concentration-time profiles.

Table 2.4.1 Patient demographics.

A Treatment details	PKDL	VL
Total no. of patients	109	264
Included no. in PK analysis		
PM model	14	26
MF model	109	264
PKDL Treatment regimens, n (%)		
LAMB + MF 28 days	54 (49.5%)	
PM + MF 42 days	55 (50.5%)	
VL Treatment regimens, n (%)		
PM + MF 28 days		167 (63.3%)
PM + MF 14 days		97 (36.7%)

B Basic characteristics (median [range])	PKDL		VL	
	Age >18 (N=4)	Age ≤18 (N=105)	Age >18 (N=73)	Age ≤18 (N=191)
Age (years)	25.5 [19.0, 30.0]	9.00 [6.00, 18.0]	23.0 [19.0, 45.0]	9.00 [4.00, 18.0]
Body weight (kg)	63.5 [51.0, 74.0]	23.0 [15.0, 49.0]	51.0 [39.7, 71.0]	25.0 [11.0, 52.0]
Body mass index (kg/m^2)	20.0 [17.0, 21.4]	14.6 [12.1, 19.7]	17.8 [14.6, 21.6]	14.2 [11.8, 23.7]
Body surface area (m^2)	1.79 [1.60, 1.98]	0.918 [0.631, 1.49]	1.58 [1.39, 1.94]	0.961 [0.532, 1.64]
Fat-free-mass (kg)	53.4 [45.6, 60.7]	18.9 [11.8, 41.9]	44.9 [31.2, 58.9]	20.1 [9.52, 45.7]
Gender (n, %)				
Male	4 (100%)	65 (61.9%)	72 (98.6%)	141 (73.8%)
Female	0 (0%)	40 (38.1%)	1 (1.4%)	50 (26.2%)

C Laboratory examinations (median [range])	PKDL	VL
Albumin (g/L)	38.8 [28.5, 59.7]	27.4 [1.50, 54.6]
ALT (U/L)	24.0 [9.00, 90.0]	24.5 [1.00, 473]
AST (U/L)	29.0 [10.0, 67.0]	53.0 [6.00, 592]
Creatinine (mg/dL)		
Day 1	0.400 [0.100, 1.00]	0.800 [0.100, 1.50]
Day 14	0.600 [0.200, 1.50]	0.800 [0.100, 10.8]
Absolute eGFR (ml/min/m^2)		
Day 1	78.5 [27.5, 407]	56.6 [14.7, 286]
Day 14	48.8 [20.6, 170]	50.2 [3.72, 326]
Absolute Neutrophil (x10^3/μL)		
Day 1	2.91 [0.810, 6.72]	1.00 [0.200, 4.30]
Day 14	3.42 [1.84, 10.9]	2.20 [0.300, 6.10]

3.2   Pharmacokinetics of paromomycin

Plasma concentration-time profiles of paromomycin were best described by a three-compartment model with first-order absorption and elimination from the central compartment, and saturable distribution to a peripheral compartment described by a B_{max} function (equation 1) (Figure 2.4.3 and Table 2.4.2). In the initial two-compartment model, samples collected 4-8 hours after administration at day 1 were over-predicted particularly in PKDL patients, indicating a fast distribution. Besides, a time-depending bias between predictions on day 1 versus day 14 was observed in goodness-of-fit plots suggesting a decrease in plasma CL/F over the treatment period. Incorporating a saturable compartment to resemble paromomycin accumulation in tissues significantly improved the model fit with dOFV of -109, and solved the time-related bias. Disease type was a significant covariate on B_{max}, suggesting that the maximum capacity for paromomycin accumulation in tissues was 1.7-fold (95%CI: 1.21-2.45) higher in PKDL patients compared to VL patients. The maximal fraction of paromomycin accumulated in tissue corresponds to 3.5% and 1.7% of the total dose given in PKDL and VL patients, respectively. No additional significant covariates were found to explain the variability in B_{max}.

2.4
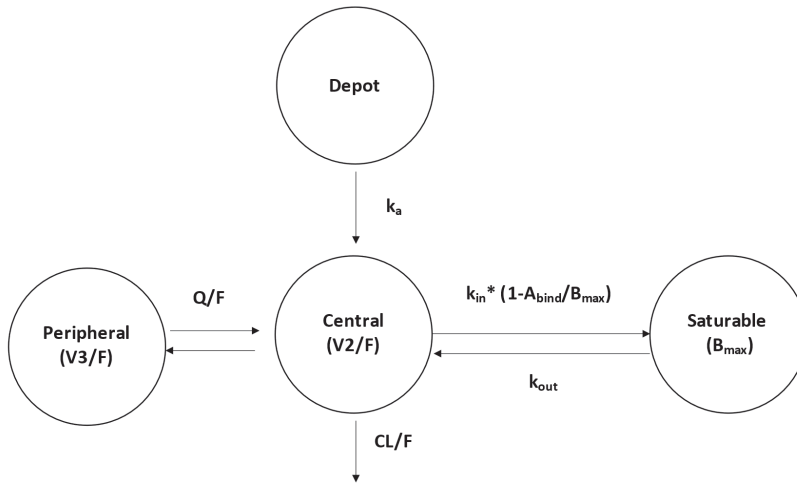
Figure 2.4.3 Structure of the final paromomycin model. CL/F, paromomycin clearance; k_a, rate of absorption; V2/F, volume of the central compartment; Q/F, inter-compartmental clearance; V3/F, volume of the peripheral compartment; k_{in}, rate constant for association; k_{out}, rate constant for dissociation; B_{max}, maximal drug accumulation in the saturable compartment represented by megalin-expressing cells.

Table 2.4.2 Paromomycin final model parameter estimates.

	Unit	Estimate	95%CI
Population parameters Rate of absorption (k_a)	1/h	2.59	2.08-3.45
Paromomycin clearance on Day1 [a] (CL_{D1}/F)	L/h	1.45	1.23-1.72
Paromomycin clearance on Day14 [a] (CL_{D14}/F)	1/h	$CL_{D1}*(CREAT_{D0}/CREAT_{D14})$ [b]	
Volume of central compartment [a] (V2/F)	L	6.72	6.40-7.03
Inter-compartmental clearance [a] (Q/F)	L/h	0.57	0.4-0.7
Volume of peripheral compartment [a] (V3/F)	L	1150	563-1844
Rate constant for association (k_{in})	1/h	0.2	0.13-0.27
Rate constant for dissociation (k_{out})	1/h	0.005	0.004-0.007
Maximal drug accumulation in peripheral compartment (B_{max})			
B_{max} in VL patients	mg	108	76-156
B_{max} in PKDL patients relative to VL patients (fractional change)	-	1.7	1.21-2.45
Between subject variability			
CL_{D1}/F	CV%	28	22-37
CL_{D14}/F	CV%	51	40-66
B_{max}	CV%	34	16-48
Residual proportional error	CV%	18	16-20

[a] Allometrically scaled based on weight with a power exponent of 0.75 for clearance and 1 for volume of distribution; [b] $CREAT_{D0}$, creatinine levels measured pre-screening; $CRETA_{D14,}$ creatinine levels measured on day 14.

PKDL patients had a lower baseline creatinine level compared to VL patients, and showed a trend of increase during the treatment, while VL patients had a relatively high but stable creatinine level at baseline and during the treatment period (Supplementary Figure S2.4.1). Variability in baseline creatinine level and $eGFR_{abs}$ could not explain the variability in paromomycin CL/F between individuals. However, the individual relative change in renal function over time, expressed as creatinine level or $eGFR_{abs}$ on day 14 divided by the baseline level, was found to be a good additional descriptor for individual changes in CL/F during the 14-day treatment period. In the final model, creatinine at baseline divided by creatinine at day 14 ($CREAT_{D0}/CREAT_{D14}$) was included as a covariate on baseline CL/F following equation 3, which resulted in a dOFV of -56.

$$CL_{D14} = CL_{D1} * (\frac{CREAT_{D0}}{CREAT_{D14}})$$

Eq. 3

The final model adequately described paromomycin observations in PKDL and VL patients. Goodness-of-fit plots (Supplementary Figure S2.4.2) and the VPC (Figure 2.4.4) based on the final model showed no major deviations. Paromomycin exposure in PKDL patients on day 1 ($AUC_{0-24, D1}$) and on day 14 ($AUC_{0-24,D14}$) was 22% and 26% lower than in VL patients, respectively (Table 2.4.3).
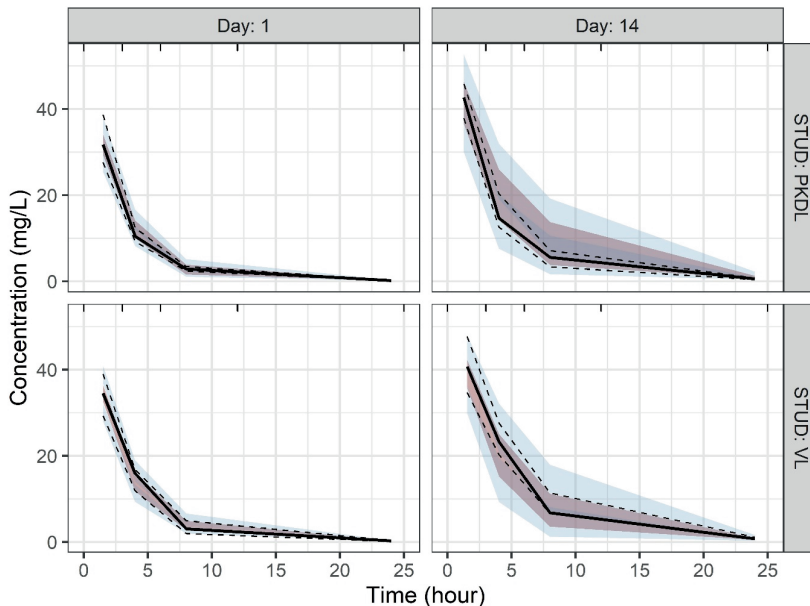
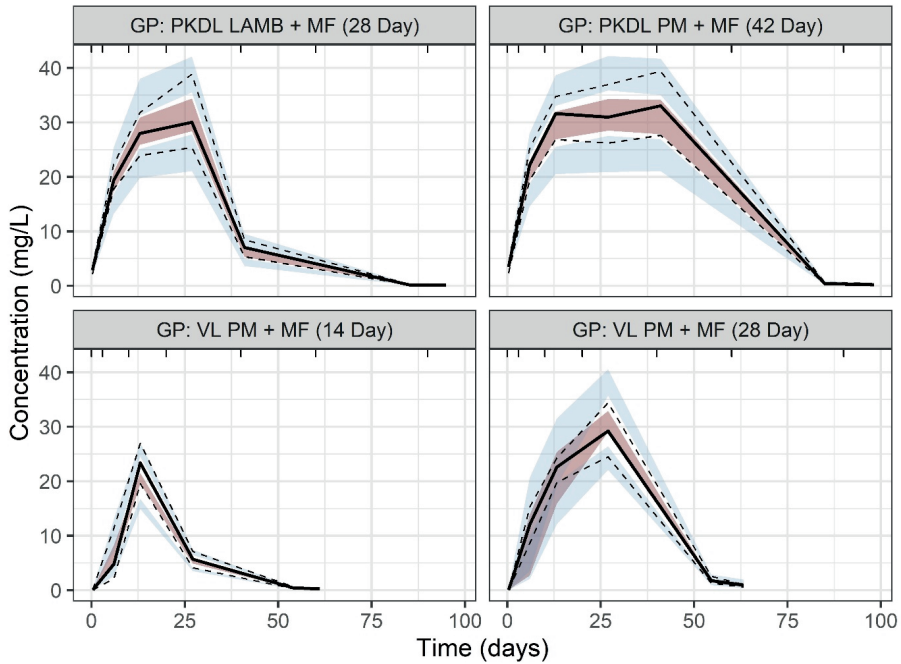**Figure 2.4.4** Prediction corrected visual predictive checks of the final paromomycin pharmacokinetic model. The solid lines represent the median of the observed values, the dashed lines the 25th and 75th percentiles of the observed values. The dark and light blue areas indicate the 95% confidence intervals of the simulated median and percentiles, based on 200 simulations.

Table 2.4.3 Paromomycin exposure and target attainment (median [range]).

	PKDL	VL
AUC$_{0-24, D1}$ (mg*hr/L)	132 [99.2, 157]	168 [108, 275]
AUC$_{0-24, D14}$ (mg*hr/L)	168 [134, 185]	226 [118, 800]

AUC$_{0-24}$: Area under the plasma concentration-time curve for 0 till 24 hours after dosing. Both PKDL and VL patients received 14 days of 20 mg/kg paromomycin.

3.3 Pharmacokinetics of miltefosine

In line with previous studies, miltefosine concentration-time profiles were best described by a two-compartment model with first-order absorption and first-order elimination. Nonlinearities in miltefosine PK were identified and were best described by changes in F, which in turn were influenced by disease (EFF $_{Disease}$), cumulative dose (EFF $_{Cumulative\ dose}$), and a drug-drug interaction with LAmB (EFF $_{LAmB}$) in the final model (Table 2.4.4). The effects on F are summarized in equation 4 and Figure 2.4.5 and the details are explained below.

$$F\ (if\ treatment\ day\ \leq 7\ ) = TVF\ *\ (1 - EFF_{Disease})\ *\ EFF\ _{Cumulative\ dose}\ *\ (1 - EFF_{LAmB})$$

Eq. 4

$$F\ (if\ treatment\ day > 7\ ) = TVF\ *\ EFF\ _{Cumulative\ dose}$$

In the concentration-time profiles, a large difference in drug accumulation and exposure in the first week of treatment between VL patients and PKDL patients was observed (Figure 2.4.2). In PKDL patients, the effect of disease on F in the first week of treatment was not identified, and was therefore fixed to 0. While in VL patients, F in the first week of treatment decreased by 69% (95% CI:62-76). In addition to the difference in F, the rate of absorption (k$_a$) in PKDL and VL was 5.43 1/day (95% CI: 4.54-6.26) and 0.99 1/day (95%CI: 0.84-1.17), respectively, indicating a much longer absorption half-life in VL patients. As PKDL patients are not affected by a systemic parasite infection, the relatively low k$_a$ and F at treatment start only in VL patients support previous hypotheses about disease-specific absorption-limiting factors, which are likely related to malabsorption[45,46].

The previously described dose-related effect on F was identified in both VL and PKDL populations and was further optimized[14]. In the final model, the decrease in F was related to cumulative miltefosine dose from the beginning of treatment, and was best described by a power function with the exponent estimated at -0.13 (95%CI: -0.16 - -0.11) (Equation 5), which resulted in a dOFV of -42. For patients given 14- and 42- day miltefosine treatment, relative bioavailability decreased by 33.7% and 40.6% from start till end of treatment, respectively.

$$EFF\ _{Cumulative\ dose}\ =\ Cumulative\ dose\ \left(\frac{mg}{kg}\right)^{\theta_{cumulative\ dose}}$$

Eq. 5

Table 2.4.4   Miltefosine final model parameter estimates.

	Unit	Estimate	95%CI
Population parameters			
Absorption rate in PKDL (k_a PKDL)	1/day	5.43	4.54-6.26
Absorption rate in VL (k_a VL)	1/day	0.99	0.84-1.17
Clearance [a] (CL/F)	L/day	1.53	1.4-1.66
Volume of central compartment [a] (V2/F)	L	13.8	12.66-14.89
Inter-compartmental clearance (Q/F)	L/day	0.039	0.032-0.049
Volume of peripheral compartment [a] (V3/F)	L	2.01	1.69-2.54
F after a week of treatment	%	100 (Fixed)	
Relative decrease in F during the first week of treatment			
PKDL patients	%	0 (Fixed)	
VL patients (EFF $_{Disease}$)	%	69	62-76
Patients co-administered with LAmB (EFF $_{LAmB}$)	%	8.6	2-15
Exponent of power relationship between cumulative MF dose and F (EFF $_{cumulative\ dose}$)	-	-0.13	(-0.16) - (-0.11)
Between subject variability			
CL/F	CV%	20	17-22
V2/F	CV%	13[b]	-
EFF $_{Disease}$	CV%	71	61-83
Residual proportional error	CV%	31	30-33

[a] Allometrically scaled based on fat-free mass with a power exponent of 0.75 for clearance and 1 for volume of distribution. Estimate is given for a standardized fat free mass of 25kg; [b] IIV in V2/ F was not identifiable, but a high correlation between CL/F and V2/F was suggested by SIR results. Therefore, the same ETA distribution was assumed for CL/F and V/F, and a scaling factor of 0.45 was estimated.

In PKDL patients who received LAmB-MF, median miltefosine concentration was 12% lower in the first week compared to patients receiving PM-MF (Figure 2.4.2), despite a similar daily dosing regimen. This prompted the evaluation of a potential interaction between LAmB and miltefosine. LAmB was tested as a binary covariate on all PK parameters, and was found to lower F in the first week by 8.6% (95%CI: 2-15) (dOFV -9.5), resulting in a 10% lower AUC$_{0-D7}$ of miltefosine when co-administered with LAmB (Table 2.4.5).

2.4

Table 2.4.5   Miltefosine exposure and target attainment (median [range]).

	PKDL		VL	
Treatment regimen	LAMB + MF (28 Day)	PM + MF (42 Day)	PM + MF (14 Day)	PM + MF (28 Day)
AUC $_{0-7D}$ (mg·day/L)	96.8 [69.2, 115]	107 [74.4, 159]	28.9 [5.42, 90.3]	27.0 [13.7, 43.2]
AUC $_{0-14D}$ (mg·day/L)	280 [209, 322]	300 [213, 484]	134 [66.3, 296]	127 [92.3, 171]
AUC $_{0-28D}$ (mg·day/L)	724 [555, 860]	727 [534, 1320]	304 [196, 600]	524 [357, 684]
AUC $_{0-60D}$ (mg·day/L)	991 [719, 1240]	1360 [1010, 2810]	352 [218, 774]	796 [487, 1190]
Time> EC$_{90}$	27.8 [22.4-31.7]	41.7 [35.5-56.0]	5.27 [0-18.3]	21.5 [12.8-28.9]
TEC$_{90}$	4.96 [3.94, 8.30]	4.11 [2.21, 7.96]	11.6 [4.73, 14.9]	12.0 [9.76, 16.2]

AUC: Area under the plasma concentration-time curve. EC$_{90}$: 90% effective miltefosine concentration, equivalent to 10.6 µg/mL. Time > EC$_{90}$: Time that the miltefosine concentration was over the in vitro susceptibility value EC$_{90}$ during the first 60 days of treatment. TEC$_{90}$: Total time that the miltefosine concentration was over the in vitro susceptibility value EC$_{90.}$
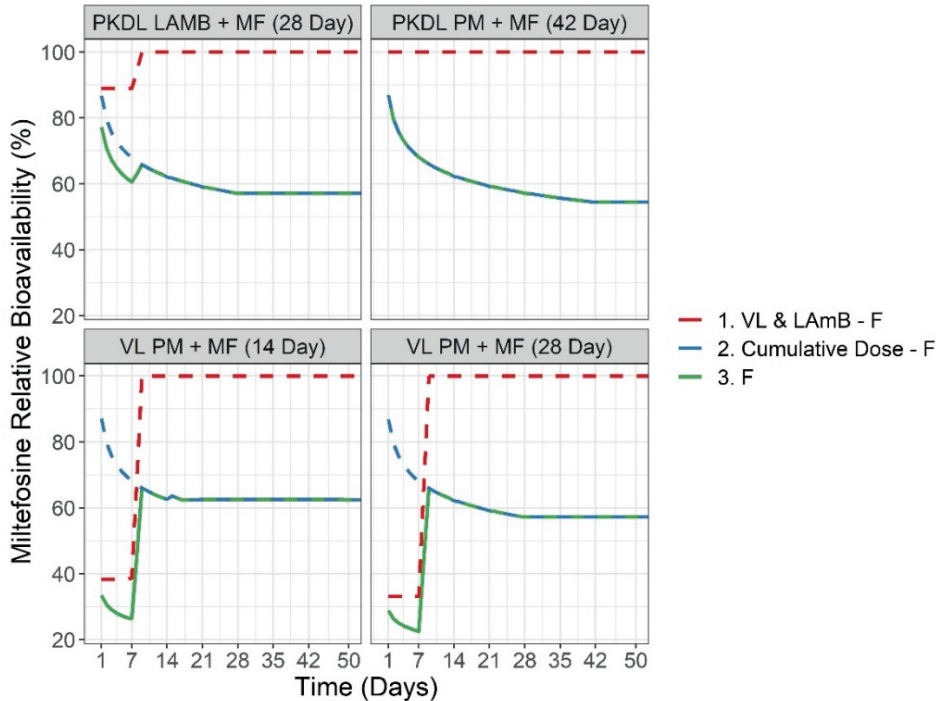
Figure 2.4.5 Miltefosine relative bioavailability over time. (1) Red dashed line describes the effect of disease (VL or PKDL) and the effect of LAmB on relative bioavailability. (2) Blue dashed line describes the effect of cumulative dose on relative bioavailability. (3) Green solid line is the resulting cumulative bioavailability of all three effects over time.

The SIR results indicated a high correlation between miltefosine CL/F and Vd/F of the central compartment (V2). Since the IIV on Vd/F could not be identified, the same ETA distribution was assumed for CL/F and Vd/F assuming 100% correlation, with a scaling factor estimated at 0.45 (dOFV -22) (Table 2.4.4). The final model, which includes effects of disease, cumulative dose, and interaction with LAmB on miltefosine F, provided an adequate description of miltefosine observations in PKDL and VL patients who received different combination regimens. Goodness-of-fit plots (Supplementary Figure S2.4.3) and the VPC (Figure 2.4.6) based on the final model showed no major deviations. Miltefosine exposure during the first week of treatment (AUC_{0-D7}) was 3.6-fold higher in PKDL patients compared to VL patients (Table 2.4.5). Overall exposure in patients receiving 28-days miltefosine treatment (AUC_{0-D28}) was 38% higher in PKDL patients compared to VL patients. Due to differences in initial drug accumulation, miltefosine plasma concentrations reached EC_{90} (TEC_{90}) already after 4 versus 12 days of treatment in PKDL and VL patients, respectively**.**

Figure 2.4.6 Prediction corrected visual predictive checks of the final miltefosine pharmacokinetic model. The solid lines represent the median of the observed values, the dashed lines the 25th and 75th percentiles of the observed values. The dark and light blue areas indicate the 95% confidence intervals of the simulated median and percentiles, based on 200 simulations.

2.4

4.   Discussion

Large and potentially clinically relevant differences in drug exposure and PK parameters of paromomycin and miltefosine were for the first time identified and quantified between PKDL and VL patients in Eastern Africa. PKDL patients had a 26% lower exposure to paromomycin at the end of treatment, which was caused by a higher maximum capacity for paromomycin accumulation in tissue (B_{max}) and higher plasma clearance due to a better renal function. Miltefosine exposure at day 28 was 38% higher in PKDL patients, caused by a higher F due to better gastrointestinal absorption. Moreover, EC_{90} was already reached after 4 days of treatment (TEC_{90}), compared to 12 days in VL patients, caused by a considerably faster miltefosine absorption rate in PKDL patients. The lower paromomycin plasma exposure in PKDL patients might explain the fewer cases of nephrotoxicity and ototoxicity found in PKDL patients, and the current maximal paromomycin dose of 20 mg/kg/day based on VL patients might be increased in PKDL patients. On the other hand, the increased miltefosine exposure and faster TEC_{90} in PKDL patients might improve treatment efficacy. These considerable

differences in exposure indicate that dosing regimens could not be directly extrapolated from VL to PKDL.

The population PK models allowed to identify different mechanistic effects to explain nonlinearities in paromomycin and miltefosine PK, as well as disease-related PK differences between VL and PKDL patients. PKDL and VL patients were from the same regions and were therefore comparable in terms of demographics such as age and body size, except for disease-associated biomarkers such as creatinine, albumin and neutrophils, and were therefore particularly suitable for the identification of disease-specific effects.

In the paromomycin model, the observed time-depending exposure was explained by both saturable distribution plus the relative change in renal function. B_{max} in PKDL patients was 1.7-fold (95%CI: 1.21-2.45) higher than in VL patients, which explained the observed faster decrease in paromomycin concentration within 4 hours post-dose. Moreover, the higher B_{max} found in PKDL patients might indicate a better toleration for aminoglycoside-induced renal toxicity, likely due to more functional cells or better cell recovery corroborated by a better baseline renal function. Aminoglycosides are known to be internalized by the transmembrane protein megalin and accumulate in cell lysosomes, which results in cell death and further toxicity (e.g., nephrotoxicity and ototoxicity). However, it is unclear whether the toxicity is related to local drug concentration or caused by the drug release from lysosomes that would take place when the accumulation reaches a critical threshold[21-23]. The framework of the current model can be extended to other aminoglycosides to further explore the relationship between drug-induced toxicity and drug accumulation in tissues.

Given that paromomycin is predominantly cleared renally, a relationship between paromomycin CL/F and renal function was expected[11]. The change in paromomycin CL/F was found to follow the individual change in creatinine levels or $eGFR_{abs}$ during the 14-day treatment period, rather than the baseline creatinine or $eGFR_{abs}$. This suggests that the measured creatinine level was not directly reflecting the baseline renal function in PKDL and VL patients, possibly due to either a lack of standardization of creatinine measurements or the lack of validated equations to estimate GFR based on creatinine in this relatively ill and malnourished population, or a combination of both[47]. The validity of current eGFR estimation methods in similar populations has been questioned previously[48].

For miltefosine, F decreased by 69% (95%CI: 62-76) in VL patients at treatment start, while in PKDL patients no initial decrease in F was presented. The k_a in VL patients was 0.99 1/day (95CI: 0.84-1.17), comparable to previously reported values of 0.4 -1.6 1/day[14,15,35]. The k_a in PKDL patients was described for the first time, equal to

5.43 1/day (95%CI: 4.54-6.26), which was much faster compared to VL patients, but comparable to the k_a of 8.64 1/day reported for cutaneous leishmaniasis patients[49]. The decreased F as well as the slower k_a in VL patients suggests a poor gastrointestinal absorption in VL patients owing to a more severe disease status. In line with the previous miltefosine model[14], the accumulation of miltefosine in plasma reached a plateau after three weeks of treatment in both PKDL and VL populations, which was explained by a decrease in F over the treatment period related to cumulative dose. Estimation of the dose effect on the absorption process over the whole treatment period was improved due to the combination of PKDL and VL patient data in one analysis.

This analysis identified a potential drug-drug interaction between miltefosine and LAmB. In PKDL patients given miltefosine together with LAmB, the F of miltefosine during the LAmB treatment period was 8.6% (95%CI: 2-15) lower than in patients given miltefosine and paromomycin combination treatment, leading to a 10% lower miltefosine exposure in the first week. In theory, free or micellular miltefosine can be incorporated into the liposomes of LAmB[39,40]. However, this additional miltefosine clearance route might actually be beneficial for increased miltefosine target-site exposure and activity/efficacy as liposomes are preferentially phagocytized by parasite-infected macrophages[50].

Exposure-response relationships should be established in PKDL patients in order to further optimize paromomycin and miltefosine dosing in more detail. Drug exposure in the skin lesions will most likely be more relevant for the exposure-efficacy relationship in PKDL. The largely decreased exposure for paromomycin in PKDL patients in combination with the improved tolerability, potentially indicates that a higher maximal mg/kg/day paromomycin dosing is applicable for PKDL patients than the 20 mg/kg/day previously established in VL patients. Particularly large observed impediments in both extent and rate of oral absorption for miltefosine in VL patients which were not present in PKDL patients, question more generally the direct extrapolation of dosing regimen from VL to PKDL. Typically, treatment regimens are being evaluated for efficacy and tolerability in VL and these regimens are then directly extrapolated, potentially with an extension in treatment duration, to PKDL. Our results indicate that this direct extrapolation is certainly not necessarily valid, particularly for oral and renally cleared drugs. Given that the current drugs in the drug development pipeline for VL are all oral new chemical entities, this should be taken into account when the first PKDL regimens for these drugs are being evaluated clinically, e.g., by the implementation of more extensive dose-finding studies.

In conclusion, we have shown that drug exposure to paromomycin was lower in PKDL patients, while miltefosine exposure was higher compared to VL patients in Eastern

2.4

Africa, for which various disease-specific mechanisms affecting the absorption, distribution and elimination of these drugs were identified and characterized. This study illustrates and highlights the difficulty of directly extrapolating dosing regimens between VL and the various other dermal clinical presentations of leishmaniasis, particularly for oral and renally cleared drugs.

Acknowledgments

Funding

References

1. Harhay MO, Olliaro PL, Vaillant M, Chappuis F, Lima MA, Ritmeijer K, et al. Who is a typical patient with visceral leishmaniasis? Characterizing the demographic and nutritional profile of patients in Brazil, East Africa, and South Asia. Am J Trop Med Hyg. 2011;84(4):543–50.
2. Zijlstra EE, Musa AM, Khalil EAG, El Hassan IM, El-Hassan AM. Post-kala-azar dermal leishmaniasis. Lancet Infect Dis. 2003;3(2):87–98.
3. Musa AM, Khalil EAG, Raheem MA, Zijlstra EE, Ibrahim ME, Elhassan IM, et al. The natural history of Sudanese post-kala-azar dermal leishmaniasis: clinical, immunological and prognostic features. Ann Trop Med Parasitol. 2002;96(8):765–72.
4. Wasunna M, Musa A, Hailu A, Khalil EAG, Olobo J, Juma R, et al. The Leishmaniasis East Africa Platform (LEAP): strengthening clinical trial capacity in resource-limited countries to deliver new treatments for visceral leishmaniasis. Trans R Soc Trop Med Hyg. 2016;110(6):321.
5. Kimutai R, Musa AM, Njoroge S, Omollo R, Alves F, Hailu A, et al. Safety and Effectiveness of Sodium Stibogluconate and Paromomycin Combination for the Treatment of Visceral Leishmaniasis in Eastern Africa: Results from a Pharmacovigilance Programme. Clin Drug Investig. 2017;37(3):259.
6. Nakweya G. Drug combination offers shorter, more effective visceral leishmaniasis treatment. Nat Africa. 2022.
7. Musa AM, Mbui J, Mohammed R, Olobo J, Ritmeijer K, Alcoba G, et al. Paromomycin and Miltefosine Combination as an Alternative to Treat Patients With Visceral Leishmaniasis in Eastern Africa: A Randomized, Controlled, Multicountry Trial. Clin Infect Dis. 2022;ciac643.
8. Musa AM, Khalil EAG, Younis BM, Elfaki MEE, Elamin MY, Adam AOA, et al. Treatment-based strategy for the management of post-kala-azar dermal leishmaniasis patients in the Sudan. J Trop Med. 2013;2013:708391.
9. Drugs for Neglected Diseases. Short Course Regimens for Treatment of PKDL (Sudan).[ClinicalTrials.gov identifier NCT03399955]. US National Library of Medicine, ClinicalTrials.gov.
10. Institute for One World Health. Application for inclusion of paromomycin in the WHO Model List of Essential Medicines. 2006. [Internet]. Available from: http://archives.who.int/eml/expcom/expcom15/applications/newmed/paromomycin/paromomycin.pdf.
11. Talbert RL. Drug Dosing in Renal Insufficiency. J Clin Pharmacol. 1994;34(2):99–110.
12. Kanyok TP, Killian AD, Rodvold KA, Danziger LH. Pharmacokinetics of intramuscularly administered aminosidine in healthy subjects. Antimicrob Agents Chemother. 1997;41(5):982–6.
13. Dorlo TPC, Balasegaram M, Beijnen JH, de vries PJ. Miltefosine: a review of its pharmacology and therapeutic efficacy in the treatment of leishmaniasis. J Antimicrob Chemother. 2012;67(11):2576–97.
14. Palic S, Kip AE, Beijnen JH, Mbui J, Musa A, Solomos A, et al. Characterizing the non-linear pharmacokinetics of miltefosine in paediatric visceral leishmaniasis patients from Eastern Africa. J Antimicrob Chemother. 2020;75(11):3260–8.
15. Dorlo TPC, Kip AE, Younis BM, Ellis SJ, Alves F, Beijnen JH, et al. Visceral leishmaniasis relapse hazard is linked to reduced miltefosine exposure in patients from Eastern Africa: A population pharmacokinetic/pharmacodynamic study. J Antimicrob Chemother. 2017;72(11):3131–40.
16. Dorlo TPC, Huitema ADR, Beijnen JH, de Vries PJ. Optimal dosing of miltefosine in children and adults with visceral leishmaniasis. Antimicrob Agents Chemother. 2012;56(7):3864–72.
17. Roseboom IC, Thijssen B, Rosing H, Mbui J, Beijnen JH, Dorlo TPC. Highly sensitive UPLC-MS/MS method for the quantification of paromomycin in human plasma. J Pharm Biomed Anal. 2020;185.
18. Dorlo TPC, Hillebrand MJX, Rosing H, Eggelte TA, de Vries PJ, Beijnen JH. Development and validation of a quantitative assay for the measurement of miltefosine in human plasma by liquid chromatography-tandem mass spectrometry. J Chromatogr B Analyt Technol Biomed Life Sci. 2008;865(1–2):55–62.
19. Verrest L, Roseboom IC, Wasunna M, Mbui J, Musa A, Olobo J, et al. Population pharmacokinetics of a combination of miltefosine and paromomycin in Eastern African children and adults with visceral leishmaniasis. Thesis Luka Verrest.
20. Verrest L, Wasunna M, Kokwaro G, Aman R, Musa AM, Khalil EAG, et al. Geographical Variability in Paromomycin Pharmacokinetics Does Not Explain Efficacy Differences between Eastern African and Indian Visceral Leishmaniasis Patients. Clin Pharmacokinet. 2021;60(11):1463–73.

2.4

21.   Mingeot-Leclercq MP, Tulkens PM. Aminoglycosides: Nephrotoxicity. Antimicrob Agents Chemother. 1999;43(5):1003.

22.   Lopez-Novoa JM, Quiros Y, Vicente L, Morales AI, Lopez-Hernandez FJ. New insights into the mechanism of aminoglycoside nephrotoxicity: an integrative point of view. Kidney Int. 2011;79(1): 33-45.

23.   Perazella MA. Pharmacology behind Common Drug Nephrotoxicities. Clin J Am Soc Nephrol. 2018; 13(12):1897.

24.   Moestrup SK, Cui S, Vorum H, Bregengård C, Bjørn SE, Norris K, et al. Evidence that epithelial glycoprotein 330/megalin mediates uptake of polybasic drugs. J Clin Invest. 1995;96(3):1404.

25.   Christensen EI, Birn H. Megalin and cubilin: multifunctional endocytic receptors. Nat Rev Mol Cell Biol 2002;3(4):258–67.

26.   Giuliano RA, Verpooten GA, Verbist L, Wedeen RP, De Broe ME. In vivo uptake kinetics of aminoglycosides in the kidney cortex of rats. J Pharmacol Exp Ther. 1986;236(2):470-475.

27.   Nagai J, Tanaka H, Nakanishi N, Murakami T, Takano M. Role of megalin in renal handling of aminoglycosides. Am J Physiol Renal Physiol. 2001;281(2): F337-44.

28.   Zheng G, Bachinsky DR, Stamenkovic I, Strickland DK, Brown D, Andres G, et al. Organ distribution in rats of two members of the low-density lipoprotein receptor gene family, gp330 and LRP/alpha 2MR, and the receptor-associated protein (RAP). J Histochem Cytochem. 1994;42(4):531–42.

29.   Nijstad AL, Chu WY, de Vos-Kerkhof E, Enters-Weijnen CF, van de Velde ME, Kaspers GJL, et al. A Population Pharmacokinetic Modelling Approach to Unravel the Complex Pharmacokinetics of Vincristine in Children. Pharm Res. 2022;39(10):2487.

30.   Levey AS, Stevens LA, Schmid CH, Zhang Y, Castro AF, Feldman HI, et al. A New Equation to Estimate Glomerular Filtration Rate. Ann Intern Med. 2009;150(9):604.

31.   Schwartz GJ, Muñoz A, Schneider MF, Mak RH, Kaskel F, Warady BA, et al. New equations to estimate GFR in children with CKD. J Am Soc Nephrol. 2009;20(3):629–37.

32.   West GB, Brown JH, Enquist BJ. A general model for the origin of allometric scaling laws in biology. Science (80-). 1997;276(5309):122–6.

33.   Nielsen R, Christensen EI, Birn H. Megalin and cubilin in proximal tubule protein reabsorption: from experimental models to human disease. Kidney Int. 2016;89(1):58–67.

34.   Zhai XY, Nielsen R, Birn H, Drumm K, Mildenberger S, Freudinger R, et al. Cubilin- and megalin-mediated uptake of albumin in cultured proximal tubule cells of opossum kidney. Kidney Int. 2000;58(4):1523–33.

35.   Dorlo TPC, Huitema ADR, Beijnen JH, De Vries PJ. Optimal dosing of miltefosine in children and adults with visceral leishmaniasis. Antimicrob Agents Chemother. 2012;56(7):3864–72.

36.   Barioni MB, Ramos AP, Zaniquelli MED, Acuña AU, Ito AS. Miltefosine and BODIPY-labeled alkylphosphocholine with leishmanicidal activity: Aggregation properties and interaction with model membranes. Biophys Chem. 2015;196:92–9.

37.   Ménez C, Buyse M, Dugave C, Farinotti R, Barratt G. Intestinal absorption of miltefosine: contribution of passive paracellular transport. Pharm Res. 2007;24(3):546–54.

38.   Ménez C, Buyse M, Farinotti R, Barratt G. Inward translocation of the phospholipid analogue miltefosine across caco-2 cell membranes exhibits characteristics of a carrier-mediated process. Lipids. 2007;42(3):229–40.

39.   Barratt G, Saint-Pierre-Chazalet M, Loiseau P. Cellular transport and lipid interactions of miltefosine. Curr Drug Metab. 2009;10(3):247–55.

40.   K S, SL C. In vitro and in vivo interactions between miltefosine and other antileishmanial drugs. Antimicrob Agents Chemother. 2006;50(1):73–88.

41.   Lindbom L, Ribbing J, Jonsson EN. Perl-speaks-NONMEM (PsN)--a Perl module for NONMEM related programming. Comput Methods Programs Biomed. 2004;75(2):85–94.

42.   Keizer RJ, van Benten M, Beijnen JH, Schellens JHM, Huitema ADR. Piraña and PCluster: A modeling environment and cluster infrastructure for NONMEM. Comput Methods Programs Biomed. 2011;101(1):72–9.

43.   Bergstrand M, Hooker AC, Wallin JE, Karlsson MO. Prediction-corrected visual predictive checks for diagnosing nonlinear mixed-effects models. AAPS J. 2011;13(2):143–51.

44.   Dosne AG, Bergstrand M, Karlsson MO. An automated sampling importance resampling procedure for estimating parameter uncertainty. J Pharmacokinet Pharmacodyn. 2017;44(6):509–20.

45. Viteri FE, Flores JM, Alvarado J, Béhar M. Intestinal malabsorption in malnourished children before and during recovery. Relation between severity of protein deficiency and the malabsorption process. Am J Dig Dis. 1973;18(3):201–11.
46. Krishnaswamy K. Drug metabolism and pharmacokinetics in malnourished children. Clin Pharmacokinet. 1989;17 Suppl 1(1):68–88.
47. Waikar SS, Sabbisetti VS, Bonventre J V. Normalization of urinary biomarkers to creatinine during changes in glomerular filtration rate. Kidney Int. 2010;78(5):486–94.
48. Fabian J, Kalyesubula R, Mkandawire J, Hansen CH, Nitsch D, Musenge E, et al. Measurement of kidney function in Malawi, South Africa, and Uganda: a multicentre cohort study. Lancet Glob Heal. 2022; 10(8):e1159–69.
49. Dorlo TPC, Van Thiel PPAM, Huitema ADR, Keizer RJ, De Vries HJC, Beijnen JH, et al. Pharmacokinetics of miltefosine in old world cutaneous leishmaniasis patients. Antimicrob Agents Chemother. 2008; 52(8):2855–60.
50. Kelly C, Jefferies C, Cryan S-A. Targeted liposomal drug delivery to monocytes and macrophages. J Drug Deliv. 2011;2011:1–11.

2.4

Supplementary material 2.4
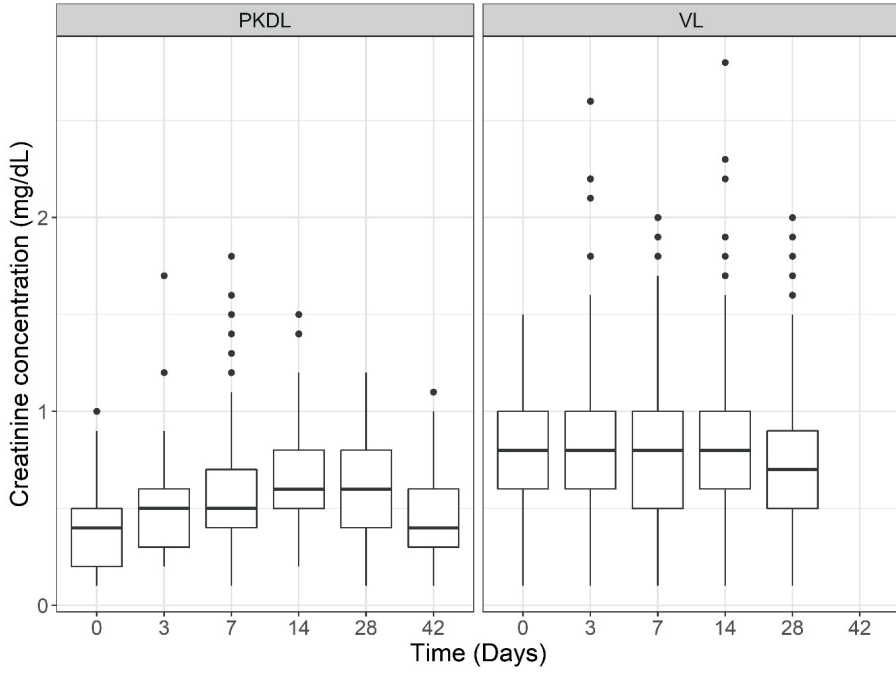
Figure S2.4.1 *Creatinine concentrations in PKDL patients (left panel) and in VL patients (right panel) over time.*
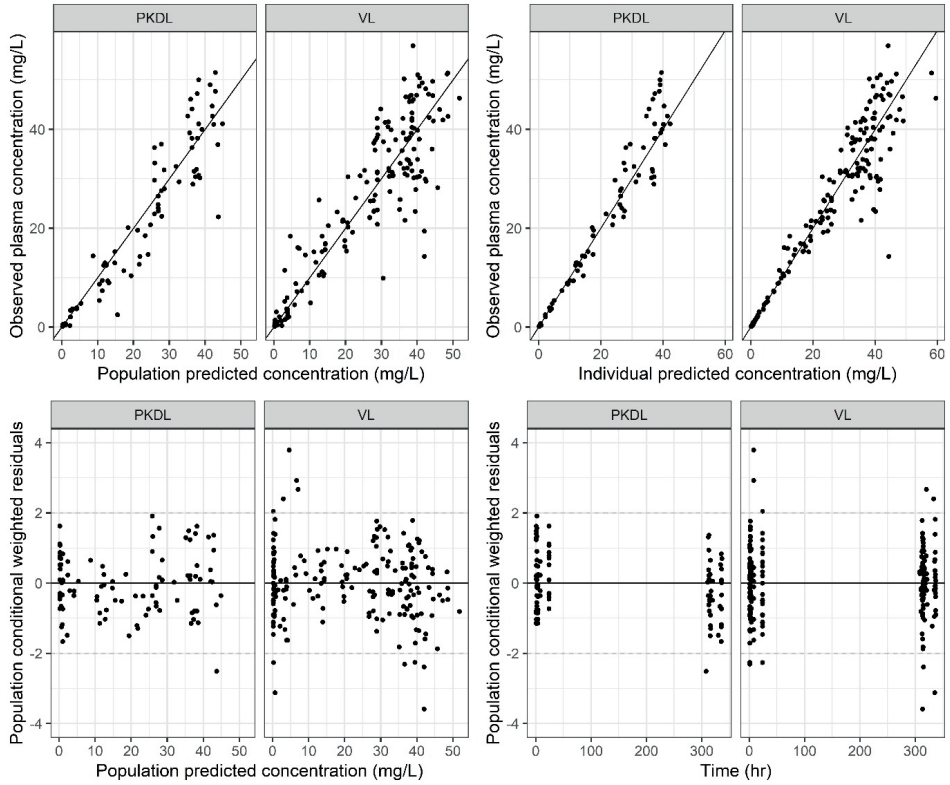
Figure S2.4.2 Goodness-of-fit plots for the final paromomycin pharmacokinetic model. (a) Observed versus population predicted paromomycin concentrations, (b) observed versus individually predicted paromomycin concentrations, (c) conditional weighted residuals (CWRES) versus population predicted concentrations, and (d) CWRES versus time after last dose.

2.4
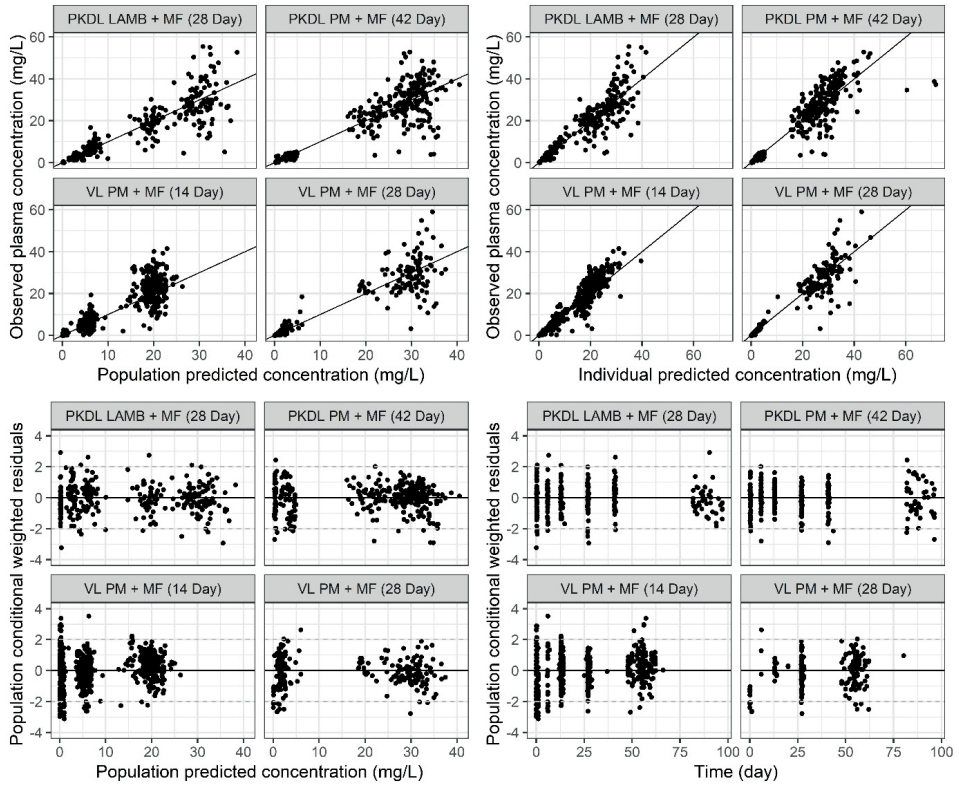
Figure S2.4.3 Goodness-of-fit plots for the final miltefosine pharmacokinetic model. (a) Observed versus population predicted paromomycin concentrations, (b) observed versus individually predicted paromomycin concentrations, (c) conditional weighted residuals (CWRES) versus population predicted concentrations, and (d) CWRES versus time after last dose.

Chapter 3

Leishmania parasite dynamics

Chapter 3.1

Blood parasite load as an early marker to predict treatment response in visceral leishmaniasis in Eastern Africa

Luka Verrest, Anke E. Kip, Ahmed M. Musa, Gerard J. Schoone, Henk D. F. H. Schallig, Jane Mbui, Eltahir A. G. Khalil, Brima M.Younis, Joseph Olobo, Lilian Were, Robert Kimutai, Séverine Monnerat, Isra Cruz, Monique Wasunna, Alexandra Solomos, Fabiana Alves, Thomas P. C. Dorlo

Abstract

Background: In order to expedite the development of new oral treatment regimens for visceral leishmaniasis (VL), there is a need for early markers to evaluate treatment response and predict long-term outcomes.

Methods: Data from three clinical trials were combined in this study, where Eastern African VL patients received various antileishmanial therapies. *Leishmania* kinetoplast DNA was quantified in whole blood with real-time quantitative PCR (qPCR) before, during and up to six months after treatment. The predictive performance of pharmacodynamic parameters for clinical relapse was evaluated using receiver-operating characteristic curves. Clinical trial simulations were performed to determine the power associated with the use of blood parasite load as a surrogate endpoint to predict clinical outcome at six months.

Results: The absolute parasite density on day 56 after start of treatment was found to be a highly sensitive predictor of relapse within six months of follow-up at a cut-off of 20 parasites/mL (AUC 0.92, specificity 0.91, sensitivity 0.89). Blood parasite loads correlated well with tissue parasite loads (ρ=0.80) and with microscopy gradings of bone marrow and spleen aspirate smears. Clinical trial simulations indicated a >80% power to detect a difference in cure rate between treatment regimens if this difference was high (>50%) and when minimally 30 patients were included per regimen.

Conclusion: Blood *Leishmania* parasite load determined by qPCR is a promising early biomarker to predict relapse in VL patients. Once optimized, it might be useful in dose finding studies of new chemical entities.

1.   Introduction

There is an urgent need to develop field-adapted oral efficacious treatments for the neglected tropical parasitic disease visceral leishmaniasis (VL), particularly in Eastern Africa. New candidates with different mechanisms of action have been identified and are progressing to clinical development[1]. To facilitate drug development, accurate tools are needed to evaluate treatment efficacy early after the treatment, which is a specific research priority for neglected tropical diseases according to the World Health Organization (WHO)[2,3]. This will allow early selection of promising drug regimens and will reduce the number of subjects exposed to regimens with poor efficacy.

Treatment evaluation is complicated, since initially cured patients can relapse due to recrudescence of parasites, which is a long-term event that is particularly difficult to predict[4]. Therefore, definitive cure in Eastern African VL clinical trials is generally assessed at six months after completion of treatment, defined as a negative parasitological test of cure at the end of treatment (absence of *Leishmania* amastigotes in spleen or bone marrow aspirate smears by microscopy), lack of VL clinical symptoms and no requirement for rescue treatment during 6 months follow-up. To speed up treatment evaluation, sensitive and specific biomarkers are needed to monitor treatment response and predict relapses. These biomarkers would be particularly useful in clinical trials with new chemical entities, where they could serve as a surrogate endpoint at an early time point after treatment.

Splenic aspiration is an invasive procedure, associated with risk of severe hemorrhage[5,6], and cannot be performed in patients with unpalpable or reduced spleen size at the end of treatment. Quantification of blood parasite load by real-time quantitative PCR (qPCR) can be an alternative: previous results suggest that positive blood parasite load after treatment is associated with a higher risk of VL relapse[7-19]. In HIV co-infected patients, blood parasite load >10 parasites/mL preceded clinical relapse[7]. However, risk of VL relapse in HIV co-infection is affected by other factors such as CD4 count[11]. In Eastern Africa, the region with the highest VL incidence globally, very limited *Leishmania* qPCR data has been published in the context of VL[20,21]; only a small study in 11 patients focused on the relation with clinical outcome[19].

3.1

To evaluate the pharmacodynamic potential of blood parasite load as a predictor for clinical relapse, we longitudinally quantified the blood parasite load using qPCR in patients from three multicenter Eastern African clinical trials. The first objective was to identify the most optimal predictor for VL treatment outcome at six months in terms of absolute or relative blood parasite load and time of sampling. Secondly, blood parasite loads were compared with tissue aspirate parasite loads to assess whether the parasite biomass in whole blood is reflecting that in the primary infected organs. Thirdly, the sensitivity of blood and tissue qPCR parasite loads were compared with microscopic

readings of tissue samples. Lastly, the predictive power was quantified for different clinical trial scenarios with variable efficacy rates where this pharmacodynamic marker could hypothetically be used as early surrogate endpoint.

2.   Methods

2.1   Study sites and patients

Data originated from three Phase II open-label randomized clinical trials, to assess the safety and efficacy of different treatment regimens in the treatment of VL in Eastern Africa: LEAP0208 (NCT01067443[21]); LEAP0714 (NCT02431143 [22]); and FEXI VL 001 (NCT01980199). Ethical approval was obtained from national and local Ethics Committees in Kenya, Sudan, and Uganda. Further patient and treatment details can be found in Supplementary Material 3.1.

2.2   Clinical assessment of efficacy and sample collection

An initial cure was defined by improvement of clinical signs and symptoms of VL and a negative parasitological test of cure by microscopy at day 28. Patients who died or required rescue treatment before completion of study treatment were considered initial treatment failures. A definitive cure at day 210 (6 months) was defined as a patient who had initial cure and remained free of VL signs and symptoms, *i.e.*, no occurrence of relapse during the follow-up period and no requirement for rescue treatment.

Microscopic parasitological assessments on aspirate smears from lymph node, bone marrow, or spleen (LEAP0208 and FEXI VL 001), or spleen or bone marrow (LEAP0714) were performed at baseline and on day 28 in all studies; it was repeated at day 56, day 210 or in an unscheduled visit if clinically indicated, due to reappearance of VL signs and symptoms, suspecting of relapse. In LEAP0714 and FEXI VL 001, part of the tissue aspirate samples intended for microscopy were also collected to perform qPCR. Whole blood EDTA samples with a volume of 200 μL were collected for pharmacodynamic assessment prior to treatment and nominally on day 3, 7, 14, 28, 56, 210 (LEAP0208), on day 3, 7, 14, 21, 28, 56 (LEAP0714), and on day 1, 3, 5, 8, 11, 14, 28, 56, 210 (FEXI VL 001).

2.3   Microscopy and molecular methods

Parasitological assessments in the studies were adapted according to the practice of tissue aspiration (spleen, bone marrow and lymph node) for VL diagnosis in the different countries. In LEAP0208, parasitological assessment by microscopy was done

on lymph node aspirates (Dooka, Kassab), spleen aspirates (Kimalel) or bone marrow aspirates (all sites). In LEAP0714, spleen aspirates were collected or, under specific circumstances (see[22]), bone marrow aspirates. In FEXI VL 001, lymph node or bone marrow samples were collected. Aspirates were smeared on two slides per sample, stained with Giemsa and graded on a semi-quantitative logarithmic scale from 0 (no parasites in 1000 microscopic fields) to 6+ (>100 parasites per microscopic field). Measurements of the *Leishmania* parasite load in whole blood samples and tissue samples were performed using a qPCR method targeting *Leishmania* kinetoplastid DNA (kDNA). A detailed description of the DNA extraction, used primers, and qPCR protocol can be found in Supplementary Material 3.1.

2.4 Data and statistical analysis

Data cleaning, statistical analysis, and clinical trial simulations were performed with R (version 3.5.1). qPCR data were excluded from the analysis for patients who were considered initial treatment failures, for samples collected after rescue treatment was given, or for samples considered unreliable. Absolute blood parasite concentrations and relative changes over time were evaluated for their ability to discriminate between cured and relapsed patients. Absolute and log-transformed data were checked for normality and equal variances using the Shapiro-Wilk test. Logistic regression was performed by an unpaired one-sided Wilcoxon signed rank test to compare blood parasite loads at baseline, day 28, and day 56 after start of treatment. Subsequently, receiver-operating characteristic (ROC) curves were generated with the R package "pROC" and "plotROC". The area under the curve (AUC) was compared to find the most predictive parameter for clinical relapse in terms of follow-up day (day 14, day 28, or day 56 after start of treatment), and absolute parasite load or relative to baseline. Furthermore, the interplay between sensitivity and specificity of blood parasite load as a biomarker was evaluated and the optimal cut-off value was determined.

3.1

To evaluate the correlation between blood parasite load and tissue parasite load obtained by qPCR, Spearman's rank correlation rho was determined. The relationship between the two sources was determined by linear regression on log-transformed data, excluding data below the limit of quantitation (BLQ). The correlation between available matched qPCR blood and tissue loads and microscopy gradings of aspirate smears was evaluated visually. To evaluate the sensitivity of the qPCR and microscopy method, the percentage of samples having detectable parasites was compared.

2.5 Surrogate endpoint evaluation

Finally, clinical trial simulations were performed to evaluate the predictive performance and power associated with the use of qPCR blood parasite load on either day 28 or day 56 as a surrogate endpoint to predict final clinical outcome at six months. For this

we used non-inferiority clinical trial scenarios where a control treatment arm (90% cure rate at six months), representing current standard of care[1], was compared to an alternative treatment arm with lower, varying, cure rates (20%, 40%, 60%, and 80%). Patient populations (n=10, 20, 30, 40, 50) were sampled with replacement from the pool of cured (n=143/147) and relapsed (n=30/32) patients on day 28/56 in our original dataset. While the actual cure rate was pre-defined, the predicted cure rate of both populations was derived based on blood parasite load at day 28 or 56, based on the optimal cut-off. To simulate the performance of the qPCR procedure realistically, previously excluded and missing samples were included in these simulations. Fisher's exact test was used to test if these populations had significantly different predicted cure rates, based on blood parasite load. Per scenario, 1000 clinical trials were simulated. The power was defined as the number of times a significant difference was found between treatment arms and was considered adequate when >80%.

3. Results

In total, blood parasite loads were available from 177 patients, (n=134 for LEAP0208, n=29 for LEAP0714, n=14 for FEXI-VL-001), treated with 5 different treatment regimens. Overall, 15.8% of blood and 16.3% of tissue qPCR data had to be excluded (Table 3.1.1). Main reasons for exclusion of data were an unreliable or incomplete DNA extraction of the sample (based on glyceraldehyde 3-phosphate dehydrogenase (GAPDH)), bad sample quality, or insufficient sample material. None of the microscopic readings were excluded.

Table 3.1.1 Overview of the data used for logistic regression (Day 0, 28, 56) and ROC analysis (Day 14, 28, 56), specifying collected and excluded qPCR blood samples, qPCR tissue samples and microscopy scores derived from splenic or bone marrow aspirates.

		Blood qPCR		Tissue qPCR		Microscopy score
Day	Study	Collected samples	Excluded samples (%)	Collected samples	Excluded samples (%)	Available readings
0	LEAP0208	131	14 (11)	N/A	N/A	131
	LEAP0714	30	13 (43)	30	0 (0)	30
	FEXI VL 001	14	5 (36)	10	0 (0)	14
	Total	175	32 (18)	40	0 (0)	174
14	LEAP0208	139	18 (13)	N/A	N/A	N/A
	LEAP0714	30	12 (40)	N/A	N/A	N/A
	FEXI VL 001	14	5 (36)	N/A	N/A	N/A
	Total	183	35 (19)	N/A	N/A	N/A
28	LEAP0208	130	13 (10)	N/A	N/A	126
	LEAP0714	29	5 (17)	29	7 (24)	28
	FEXI VL 001	14	5 (36)	13	5 (38)	14
	Total	173	23 (13)	42	12 (29)	168
56	LEAP0208	136	12 (9)	N/A	N/A	8
	LEAP0714	29	2 (7)	1	0 (0)	1
	FEXI VL 001	13	4 (31)	4	1 (25)	N/A
	Total	178	18 (10)	5	1 (20)	9

A difference in blood parasite load dynamics between cured and relapsed patients could be observed in all treatment groups (Figure 3.1.1). In total, cured patients had a significantly lower parasite load on day 28 (p=3.91^{-06}) and on day 56 (p=2.58^{-14}) (Table 3.1.2). Remarkably, cured patients also had a significantly lower baseline parasite load (p=0.030). This correlation has been demonstrated earlier for tissue baseline parasite loads detected by microscopy in HIV co-infected patients[23]. Baseline parasite loads were not significantly different between treatment groups.
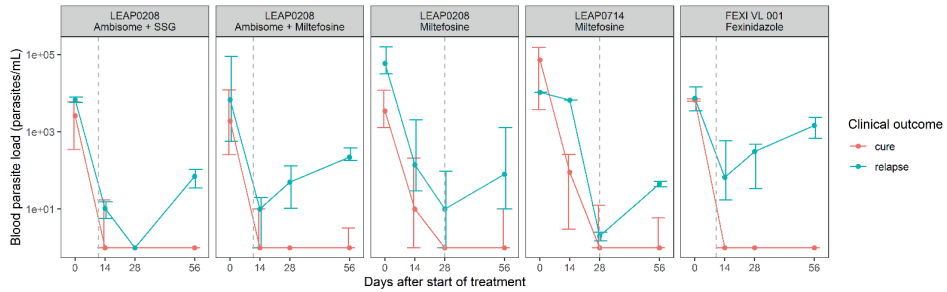
Figure 3.1.1 Median absolute parasite load of cured patients (red line) and relapsed patients (blue line) at baseline, day 14, 28 and 56, stratified per treatment arm. Error bars represent the inter-quartile range. Grey dashed lines represent end of treatment.

Table 3.1.2 Blood parasite loads quantified by qPCR at baseline, day 28, and day 56, stratified by clinical outcome at 6 months follow-up.

Day	Total N	Cure N	Parasites/mL[a]	Relapse N	Parasites/mL[a]	Difference p-value[b]
0	143	117	3070 (720-16290)	26	9760 (2574-63195)	0.030*
28	150	123	0 (0-1.5)	27	20 (0-230)	3.91e-06*
56	156	130	0 (0-2.75)	26	270 (59.2-1242)	2.58e-14*

[a]Values are given as median (inter-quartile range); [b]Wilcoxon test on absolute parasite concentrations; * Significant difference when p<0.05.

3.1

The ROC AUC for absolute blood parasite load classifying clinical relapse (Figure 3.1.2) was highest on day 56 (0.92), compared to day 14 (0.71) and day 28 (0.74). The optimal cut-off value on day 56 was 20 p/mL, corresponding to a sensitivity of 89% and a specificity of 91%. ROC curves of relative parasite load at day 14, 28, or 56 in relation to baseline were also evaluated, resulting in comparable AUCs (0.93 on day 56), and thus the absolute parasite load was preferred since only a single sample is needed. Based on a threshold of 20 p/mL on day 56, 67.6% of patients in this study were correctly categorized as relapsed for day 210 outcome, taking into account missing samples to evaluate the overall performance of the sampling procedure, extraction, and qPCR method. Without missing samples, 85.2% of patients were correctly categorized as relapsed, representing the performance of the qPCR method. Relapsed patients not

predicted at day 56 relapsed at day 68, 86, 108, and 112, whereas correctly predicted relapsed patients relapsed at day 102 (median) (IQR 64.5-136.5).
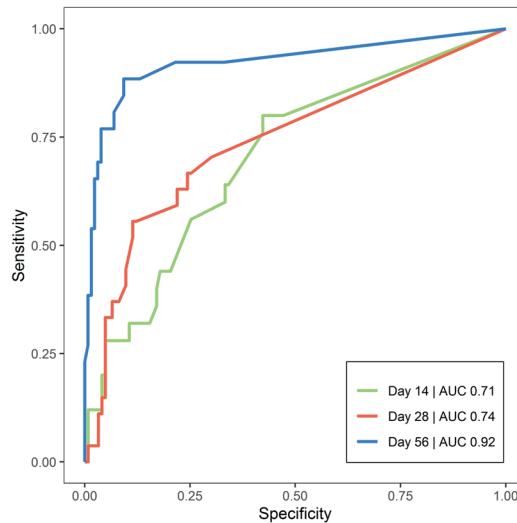
Figure 3.1.2 ROC curves of absolute parasite load as predictor of clinical relapse on day 14, 28, and 56 of follow-up. AUC represents the integrated area under the ROC curve. Green line: day 14 (AUC 0.71). Red line: day 28 (AUC 0.74). Blue line: day 56 (AUC 0.92).

There was a significant correlation between matching log-transformed blood and tissue qPCR results (ρ = 0.80), indicating an approximately 2 log higher parasite load in spleen, bone marrow, or lymph node compared to whole blood (Figure 3.1.3). In total, 302 blood qPCR samples and 71 tissue qPCR samples were compared to matching microscopy gradings of tissue aspirate smears (Figure 3.1.4 and 3.1.5). When stratified by tissue source, there was a positive trend between the two scores, especially in samples from bone marrow and spleen. At start of treatment, parasites were detectable by microscopy in all tissue samples (microscopy grading >0), whereas 6% of matching blood qPCR samples were negative (Table 3.1.3). When no parasites were detected by microscopy on day 28, parasites were still detected by qPCR in 36% of blood samples (Table 3.1.3). Parasites were detectable by qPCR in all of the available tissue samples (data not shown).

In the clinical trial simulations, absolute blood parasite load on either day 28 or day 56 was evaluated as a surrogate endpoint to predict clinical cure for various treatment regimens, with a threshold of ≤20 p/mL based on the ROC curves. The power of different simulation scenarios is shown in Figure 3.1.6. Clinical trial simulations demonstrated that the power to detect a difference in cure rate was higher when blood parasite load on day 56 was used, instead of day 28, in accordance with the ROC curves.

When blood parasite load on day 56 was used, clinical trials only achieved a >80% power when the difference in cure rate was high (>50%) between the hypothetical investigational regimen and a standard of care regimen with an efficacy of 90%, and when sufficient patients were included. For example, to identify an insufficient treatment regimen with 40% cure rate, at least 30 patients per treatment regimen need to be included. For alternative treatment regimens with higher cure rates, no adequate power was achieved with a sample size ≤50 subjects per treatment regimen.

Table 3.1.3 Number (%) of positive and negative blood qPCR loads versus microscopy gradings for matching samples at day 0 (N=143) and day 28 (N=135). Microscopy gradings >0 were considered positive.

	Day 0		Day 28	
	Microscopy grading		Microscopy grading	
	Positive	Negative	Positive	Negative
Total (N)	143	0	10	135
Matching blood qPCR loads				
Positive (N (%))	135 (94%)	0 (0%)	7 (70%)	48 (36%)
Negative (N (%))	8 (6%)	0 (0%)	3 (30%)	87 (64%)
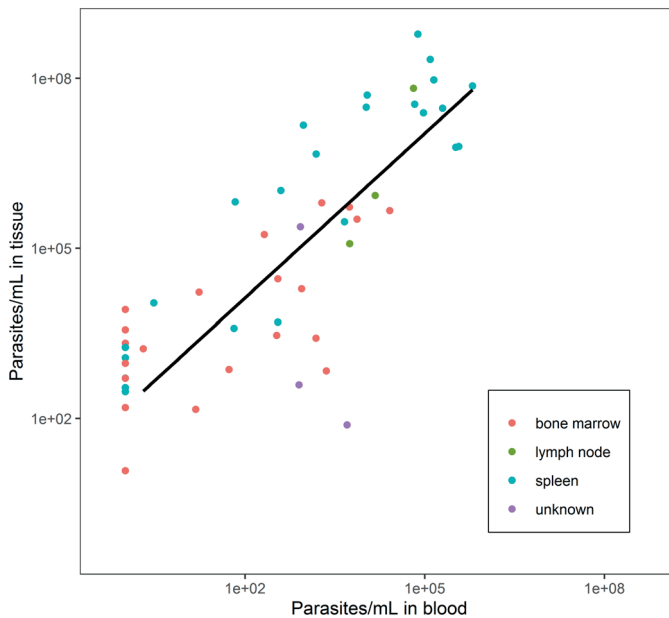
Figure 3.1.3 Correlation between log-transformed qPCR blood and tissue parasite load (matching ID/timepoint) determined in bone marrow aspirates (red), lymph nodes (green), and spleen aspirates (blue). Tissue samples include 4 drops of bone marrow aspirate (~200 μL), or the remainder in the needle of the spleen or lymph node aspiration. Data below the limit of quantification are shown as 1 p/mL. Linear regression line (solid line) is based on the combined data, excluding data below the limit of quantification: y = 1.5 + 0.97x.

3.1
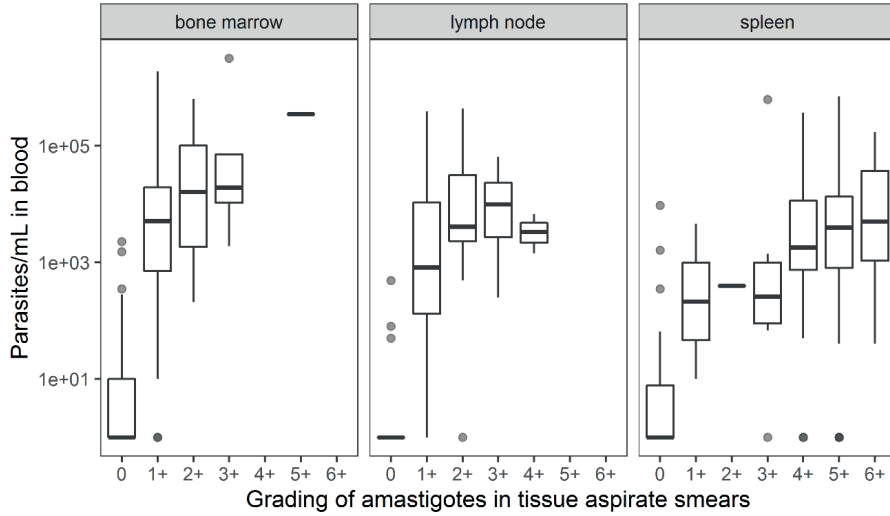
Figure 3.1.4 Correlation between log-transformed qPCR blood parasite load and grading of amastigotes in aspirate smears by microscopy, stratified by parasite load according to tissue source.
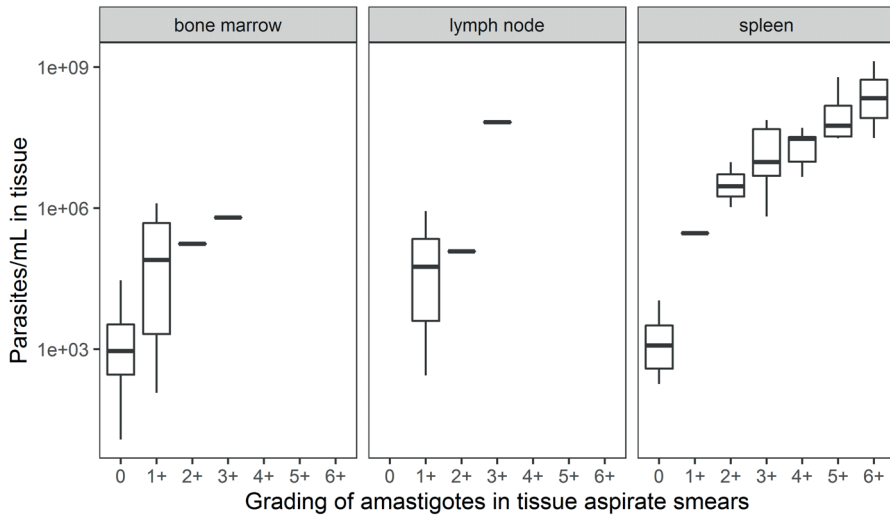
Figure 3.1.5 Correlation between log-transformed qPCR tissue parasite load and grading of amastigotes in aspirate smears by microscopy, stratified by parasite load according to tissue source. Tissue samples include 4 drops of bone marrow aspirate (~200 μL), or the remainder in the needle of the spleen or lymph node aspiration.
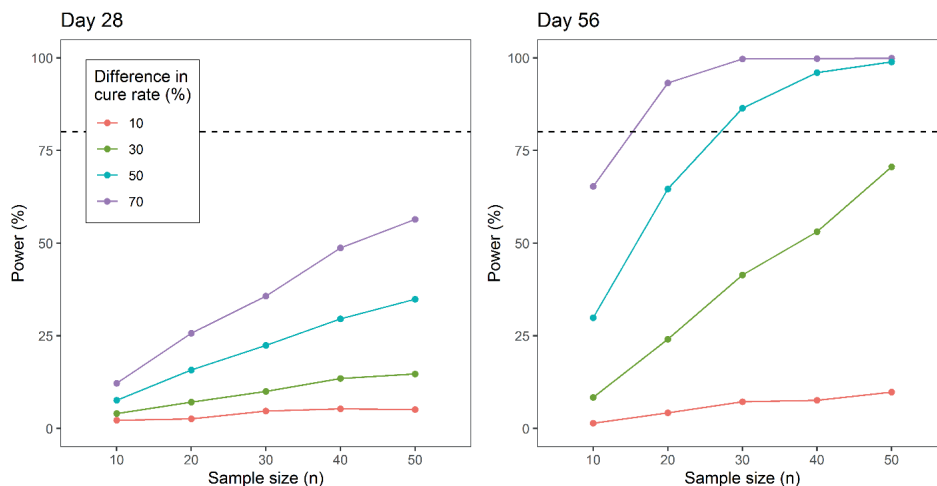
Figure 3.1.6 Predictive power of blood parasite load is shown for day 28 (left panel) and day 56 (right panel), with clinical cure defined as parasite load <=20 p/mL. The difference in cure rate is the difference between the alternative treatment regimens (20%, 40%, 60%, or 80% cure rate) and the reference treatment regimen (90% cure rate). Sample size ranges from n=10 to n=50. Dotted horizontal line represents the 80% power cut-off.

4.   Discussion

In this study, various parasitemia parameters were evaluated for their sensitivity and specificity in classifying and predicting final treatment outcome in a large Eastern African VL patient population. Absolute parasite load on day 56 was a highly sensitive predictor of relapse at a cut-off of 20 p/mL. When compared to other approaches, the surrogate marker can be assessed early (day 56 instead of 6 months) compared to IgG1 antigen detection[24] and more specific compared to antigen detection in urine[25]. The low cut-off value found in this study indicates that blood parasite loads as low as 20 p/mL are associated with a higher risk of disease relapse, even when patients do not yet present reoccurrence of clinical symptoms. Previously this has only been demonstrated in HIV co-infected patients, where values ranging from 0.03-42 p/mL indicated relapse[7,17,18,26].

A potential drawback of this biomarker is that blood represents only a proximal site for the total parasite biomass in the human host, of which the mainstay is resident in infected organs (e.g., liver, spleen and bone marrow). This is in line with our findings, as qPCR was approximately 2-log higher in tissue compared to whole blood. Another potential source of bias might be lingering kDNA of dead parasites in the circulation. However, a rapid clearance of circulating *Leishmania* kDNA immediately after

3.1

treatment initiation has been shown previously, following clinical recovery[13]. Additionally, qPCR blood parasite load showed a good correlation with qPCR parasite load in tissue (ρ=0.80), indicating that whole blood is a good proxy compartment to monitor the parasite biomass in the infected tissues.

qPCR has been shown to be a sensitive method to measure blood parasite load previously[16,18,19,27,28], as well as in this study. Both blood and tissue qPCR parasite loads showed a correlation with microscopy gradings from aspirate smears; the clearest trend was observed between spleen qPCR and microscopy gradings. The observed correlation is in line with previous data from India[29]. qPCR analysis seems to be a more sensitive method, as parasites were detectable by qPCR in all tissue samples and in 76.7% of blood samples, compared to 60.5% of tissue samples by microscopy. The high sensitivity of qPCR on whole blood, as well as the convenience for the patient, suggest that qPCR is a suitable method for regular patient monitoring. Noteworthy, detectable qPCR blood or tissue parasite loads at end of treatment or during follow-up were observed in patients considered clinically cured. This could indicate that patients can still harbor *Leishmania* parasites at low levels, but nevertheless remain asymptomatic. In the context of a clinical trial this means negative blood qPCR loads cannot replace the gold standard of microscopic examination as a test of cure to define initial cure and the clinical value of a positive qPCR in a patient without clinical signs and symptoms of disease remains to be defined. It could indicate the need for closer follow-up but not directly rescue treatment, as for an immunocompetent patient the immune system is expected to control the infection, conferring long-lasting protection[30,31].

To evaluate the usefulness of early blood parasite load as a surrogate endpoint for long-term clinical outcome in clinical trials evaluating novel drug regimens, clinical trial simulations were performed. The use of blood parasite load on day 56 might be suitable to identify insufficient treatment regimens or dose levels with a very poor cure rate of 40% or less and stop early for futility. However, the power will improve when the number of excluded samples can be reduced, e.g., by improving the performance of DNA extraction.

With the introduction of new chemical entities as clinical candidates for VL treatment, there is a need for better and more accurate tools to evaluate their efficacy at early time-points, as to allow for adaptive study design to select promising drug regimens and reduce the number of subjects exposed to regimens with poor activity. This is the first study that evaluated the predictive value of qPCR for long-term clinical outcome and its use as a surrogate endpoint in clinical trials for VL, by using a large dataset from different studies in Eastern African VL patients, including treatment regimens with different cure rates. The absolute parasite load on day 56 was a highly sensitive predictor of relapse at a cut-off of 20 p/mL, and its potential application has been shown by clinical trial simulations. However, this cut-off value is based on the studied data only, and the exact threshold and time-point may need to be optimized for future

compounds, depending on their pharmacokinetic properties, treatment duration, and ultimately their effect on parasite dynamics. With the increase in molecular biology capacity in areas endemic for VL, we expect that it would be feasible to put this tool into practice in clinical trial settings. In the near future, validation of molecular biology tools in blood could be envisaged to replace the current invasive tissue aspiration procedures for parasitological diagnosis and treatment monitoring.

Acknowledgments

Funding

3.1

References

1.   Alves F, Bilbe G, Blesson S, et al. Recent Development of Visceral Leishmaniasis Treatments: Successes, Pitfalls, and Perspectives. Clin Microbiol Rev 2018;31:1–30.

2.   World Health Organization. Ending the neglect to attain the Sustainable Developmetn Goals - A road map for neglected tropical diseases 2021–2030. 2020; :1–13. Available at: https://www.who.int/neglected_diseases/Revised-Draft-NTD-Roadmap-23Apr2020.pdf?ua=1.

3.   Control of the leishmaniases. Report of a meeting of the WHO Expert Committee on the Control of Leishmaniases, Geneva. 2010; Available at: https://apps.who.int/iris/bitstream/handle/10665/44412/WHO_TRS_949_eng.pdf?sequence=1.

4.   Rijal S, Ostyn B, Uranw S, et al. Increasing failure of miltefosine in the treatment of kala-azar in nepal and the potential role of parasite drug resistance, reinfection, or noncompliance. Clin Infect Dis 2013; 56:1530–1538.

5.   Chulay JD, Bryceson ADM. Quantitation of amastigotes of Leishmania donovani in smears of splenic aspirates from patients with visceral leishmaniasis. Am J Trop Med Hyg 1983;32:475–479.

6.   Chappuis F, Sundar S, Hailu A, et al. Visceral leishmaniasis: what are the needs for diagnosis, treatment and control? Nat Rev Microbiol 2007;5:873.

7.   Bossolasco S, Gaiera G, Olchini D, et al. Erratum: Real-Time PCR Assay for Clinical Management of Human Immunodeficiency Virus-Infected Patients with Visceral Leishmaniasis. J Clin Microbiol 2004; 42:1858.

8.   Cascio A, Calattini S, Colomba C, et al. Polymerase chain reaction in the diagnosis and prognosis of Mediterranean visceral leishmaniasis in immunocompetent children. Pediatrics 2002;109.

9.   Pizzuto M, Piazza M, Senese D, et al. Role of PCR in Diagnosis and Prognosis of Visceral Leishmaniasis in Patients Coinfected with Human Immunodeficiency Virus Type 1. J Clin Microbiol 2001;39:357–361.

10. Sudarshan M, Weirather JL, Wilson ME, Sundar S. Study of parasite kinetics with antileishmanial drugs using real-time quantitative PCR in Indian visceral leishmaniasis. J Antimicrob Chemother 2011; 66:1751–1755.

11. Cota GF, de Sousa MR, de Assis TSM, Pinto BF, Rabello A. Exploring prognosis in chronic relapsing visceral leishmaniasis among HIV-infected patients: Circulating Leishmania DNA. Acta Trop 2017; 172:186–191.

12. Cruz I, Cañavate C, Rubio JM, et al. A nested polymerase chain reaction (Ln-PCR) for diagnosing and monitoring Leishmania infantum infection in patients co-infected with human immunodeficiency virus. Trans R Soc Trop Med Hyg 2002;96:S185–S189.

13. Disch J, Oliveira MC, Orsini M, Rabello A. Rapid clearance of circulating Leishmania kinetoplast DNA after treatment of visceral leishmaniasis. Acta Trop 2004;92:279–283.

14. Fisa R, Riera C, Ribera E, Gállego M, Portús M. A nested polymerase chain reaction for diagnosis and follow-up of human visceral leishmaniasis patients using blood samples. Trans R Soc Trop Med Hyg 2002;96:S191–S194.

15. Kip AE, Balasegaram M, Beijnen JH, Schellens JHM, Vries PJ De, Dorlo TPC. Systematic Review of Biomarkers To Monitor Therapeutic Response in. Antimicrob Agents Chemother 2015;59:1–14.

16. Lachaud L, Dereure J, Chabbert E, et al. Optimized PCR using patient blood samples for diagnosis and follow-up of visceral leishmaniasis, with special reference to AIDS patients. J Clin Microbiol 2000; 38:236–240.

17. Mary C, Faraut F, Drogoul MP, et al. Reference values for Leishmania infantum parasitemia in different clinical presentations: Quantitative polymerase chain reaction for therapeutic monitoring and patient follow-up. Am J Trop Med Hyg 2006;75:858–863.

18. Mary C, Faraut F, Lascombe L, Dumon H. Quantification of Leishmania infantum DNA by a real-time PCR assay with high sensitivity. J Clin Microbiol 2004;42:5249–5255.

19. Nuzum E, White F, Thakur C, et al. Diagnosis of symptomatic visceral leishmaniasis by use of the polymerase chain reaction on patient blood. J Infect Dis 1995;171:751–754.

20. Khalil EAG, Weldegebreal T, Younis BM, et al. Safety and Efficacy of Single Dose versus Multiple Doses of AmBisome H for Treatment of Visceral Leishmaniasis in Eastern Africa : A Randomised Trial. PLoS Negl Trop Dis 2014;8.

21. Wasunna M, Njenga S, Balasegaram M, et al. Efficacy and Safety of AmBisome in Combination with Sodium Stibogluconate or Miltefosine and Miltefosine Monotherapy for African Visceral Leishmaniasis: Phase II Randomized Trial. PLoS Negl Trop Dis 2016:1–18.

22. Mbui J, Olobo J, Omollo R, et al. Pharmacokinetics, Safety, and Efficacy of an Allometric Miltefosine Regimen for the Treatment of Visceral Leishmaniasis in Eastern African Children : An Open-label , Phase II Clinical Trial. Clin Infect Dis 2019;68.

23. Abongomera C, Diro E, Vogt F, et al. The Risk and Predictors of Visceral Leishmaniasis Relapse in Human Immunodeficiency Virus-Coinfected Patients in Ethiopia: A Retrospective Cohort Study. Clin Infect Dis 2017;65:1703–1710.

24. Marlais T, Bhattacharyya T, Singh OP, et al. Visceral Leishmaniasis IgG1 Rapid Monitoring of Cure vs. Relapse, and Potential for Diagnosis of Post Kala-Azar Dermal Leishmaniasis. Front Cell Infect Microbiol 2018;8:427.

25. Vogt F, Mengesha B, Asmamaw H, et al. Antigen detection in urine for noninvasive diagnosis and treatment monitoring of visceral leishmaniasis in human immunodeficiency virus coinfected patients: An exploratory analysis from Ethiopia. Am J Trop Med Hyg 2018;99:957–966.

26. Molina I, Fisa R, Riera C, et al. Ultrasensitive real-time pcr for the clinical management of visceral leishmaniasis in HIV-infected patients. Am J Trop Med Hyg 2013;89:105–110.

27. Adams ER, Schoone G, Versteeg I, et al. Development and evaluation of a novel loop-mediated isothermal amplification assay for diagnosis of cutaneous and visceral leishmaniasis. J Clin Microbiol 2018;56:1–8.

28. Piarroux R, Gambarelli F, Dumon H, et al. Comparison of PCR with direct examination of bone marrow aspiration, myeloculture, and serology for diagnosis of visceral leishmaniasis in immunocompromised patients. J Clin Microbiol 1994;32:746–749.

29. Sudarshan M, Singh T, Chakravarty J, Sundar S. A correlative study of splenic parasite score and peripheral blood parasite load estimation by quantitative PCR in visceral leishmaniasis. J Clin Microbiol 2015;53:3905–3907.

30. Khalil EAG, Ayed NB, Musa AM, et al. Dichotomy of protective cellular immune responses to human visceral leishmaniasis. Clin Exp Immunol 2005;140:349–353.

31. Zijlstra EE, El-Hassan AM, Ismael A, Ghalib HW. Endemic kala-azar in Eastern Sudan: A longitudinal study on the incidence of clinical and subclinical infection and post kala-azar dermal leishmaniasis. Am J Trop Med Hyg 1994;51:826–836.

3.1

Supplementary material 3.1

Methods

Study sites and patients

Analyzed samples originated from three Phase II open-label randomized clinical trials, to assess the safety and efficacy of different treatment regimens in the treatment of VL in Eastern Africa. Firstly, clinical trial LEAP0208 (NCT01067443[1]) compared three different treatment regimens: (1) a combination of 10 mg/kg liposomal amphotericin B (IV) on day 1 followed by 10 days of (IM) 20 mg/kg sodium stibogluconate from day 2-11 (*n*=51), (2) a combination of 10 mg/kg liposomal amphotericin B (IV) on day 1 followed by 10 days of 2.5 mg/kg/day (maximally 150 mg/day) miltefosine (oral) from day 2–11 (*n*=49), (3) monotherapy with 2.5 mg/kg/day (maximally 150 mg/day) miltefosine (oral) for 28 days (*n*=51). Patients were recruited in Kenya (Kimalel) and Sudan (Dooka and Kassab) and were between 7 and 60 years of age.

Secondly, clinical trial LEAP0714, (NCT02431143[2]) studied paediatric patients aged 4-12 years who received a monotherapy of allometric miltefosine dosing for 28 days (ranging between 30 and 100 mg/day). 30 patients were recruited in Kenya (Kacheliba) and Uganda (Amudat). Thirdly, clinical trial FEXI VL 001 (NCT01980199) studied a flat dosing of 1800 mg/day fexinidazole for 4 days, followed by 1200 mg/day for 6 days. 14 adult patients were recruited in Sudan (Dooka).

For all studies, included patients showed VL clinical signs and symptoms (fever clearance, reduction of spleen size and improvement of haematological parameters) and had a confirmatory parasitological microscopic diagnosis. All recruited patients were HIV negative. None presented severe VL, suffered severe malnutrition (BMI<11) or any serious underlying disease or concomitant severe infection, at the time of diagnosis.

All trials were conducted in accordance with the trial protocols, the International Conference on Harmonization guidelines for Good Clinical Practice, local regulations, and the Declaration of Helsinki. Ethical approvals were obtained from national and local Ethics Committees in Kenya, Sudan, and Uganda prior to the start of the trial in each country. Ethical approval was also granted by LSHTM's Ethics Committee (#5543), and the Academic Medical Center Medical Ethics Committee issued a 'declaration of no objection'. Study participants or their parents/guardians (for children) gave a written signed informed consent before enrolment into the study, including participation in the data collection for pharmacokinetic and parasitological assessments.

Microscopy and molecular methods

200 µL from blood samples, 4 drops of bone marrow aspirate corresponding to about 200 µL, or the remainder in the needle of the spleen or lymph node aspiration samples after preparation of the microscopic slides, was used for analysis. DNA isolation was performed partially on site following a modified Boom method using guanidine thiocyanate and silica as described previously[3], after which silica samples were stored and transported at minimally -20°C until the moment of further extraction and analysis. The silica samples were washed subsequently with L2-buffer, ethanol 70% and acetone, and DNA and RNA were eluted using 50 µl MilliQ water.

A duplex *Leishmania* kDNA and human glyceraldehyde 3-phosphate dehydrogenase (GAPDH) DNA qPCR was performed by adding an aliquot of 1.25 µl of DNA added to 11.3 µl amplification mixture containing 6.25 µl iQ Supermix (catalog no. 170-8862; Bio-Rad) or VeriQuest Probe qPCR Master Mix with No Reference Dye (catalog no. 75660), 0.25 µM kDNA forward primer (5'-TCCCAAACTTTTCTGGTCCT-3'), 0.25 µM kDNA reverse primer (5'-TTACACCAACCCCCAGTTTC-3'), 0.12 µM kDNA probe (5'-6-carboxyfluorescein [FAM]-TTCTGCGAAAACCGAAAAATGGGTGC-BHQ-3'), 0.025µM GAPDH forward primer (5'-GAAGGTGAAGGTCGGAGTC-3'), 0.025 µM GAPDH reverse primer (5'-GAAGATGGTGATGGGATTTC-3'), and 0.12 µM GAPDH probe (5' Texas Red-CAAGCTTCCCGTTCTCAGCC-BHQ-3'). The qPCR protocol was as follows: 10 min at 50˚C, 5 min at 95˚C, followed by 40 cycles of 15 s at 95˚C and 45 s at 59˚C, performed using a CFX-96 real-time machine (Bio-Rad).

Human GAPDH DNA was used as internal control for validation of the extraction procedure. GAPDH and kDNA were amplified in the same PCR reaction, leading to a quenching of the GAPDH signal at high parasite loads, which was taken into account when assessing the extraction efficiency. Samples were excluded if the GAPDH response indicated unreliable or incomplete DNA extraction of the sample, if the sample quality was bad or if there was not sufficient sample material.

3.1

References

1. Wasunna M, Njenga S, Balasegaram M, et al. Efficacy and Safety of AmBisome in Combination with Sodium Stibogluconate or Miltefosine and Miltefosine Monotherapy for African Visceral Leishmaniasis: Phase II Randomized Trial. PLoS Negl Trop Dis 2016;10(9):e0004880.
2. Mbui J, Olobo J, Omollo R, et al. Pharmacokinetics, Safety, and Efficacy of an Allometric Miltefosine Regimen for the Treatment of Visceral Leishmaniasis in Eastern African Children : An Open-label , Phase II Clinical Trial. Clin Infect Dis 2019;68:1530-1538.
3. Basiye FL, Schoone GJ, Beld M, et al. Comparison of short-term and long-term protocols for stabilization and preservation of RNA and DNA of Leishmania, Trypanosoma, and Plasmodium. Diagn Microbiol Infect Dis 2011;69:66–73.

Chapter 3.2

Leishmania blood parasite dynamics during and after treatment of visceral leishmaniasis in Eastern Africa: a pharmacokinetic-pharmacodynamic model

Luka Verrest, Séverine Monnerat, Ahmed M. Musa, Jane Mbui, Eltahir AG Khalil, Joseph Olobo, Monique Wasunna, Alwin D.R. Huitema, Jos H. Beijnen, Henk D.F.H. Schallig, Fabiana Alves, Thomas P.C. Dorlo

Abstract

Background: With the current treatment options for visceral leishmaniasis (VL), recrudescence of the parasite is seen in a proportion of patients. To improve treatment efficacy and to predict patient relapse in VL cases, an understanding of the parasite dynamics is crucial. This study aimed to characterize the kinetics of circulating *Leishmania* parasites in blood, during and after different antileishmanial therapies and to find predictors for clinical relapse of disease.

Methods: Data from three clinical trials were combined in this study, where Eastern African VL patients received various antileishmanial regimens. *Leishmania* kinetoplast DNA was quantified in whole blood with real-time quantitative PCR (qPCR) before, during and up to six months after treatment. An integrated PK-PD model was developed using non-linear mixed effects modelling.

Results: Parasite proliferation was best described by an exponential growth model, with an *in vivo* parasite doubling time of 7.8 days (RSE 12%). Parasite killing by fexinidazole, liposomal amphotericin B, sodium stibogluconate and miltefosine was best described by linear models directly relating drug concentrations to the parasite elimination rate. After treatment, parasite growth was assumed to be suppressed by the host's immune system, described by an E_{max} model driven by the time after treatment. No predictors could be identified for the high variability in onset and magnitude of the immune response. Model-based individual predictions of blood parasite load at Day 28 and Day 56 after start of treatment were predictive for clinical relapse of disease.

Conclusion: This semi-mechanistic pharmacokinetic-pharmacodynamic model adequately captured the blood parasite dynamics during and after treatment and revealed that high blood parasite loads at Day 28 and Day 56 after start of treatment are an early indication for VL relapse, which could be a useful biomarker to assess treatment efficacy of a treatment regimen in a clinical trial setting.

1.   Introduction

In Eastern Africa, the region with the highest visceral leishmaniasis (VL) incidence globally, efficacy rates of currently available VL therapies range from 72% to 91%[1-3]. Almost all patients show improvement of the clinical sings and symptoms and have a negative parasitological test of cure by microscopy at the end of treatment, defined as initial cure, as a result of a good initial response to the drug treatment. Therapy failure occurs mainly by relapse of disease after initial successful treatment due to recrudescence of parasites, which is a long-term event that can occur up till 12 months after treatment or even longer[4]. Following successful treatment of VL infection, parasites can still be latently present and result in reactivation of the infection and recurrence of VL once immunity is compromised[5-8]. Patients who start VL treatment are mostly malnourished and severely sick, often presenting fever, hypergamma-globulinemia, and hematological depletions such as anemia, neutropenia, and leucopenia[9]. These complications might lead to an impaired functioning of the immune system, unable to suppress or eradicate *Leishmania* parasites[10]. Once the patient will improve after start of treatment, the immune system might recover and can clear or control the parasites.

It is particularly difficult to predict which patients will relapse, as almost all patients are clinically cured at the end of treatment, although some parasites may still remain. The quantification of the total *Leishmania* parasite burden in patients might be a good approximation of severity of disease and response to treatment. The gold standard in clinical trials is quantification of parasites by microscopy in aspirates from spleen or bone marrow, where the mainstay of parasites is resident, performed before start of treatment to confirm VL infection, at the end of treatment to assess initial cure, and when relapse is suspected. However, aspiration is a highly invasive procedure and therefore not suitable for more regulator monitoring. Quantification of circulating *Leishmania* kinetoplast DNA (kDNA) in blood by real-time quantitative PCR (qPCR) is an attractive patient-friendly alternative, which allows the collection of longitudinal data. Previously, qPCR blood parasite load showed a good correlation with qPCR parasite load in aspirated organ tissue (ρ=0.80)[11], indicating that whole blood is an adequate proxy compartment to monitor the parasite biomass in the infected organs. Positive blood parasite load after treatment has been associated with a higher risk of VL relapse[12-24], and the blood parasite load on day 56 after start of treatment was found to be a highly sensitive predictor of relapse at a cut-off of 20 parasites/mL[11]. This low cut-off value indicates that very low blood parasite loads are already associated with a higher risk of disease relapse, even when patients do not yet present reoccurrence of clinical symptoms.

The phenomenon of asymptomatic recrudescence of parasites without the emergence of clinical relapse complicates the analysis of parasite dynamics in relation to clinical

3.2

response[11]. The analysis of the parasite dynamics is further complicated by the large baseline variability of the parasite load and the large inter-patient variability in response[11]. Factors that affect the parasite dynamics and the treatment response may depend on the initial degree of parasite depletion by the treatment, but also on parasite-related factors such as of the total burden of parasites present at the start of treatment or the virulence of the parasite. To achieve long-lasting cure, sufficient suppression of the parasite by a proper functioning immune system of the host is of crucial importance, which might be affected by patient specific factors such as severity of VL infection, co-infections such as HIV, or malnutrition.

A dynamic pharmacokinetic-pharmacodynamic model is needed to capture the interplay between parasite growth, drug exposure, drug-induced parasite clearance, and suppression of parasite regrowth after treatment by the host. Whereas such pharmacokinetic-pharmacodynamic models have shown to be useful in the understanding of other parasitic diseases such as malaria[25-28], for *Leishmania* parasite dynamics, *in vivo* parasite replication rate or parasite clearance by VL drugs, have not been studied and quantified before. Longitudinal analysis of repeated blood parasite loads during and after VL treatment will enable characterization of these dynamics[11].

In this study, we aimed to develop a pharmacokinetic-pharmacodynamic model of *Leishmania* blood parasite loads in VL patients receiving various drug regimens, to get a better understanding of the interplay between parasite, drugs and host. Moreover, using a semi-mechanistic model we characterized the different effects of VL treatment on parasite clearance during treatment, to further enable optimization of dosing regimens or new combination regimens. Lastly, to predict the long-term response of *Leishmania* parasites to treatment, we aimed to identify early biomarkers or model-derived predictors for parasite recrudescence and clinical relapse of disease.

2. Methods

2.1 Study design, patients, and clinical assessment of efficacy

Analysed samples originated from three Phase II open-label randomized clinical trials, to assess the safety and efficacy of different VL treatment regimens in Eastern Africa (Table 3.2.1). Clinical trial LEAP0208 (NCT01067443[1]) compared three different treatment regimens in patients from Kenya (Kimalel) and Sudan (Dooka and Kassab): (1) a combination of 10 mg/kg liposomal amphotericin B (IV) on day 1 followed by 10 days of 20 mg/kg sodium stibogluconate (IM) from day 2–11 (*n*=51) (AmB+SSG10D), (2) a combination of 10 mg/kg liposomal amphotericin B (AmBisome) (IV) on day 1 followed by 10 days of 2.5 mg/kg/day (maximally 150 mg/day) miltefosine (oral) from

day 2–11 (*n*=49) (AmB+MF10D), (3) monotherapy of conventional miltefosine dosing for 28 days of 2.5 mg/kg/day (maximally 150 mg/day) (*n*=51) (MFC28D). Clinical trial LEAP0714, (NCT02431143[2]) studied 30 paediatric patients from Kenya (Kacheliba) and Uganda (Amudat) who received a monotherapy of allometric miltefosine dosing for 28 days (ranging between 30 and 100 mg/day) (MF28D). Clinical trial FEXI-VL-001 (NCT01980199) studied a flat dosing of 1800 mg/day fexinidazole for 4 days, followed by 1200 mg/day for 6 days in 14 adult patients from Sudan (Dooka) (Fexi10D). For all studies, included patients showed VL clinical symptoms (fever and splenomegaly) and had a confirmatory parasitological microscopic diagnosis. All recruited patients were HIV negative. None presented with severe VL, suffered severe malnutrition (BMI<11) or any serious underlying disease or concomitant severe infection, at the time of diagnosis.

Ethical approval was obtained from national and local Ethics Committees in Kenya and Sudan, the LSHTM's Ethics Committee (#5543), and the Academic Medical Center Medical Ethics Committee (LEAP0208), and from institutional ethics committees at the Kenya Medical Research Institute and at Makerere University, Uganda (LEAP0714). Study participants or their parents/guardians (for children under 18 years) gave a written signed informed consent before enrolment into the study, including participation in the pharmacokinetic and parasitological assessments.

Clinical assessment of efficacy was defined by initial cure: a negative parasitological test of cure by microscopy at Day 28; final cure: initial cure and absence of VL symptoms until Day 210 (6 months), *i.e.*, no occurrence of relapse during the follow-up period and no requirement for rescue treatment; or initial treatment failure: patients who died or required rescue treatment before completion of study treatment.

Table 3.2.1   Patient characteristics and data overview.

Study	LEAP0208			LEAP0714	FEXI-VL-001	Total
Treatment	AmB+SSG10D	AmB+MF10D	MFC28D	MFA28D	Fexi10D	
Subjects[a] (*n*)	40	44	46	29	13	172
Cured patients (*n* [%])	37 (93)	37 (84)	35 (76)	27 (93)	2 (15)	138 (80)
Male (*n* [%])	28 (70)	36 (82)	41 (89)	8 (28)	1 (8)	114 (66)
Age (years)[b]	14 (7-40)	14 (7-30)	15 (7-37)	8 (4-12)	26 (16-50)	14 (4-50)
Body weight (kg)[b]	33 (15-69)	34 (15-57)	36 (16-60)	22 (13-30)	51 (42-64)	34 (13-69)
PD samples[c] collected (n)	306	306	313	208	127	1260
PD samples[c] included (n [% excluded])	243 (21)	256 (16)	278 (11)	138 (34)	77 (39)	992 (21)

AmB+MF10D: Amphotericin B 10 mg/kg (1 day) + miltefosine 2.5 mg/kg (10 days); AmB+SSG10D: Amphotericin B 10 mg/kg (1 day) + SSG 20 mg/kg (10 days); Fexi10D: Fexinidazole 1800 mg (4 days), 1200 mg (6 days); MFC28D: Miltefosine conventional 2.5 mg/kg (28 days), MFA28D: Miltefosine allometric dosing (28 days). [a] Patients included in the analysis; [b] Mean (range) at baseline; [c] Samples for quantification of blood parasite load by qPCR.

3.2

2.2 Sample collection, bioanalysis and data exclusion

Pharmacokinetic samples were collected for miltefosine (LEAP0208 and LEAP0714) and fexinidazole and its active metabolites fexinidazole sulfoxide (M1) and fexinidazole sulfone (M2) (FEXI-VL-001). Miltefosine sample collection was performed in all patients receiving miltefosine monotherapy or a combination therapy with miltefosine. Sample collection and bioanalysis has been described previously[1,29,30]. In FEXI-VL-001, dried-blood spot (DBS) samples were collected on multiple time points during treatment in all patients receiving fexinidazole treatment, with more dense sampling on Day 1 and Day 10 of treatment. Whole blood concentrations of fexinidazole, M1 and M2 were quantified, as described by an internal report. Whole blood EDTA samples with a volume of 200 µL were collected for pharmacodynamic assessment in all patients prior to treatment and on day 3, 7, 14, 28, 56, 210 (LEAP0208), on day 3, 7, 14, 21, 28, 56 (LEAP0714), and on day 1, 3, 5, 8, 11, 14, 28, 56, 210 (FEXI VL 001). *Leishmania* kinetoplastid DNA (kDNA) was quantified in these samples using a qPCR method, to represent the parasite load in the patient (hereafter referred to as blood parasite load). Human glyceraldehyde 3-phosphate dehydrogenase (GAPDH) DNA was used as internal control for validation of the extraction procedure. The lower limit of quantification (LLOQ) was set to 1 parasite/mL. A detailed description of the DNA extraction, used primers, and qPCR protocol has been described earlier[11].

qPCR data were excluded from the analysis for patients who were considered initial treatment failures and did not complete the study treatment, for samples collected after rescue treatment was given to relapsed patients, for samples considered unreliable, (*i.e.,* if the GAPDH response indicated unreliable or incomplete DNA extraction of the sample, if the sample quality was low or if there was not sufficient sample material). qPCR data was also excluded if values were physiologically not possible. Furthermore, patients who received miltefosine or fexinidazole for whom no pharmacokinetic data was available were also excluded.

2.3 Population pharmacokinetic-pharmacodynamic analysis

An integrated pharmacokinetic-pharmacodynamic model was developed using the nonlinear mixed effects modelling software NONMEM (version 7.5, ICON Development Solutions, USA) using the first-order conditional estimation method with interaction (FOCE-I). Data cleaning and visualization of the data was performed using R (version 4.0.2), and model evaluation using Perl-speaks-NONMEM (PsN, version 5.2.6) and the interface Pirana (version 3.0.0). Model development was performed in three consecutive steps: 1) characterization of parasite growth, 2) characterization of drug-induced parasite clearance during treatment, and 3) characterization of host-induced parasite suppression after treatment. In each step, a relevant subset of the data was used to be able to estimate the different model parameters. Blood parasite loads below

the limit of quantification (BLQ) were fixed to half the BLQ (0.5 parasites/mL). Between-subject variability (BSV) was evaluated on all parameters, and implemented using an exponential error model. Residual variability was modeled using a combined additive and proportional error models, with the additive error fixed to the LLOQ of 1 parasite/mL.

2.3.1 Parasite growth

No pharmacodynamic data was available before start of treatment, complicating the characterization of the natural parasite growth in primary VL patients. *In vivo* parasite growth was therefore modelled and estimated based on data from patients treated with fexinidazole (n=13), where an inadequate drug response that resulted in a rapid parasite recrudescence directly after treatment was observed in the majority of patients. To describe parasite proliferation, turn-over and exponential growth models were evaluated.

2.3.2 Drug-induced parasite clearance during treatment

Previously developed population pharmacokinetic models of miltefosine[29] and fexinidazole and its active metabolites M1 and M2 (internal report) were used to derive individual predicted pharmacokinetic concentrations, used as pharmacokinetic input to the model. For liposomal amphotericin B and SSG, a kinetic-pharmacodynamic approach was used assuming a 1 compartment model with first-order elimination, using the administered drug amounts and previously reported elimination half-lives of 6 hours for liposomal amphotericin B[31] and 2 hours for SSG[32,33]. Direct and delayed sigmoidal E_{max} and linear models were evaluated to model the drug-induced killing of parasites driven by individual predicted concentration-time curves for the drugs.

2.3.3 Host-induced parasite suppression after treatment

Visual inspection of individual blood parasite loads over time indicated diverse and highly variable profiles after treatment (Supplementary Figure S3.2.1). Typical profiles after treatment included 1) complete parasitological cure, with no parasite recrudescence during follow-up after complete parasite clearance by the treatment, 2) initial parasite clearance followed by parasite recrudescence, where parasite regrowth is initiated at different time points during the follow-up period, and 3) initial parasite clearance followed by parasite recrudescence early after treatment, followed by parasite clearance later during follow-up.

The aim of this part of the model building was to enable the description of these three distinct typical parasite load-time profiles during the follow-up phase after treatment. Based on the hypothesis that parasite suppression after treatment, in the absence of drug pressure, is driven by the hosts' immune system, the variable onset in parasite

3.2

suppression and clearance after the end of treatment by the host's immune system was implemented by a sigmoidal E_{max} function, driven empirically by the time after treatment, to capture the differences in onset and magnitude of parasite recrudescence among patients (eq. 1). To allow for a clinically meaningful parasite recrudescence after complete drug-induced parasite depletion, the parasite compartment was restricted to ≥1 parasite/mL.

$$k_{imm} = \frac{I_{max}^{5} * time}{IT_{50}^{5} + time}$$ Eq. 1

In equation 1, k_{imm} is the parasite suppression by the immune system, time is the time after start of treatment, I_{max} the maximum inhibitory effect of the immune system, and IT_{50} the time after treatment of half the maximal immune effect.

With the aim to find biomarkers predictive of (suppression of) parasite recrudescence after therapy, hematological and biochemical markers were evaluated as drivers for parasite suppression (k_{imm}) instead of time after treatment. Available hematological and biochemical data included hemoglobin, white blood cells, platelets and creatinine for all patients, neutrophils, lymphocytes and monocytes (LEAP0714 and FEXI-VL-001), and total protein and albumin (FEXI-VL-001). All these covariates were evaluated graphically to assess their relationship with parasite recrudescence and suppression. White blood cell count was a physiologically plausible covariate as it may reflect the overall activity of the immune system. White blood cell count on Day 56, either absolute or relative to baseline, were evaluated on the extent of suppression of parasite regrowth (I_{max}) after treatment (eq. 2) and the onset of parasite suppression after treatment (IT_{50}) (eq. 3).

$$P_{TV} = P_{pop} * (1 + (WBC_i - WBC_{med}) * l)$$ Eq. 2

$$k_{imm} = \frac{I_{max}^{5} * WBC_i}{IT_{50}^{5} + WBC_i}$$ Eq. 3

where P_{TV} is the typical parameter value for IT_{50} or k_{imm} at covariate value WBC_i, P_{pop} the population estimate of IT_{50} or k_{imm}, WBC_i the white blood cell count or the white blood cell count relative to baseline for individual i at Day 56, WBC_{med} the median covariate value in the population, and l the slope factor.

2.4   Model evaluation

The aim of this modeling analysis was to describe the parasite clearance rates by the different treatment regimens, as well as to capture the different parasite profiles after treatment, driven by the immune system. Standard goodness of fit plots and individual prediction plots were used to guide model development. Model selection was based on scientific plausibility and minimum objective function value (OFV), where a decrease of 6.63 points in OFV corresponding to a P value <0.01 was considered significant, with

1 degree of freedom following a χ^2 distribution. Precision in parameter estimates was obtained by sampling importance resampling (SIR). To further assess the goodness of fit and to compare the model description of the parasite clearance during the treatment period in more detail, a visual predictive check (VPC) of the blood parasite loads during treatment was performed, stratified by the different treatment regimens. Simulations were performed of parasite profiles in a typical patient receiving different treatment regimens, and having different activity of the immune system, to illustrate the effect of different drugs and different immune effects.

2.5 Evaluation of the correlation between parasite exposure and clinical outcome

One of the goals of the model was to evaluate the predictiveness of parasite load or parasite clearance for subsequent clinical relapse of VL later during follow-up. To characterize the relationship of early drug-induced parasite clearance and long-term clinical outcome, different parasite exposure metrics during and early after treatment were evaluated. The sensitivity and specificity to predict clinical relapse based on blood parasite load on Day 10, Day 28 and Day 56 and the optimal cutoff values were derived by receiver-operating characteristic (ROC) curves, generated using the R packages "pROC" and "plotROC". The area under the ROC curve (AUC_{ROC}) was compared to find the most predictive parameter for clinical relapse in terms of follow-up day (Day 10, Day 28, or Day 56). The fraction of patients having a blood parasite load below the optimal cutoff value resulting from the ROC curve was compared between treatment regimens and between cured and relapsed patients. Second, model-based predictions of parasite load and parasite exposure during and early after treatment (at baseline and Day 10, 28 and 56) were compared between treatment regimens and to clinical outcome. As a measure of parasite clearance during therapy, cumulative exposure to parasites during and after the treatment, expressed as the area under the blood parasite load-time curve (AUC), was also compared. This parameter incorporates both drug-induced parasite clearance rate and the baseline parasite load, which was highly variable among patients. The parasite AUC during the first 10, 28 and 56 days were compared. To assess any treatment-related effects on the suppression of parasite recrudescence after treatment, I_{max} and IT_{50} were compared.

3.2

3. Results

3.1 Data

In total, 1260 blood samples from 188 patients were available for qPCR analysis (Table 3.2.1). The following qPCR observations were excluded from the analysis: 2 initial treatment failures (7 observations); 21 observations collected after rescue treatment;

190 unreliably extracted samples; and 44 physiologically impossible observations (3.5%). One patient who received AmB+MF10D lacking pharmacokinetic data was excluded (6 observations). Out of 992 blood parasite load observations included in the analysis, 359 observations (36%) were BLQ. An overview of the data included in the analysis up to Day 56 is shown in Figure 3.2.1 to display trends in the data during and early after treatment between treatment regimens.
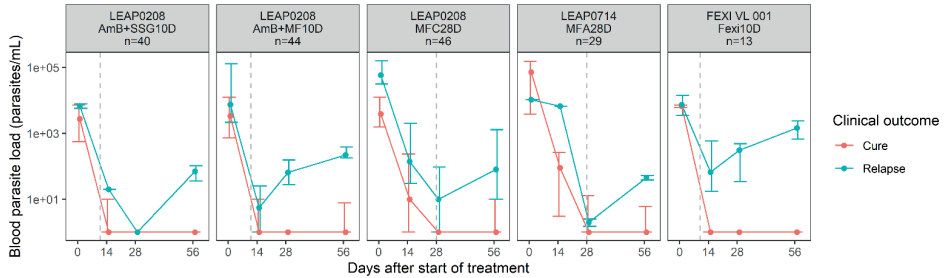

Figure 3.2.1 Blood parasite loads in Eastern African visceral leishmaniasis patients during treatment and early follow-up. Depicted are median (IQR) observed blood parasite loads colored by treatment outcome (cured patients in red and relapsed patients in blue), stratified by treatment regimen. AmB+SSG10D: 10 mg/kg amphotericin B (day 1) + 20 mg/kg/day SSG (day 2 to 11); AmB+MF10D: 10 mg/kg amphotericin B (day 1) + 100 mg/day miltefosine (day 2 to 11); MFC28D: miltefosine conventional dose (100 mg/day) (28 days); MFA28D: miltefosine allometric dose (28 days); Fexi10D: 1800 mg/day fexinidazole (4 days) + 1200 mg/day fexinidazole (6 days). Gray dashed lines represent the end of treatment.

3.2 Population pharmacokinetic-pharmacodynamic model

3.2.1 Parasite growth and drug-dependent parasite clearance

Parasite proliferation was best described by an exponential growth model (Figure 3.2.2), with an *in vivo* parasite doubling time of 7.8 days (RSE 12%) (Table 3.2.2, Figure 3.2.2). The model-derived individual predictions for the Fexi10D regimen indicated that parasite proliferation was adequately described, as the model captured the parasite growth after treatment in these patients (Supplementary Figure S3.2.1). Drug-dependent parasite killing was best described by first-order linear pharmacokinetic-pharmacodynamic models (fexinidazole and miltefosine) or kinetic-pharmacodynamic models (liposomal amphotericin B and SSG), where the parasite killing rate was directly proportional to the drug concentration. The VPC shows that the model quite adequately described the parasite clearance by the different treatment regimens (Figure 3.2.3). There were some discrepancies between the observed data and the model simulations, i.e., parasite recrudescence in Fexi10D was under-predicted by the model, baseline blood parasite load in MFA10D was under-predicted, and the parasite clearance rate in AmB+MF10D was under-predicted, especially the upper boundary of

the prediction interval. The time course of drug exposure in the different treatment regimens was simulated for a typical patient (Figure 3.3.4), illustrating variable durations of exposure depending on the treatment drugs and there corresponding half-lifes, which was much longer for miltefosine. This resulted in persistent drug exposure of about 11 days for the AmB+SSG10D and Fexi10D regimens, 30 days for the AmB+MF10D regimen, and 50 days for the MF28D regimen. The individual model-based predictions during treatment further illustrate the different parasite clearance rates for the various drug regimens (Supplementary Figure S3.2.1 and S3.2.2). The differential pharmacokinetic profiles in combination with the drug-specific drug effects on the parasite clearance, led to different typical parasite dynamics during the treatment period for each treatment regimen (Figure 3.2.5A). A fast and strong parasite clearance was induced by liposomal amphotericin B treatment (AmB+SSG10D and AmB+MF10D), while a slow onset and later parasite clearance was observed for miltefosine (MFC28D and MFA28D), and a weak response was observed for fexinidazole (Fexi10D).

Table 3.2.2 Parameter estimates for the final population pharmacokinetic-pharmacodynamic model.

Parameter	Parameter estimate	RSE (%)[a]	BSV (CV%)	RSE (%)[a]	Shrinkage (%)
E_{BASE} (p/mL)	5324	16	243	12	3
k_{GR} (h^{-1})	0.0037	12	-	-	-
λ_{fexi} (µg^{-1}*L*h^{-1})	0.0011	15	44	59	3
λ_{MF} (µg^{-1}*L*h^{-1})	0.0010	5	42	21	5
λ_{Amb} (mg^{-1}*kg*h^{-1})	0.0245	8	-	-	-
λ_{SSG} (mg^{-1}*kg*h^{-1})	0.0112	5	-	-	-
I_{max} (h^{-1})	0.037 (fixed)[b]	-	298	16	52
IT_{50} (days)	33.7	0.1	230	12	40
Proportional residual error (%)	101	-		0.7	18
Additive residual error (%)	70 (fixed)[c]	-		-	18

BSV: between-subject variability; CV: coefficient of variation; E_{BASE}: Baseline blood parasite load; I_{max}: maximum inhibition by immune response; IT_{50}: time at half-maximum inhibition; k_{GR}: parasite growth constant; λ_{Amb}: linear drug effect Amphotericin B; λ_{fexi}: linear drug effect fexinidazole; λ_{MF}: linear drug effect miltefosine; λ_{SSG}: linear drug effect SSG; RSE: relative standard error. [a] Obtained by SIR; [b] Fixed to ten times k_{GR}; [c] Fixed to half the lower limit of quantification.

3.2

3.2.2   Parasite suppression after treatment

Parasite suppression after treatment was best described by a first-order elimination process with an E_{max} model driven by the time after treatment, representing the onset and magnitude of parasite suppression by the host's immune system after start of treatment, including BSV on I_{max} and IT_{50} (Figure 3.2.2). The model captured the different parasite profiles after treatment, including complete parasite suppression, parasite regrowth at different time points during follow-up, and initial parasite regrowth followed by later suppression, and could therefore describe most of the individual profiles of parasite recrudescence during follow-up (Supplementary Figure S3.2.1 and S3.2.3). High variability in recrudescence profiles was reflected by a very

large and non-normally distributed BSV (>200 CV%) for baseline parasite load, I_{max} and IT_{50}. Typical value plots, as depicted in Figure 5B, illustrate the effect of different onset times of the immune suppression (different IT_{50}) on the parasite dynamics during follow-up. None of the hematological markers correlated with parasitological response (Supplementary Figure S3.2.4) and white blood cell counts was no significant covariate for k_{imm} or IT_{50}. Profiles with complete parasite clearance during treatment, followed by a fast and strong parasite recrudescence, could not be fully captured by the model (Supplementary Figure S3.2.1), despite the restriction of low parasite loads to ≥1 parasites/mL in the model. Using the consecutive estimation approach, drug effects and baseline parasite load could be estimated with good precision. Individual immune effect parameter estimates (I_{max} and IT_{50}) were difficult to differentiate from parasite growth due to the sparseness of data during the follow-up period, corroborated by sensitivity for initial values, convergence issues indicating that the global minima of the parameter values were not reached.
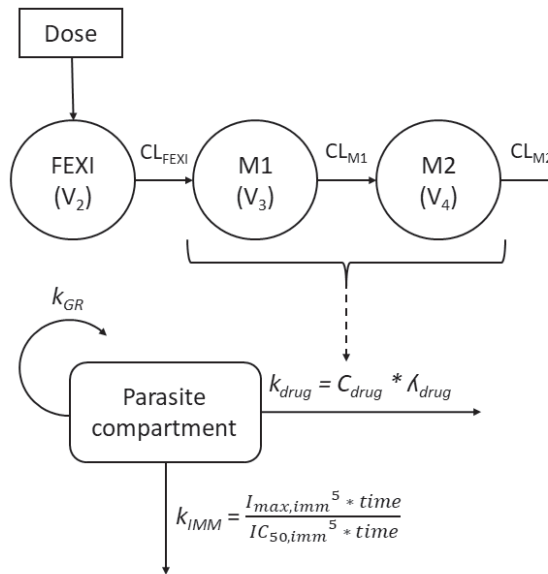
Figure 3.2.2 Schematic overview of the final pharmacokinetic-pharmacodynamic model, exemplified with the pharmacokinetic model for fexinidazole and its active metabolites M1 and M2. In the parasite model, k_{GR} is the parasite replication rate, k_{drug} is the drug-driven parasite clearance rate, λ_{drug} the drug-specific linear effect, and C_{drug} the drug concentration of either miltefosine, the sum of M1 and M2 for fexinidazole, amphotericin B, or SSG. k_{IMM} is the immune-driven parasite clearance, I_{max} the maximum inhibition by the immune response, and IT_{50} the time at half-maximum inhibition. In the fexinidazole pharmacokinetic model, CL is the clearance of fexinidazole, M1 or M2, and V_2, V_3, and V_4 the volume of distribution of fexinidazole, M1, and M2, respectively.
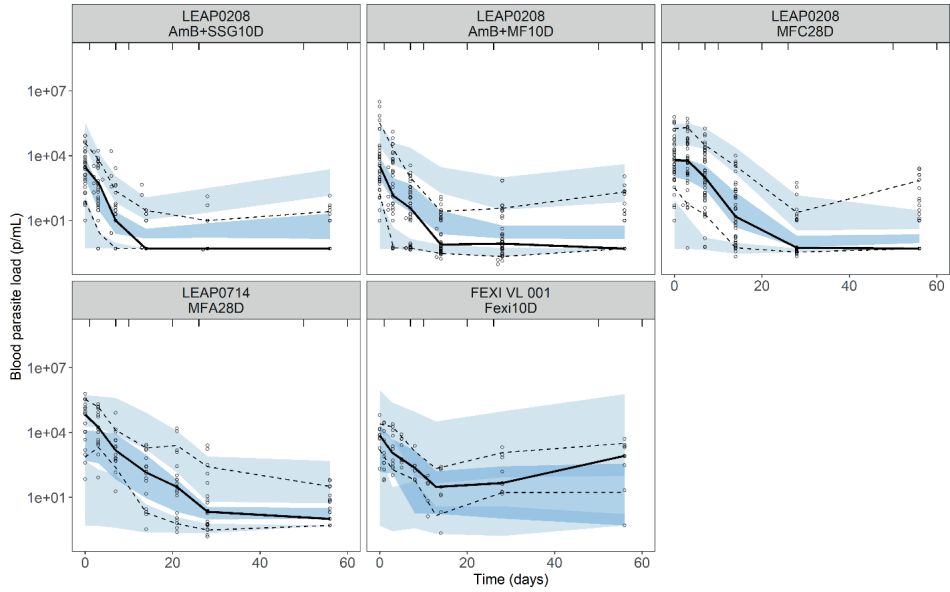
Figure 3.2.3 Prediction-corrected visual predictive checks for the final pharmacokinetic-pharmacodynamic blood *Leishmania* parasite load model until Day 56 after start of treatment. Solid lines: median of the observed values; dashed lines: the 10th and 90th percentiles of the observed values; dark and light blue areas: the 90% confidence intervals of the simulated median and percentiles, based on 1000 simulations.

3.2
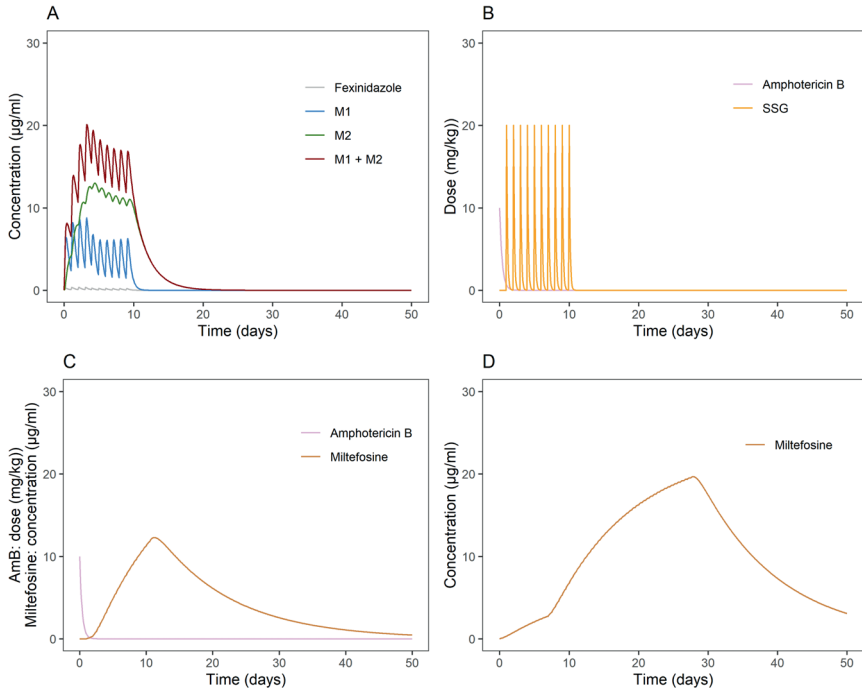
Figure 3.2.4 Simulations of typical pharmacokinetic profiles of patients receiving A) 1800 mg/day fexinidazole (4 days) + 1200 mg/day fexinidazole; B) 10 mg/kg amphotericin B (day 1) + 20 mg/kg/day SSG (day 2 to 11); C) 10 mg/kg amphotericin B (day 1) + 100 mg/day miltefosine (day 2 to 11); or D) 100 mg/day miltefosine (28 days).
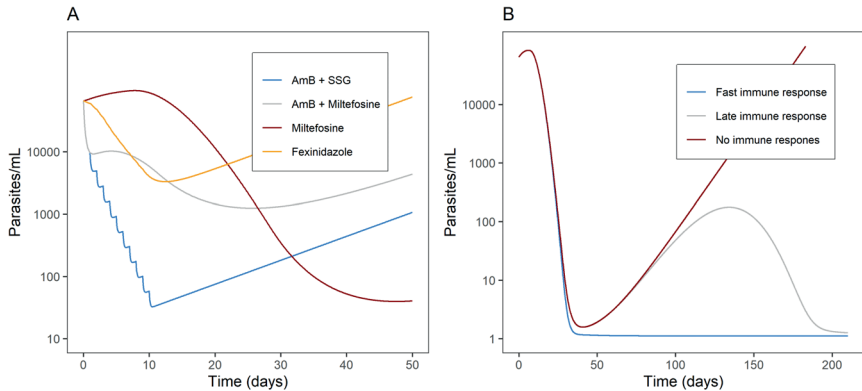
Figure 3.2.5 A: Simulation of drug effects of different VL therapies of typical patients receiving 1) 10 mg/kg amphotericin B (day 1) + 20 mg/kg/day SSG (day 2 to 11) (blue curve), 2) 10 mg/kg amphotericin B (day 1) + 100 mg/day miltefosine (day 2 to 11) (grey curve), 3) 100 mg/day miltefosine (28 days) (red curve), or 4) 1800 mg/day fexinidazole (4 days) + 1200 mg/day fexinidazole (6 days) (yellow curve). No immune response after the end of treatment was present. Other parameters were fixed to the population values. B: Simulation of typical patients receiving 150 mg/day miltefosine for 28 days. Patients have an IT$_{50}$ of 1000h (blue curve), 5000h (grey curve) and 100.000h (red curve). Other parameters were fixed to the population values.

3.3   Correlation between parasite exposure and clinical outcome

The AUC$_{ROC}$ for blood parasite load classifying clinical relapse (Figure 3.2.6) was highest on Day 28 (0.82) and Day 56 (0.87), compared with Day 10 (0.64) (Table 3.2.3). The optimal cutoff values for classifying relapse were around 10 p/mL (9 p/mL on Day 28 and 11 p/mL on Day 56). The fraction of patients having a blood parasite load <10 p/mL on Day 28 and Day 56 was therefore compared between treatment regimens and between final clinical outcome (Table 3.2.4). There were considerably more patients (73-86%) with an adequate parasite clearance (parasite load <10 p/mL) at Day 56 in relatively effective treatment regimens (AmB+SSG10D, AmB+MF10D, MFC28D, MFA28D), compared to only 10% in the non-efficacious Fexi10D regimen. Based on the cutoff value of 10 p/mL, 74% and 76% of relapsed patients were correctly categorized as relapse on Day 28 and Day 56, respectively.

Table 3.2.3 Predictiveness of clinical relapse by blood parasite load on different days after treatment, based on ROC curves.

Day[a]	AUC$_{ROC}$[b]	Cutoff value (p/mL)[c]	Sensitivity	Specificity
10	0.64	51	0.44	0.85
28	0.82	9	0.77	0.82
56	0.87	11	0.88	0.77

[a] Day after start of treatment; [b] Area under the ROC curve; [c] Optimal cutoff value of blood parasite load to predict clinical relapse.
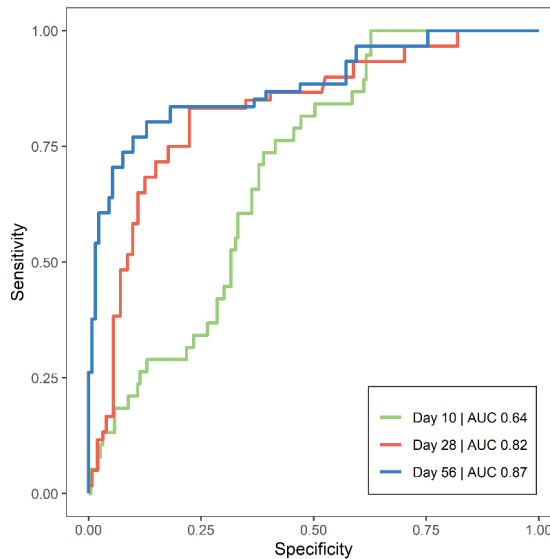
Figure 3.2.6 ROC curves of blood parasite load as predictor of clinical relapse on Day 10, 28, and 56 after start of treatment. AUC represents the integrated area under the ROC curve. Green line: day 10 (AUC 0.64); red line: day 28 (AUC 0.82); blue line: day 56 (AUC 0.87). Abbreviations: AUC, area under the curve; ROC, receiver operating characteristic.

Various other individual model-based secondary blood parasite load metrics were compared between treatment regimens and final clinical outcome (Table 3.2.4). Individual predicted blood parasite loads were higher on Day 10 in the miltefosine monotherapy regimens (MFC28D and MFA28D), and were higher on Day 28 and Day 56 in the Fexi10D treatment arm with poor efficacy. Blood parasite loads on Day 10, Day 28 and Day 56 were substantially higher in relapsed patients (Table 3.2.4, Figure 3.2.7).
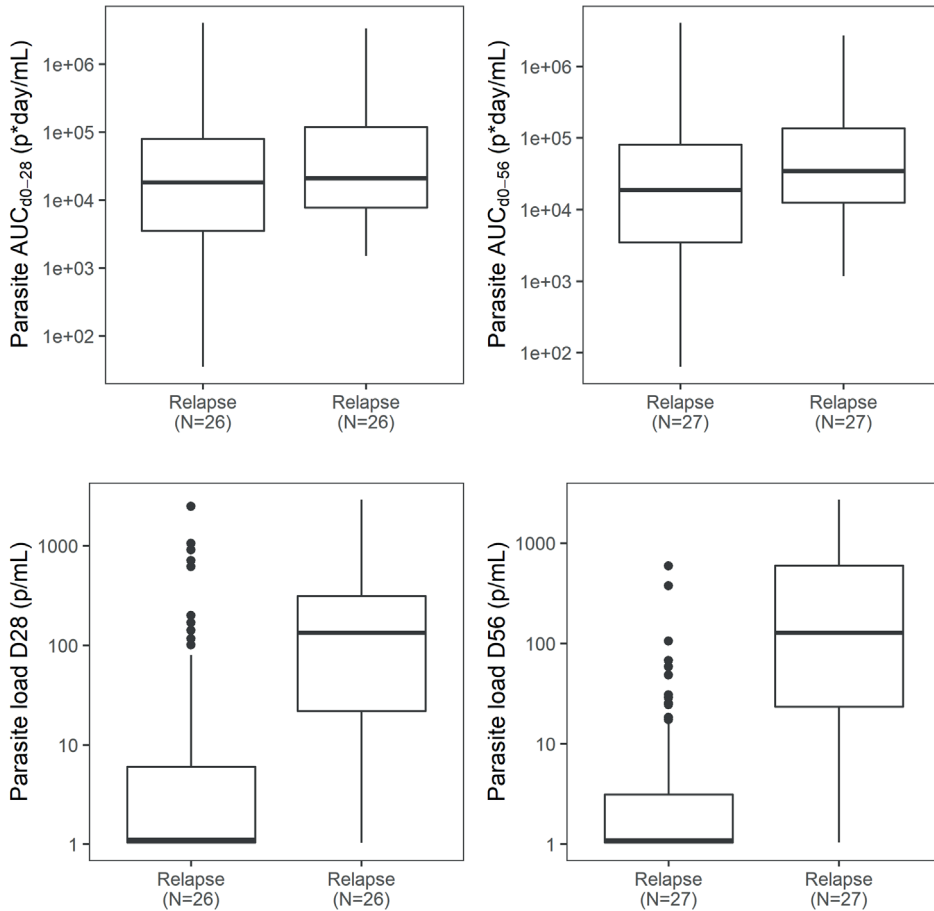
Figure 3.2.7 Parasite AUC_{d0-28} and AUC_{d0-56} and parasite load on Day 28, and Day 56 versus clinical outcome.

A low parasite AUC for different durations (AUC_{D0-10}, AUC_{D0-28}, AUC_{D0-56}) was not associated with favorable clinical outcome, except for a slightly lower AUC_{D0-56} of 18884 (3464-85774) p·day/mL in cured patients compared to 41931 (14171-173361) p·day/mL in relapsed patients. The parasite AUCs were considerably higher in the miltefosine

monotherapy regimens (MFC28D and MFA28D), which is in accordance with the slow miltefosine drug accumulation and slow onset of miltefosine-induced parasite clearance. The extent of suppression of parasite regrowth after treatment (I_{max}) did not clearly correlate with treatment efficacy, but the onset of the suppressive immune response (IT_{50}) was substantially delayed in the Fexi10D treatment arm with poor efficacy, indicating that a weak drug effect and partial parasite clearance during treatment negatively influences the onset of the immune response. This was in accordance with the delayed IT_{50} in relapsed patients compared to cured patients.

4.   Discussion

A semi-mechanistic pharmacokinetic-pharmacodynamic model was developed based on pharmacokinetic and blood parasite load data from Eastern African VL patients receiving five different (combination or monotherapy) treatment regimens, to characterize the complicated interaction between parasite replication, drug-induced parasite clearance and parasite clearance due to an emerging host immune response. The model adequately captured the blood parasite dynamics during and after treatment and revealed that blood parasite loads higher than 10 p/mL at Day 28 and Day 56 after start of treatment are an early indication for VL relapse, which could serve as a biomarker to predict long-term clinical outcome, although not yet ideal, based on the sensitivity and specificity. Until now, it is not possible to predict relapse, a long-term event that can occur up to 12 months or even longer after treatment. Moreover, the model indicated that long-term clinical outcome depends on both the initial parasite clearance by the treatment, as well as parasite suppression after treatment, which is probably achieved by an adequate hosts' immunological response. A better understanding of this immunological response by additional host biomarkers could potentially lead to an improved prediction of relapse.

Parasite replication and drug-induced parasite clearance by five different VL drug regimens were adequately characterized by the developed pharmacokinetic-pharmacodynamic model. To our knowledge, the model provided the first-ever estimation of the *in vivo Leishmania* parasite doubling time in human of 7.8 days, which was only slightly slower compared to previously reported *in vitro* intracellular *L. donovani* amastigote replication rates within macrophages, corresponding to parasite doubling times of 4.2 days and 2.9 days[34,35]. However, a limitation of this analysis is the lack of data on parasite growth before treatment. Parasite growth was estimated based on patient data after treatment (Fexi10D), and thus parasite growth might be influenced by the treatment. Moreover, identification of parasite growth is also dependent on the sampling scheme, and parasite growth rate might be variable among patients, depending on host-related factors such as activity of the immune system.

3.2

Table 3.2.4 Individual model-based predictions of parasite exposure per treatment arm and clinical outcome.

Study	LEAP0208		LEAP0714		FEXI-VL-001		
Treatment/outcome	AmB+SSG10D	AmB+MF10D	MFC28D	MFA28D	Fexi10D	Cure	Relapse
Subjects[a] (n)	40	44	46	29	13	138	34
Cured patients (n [%])	37 (93)	37 (84)	35 (76)	27 (93)	2 (15)	138 (100)	0 (0)
Parasite load <10p/mL at D28 (n [%])	31 (78)	31 (70)	32 (70)	18 (62)	3 (10)	106 (77)	9 (26)
Parasite load <10p/mL at D56 (n [%])	33 (83)	32 (73)	34 (74)	25 (86)	3 (10)	119 (86)	8 (24)
Parasite load D1[b] (p/mL)	23802 (4904-51372)	4493 (553-34633)	4583 (1008-29194)	33363 (6091-77096)	3732 (2605-14467)	7142 (1231-40157)	14467 (4493-62465)
Parasite load D10[b] (p/mL)	11.8 (2.8-35.9)	137 (4.0-807)	2027 (226-12355))	2378 (429-44318)	105 (25.1-249)	150 (8.8-2094)	333 (122-5985)
Parasite load D28[b] (p/mL)	1.1 (1.0-6.1)	2.1 (1.0-22.9)	1.1 (1.0-135)	1.3 (1.1-42.2)	112 (18.2-216)	1.1 (1.0-6.1)	105 (11.6-313)
Parasite load D56[b] (p/mL)	1.0 (1.0-5.7)	1.1 (1.0-10.1)	1.3 (1.0-10.4)	1.2 (1.1-3.1)	486 (11.1-1073)	1.1 (1.0-2.7)	125 (11.9-613)
Parasite $AUC_{00\text{-}10}$[b] (p·day/mL)	7284 (2385-19935)	5970 (641-41824)	32509 (8631-162007)	39558 (7638-417250)	8482 (4827-36350)	15648 (3241-52869)	17209 (5012-97125)
Parasite $AUC_{00\text{-}28}$[b] (p·day/mL)	7371 (2537-20370)	7061 (804-47564)	56327 (18322-223201)	74829 (14150-604792)	10260 (5644-37750)	18642 (3382-80241)	24596 (7042-129150)
Parasite $AUC_{00\text{-}56}$[b] (p·day/mL)	7400 (3094-20972)	10905 (906-52583)	56906 (18973-223236)	75175 (15254-604833)	33768 (8532-69033)	18884 (3464-85774)	41931 (14171-173361)
I_{max} (day^{-1})[c]	2.3 (1.7)	1.9 (2.0)	1.4 (1.6)	1.2 (0.7)	0.9 (0.7)	1.9 (1.7)	0.7 (0.5)
IT_{50} (day)[c]	23 (21)	45 (58)	59 (73)	60 (50)	77 (57)	40 (51)	84 (65)

AmB+MF10D: Amphotericin B 10 mg/kg (1 day) + miltefosine 2.5 mg/kg (10 days); AmB+SSG10D: Amphotericin B 10 mg/kg (1 day) + SSG 20 mg/kg (10 days); BLQ: below the limit of quantification; Fexi10D: Fexinidazole 1800 mg (4 days), 1200 mg (6 days); I_{max}: maximum inhibitory effect of the immune system; IT_{50}: time after treatment of half the maximal immune effect; MFA28D: miltefosine allometric dosing (pediatrics); MFC28D: Miltefosine conventional dosing (2.5 mg/kg) (adults). [a] Patients included in the analysis; [b] Median (IQR); [c] Mean (sd). I_{max} and IT_{50} represent the activity of the immune system to suppress the parasites.

The combination regimens of liposomal amphotericin B with SSG or miltefosine led to a rapid drug-induced parasite clearance, resulting in undetectable blood parasite loads by the end of drug exposure in most patients (70-78% of patients had a parasite load <10p/mL at Day 28). Miltefosine monotherapy resulted in a slower or delayed onset of parasite clearance, in line with the slow accumulation of miltefosine in the first week of treatment. Miltefosine treatment outcome has been shown to be associated with the time above a target concentration[36]. On the other hand, the long half-life of the drug results in an adequate above-target exposure, extending for a considerable period of time after the end of the 28-day monotherapy (MFC28D and MFA28D) and resulting in complete parasite clearance by Day 56 (parasite load <10p/mL at Day 56 in 74-86% of patients). Fexinidazole treatment resulted in only partial drug-induced parasite clearance in most patients, with only 2/13 patients having complete parasite clearance by the end of treatment, as measured by qPCR. These model results suggest that adequate parasite clearance by the drug is important to achieve long-term clinical cure, as almost all patients on fexinidazole therapy who had incomplete drug clearance by the treatment failed therapy. This was confirmed by the ROC analysis, as the optimal blood parasite load cutoff values for classifying clinical relapse were around 10 p/mL, meaning that very low parasite levels by the end of treatment are already associated with higher risk of clinical relapse. This was in line with previous results of a descriptive analysis of these data, concluding that the blood parasite load at Day 56 was the best time to predict clinical outcome, with a comparable optimal cutoff value of 20 p/mL[11].

Parasite suppression after treatment, presumably driven by the hosts' immune system, was described in the model by an E_{max} function with variable onset and magnitude of parasite clearance. Parasite dynamics after treatment was highly variable among patients. The model suggested that patients with complete parasite suppression had a fast onset of the host immune response, relatively rapid after end of treatment, while patients with parasite recrudescence somewhere during the follow-up had a late onset or weak magnitude of the suppressive immune effect. Although we used a sophisticated analysis method to incorporate the complex interplay between parasites, drugs and host, the explored hematological and biochemical data could not be identified as predictors to explain the between-patient variability in onset and magnitude of the post-treatment suppression or conversely recrudescence of parasites.

3.2

Because of the multitude of effects that play a role in the parasite dynamics, such as parasite growth and simultaneous parasite clearance by the treatment or parasite suppression by the immune system, simultaneous estimation of all parameters led to over-parameterization of the model. However, by estimating the parasite growth rate, the drug effects, and the immune effect separately based on representative subsets of the data, we could adequately estimate a parasite growth rate and drug effects for all drugs. Precise parameter estimates of the immune response model were nevertheless

difficult to obtain. To improve the stability and the convergence of the model, various estimation methods were attempted as well implementing a mixture model with different k_{imm}'s for cured and relapsed patients, but this did not result in stable parameter estimates. In future studies, more frequent blood sampling, especially during the follow-up phase, in combination with measurement of other host biomarkers, might improve the characterization of the host suppression of the parasite load after treatment.

To predict parasite response after treatment, attempts were made to identify biomarkers for the activity of the immune system, by explaining variability in k_{imm}, but could nevertheless not be identified. Identification of a biomarker for activity of the immune system is complicated because there are many factors involved. White blood cell count was evaluated as a predictor for the activity of the hosts' immune system, but was not identified. Lymphocyte and albumin levels were higher in cured patients, and total protein levels were lower in cured patients, although these results should be interpreted with caution as these were available for only a small portion of patients (Supplementary Figure S3.2.3). Depletion of lymphocytes and albumin is a manifestation of VL infection, and could therefore reflect severity of disease, and subsequently the ability of the patient to clear the parasite. Moreover, lymphocyte count might directly reflect the function of the immune system, as probably a Th1 response is responsible for activation of infected macrophages that can lead to intracellular *L. donovani* killing[37], once there are sufficient amounts of active T cells[10]. It would be worthwhile to collect blood cell counts and albumin levels in patients during treatment and follow-up in future clinical trials, as well as to explore other parameters related to the immune response, to further investigate this relationship.

Using the developed model, individually model-based predictions of parasite AUC and parasite loads at different time points were compared to final clinical outcome. Parasite load at start of treatment was not related to relapse, indicating that the severity of infection at start of treatment is not indicative for the final treatment outcome. Parasite AUC was not predictive for clinical outcome either, which might be due to the aforementioned differences in pharmacokinetics between the treatment regimens. For example, the onset of parasite clearance due to miltefosine is much slower due the initial slow accumulation of miltefosine, resulting in higher AUCs until Day 10, 28 and 56 for the miltefosine monotherapies compared to combination therapies with liposomal amphotericin B, but resulted nevertheless in a comparable final treatment outcome. The parasite load at Day 28 and Day 56 after start of treatment was related to relapse, indicating that an adequate drug response is needed, as well as an early onset of immune system activation. Although the blood parasite load on Day 28 or Day 56 could not correctly predict relapse in all individual patients (26% and 24% of relapsed patients were classified as cured based on the ROC results, respectively), the fraction of patients

having a blood parasite load <10 p/mL by the end of treatment in a group of patients receiving the same VL treatment is an indication for the efficacy of the treatment in this population. This might be useful in clinical trials where new dosing regimens or new combinations will be tested, to get an early indication of the long-term efficacy of this treatment. In the future, optimization of qPCR as a parasitological marker, possibly combined with other host biomarkers could improve the sensitivity/specificity of a predictor for VL relapse, and be used as an endpoint in future VL trials to reduce the need for long periods of follow-up.

This is the first time that the complex mechanisms of parasite replication, treatment effects and host response are integrated in a comprehensive semi-mechanistic model, which provides insight into the *in vivo* parasite growth rate and parasite clearance rates by different drugs. The model could serve as a framework for treatment optimization of VL treatment regimens, and blood parasite load at the end of treatment could be a useful biomarker to assess treatment efficacy of a treatment regimen in a clinical trial setting.

Acknowledgments

Funding

3.2

References

1. Wasunna M, Njenga S, Balasegaram M, Alexander N, Omollo R, Edwards T, et al. Efficacy and Safety of AmBisome in Combination with Sodium Stibogluconate or Miltefosine and Miltefosine Monotherapy for African Visceral Leishmaniasis: Phase II Randomized Trial. PLoS Negl Trop Dis. 2016;10(9): e0004880.
2. Mbui J, Olobo J, Omollo R, Solomos A, Kip AE, Kirigi G, et al. Pharmacokinetics, Safety, and Efficacy of an Allometric Miltefosine Regimen for the Treatment of Visceral Leishmaniasis in Eastern African Children: An Open-label, Phase II Clinical Trial. Clin Infect Dis. 2019;68(9):1530-1538.
3. Musa AM, Mbui J, Mohammed R, Olobo J, Ritmeijer K, Alcoba G, et al. Paromomycin and Miltefosine Combination as an Alternative to Treat Patients with Visceral Leishmaniasis in Eastern Africa: A Randomized, Controlled, Multicountry Trial. Clin Infect Dis. 2022;ciac643.
4. Rijal S, Ostyn B, Uranw S, Rai K, Bhattarai NR, Dorlo TPC, et al. Increasing failure of miltefosine in the treatment of kala-azar in nepal and the potential role of parasite drug resistance, reinfection, or noncompliance. Clin Infect Dis. 2013;56(11):1530–8.
5. Gorski S, Collin SM, Ritmeijer K, Keus K, Gatluak F, Mueller M, et al. Visceral leishmaniasis relapse in Southern Sudan (1999-2007): A retrospective study of risk factors and trends. PLoS Negl Trop Dis. 2010; 4(6):e705.
6. Burza S, Croft SL, Boelaert M. Leishmaniasis. Vol. 392, The Lancet. Lancet Publishing Group; 2018: 951-970.
7. Murray HW, Hariprashad J, Fichtl RE, Murray HW. Models of Relapse of Experimental Visceral Leishmaniasis. J lnfect Dis. 1996;173:1041–1044.
8. Leta S, Dao THT, Mesele F, Alemayehu G. Visceral Leishmaniasis in Ethiopia: An Evolving Disease. PLoS One. 2014;8(9):e3131.
9. Varma N, Naseem S. Hematologic changes in visceral Leishmaniasis/Kala Azar. Indian J Hematol Blood Transfus. 2010;26(3):78–82.
10. Rodrigues V, Cordeiro-Da-Silva A, Laforge M, Silvestre R, Estaquier J. Regulation of immunity during visceral Leishmania infection. Parasit Vectors. 2016;9(1):1–13.
11. Verrest L, Kip AE, Musa AM, Schoone GJ, Schallig HDFH, Mbui J, et al. Blood Parasite Load as an Early Marker to Predict Treatment Response in Visceral Leishmaniasis in Eastern Africa. Clin Infect Dis. 2021;73(5):775–782.
12. Bossolasco S, Gaiera G, Olchini D, Gulletta M, Martello L, Bestetti A, et al. Erratum: Real-Time PCR Assay for Clinical Management of Human Immunodeficiency Virus-Infected Patients with Visceral Leishmaniasis. J Clin Microbiol. 2004;42(4):1858.
13. Cascio A, Calattini S, Colomba C, Scalamogna C, Galazzi M, Pizzuto M, et al. Polymerase chain reaction in the diagnosis and prognosis of Mediterranean visceral leishmaniasis in immunocompetent children. Pediatrics. 2002;109(2):E27.
14. Cruz I, Cañavate C, Rubio JM, Morales MA, Chicharro C, Laguna F, et al. A nested polymerase chain reaction (Ln-PCR) for diagnosing and monitoring Leishmania infantum infection in patients co-infected with human immunodeficiency virus. Trans R Soc Trop Med Hyg. 2002;96:S185–S189.
15. Disch J, Oliveira MC, Orsini M, Rabello A. Rapid clearance of circulating Leishmania kinetoplast DNA after treatment of visceral leishmaniasis. Acta Trop. 2004;92(3):279–283.
16. Fisa R, Riera C, Ribera E, Gállego M, Portús M. A nested polymerase chain reaction for diagnosis and follow-up of human visceral leishmaniasis patients using blood samples. Trans R Soc Trop Med Hyg. 2002;96:S191–S194.
17. Kip AE, Balasegaram M, Beijnen JH, Schellens JHM, Vries PJ De, Dorlo TPC. Systematic Review of Biomarkers To Monitor Therapeutic Response in. Antimicrob Agents Chemother. 2015;59(1):1–14.
18. Lachaud L, Dereure J, Chabbert E, Reynes J, Mauboussin JM, Oziol E, et al. Optimized PCR using patient blood samples for diagnosis and follow-up of visceral leishmaniasis, with special reference to AIDS patients. J Clin Microbiol. 2000;38(1):236–240.
19. Mary C, Faraut F, Drogoul MP, Xeridat B, Schleinitz N, Cuisenier B, et al. Reference values for Leishmania infantum parasitemia in different clinical presentations: Quantitative polymerase chain reaction for therapeutic monitoring and patient follow-up. Am J Trop Med Hyg. 2006;75(5):858–863.

20. Mary C, Faraut F, Lascombe L, Dumon H. Quantification of Leishmania infantum DNA by a real-time PCR assay with high sensitivity. J Clin Microbiol. 2004;42(11):5249–5255.

21. Nuzum E, White F, Thakur C, Dietze R, Wages J, Grogl M, et al. Diagnosis of symptomatic visceral leishmaniasis by use of the polymerase chain reaction on patient blood. J Infect Dis. 1995;171(3): 751-754.

22. Pizzuto M, Piazza M, Senese D, Scalamogna C, Calattini S, Corsico L, et al. Role of PCR in Diagnosis and Prognosis of Visceral Leishmaniasis in Patients Coinfected with Human Immunodeficiency Virus Type 1. J Clin Microbiol. 2001;39(1):357–361.

23. Sudarshan M, Weirather JL, Wilson ME, Sundar S. Study of parasite kinetics with antileishmanial drugs using real-time quantitative PCR in Indian visceral leishmaniasis. Journal of Antimicrobial Chemotherapy. 2011;66(8):1751–1755.

24. Cota GF, de Sousa MR, de Assis TSM, Pinto BF, Rabello A. Exploring prognosis in chronic relapsing visceral leishmaniasis among HIV-infected patients: Circulating Leishmania DNA. Acta Trop. 2017;172:186–191.

25. Abd-Rahman AN, Marquart L, Gobeau N, Kümmel A, Simpson JA, Chalon S, et al. Population Pharmacokinetics and Pharmacodynamics of Chloroquine in a Plasmodium vivax Volunteer Infection Study. Clin Pharmacol Ther. 2020;108(5):1055–1066.

26. Krause A, Dingemanse J, Mathis A, Marquart L, Möhrle JJ, McCarthy JS. Pharmacokinetic/ pharmacodynamic modelling of the antimalarial effect of Actelion-451840 in an induced blood stage malaria study in healthy subjects. Br J Clin Pharmacol. 2016;412–421.

27. Wattanakul T, Baker M, Mohrle J, Mcwhinney B, Hoglund RM, Mccarthy JS, et al. Semimechanistic Pharmacokinetic and Pharmacodynamic Modeling of Piperaquine in a Volunteer Infection Study with Plasmodium falciparum Blood-Stage Malaria. Antimicrob Agents Chemother. 2021;65(4):e01583-20.

28. Tarning J, Thana P, Phyo AP, Lwin KM, Hanpithakpong W, Ashley EA, et al. Population pharmacokinetics and antimalarial pharmacodynamics of piperaquine in patients with Plasmodium vivax Malaria in Thailand. CPT Pharmacometrics Syst Pharmacol. 2014;3(8):e132.

29. Palic S, Kip AE, Beijnen JH, Mbui J, Musa A, Solomos A, et al. Characterizing the non-linear pharmacokinetics of miltefosine in paediatric visceral leishmaniasis patients from Eastern Africa. J Antimicrob Chemother. 2020;75:3260–3268.

30. Dorlo TPC, Hillebrand MJX, Rosing H, Eggelte TA, de Vries PJ, Beijnen JH. Development and validation of a quantitative assay for the measurement of miltefosine in human plasma by liquid chromatography-tandem mass spectrometry. J Chromatogr B Analyt Technol Biomed Life Sci. 2008;865(1–2):55–62.

31. Bekersky I, Fielding RM, Dressler DE, Lee JW, Buell DN, Walsh TJ. Plasma protein binding of amphotericin B and pharmacokinetics of bound versus unbound amphotericin B after administration of intravenous liposomal amphotericin B (AmBisome) and amphotericin B deoxycholate. Antimicrob Agents Chemother. 2002;46(3):834–840.

32. Chulay JD, Fleckenstein L, Smith DH. Pharmacokinetics of antimony during treatment of visceral leishmaniasis with sodium stibogluconate or meglumine antimoniate. Trans R Soc Trop Med Hyg. 1988;82(1):69–72.

33. Cruz A, Rainey PM, Herwaldt BL, Stagni G, Palacios R, Trujillo R, et al. Pharmacokinetics of antimony in children treated for leishmaniasis with meglumine antimoniate. J Infect Dis. 2007;195(4):602–608.

34. Tegazzini D, Díaz R, Aguilar F, Peña I, Presa JL, Yardley V, et al. A Replicative In Vitro Assay for Drug Discovery against Leishmania donovani. Antimicrob Agents Chemother. 2016;60(6):3524–3532.

35. Castilla JJ, Sanchez-Moreno M, Mesa C, Osuna A. Leishmania donovani: In vitro culture and [1H] NMR characterization of amastigote-like forms. Mol Cell Biochem. 1995;142(2):89–97.

36. Dorlo TPC, Kip AE, Younis BM, Ellis SJ, Alves F, Beijnen JH, et al. Visceral leishmaniasis relapse hazard is linked to reduced miltefosine exposure in patients from Eastern Africa: A population pharmacokinetic/pharmacodynamic study. J Antimicrob Chemother. 2017;72(11):3131–3140.

37. McElrath MJ, Murray HW, Cohn ZA. The dynamics of granuloma formation in experimental visceral leishmaniasis. J Exp Med. 1988;167(6):1927–1937.
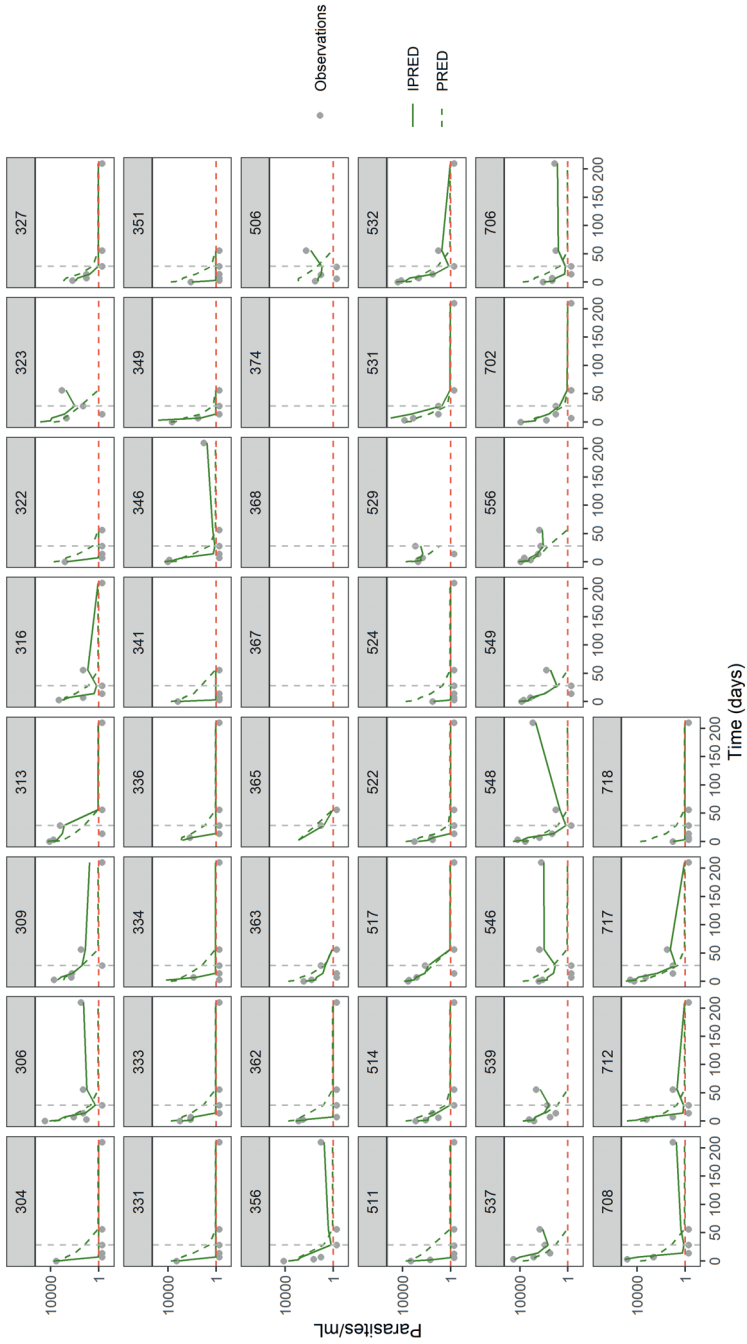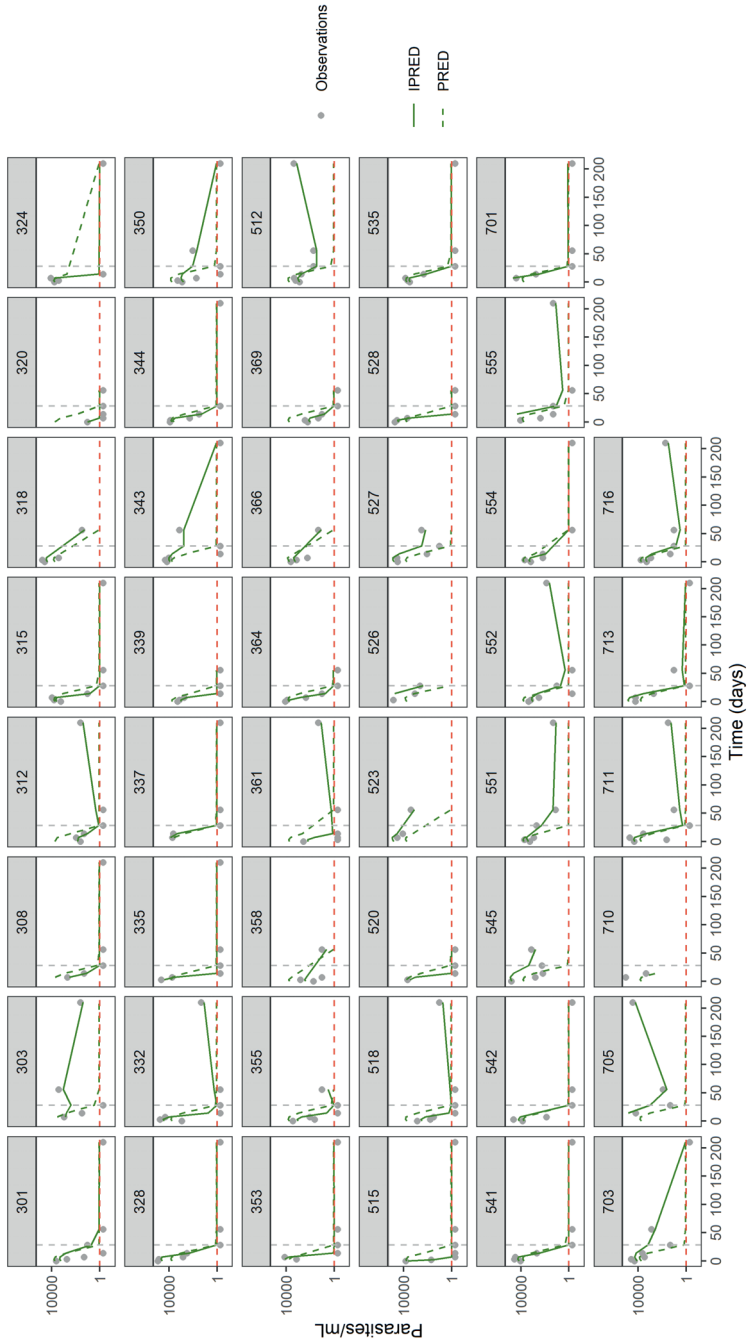
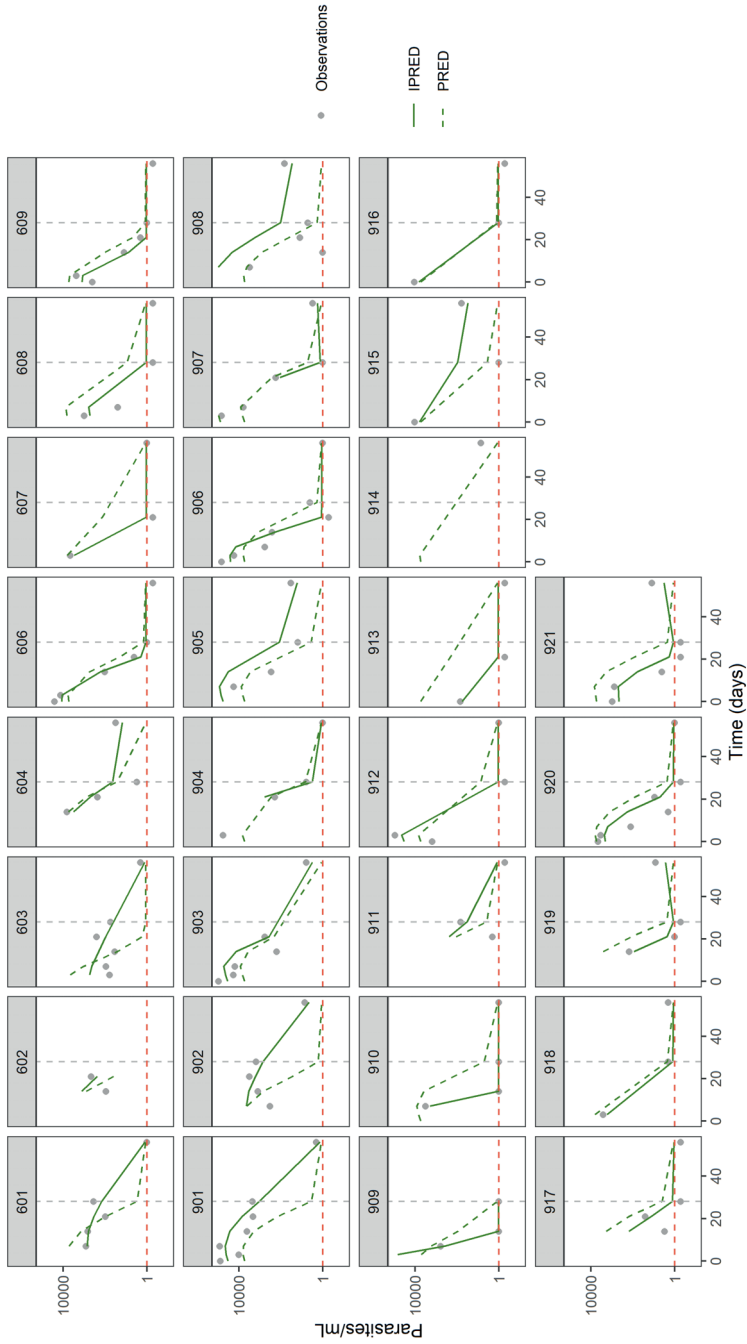**3.2**

Supplementary material 3.2
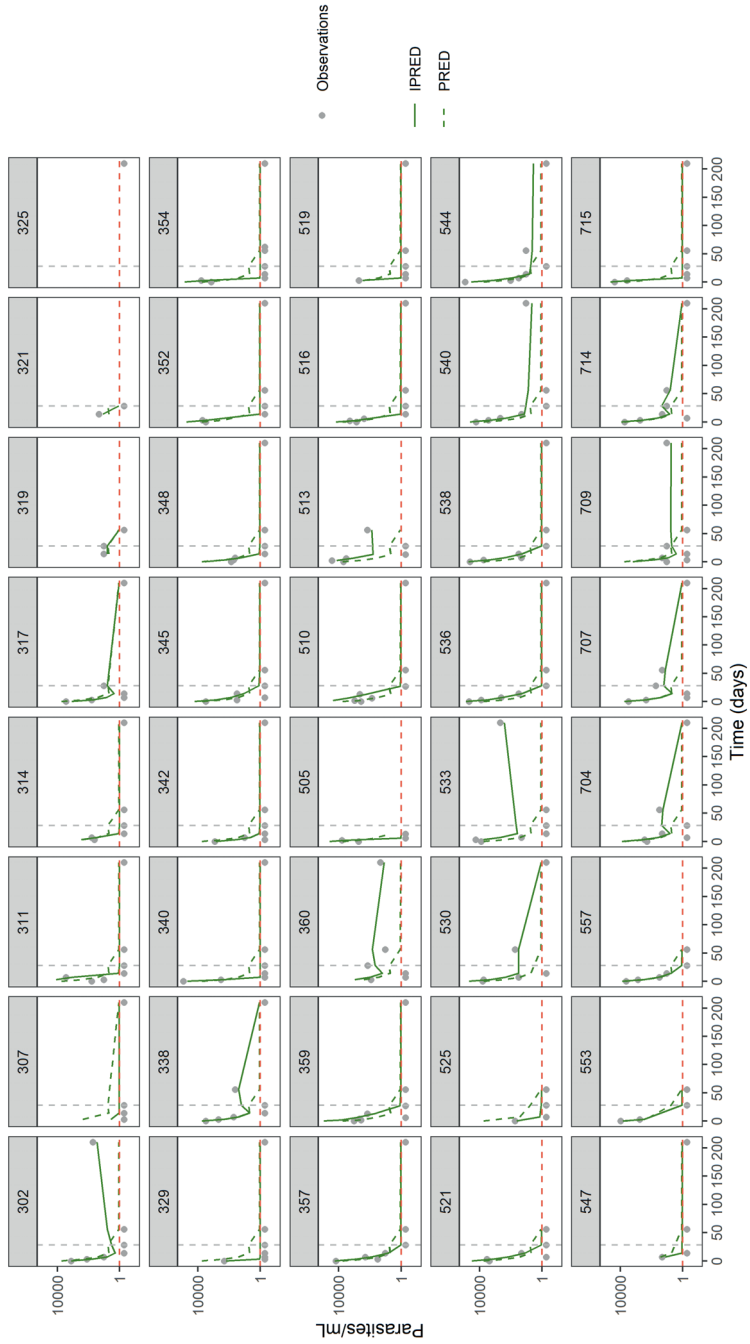
B. LEAP0208 AmB+MF10D

3.2

C. LEAP0208 MF28D
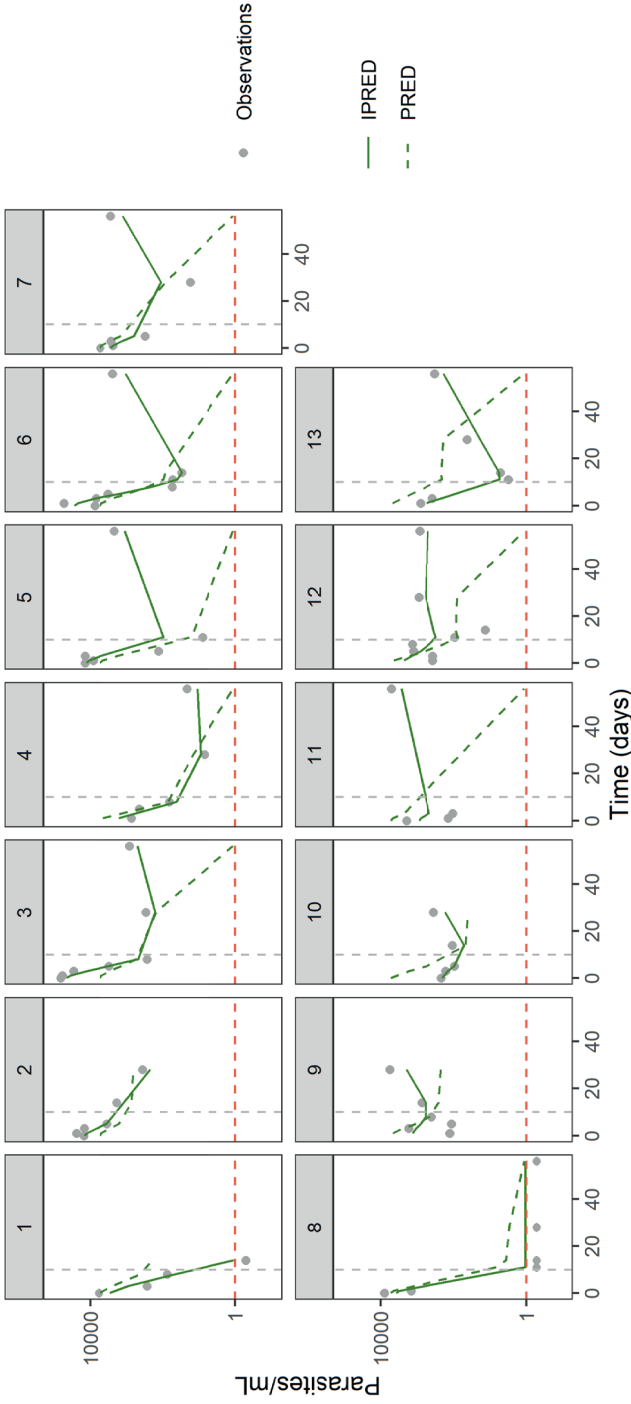
D. LEAP0714 MF28D

3.2

Figure S3.2.1 Individual model-based predictions of blood parasite loads per treatment arm.
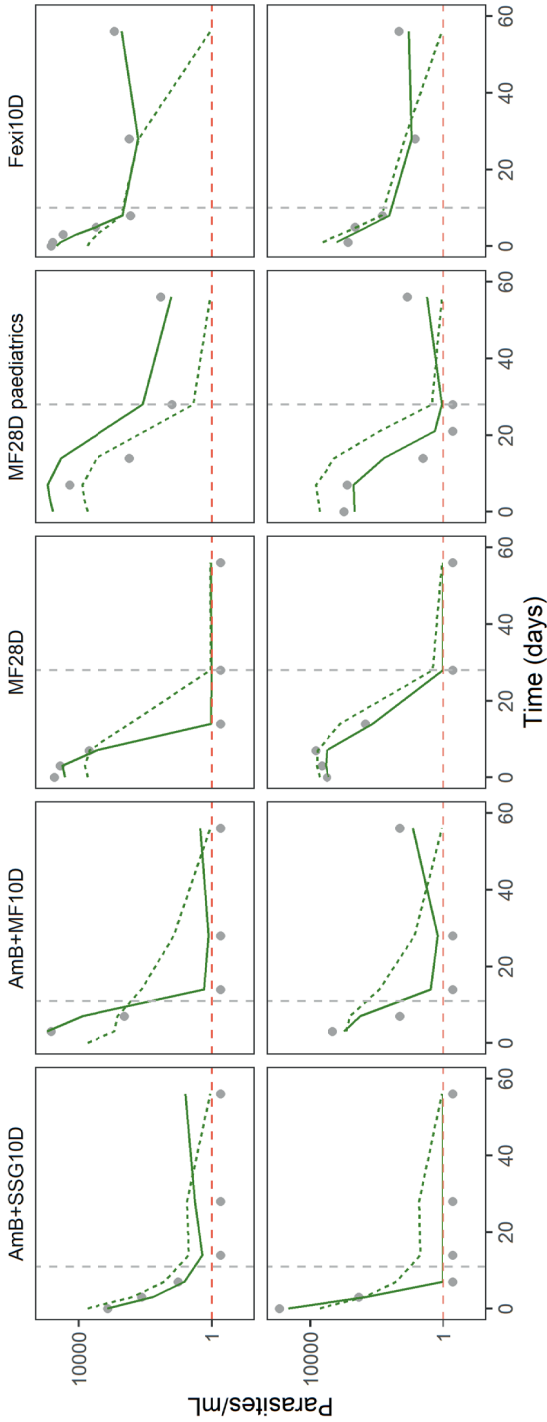
Figure S3.2.2 Individual model fits in a selection of patients presenting different parasite profiles. Grey dots: observed blood parasite loads; dashed green line: population predictions; solid green line: individual predictions; dashed red line: lower limit of quantification; dashed grey line: end of treatment.
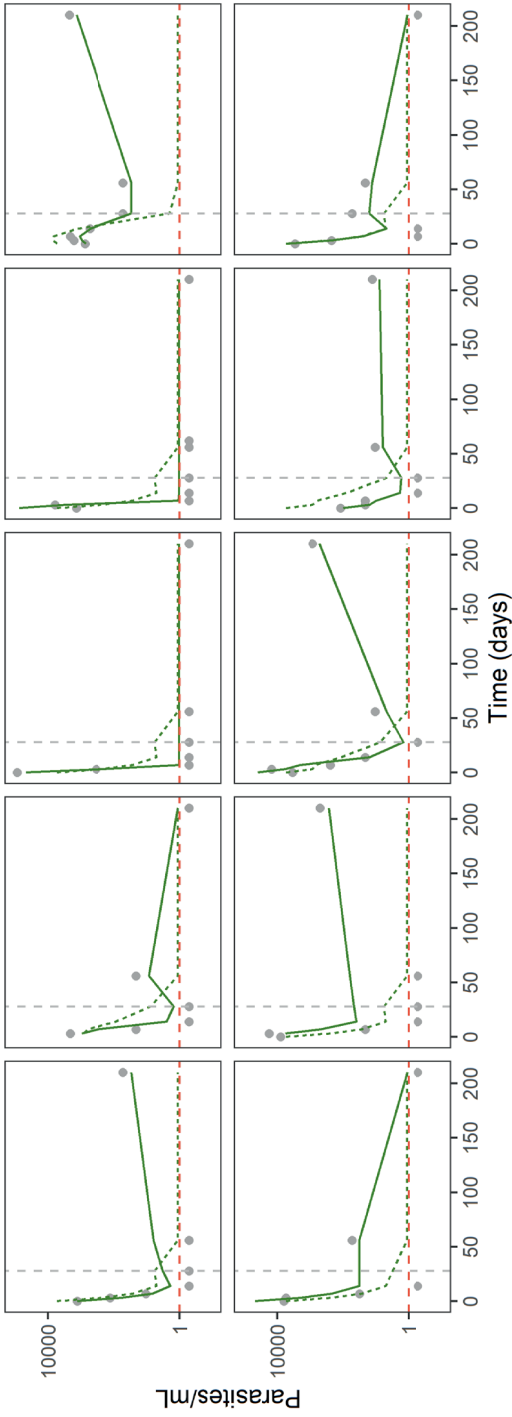
3.2

Figure S3.2.3 Individual model fits of parasite loads during and after treatment in a selection of patients receiving different treatment regimens. Grey dots: observed blood parasite loads; dashed green line: population predictions; solid green line: individual predictions; dashed red line: lower limit of quantification; dashed grey line: end of treatment.
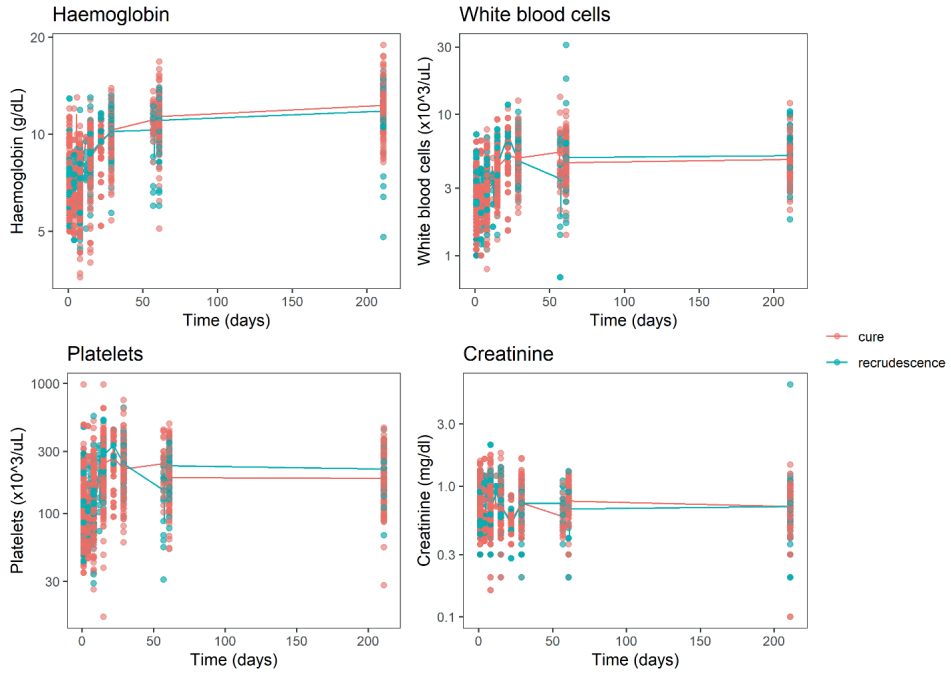
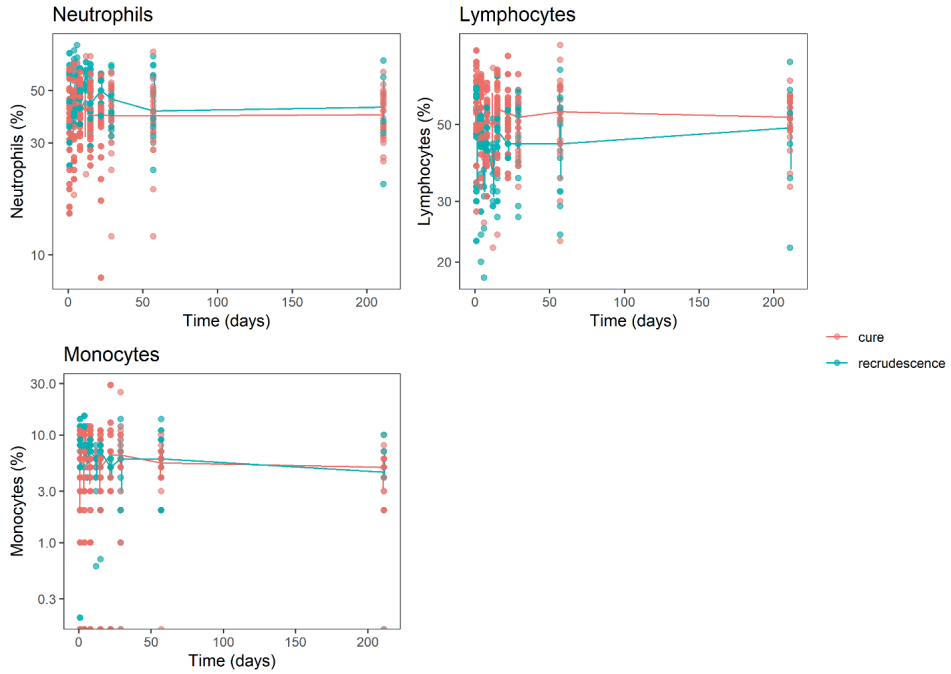**Figure S3.2.4a**   Hematological data available of all studies, colored by parasitological response.

Figure S3.2.4b   Hematological data available of LEAP0714 and FEXI-VL-001, colored by parasitological response.
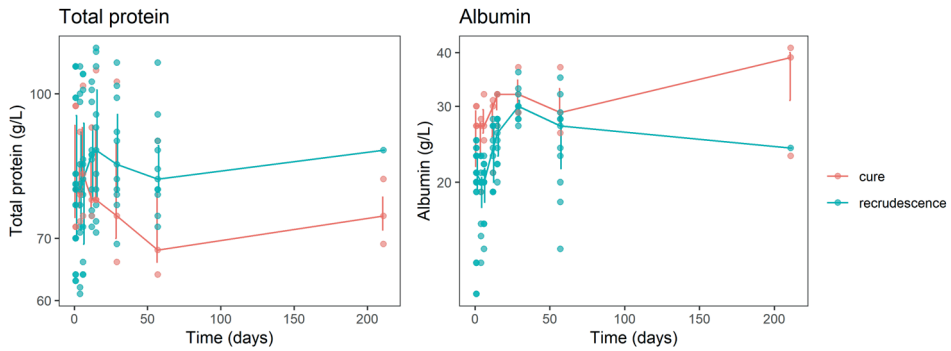

Figure S3.2.4c   Hematological data available of FEXI-VL-001, colored by parasitological response.

NONMEM control stream

; Description: Final PK-PD model
; Author: L. Verrest

$PROBLEM PK PD MODEL

$INPUT ID STUDY ARM TIME DAY DV CMT EVID MDV AMT II ADDL FLAG FLAG2 FLAG3
FLAG4 DROP CURE RDAY CODE SITE WT HT FV2 FV3 FV4 FQM1 FQM2 FCLM2 FKA MCL
MV2 MQ MV3 MKA MF1 AGE SEX WBC0 WBC56 WBC56R DROP

; Dataset description
; ID: unique subject number
; STUDY: 208: LEAP0208, 714: LEAP0714, 1: Fexi-VL-001
; ARM: 1: 0208 Ambisome (1 dose) + SSG (10 days), 2: 0208 Ambisome (1 dose) +
Miltefosine
; (10 days), 3: 0208 Miltefosine (28 days), 4: 0714 Miltefosine (28 days), 5: Fexinidazole
(10 days)
; TIME: time after start of treatment (hours)
; DAY: reported sampling day (start of treatment = DAY 0)
; DV: dependent variable
; CMT: 1: Fexi dose, (2: Fexi central comp, not used), (3: M1 comp, not used), (4: M2
comp, not used),
; 5: MF dose LEAP0208, (6: MF central comp, not used), (7, MF periph comp, not used),
8: AmBisome
; mg/kg dose (10mg/kg), 9: SSG mg/kg dose (20mg/kg), 10: PD dose (blood qPCR
parasite load,
; parasites/mL)
; EVID: event ID (1: dosing record, 2: DV record, 3: other record)
; MDV: missing dependent variable
; AMT: amount (p/mL for blood parasite load)
; II: interdose interval
; ADDL: additional identical doses given
; FLAG: Flag to mark blood samples. 1: unreliable, 2: initial failure, 3: questionable, 4:
samples after
; rescue treatment is given
; FLAG2: IDs 0208 ARM 2 and 3 without PK observations (ID 534)
; FLAG3: IDs 0208 without PD observations (ID 509)
; FLAG4: outlier IDs 0208 and Fexi
; CURE: 1: cure, 0: relapse (1 outcome per ID), 2: initial failure
; RDAY: Relapse day. NOTE: for 0714, rescue treatment day is used here!
; CODE: parasite response. 0: parasitological cure, 1: parasitological relapse, 2: late cure

3.2

; SITE: Study site. 1: Doka (Sudan) (0208 and Fexi), 2: Kassab (Sudan) (0208), 3: Kimalel (Kenya)
; (0208), 4: Amudat (Uganda) (0714), 5: Kacheliba (Kenya) (0714)
; WT: Body weight (kg)
; HT: Height (cm)
; FV2, FV3, FV4, FQM1, FQM2, FCLM2, FKA: fexi PK individual model estimates
; MCL, MV2, MQ, MV3, MKA, MF1: miltefosine PK individual model estimates
; AGE: Age (years)
; SEX : 0: male, 1: female
; WBC0: white blood cell count Day 1
; WBC56: white blood cell count Day 56
; WBC56R: change in white blood cell count Day 56 relative to baseline

$DATA   nm.qPCR.PK.C.v8.csv
IGNORE=@
IGNORE(FLAG.NE.0)
IGNORE(FLAG2.NE.0)
IGNORE(FLAG3.NE.0)
IGNORE(FLAG4.EQ.1)

$SUBROUTINE ADVAN13 TOL=6

$MODEL
COMP=(DEPOT DEFDOSE)
COMP=(CENTR1) ; Fexi
COMP=(MET1)
COMP=(MET2)
COMP=(ABS2)   ; MF 0208
COMP=(CENTR2)
COMP=(PERI2)
COMP=(AMB) ; Amphotericin B dose (10 mg/kg iv)
COMP=(SSG) ; SSG dose (20 mg/kg im)
COMP=(PML) ; blood parasite load (p/mL)

$PK
;;; PK
; FEXI
F1   = 1
KA1 = FKA
CL2 = FQM1 * (1-(DAY-1)*(-0.0403))
CL3 = FQM2

```
CL4  = FCLM2
V2   = FV2
V3   = FV3
V4   = FV4
K23  = CL2 / V2
K34  = CL3 / V3
K40  = CL4 / V4

; MF
F5   = MF1
KA2  = MKA
CL6  = MCL
V6   = MV2
V7   = MV3
Q    = MQ
K60  = CL6 / V6
K67  =  Q / V6
K76  =  Q / V7


; AmfoB
K80 = 0.1155 ; Based on elimination half-life 6hr (Bekersky 2002)

; SSG
K90 = 0.3465 ; Based on elimination half-line 2hr (Cruz 2007, Chulay 1988)

;;; PD
EBASE  =  THETA(1) * EXP(ETA(1))     ; Baseline parasite load
KG    =  THETA(2) * EXP(ETA(2))      ; Parasite growth constant
A_0(10)=  EBASE                      ; Set effect compartment initial value
; Drug effects
LAMBF  =  THETA(3) * EXP(ETA(3))   ; Fexi
LAMBM =  THETA(4) * EXP(ETA(4))    ; Miltefosine
LAMBA = THETA(5) * EXP(ETA(5))     ; AmfoB
LAMBS = THETA(6) * EXP(ETA(6))     ; SSG
; Immune effect
GM = THETA(7) * EXP(ETA(7))
IMAX = THETA(8) * EXP(ETA(8))
IT50 = THETA(9) * EXP(ETA(9))

; Scaling parameters
```

3.2

```
S2  = V2                    ; MW Fexi 279.31
S3  = V3  * (279.31/295.32) ; Scaling M1, MW 295.32
S4  = V4  * (279.31/311.32) ; Scaling M2, MW 311.32
S6  = V6
S7  = V7
```

$DES
```
DEL = 1E-12

C2 = A(2)/(S2+DEL) ; FEXI Concentration
C3 = A(3)/(S3+DEL) ; M1 Concentration
C4 = A(4)/(S4+DEL) ; M2 Concentration
C6 = A(6)/(S6+DEL) ; MF Concentration
C34 = C3 + C4 + DEL
A8 = A(8)
A9 = A(9)

KGR = KG
KFEX   = LAMBF*C34
KMIL   = LAMBM*C6
KAMB   = LAMBA*A8
KSSG   = LAMBS*A9
KIMM   = IMAX * T**GM / (IT50**GM + T**GM)

DADT(1)  =  - KA1 * A(1)
DADT(2)  =  KA1 * A(1) - K23 * A(2) ; Central comp Fexi
DADT(3)  =  K23 * A(2) - K34 * A(3) ; M1
DADT(4)  =  K34 * A(3) - K40 * A(4) ; M2
DADT(5)  =  - KA2 * A(5)
DADT(6)  =  KA2 * A(5) - K67 * A(6) + K76 * A(7) - K60 * A(6) ; Central comp MF
DADT(7)  =  K67 * A(6) - K76 * A(7)                           ; Peripheral comp MF
DADT(8)  =   - K80 * A(8)   ; AMB
DADT(9)  =   - K90 * A(9)   ; SSG
DADT(10) =   KGR*A(10) - KMIL*(A(10)-1) - KFEX*(A(10)-1) - KAMB*(A(10)-1) -
KSSG*(A(10)-1)  - KIMM*(A(10)-1) ; Parasite effect compartment
```

$ERROR
```
A1   = A(1)
FEXI = A(2)/S2
M1   = A(3)/S3
M2   = A(4)/S4
```

```
M1M2 = M1 + M2
MF   = A(6)/S6
AMB  = A(8)
SSG  = A(9)
E    = A(10)   ; parasite effect comp

DELL  = 1E-12
IPRED= LOG(E+DELL)
IF(CMT.EQ.10) IPRED = E+DELL
W = 1
IRES=DV-IPRED
IWRES=IRES/W
Y = IPRED * (1+ EPS(1)) + EPS(2)
$THETA
(5330) FIX  ; EBASE
(0.0037) FIX  ; KG
(0.00106) FIX ; LAMB FEXI
(0.001) FIX  ; LAMB MF
(0.0245) FIX ; LAMB AmfoB
(0.0112) FIX ; LAMB SSG
(5) FIX ; GM
(0.037) FIX  ; IMAX
(0, 808)  ; IT50


$OMEGA
 5.93 FIX  ; EBASE
 0 FIX    ;KG
 0.195 FIX  ; LAMB FEXI
 0.18 FIX   ; LAMB MF
 0 FIX  ; LAMB AmfoB
 0 FIX  ; LAMB SSG
 0 FIX  ; GM
 5.84   ; IMAX
 5.17   ; IT50


$SIGMA
 1.02   ; Prop error
 0.5 FIX   ; Add error


$ESTIMATION METHOD=1 INTER MAXEVAL=2000 NOABORT PRINT=10 POSTHOC
NSIG=2 SIGL=6
```
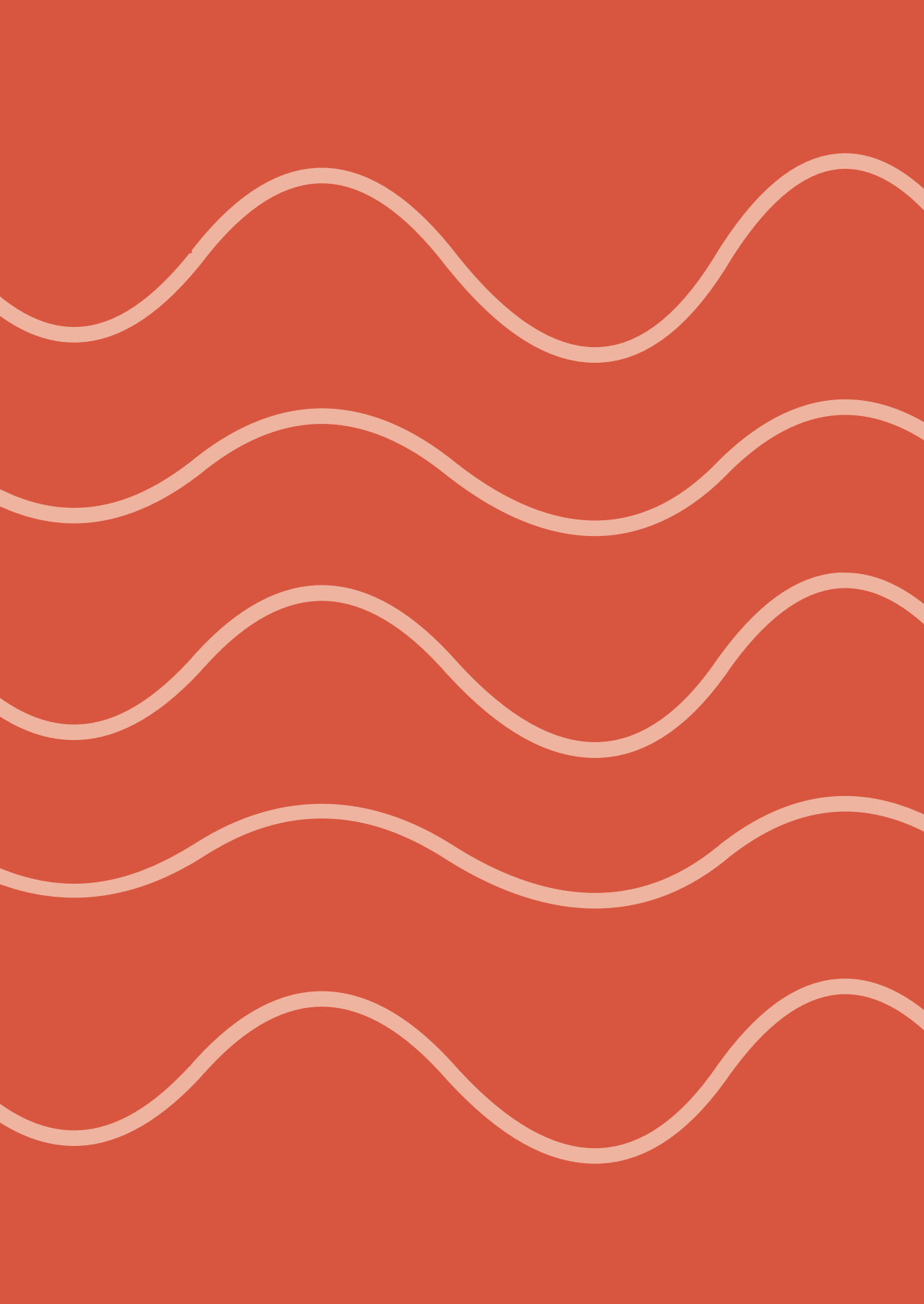
3.2

$COVARIANCE PRINT=E MATRIX=S

$TABLE ID TIME DAY DV CMT AMT EVID CWRES IPRED STUDY ARM
EBASE KG FEXI M1 M2 M1M2 MF AMB SSG E KG KMIL KFEX KAMB KSSG KIMM
C2 C3 C4 C6 C34 A8 A9 CODE AGE SEX WBC0 WBC56 WBC56R ETA1 ETA2 ETA3 ETA4
ETA5 ETA6 ETA7 ETA8 ETA9 CURE RDAY WT HT ONEHEADER NOPRINT FILE=tab10

Chapter 4

Conclusions and perspectives

Conclusions and perspectives

Neglected tropical diseases (NTDs) are a diverse group of 20 diseases, including visceral leishmaniasis (VL), that mostly affect impoverished communities and disproportionately affect children[1]. These diseases cause devastating health, social and economic consequences to more than one billion people. Due to a structural lack of funding, development of interventions to tackle NTDs is barely performed, and, therefore, treatment for most NTDs is suboptimal. Many of the currently available drugs were developed over 50 years ago and many of them exhibit high toxicity. Moreover, treatment efficacy is variable among patient populations and often suboptimal. Adequate dosing is of utmost importance to obtain adequate exposure within the therapeutic range, to minimize the risks for either treatment failure or toxicity. However, dose-optimization studies or studies in specific patient populations particularly affected by NTDs (e.g., pediatric or HIV co-infected patients) have rarely been reported (**chapter 1.1**).

Adequate dosing of patients affected by NTDs comes with many challenges. These patient populations are highly heterogeneous owing to variability in clinical characteristics such as degree of liver impairment, malnourishment, or concomitant underlying infections, which subsequently can lead to large inter-individual variability in various aspects of the absorption, distribution, metabolism and excretion of VL drugs. Moreover, because of limited financial resources, elaborate pharmacokinetic studies are rarely performed, which is further complicated by the remote setting where most patients live, impeding long-term follow-up of patients. These aspects generally lead to heterogeneous and often underpowered pharmacokinetic studies, with only sparse sampling and small sample sizes.

The treatment of VL, a NTD with dramatic health impact, in Eastern Africa comes with all the above-mentioned challenges. To improve VL treatment in Eastern Africa, dosing should be adjusted to Eastern African patients, in order to obtain adequate drug exposure in this vulnerable population. Moreover, VL patients are typically hematologically depleted at start of treatment, resulting in an impaired immune function to combat the VL infection. A better understanding of the parasite dynamics is needed to understand the interplay between growth of *Leishmania* parasites and clinical representation of VL in the patient. In this thesis, we aim to improve VL treatment in Eastern Africa by improved understanding of (i) the pharmacokinetics of anti-leishmanial drugs and (ii) the pharmacodynamics of the *Leishmania* parasite. Key points that can be extracted from this thesis are summarized and further discussed below.

4

Key points

1. To optimize VL treatment in Eastern Africa, population pharmacokinetic-pharmacodynamic studies are crucial for this largely pediatric and highly malnourished patient population

2. Nutritional conditions and severity of VL disease are affecting the bioavailability and disposition of antileishmanial drugs and should be taken into account in current pharmacotherapy but also in the design of future clinical trials.

3. Blood parasite load is a useful and widely implementable biomarker to understand the parasite dynamics and to monitor relapse of disease.

1. To optimize VL treatment in Eastern Africa, population pharmacokinetic-pharmacodynamic studies are crucial for this largely pediatric and highly malnourished patient population

Like most patient populations affected by NTDs, VL patients are typically malnourished to a variable extent, are severely sick, anemic, and often suffer from co-infections, with 50-60% being children under 12 years old. These are all aspects that can lead to heterogeneous drug pharmacokinetics and treatment efficacy. Moreover, the fragility of typical VL patients do not allow extensive blood sampling, as this can be considered too invasive for this vulnerable patient population. Taking into account the heterogeneous patient population and the often limited data, a population-based approach for pharmacokinetic-pharmacodynamic analysis is the only relevant option to obtain the urgently needed pharmacokinetic data to support dosing strategies and decisions. It allows to determine drug exposure in different populations based on very heterogeneous, sparse and limited data. Moreover, it allows to characterize and to explain inter-individual differences in pharmacokinetics by patient characteristics (e.g., body weight, age, and concomitant medication). Once pharmacokinetic-pharmacodynamic models are developed and exposure-response relationships are established, optimal dosing schemes can be designed to reach the desired drug exposure and effect in all patients. This can be achieved by simulations of various dose regimens, taking into account the actual variability in patient characteristics in the target population.

Variability in efficacy of paromomycin and miltefosine monotherapies, or in a combination with other drugs, have been observed previously[2-4]. Higher doses of miltefosine and paromomycin have been used in Eastern Africa compared to those applied in India, but monotherapies of these drugs still result in suboptimal efficacy[2,5]. To assess if the suboptimal efficacy is related to underexposure to the drugs, exposure-response relationships for paromomycin and miltefosine in the Eastern African population need to be established. An exposure-response relationship for miltefosine in Eastern African patients has been characterized before. The VL relapse hazard was related to underexposure to the drug, particularly in children[6]. An adapted dosing regimen for pediatrics based on allometric scaling led to higher miltefosine exposure and efficacy comparable to adults[7,8]. A pharmacokinetic-pharmacodynamic analysis was

used to define a target for miltefosine exposure needed for optimal efficacy[9]. The pharmacokinetics of paromomycin in VL patients has not been studied before. The population pharmacokinetic analysis of paromomycin in this thesis (**chapter 2.1**) revealed important pharmacokinetic differences between Indian and Eastern African patients, and within Eastern African regions[3,4]. The known geographical differences in paromomycin and miltefosine efficacy, and the geographical pharmacokinetic differences studied in this thesis, demonstrate that it is not possible to simply extrapolate VL dosing schemes developed elsewhere, to Eastern African patients. The different exposure-response relationships in Eastern African patients are most likely one of the reasons for the geographical efficacy differences. Exposure-response relationships of paromomycin and miltefosine need to be established in the Eastern African population in order to develop an adequate dosing regimen.

In this thesis, the knowledge on the effective and tolerable doses of paromomycin and miltefosine Eastern African patients[2,4,5,8], as well as the knowledge on the miltefosine exposure-response relationship in Eastern African adults and pediatrics[6,7,9], were integrated to develop a new paromomycin-miltefosine combination regimen in Eastern African VL patients (**chapter 2.2**). This regimen consisted of a higher paromomycin dose for a longer period of time in combination with a longer miltefosine treatment duration of 14 days compared to the 10-day Indian treatment regimen[10]. This led to a paromomycin exposure comparable to the earlier pharmacokinetic study in Eastern African patients (**chapter 2.1 and 2.3**). The proposed allometric dosing of miltefosine was verified in this study and in **chapter 2.3** it was shown that miltefosine exposure in children and adults was comparable to previous studies in Eastern African adult VL patients, confirming adequate miltefosine dosing in this new combination regimen. Moreover, the miltefosine allometric dosing regimen let to similar exposure in pediatrics comparable to adult exposure, confirming the importance of an appropriate body size-based dosing scheme.

2. Nutritional conditions and severity of VL disease are affecting the bioavailability and disposition of antileishmanial drugs

The majority of patients affected by VL are malnourished and suffer from clinical manifestations of the disease, such as fever and hematological depletions such as anemia, neutropenia, or even pancytopenia. These complications lead to physiological alterations that potentially affect drug pharmacokinetics and pharmacodynamics, a mechanism that played a key role in multiple studies described in this thesis. As described in **Key point 1**, variability in paromomycin and miltefosine pharmacokinetics was observed among different VL populations. One of our goals was to find determinants that could explain the variability in pharmacokinetics and pharmacodynamics of antileishmanial drugs.

An extensive systematic review on all pharmacokinetic studies performed in poverty-related infectious diseases (PRDs) (**chapter 1.2**) demonstrated that malnutrition affects

4

the pharmacokinetics for most of the studied drugs. The effects of malnutrition were heterogeneous, due to different definitions and degrees of malnutrition, lack of controlled trials, and lack of non-malnourished comparator groups. However, general trends could be extracted for specific classes of drugs and different types and degrees of malnutrition. Clinically relevant effects were mainly observed in severely malnourished and kwashiorkor patients. In our modeling studies (**chapter 2.1, 2.3, 2.4, and 3.2**), nutritional status of the patient could not be identified as a significant covariate explaining variability in paromomycin or miltefosine pharmacokinetics.

A reason that none of these relationships could be identified could be the lack of variability in nutritional status among the studied patients. In the VL population, the majority of patients is malnourished, which makes it difficult to compare pharmacokinetics to well-nourished patients. Additionally, patients who were severely malnourished or had kwashiorkor were excluded from the clinical trials, which is in particular the population mostly at risk for clinically relevant pharmacokinetic changes that may affect treatment response. Outside the clinical trial setting, these severely malnourished patients do get affected by VL, and especially these highly vulnerable patients require optimal and individualized drug treatment. To optimize treatment in these neglected subpopulations, adequate pharmacokinetic studies are highly needed, including severely malnourished or kwashiorkor patients.

Based on the results of the systematic review (**chapter 1.2**) and the pharmacokinetic properties of paromomycin and miltefosine, it might be expected that for paromomycin, the volume of distribution of this hydrophilic drug will be increased in severely malnourished patients, due to decreased lean body mass and increased extracellular body water. This can potentially lead to decreased peak concentrations (C_{max}) and/or an extended elimination half-life and prolonged exposure. Typical for aminoglycosides, this might lead to lower efficacy (related to C_{max}) and higher risk of toxicity (related to prolonged exposure). Moreover, in kwashiorkor the glomerular filtration rate is decreased, so renal clearance might be decreased as well, the main route of paromomycin elimination. Based on these expectations, we would recommend to use a lower paromomycin dose in severely malnourished patients. In severe malnutrition, miltefosine absorption might be increased due to decreased activity of p-glycoprotein transporters in the gut. Miltefosine is highly protein-bound, with a preference for albumin, and therefore volume of distribution might be increased and miltefosine plasma levels decreased, due to low albumin plasma levels. The resulting effect of the change in plasma concentration on miltefosine efficacy is difficult to predict, as a change in plasma concentration does not necessarily lead to altered exposure at the target sites.

Although the expected effects of severe malnutrition on paromomycin pharmacokinetics were not identified in the paromomycin pharmacokinetic analysis (**chapter 2.1, 2.3 and 2.4**), changes in pharmacokinetics were related to manifestations of VL infection. In **chapter 2.4**, the pharmacokinetics of paromomycin and miltefosine

were compared between VL and post kala-azar dermal leishmaniasis (PKDL) patients to evaluate the effect of disease-associated factors on the pharmacokinetics. Patients were from the same geographical regions, and therefore populations were comparable in terms of demographics such as age and body size, except for disease-associated factors. VL patients are more severely sick and suffer from fever, hematological depletions and worse kidney function, factors that can all influence the pharmacokinetics. On the other hand, PKDL patients are relatively healthy, with hematological values within the normal range at start of treatment. Paromomycin clearance was lower in VL patients compared to PKDL patients, due to worse kidney function in VL patients (**chapter 2.4**). This finding is in line with earlier results. A decrease in paromomycin clearance between the start and end of treatment in VL patients was observed (**chapter 2.1 and 2.3**), and was significantly correlated to recovering plasma neutrophil levels that were measured longitudinally during treatment (**chapter 2.3**). All VL patients were neutropenic at start of treatment, one of the manifestations of the disease, and neutrophil levels did recover during and after treatment. Consequently, this led to a potentially clinically relevant increased paromomycin exposure from start to end of treatment. The decrease in paromomycin clearance has not been observed in PKDL patients, who had overall a better renal function (**chapter 2.4**). For miltefosine, a 60% lower bioavailability during the first week of treatment was only observed in VL patients, due to malabsorption related to patient illness (**chapter 2.4**). These pharmacokinetic differences led to a 26% lower paromomycin and 38% higher miltefosine exposure in PKDL patients compared to VL patients when receiving the same dosing regimen. These results highlight the substantial impact of disease-specific factors on renal function (paromomycin) and the extent of gastrointestinal absorption (miltefosine), and consequently on drug exposure.

Given that dosing regimens for PKDL patients are generally directly extrapolated from those for VL patients, this could lead to exposure in PKDL patients outside the therapeutic range. The lower paromomycin plasma exposure might explain the fewer cases of nephrotoxicity and ototoxicity found in PKDL patients, as toxicity of aminoglycosides is related to the maximum plasma concentration. On the other hand, the increased miltefosine exposure and faster time to reach the miltefosine target concentration (EC_{90}) in PKDL patients might be beneficial for treatment efficacy. However, the target exposure of paromomycin and miltefosine in PKDL patients is still unknown, and exposure-response relationships should be established in PKDL patients in order to optimize paromomycin and miltefosine dosing. PKDL is mainly manifested in the skin, so drug exposure in the skin lesions will be highly relevant for the exposure-response relationship. Therefore, pharmacokinetic-pharmacodynamic studies including pharmacokinetics in plasma as well as the target-site are required to establish exposure-response relationships and optimize dosing in PKDL patients.

Because of lack of knowledge about the exposure-response relationships in severely malnourished patients and PKDL patients, paromomycin and miltefosine dosing is extrapolated from the VL patient population that is generally studied, who are normally

4

nourished or moderately malnourished. The results from this thesis highlights that the extrapolation of dosing regimens should be performed with caution when the pharmacokinetics in the studied population are unknown, not only between geographical regions but also between clinical indications. Based on the theoretical effects of malnutrition on paromomycin and miltefosine pharmacokinetics (**chapter 1.2**), as well as the identified disease-specific effects (**chapter 2.1, 2.3, and 2.4**), a higher paromomycin dose could potentially be considered for PKDL patients, compared to VL patients. Based on the results in this thesis, we would not recommend a dose adjustment for miltefosine in severely malnourished patients or PKDL patients. In Sudanese PKDL patients, a higher miltefosine exposure was observed, which appeared nevertheless well tolerable. Adequate pharmacokinetic studies including severely malnourished and PKDL patients are needed to confirm these recommendations.

3. Blood parasite load is a useful biomarker to understand the parasite dynamics and to monitor relapse of disease

One of the challenges in both VL drug development and individual VL patient management is the early evaluation of treatment response, which has been a focus point in this thesis. After initial cure by the end of treatment, relapses occur in a portion of patients, which is difficult to predict as there are no known determinants for parasite recrudescence and clinical relapse of disease. To be able to early predict relapse later during follow-up, a better understanding of the parasite dynamics is needed, as well as sensitive and specific biomarkers to monitor disease activity during or early after the treatment. Little is known about the parasite dynamics in the host, how and how fast the parasite replicates, how its replication is suppressed or how the parasite is killed by different therapies, and how the host's immune system is involved in successful clearance of the parasite. To characterize the parasite dynamics and to predict patient relapse, sensitive and specific biomarkers that reflect the parasite activity in the host are needed. At the moment, such biomarkers that are easy and safe to use for regular monitoring are not available. The gold standard for VL diagnosis and confirmation of clinical relapse is the quantification of *Leishmania* amastigotes in spleen or bone marrow aspirate smears by microscopy, which is a highly invasive procedure and comes with the risk of severe abdominal bleeding in case of splenic aspiration. For these reasons, assessment of parasites in these infected organs is not suitable for regular monitoring and limited to clinical suspicion of treatment failure or relapse. Quantification of blood parasite load by real-time quantitative polymerase chain reaction (qPCR) might be a patient-friendly and relatively cheap alternative for disease monitoring. Both blood and tissue qPCR parasite loads showed a correlation with microscopy gradings from aspirate smears in Eastern African VL patients, and the absolute blood parasite load on Day 56 turned out to be a highly sensitive predictor of relapse (**chapter 3.1**). In clinical practice, this could be very useful to get an early indication of long-term treatment outcome. A positive blood parasite load (>20

parasites/mL) on Day 56 is a strong indication for clinical relapse, suggesting the need for more frequent monitoring of these patients. The predictiveness of Day 56 parasite load was confirmed by our pharmacokinetic-pharmacodynamic parasite model, which demonstrated that individual predictions of parasite levels on Day 28 and Day 56 correlated with long-term clinical outcome (**chapter 3.2**). Moreover, the parasite dynamics model provided estimates of the clinical *in vivo* replication rate of the parasite, which has not been described before, and could adequately describe the effects of different VL therapies on parasite clearance during the treatment. This is very useful in the understanding of the relationship between parasite clearance and clinical response, as it indicates that sufficient parasite clearance by the treatment is needed to successfully cure the patient, as really low blood parasite loads are already an indication of patient relapse, even when clinical symptoms of VL are not yet present. For example, there were considerably more patients (80-93% of patients) with sufficient parasite clearance at Day 56 (defined as parasite load <20 parasites/mL) in the treatment regimens with a good efficacy of 76-93%, compared to sufficient parasite clearance in only 14% of patients receiving fexinidazole with a really bad efficacy of 15%.

A second insight from these studies was that parasite clearance by the treatment is not solely responsible for relapse of disease. Low parasite levels by the end of treatment are associated with successful cure, but complete parasite eradication has not been reached in most cases. Detectable qPCR blood or tissue parasite loads at end of treatment were observed in patients considered clinically cured, and even during the follow-up (**chapter 3.1**). This suggests that patients can still harbor *Leishmania* parasites at low levels, but nevertheless remain asymptomatic. A positive qPCR in a patient without clinical signs and symptoms of disease could indicate the need for closer follow-up but not directly rescue treatment, as for an immuno-competent patient the immune system is expected to control the infection, conferring long-lasting protection. Moreover, this insight highlights the contribution of the hosts' immune response to suppress or to clear the parasite. After treatment of VL infection, it has been demonstrated that life-long immune suppression is needed[11,12]. Even after years, latent parasites can reactivate once the immune system gets impaired[13], for example in case of HIV infection. In the same way as malnutrition or VL disease symptoms can affect drug pharmacokinetics, these factors can also influence the functionality of the patients' immune system. In order to describe parasite suppression and predict patient relapse, biomarkers that reflect the patient's immune response are studied in this thesis.

In our modeling analysis (**chapter 3.2**), we evaluated different parasite- and host-related factors, such as hematological markers, that could reflect the activity of the host's immune system against the parasite. We were, however, unable to find predictive markers that correlated with parasite response after the treatment, or with

4

clinical outcome. It appeared difficult to find a single marker that reflects the complex mechanism of host-related parasite clearance and suppression of parasite recrudescence during follow-up, even though an advanced method such as a non-linear mixed-effects modeling approach was used to characterize the longitudinal interplay between parasite, drugs and host. Moreover, the sparseness of biomarker data during the follow-up phase might have complicated the identification of potential relationships.

Future perspectives

The studies described in this thesis are a step forward towards improved treatment of VL in Eastern Africa. The pharmacokinetics of paromomycin and miltefosine have been studied in Eastern African patients, with the aim to optimize dosing of these drugs in all Eastern African patients, including pediatric patients. The paromomycin/miltefosine 14-day combination regimen is an improvement over the currently used therapies because of the shorter required hospitalization period and the absence of the highly toxic sodium stibogluconate component (**chapter 2.2**) and resulted in adequate efficacy comparable to the standard of care. At the same time, overall toxicity was low for this new regimen and generally well tolerated. Once this treatment is implemented as standard therapy for VL in Eastern Africa, it will be important to closely monitor these patients, to confirm the outcomes of this Phase III clinical trial. The real-world VL population is more diverse compared to the clinical trial population, where e.g., severely malnourished and severely ill patients are typically excluded. These population differences might impact treatment efficacy and/or the pharmacokinetics. To verify if drug exposure is adequate in the whole VL population, the pharmacokinetics should be analyzed once this treatment is being used.

To further optimize the use of this new combination regimen, e.g., treatment duration might even be shortened, dosing might be further optimized/individualized, and other oral companion drugs could be used to replace intramuscular paromomycin in the future. Shorter treatment duration of paromomycin will lead to a shorter hospitalization period, saving costs and improving convenience for the patient. Shorter treatment duration of miltefosine might also be an option, however, given the slow absorption and long duration before effective concentrations are reached, a loading dose regimen might be required, possibly combined with a gastroprotective agent to avoid dose-limiting gastro-intestinal side effects. A food-effect study might be useful in this context, as it is currently unknown whether higher doses of miltefosine would be tolerable together with a certain type or amount of food.

This thesis sheds a very first light on the clinical *in vivo* parasite dynamics during treatment in VL and the relationship with clinical manifestations of the disease. Moreover, factors that affect parasite dynamics, the patient's immune response and

clinical outcome were studied, with the aim to identify early biomarkers or predictors that correlate with clinical outcome. This might be particularly useful to predict long term treatment response already during or early after the treatment in clinical trials with new dosing regimens or new combination therapies, to get an early indication of the long-term response to the treatment. More regular monitoring during treatment and follow-up can potentially further improve the understanding of parasite dynamics and the correlation with biomarkers. For example, it was not possible to identify biomarkers reflecting the hosts' capacity to suppress parasite recrudescence (**chapter 3.2**), which might be very helpful in predicting VL relapse. To identify these biomarkers in the future, longitudinal monitoring of markers that could reflect the patients' immune function should be performed in novel clinical trials, such as frequent measurement of lymphocytes, neutrophils and albumin. These hematological markers are known to be related to severity of VL disease, and lymphocytes and neutrophils are also directly related to the immune response against *Leishmania* parasites.

Blood parasite load on Day 28 after start of treatment showed to be a sensitive and specific biomarker for clinical outcome, which is an improvement compared to the standard determination of response 6 months after treatment. Although this biomarker could distinguish long-term outcome between treatment regimens with different efficacy rates, it could not correctly predict relapse in every single patient, and could therefore not yet replace the standard diagnostic of parasite assessment in spleen aspirates to define VL cure. The correlation of blood parasite load by qPCR with clinical outcome could be improved by improving the logistics for sample extraction and preparation, and by improving the qPCR extraction method, as a substantial portion of qPCR samples and parasite load measurements were missing (**chapter 3.1**). With the increase in molecular biology capacity in areas endemic for VL, we expect that it would be feasible to put this tool into practice in clinical trial settings, and that technical issues with stability of kDNA and reproducibility of sample extraction would be reduced. Once molecular biology tools in blood such as qPCR are improved, this method might even replace the current invasive tissue aspiration procedures for parasitological diagnosis and long-term treatment monitoring. This patient-friendly alternative of blood sampling can be performed more frequently, which promotes frequent monitoring of patients on a large scale in clinical trials.

4

References

1. World Health Organization. Neglected tropical diseases (NTDs) [Internet]. 2022 [cited 2022 Nov 11]. Available from: https://www.who.int/health-topics/neglected-tropical-diseases#tab=tab_1
2. Wasunna M, Njenga S, Balasegaram M, Alexander N, Omollo R, Edwards T, et al. Efficacy and Safety of AmBisome in Combination with Sodium Stibogluconate or Miltefosine and Miltefosine Monotherapy for African Visceral Leishmaniasis: Phase II Randomized Trial. PLoS Negl Trop Dis. 2016;10(9):e0004880.
3. Hailu A, Musa A, Wasunna M, Balasegaram M, Yifru S, Mengistu G, et al. Geographical variation in the response of visceral leishmaniasis to paromomycin in East Africa: A multicentre, open-label, randomized trial. PLoS Negl Trop Dis. 2010;4(10):e709.
4. Musa AM, Younis B, Fadlalla A, Royce C, Balasegaram M, Wasunna M, et al. Paromomycin for the treatment of visceral leishmaniasis in Sudan: A randomized, open-label, dose-finding study. PLoS Negl Trop Dis. 2010;4(10):4–10.
5. Musa A, Khalil E, Hailu A, Olobo J, Balasegaram M, Omollo R, et al. Sodium stibogluconate (SSG) & paromomycin combination compared to SSG for visceral leishmaniasis in East Africa: A randomised controlled trial. PLoS Negl Trop Dis. 2012;6(6):e1674.
6. Dorlo TPC, Rijal S, Ostyn B, de Vries PJ, Singh R, Bhattarai N, et al. Failure of miltefosine in visceral leishmaniasis is associated with low drug exposure. J Infect Dis. 2014;210(1):146–153.
7. Palic S, Kip AE, Beijnen JH, Mbui J, Musa A, Solomos A, et al. Characterizing the non-linear pharmacokinetics of miltefosine in paediatric visceral leishmaniasis patients from Eastern Africa. J Antimicrob Chemother. 2020;75:3260–3268.
8. Mbui J, Olobo J, Omollo R, Solomos A, Kip AE, Kirigi G, et al. Pharmacokinetics, Safety, and Efficacy of an Allometric Miltefosine Regimen for the Treatment of Visceral Leishmaniasis in Eastern African Children: An Open-label, Phase II Clinical Trial. Clin Infect Dis. 2019;68(9):1530-1538.
9. Dorlo TPC, Kip AE, Younis BM, Ellis SJ, Alves F, Beijnen JH, et al. Visceral leishmaniasis relapse hazard is linked to reduced miltefosine exposure in patients from Eastern Africa: A population pharmacokinetic/pharmacodynamic study. Journal of Antimicrobial Chemotherapy. 2017;72(11): 3131-3140.
10. Sundar S, Sinha PK, Rai M, Verma DK, Nawin K, Alam S, et al. Comparison of short-course multidrug treatment with standard therapy for visceral leishmaniasis in India: An open-label, non-inferiority, randomised controlled trial. Lancet. 2011;377(9764):477–486.
11. Gorski S, Collin SM, Ritmeijer K, Keus K, Gatluak F, Mueller M, et al. Visceral leishmaniasis relapse in Southern Sudan (1999-2007): A retrospective study of risk factors and trends. PLoS Negl Trop Dis. 2010; 4(6):e705.
12. Leta S, Dao THT, Mesele F, Alemayehu G. Visceral Leishmaniasis in Ethiopia: An Evolving Disease. PLoS One. 2014;8(9):e3131.
13. Murray HW, Hariprashad J, Fichtl RE, Murray HW. Models of Relapse of Experimental Visceral Leishmaniasis. J Infect Dis. 1996;173:1041–1044.
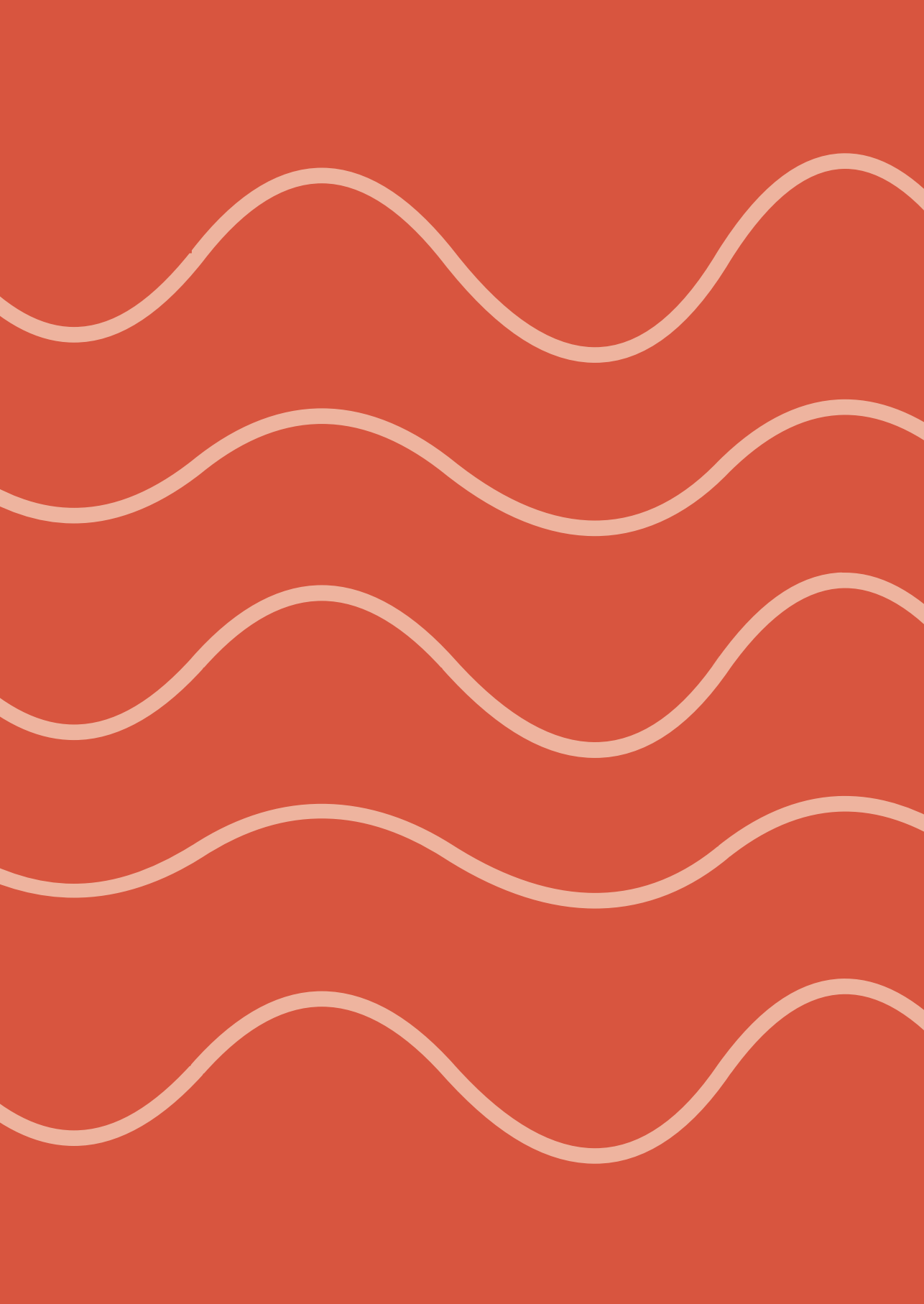
Appendix

Summary

Chapter 1

Neglected tropical diseases (NTDs) are a group of 20 diseases, including visceral leishmaniasis (VL), that mostly affect impoverished communities and disproportionately affect children. Due to a structural lack of funding, development of interventions to tackle NTDs is barely performed, and, therefore, treatment for most NTDs is suboptimal. Many of the currently available drugs were developed over 50 years ago and many of them exhibit high toxicity. Moreover, treatment efficacy is variable among patient populations and often suboptimal. Adequate dosing is of utmost importance to obtain adequate drug exposure within the therapeutic range, to minimize the risks for either treatment failure or toxicity. To achieve adequate drug exposure in all patients, pharmacokinetic studies are needed in patient populations affected by NTDs, preferably by applying population-based modeling and simulation techniques to enable the design of improved dosing regimens in specific patient populations and to optimally use the often limited resources and available data. In **chapter 1.1** we discovered that for most NTDs, adequate pharmacokinetic studies are lacking. In particular population-based pharmacokinetic dose-optimization studies or studies in patient populations particularly affected by NTDs (e.g., pediatric or HIV co-infected patients) have rarely been reported, while these studies can make a substantial improvement in treatment optimalization for NTDs.

NTD patient populations are highly heterogeneous owing to variability in clinical characteristics such as degree of liver impairment, malnourishment, or concomitant underlying infections, which subsequently can lead to large inter-individual variability in various aspects of the absorption, distribution, metabolism and excretion of NTD drugs. In **chapter 1.2** we demonstrated that malnutrition affects the pharmacokinetics for most of the studied drugs used to treat poverty-related diseases (PRDs). Although the effects of malnutrition were heterogeneous, general trends could be extracted for specific classes of drugs and different types and degrees of malnutrition. Clinically relevant effects were mainly observed in severely malnourished and kwashiorkor patients. As a significant portion of the patients affected by PRDs are malnourished, the effects of malnourishment on pharmacokinetics should be taken into account when dosing regimens are extrapolated to these populations, and clinical pharmacokinetic studies with PRD drugs should preferably include (severely) malnourished patients.

Chapter 2

VL, one of the NTDs, is a devastating disease caused by the *Leishmania* parasite that affects the poorest of the poor, with the highest burden in Eastern Africa, mainly affecting children. Current treatment for VL is far from optimal, since it entails

hospitalization during the whole treatment period with painful injections twice daily, and the risk of potentially life-threatening antimony-related toxicities. Paromomycin and miltefosine are favorable treatment options because of their relatively good safety profile and suitability for use in remote areas. However, treatment efficacy of these drugs is suboptimal in Eastern Africa, and efficacy is highly variable among patient populations. To assess if the suboptimal efficacy is related to underexposure to the drugs, the pharmacokinetics of paromomycin and miltefosine in the Eastern African population was studied with the aim to establish exposure-response relationships. In **chapter 2.1**, the pharmacokinetics of paromomycin was characterized in Eastern African and Indian VL patients for the first time, and revealed substantial variability in paromomycin pharmacokinetics among geographical regions. However, the lower paromomycin efficacy in Eastern Africa compared to India could not be related to paromomycin exposure, and thus the exposure-response relationship of paromomycin seem to be different in Eastern Africa, which is also the case for miltefosine.

The knowledge on geographical efficacy differences and pharmacokinetics has been used to develop an adapted 14-day paromomycin-miltefosine regimen. This new combination regimen has been studied in Eastern African VL patients (**chapter 2.2**), and demonstrated adequate efficacy comparable to the current standard of care. With 1 less injection each day, reduced treatment duration, and no risk of SSG-associated life-threatening cardiotoxicity, this 14-day paromomycin-miltefosine combination is a more patient-friendly alternative for pediatric and adult VL patients in Eastern Africa. In **chapter 2.3**, the pharmacokinetics of paromomycin and miltefosine were studied in these patients using a population-based approach. The pharmacokinetics of both drugs were in accordance with earlier pharmacokinetic studies, and miltefosine exposure and target attainment was adequate in both adults and pediatrics, a specific research question as children have been underexposed to miltefosine before. This confirms the improvement of the miltefosine allometric dosing regimen over the conventional dosing regimen.

In **chapter 2.4**, the pharmacokinetics of paromomycin and miltefosine was compared between post kala-azar dermal leishmaniasis (PKDL) patients and VL patients, and revealed substantial differences in pharmacokinetics between the two clinical representations of the disease. These findings highlight the impact of disease-associated physiological alterations on the pharmacokinetics of antileishmanial drugs, with potentially clinically relevant effects on drug exposure. Given that dosing regimens for PKDL patients are generally directly extrapolated from those for VL patients, this could lead to exposure in PKDL patients outside the therapeutic range. This study demonstrates that dosing regimens could not be directly extrapolated between different disease populations, and pharmacokinetic studies in PKDL patients should be performed to develop adequate dosing regimens for these patients.

Chapter 3

One of the challenges in both VL drug development and individual VL patient management is the early evaluation of treatment response. Although most VL patients seem initially cured by the end of treatment, relapses occur in a fraction of patients, which is a particularly long-term event that can occur within 12 months or even longer after treatment and is difficult to predict. To be able to early predict relapse later during follow-up, a better understanding of the parasite dynamics is needed, as well as sensitive and specific biomarkers to monitor disease activity during or early after the treatment. At the moment, such biomarkers that are easy and safe to use for regular monitoring are not available. In this chapter, we studied the use of blood parasite load quantified by real-time quantitative polymerase chain reaction (qPCR) as a biomarker to reflect the parasite activity in the host, which might be a patient-friendly and relatively cheap alternative for disease monitoring. In **chapter 3.1**, we demonstrated that both blood and tissue qPCR parasite loads showed a correlation with microscopy gradings from aspirate smears (the gold standard for disease monitoring) in Eastern African VL patients, and the blood parasite load on day 56 after start of treatment turned out to be a highly sensitive predictor of relapse, which was confirmed by the pharmacokinetic-pharmacodynamic parasite model described in **chapter 3.2.** In clinical practice, this could be very useful to get an early indication of long-term treatment outcome. Moreover, the model for parasite dynamics during and after treatment provided estimates of the clinical *in vivo* replication rate of the parasite, which has not been described before, and could adequately describe the effects of different VL therapies on parasite clearance during the treatment. This is very useful in the understanding of the relationship between parasite clearance and clinical response. The model demonstrated that sufficient parasite clearance by the treatment is needed to successfully cure the patient, but also a proper functioning immune system of the host to control the infection after treatment, conferring long-lasting protection.

In conclusion, the pharmacokinetics of paromomycin and miltefosine was studied in Eastern African VL patients, and provided insight in the exposure-response relationships of the drugs. This knowledge was used to develop an adapted paromomycin-miltefosine combination regimen in Eastern African VL patients, resulting in satisfactory cure rates and desired drug exposure levels in both pediatric and adult patients. Moreover, the impact of malnutrition and severity of disease on drug pharmacokinetics and exposure was studied, and substantial and potentially clinically relevant effects were discovered. Secondly, the *Leishmania* parasite dynamics has been characterized in VL patients and the potential use of blood parasite load as an early biomarker to predict clinical relapse of disease has been studied. The knowledge gained in this thesis is a step forward to optimization, individualization and monitoring of VL treatment in Eastern Africa.

A

Nederlandse samenvatting

Hoofdstuk 1

Momenteel worden er twintig ziekten beschouwd als verwaarloosde tropische ziekten of 'Neglected Tropical Diseases (NTD's)', waaronder viscerale leishmaniasis (VL). Deze ziekten komen voornamelijk voor in lage- en middeninkomenslanden en treffen vooral kinderen. Vaak zijn er geen goede behandelingen beschikbaar en door een structureel tekort aan financiering worden er ook nauwelijks nieuwe geneesmiddelen ontwikkeld ter behandeling van deze NTD's. Veel van de gebruikte middelen zijn al meer dan 50 jaar geleden ontwikkeld en vertonen vaak ernstige toxiciteit. Daarbij is de effectiviteit van deze middelen zeer variabel tussen patiëntenpopulaties en vaak niet toereikend. Om het risico op zowel toxiciteit als onvoldoende effectiviteit te minimaliseren is een juiste blootstelling van het geneesmiddel in de patiënt belangrijk en hiervoor is een juiste dosering nodig. Om een juiste blootstelling in alle patiënten te bereiken zijn farmacokinetische (PK) studies nodig, waarbij de absorptie, verdeling, metabolisme en excretie van geneesmiddelen in kaart kunnen worden gebracht. Door gebruik te maken van modellering van de hele populatie kan zoveel mogelijk informatie uit de vaak beperkte data gehaald worden en kunnen optimale doseerschema's ontwikkeld worden voor verschillende patiëntenpopulaties. **Hoofdstuk 1.1** liet zien dat voor de meeste NTD's goede PK studies missen. Vooral populatie PK studies in typische NTD patiëntenpopulaties zoals kinderen of patiënten met HIV-coïnfectie zijn nauwelijks gerapporteerd, terwijl deze studies juist substantieel de behandeling van NTD's kunnen verbeteren.

NTD patiënten verschillen sterk in klinische eigenschappen zoals de mate van leverschade, ondervoeding, of andere onderliggende infecties. Dit kan leiden tot grote verschillen in diverse aspecten van de PK van NTD geneesmiddelen. In **hoofdstuk 1.2** werd aangetoond dat ondervoeding de PK beïnvloedt van de meeste geneesmiddelen voor aan armoede-gerelateerde infectieziekten of 'Poverty-Related Diseases (PRD's)'. Hoewel de effecten van ondervoeding erg verschillend waren, konden er trends ontdekt worden voor bepaalde geneesmiddelgroepen en voor verschillende typen ondervoeding. Klinisch relevante effecten werden vooral gevonden in ernstig ondervoede patiënten. Omdat een groot deel van de PRD populatie ondervoed is, zou hier rekening mee gehouden moeten worden bij het extrapoleren van doseerschema's naar deze populaties en bij voorkeur omvatten PK studies van PRD geneesmiddelen ook ondervoede patiënten om beter de PRD patiëntenpopulatie te reflecteren.

Hoofdstuk 2

VL, een van deze NTD's, is een levensbedreigende ziekte die wordt veroorzaakt door de *Leishmania* parasiet. Besmettingen komen het meest voor in Oost Afrika, waar het

A

vooral armen en kinderen treft. De behandeling die momenteel gebruikt wordt, is verre van optimaal, omdat ziekenhuisopname gedurende de hele 17-daagse behandeling nodig is, met dagelijks twee pijnlijke injecties en het risico op ernstige antimoon-gerelateerde toxiciteit. Paromomycine en miltefosine zijn mogelijk goede behandelopties omdat ze relatief veilig zijn en makkelijker in gebruik in afgelegen gebieden waar VL het meest voorkomt. De effectiviteit van de standaard doseringsregimes van deze middelen is echter ontoereikend in Oost Afrika en verschilt sterk tussen geografische gebieden. Om te achterhalen of de lagere effectiviteit in Oost Afrika gerelateerd is aan een te lage blootstelling van de geneesmiddelen is de PK van paromomycine en miltefosine in Oost Afrikaanse patiënten onderzocht. In **hoofdstuk 2.1** is voor het eerst de PK van paromomycine in Oost Afrikaanse en Indiase patiënten in kaart gebracht, en toonde aanzienlijke geografische verschillen in PK. Deze verschillen in PK konden echter niet gerelateerd worden aan de verschillen in effectiviteit, wat aantoont dat de relatie tussen blootstelling en effectiviteit voor deze middelen anders is in Oost Afrika, wat ook het geval is voor miltefosine.

Deze kennis over geografische verschillen in effectiviteit en PK is gebruikt om een 14-daagse paromomycine-miltefosine combinatiebehandeling te ontwikkelen in Oost Afrikaanse patiënten. Deze nieuwe combinatiebehandeling had een vergelijkbare effectiviteit als de standaardbehandeling (**hoofdstuk 2.2**). Deze behandeling heeft daarbij een kortere behandelduur met dagelijks één injectie minder en heeft geen risico op ernstige antimoon-geassocieerde toxiciteit. Daarom is deze behandeling een patiëntvriendelijker alternatief voor kinderen en volwassenen met VL in Oost Afrika. In **hoofdstuk 2.3** is de PK van paromomycine en miltefosine in deze combinatie-behandeling onderzocht met behulp van populatie modellering. De PK van beide middelen was vergelijkbaarmet eerdere PK studies en de miltefosine blootstelling bleek adequaat in zowel kinderen als volwassenen. Dit laatste was een specifieke onderzoeksvraag omdat kinderen in eerdere studies een te lage miltefosine blootstelling bleken te hebben. Dit bevestigt de verbetering van het nieuwe miltefosine doseerschema in kinderen gebaseerd op allometrische schaling ten opzichte van de eerdere standaarddosering op basis van mg/kg.

In **hoofdstuk 2.4** is de PK van paromomycine en miltefosine vergeleken tussen post kala-azar dermal leishmaniasis (PKDL) patiënten, waarbij de *Leishmania* parasiet laesies in de huid veroorzaakt, en VL patiënten, een systemische infectie van de parasiet waarbij onder andere de lever en milt worden aangetast. De studie toonde substantiële verschillen in PK tussen deze twee populaties. Deze resultaten laten de impact zien van ziekte-geassocieerde fysische veranderingen op de PK van anti-leishmaniale middelen en de mogelijk klinische relevante veranderingen in blootstelling van de middelen. Aangezien doseerschema's voor PKDL patiënten op dit moment gebaseerd zijn op doseringen gebruikt in VL patiënten kan dit tot blootstelling in PKDL patiënten leiden

buiten de therapeutische breedte. Deze studie laat zien dat doseerschema's niet direct geëxtrapoleerd kunnen worden tussen verschillende ziekten en dat PK studies in PKDL patiënten nodig zijn om juiste behandelschema's te ontwikkelen voor deze patiënten.

Hoofdstuk 3

Een van de uitdagingen in zowel VL geneesmiddelontwikkeling als in de behandeling van individuele VL patiënten is het gebrek aan indicatoren voor de lange-termijn behandeluitkomst. Hoewel de meeste VL patiënten genezen lijken aan het eind van de behandeling, komt bij een deel van de patiënten terugval van de ziekte voor. Deze terugval kan nog tot 12 maanden of langer na VL behandeling optreden en is moeilijk te voorspellen. Om VL terugval vroegtijdig te kunnen voorspellen is een beter begrip van de parasieten dynamiek nodig, maar ook sensitieve en specifieke biomarkers om ziekteactiviteit te monitoren tijdens en kort na de behandeling. Op dit moment zijn zulke biomarkers die makkelijk en veilig in gebruik zijn niet beschikbaar. In dit hoofdstuk werd onderzocht of de concentratie kinetoplast DNA van de parasieten in het bloed, gekwantificeerd door middel van 'real-time quantitative polymerase chain reaction (qPCR)', een geschikte biomarker is voor de parasietenactiviteit in de patiënt. Dit zou een patiëntvriendelijk en relatief goedkoop alternatief kunnen zijn voor het monitoren van de ziekteactiviteit. In **hoofdstuk 3.1** werd aangetoond dat de parasietenconcentraties in bloed gecorreleerd waren met microscopiescores van de geïnfecteerde weefsels, de huidige gouden standaard voor het monitoren van ziekteactiviteit. De parasietenconcentratie in bloed op dag 56 na start van de behandeling bleek de meest sensitieve voorspeller voor VL terugval en dit werd bevestigd door het parasieten model beschreven in **hoofdstuk 3.2**. In de klinische praktijk zou dit erg nuttig kunnen zijn om een vroege indicatie te krijgen van de behandeluitkomst op de lange termijn. Daarbij geeft dit model voor de dynamiek van de parasieten tijdens en na de behandeling voor het eerst een schatting van de groeisnelheid van de parasiet in de patiënt, en kan het model de effecten beschrijven van de verschillende VL behandelingen op de parasietenklaring. Dit is erg nuttig voor het begrijpen van de relatie tussen parasietenklaring en klinische uitkomst. Het model toonde aan dat voldoende parasietenklaring tijdens de behandeling nodig is voor genezing van de patiënt, maar dat daarnaast ook een goed functionerend immuunsysteem van de patiënt nodig is om de infectie na de behandeling onder controle te houden.

In dit proefschrift is de farmacokinetiek van paromomycine en miltefosine onderzocht in VL patiënten uit Oost Afrika, wat inzicht heeft gegeven in de relatie tussen blootstelling en effectiviteit van deze geneesmiddelen in deze populatie. Deze kennis is gebruikt om een nieuwe paromomycine-miltefosine combinatietherapie te ontwikkelen voor Oost Afrikaanse VL patiënten, wat resulteerde in een adequate effectiviteit en een juiste blootstelling van de geneesmiddelen in zowel kinderen als volwassenen. Daarbij

A

is de invloed van ondervoeding en mate van ziekte op de farmacokinetiek en blootstelling van deze geneesmiddelen onderzocht, wat resulteerde in substantiële en mogelijk klinisch relevante verschillen. Daarnaast is de *Leishmania* parasietendynamiek bestudeerd en de voorspellende waarde van parasietenconcentraties in het bloed om vroegtijdig de lange-termijnuitkomst van VL behandelingen te voorspellen. De opgedane kennis van de studies beschreven in dit proefschrift draagt bij aan optimalisatie, individualisatie en het monitoren van VL behandelingen in Oost Afrika.

Authorship contribution

Preface
Author's contribution: The general research question and its general scientific and social perspective were proposed by my copromotor. I delineated the research objectives, described how it fits in the current scientific literature and described its potential social impact. I wrote the first draft of the preface and implemented the input and feedback from my supervisory team.

Chapter 1.1 Lack of Clinical Pharmacokinetic Studies to Optimize the Treatment of Neglected Tropical Diseases: A Systematic Review
Author's contribution: I contributed to conception and design of the review, performed the literature survey, carried out the data extraction, and drafted an initial version of the manuscript.

Chapter 1.2 Influence of Malnutrition on the Pharmacokinetics of Drugs Used in the Treatment of Poverty-Related Diseases: A Systematic Review
Author's contribution: I contributed to conception and design of the review, collected and summarized the study data, and contributed to the interpretation of the study results. I wrote the first version of the manuscript and implemented the contribution of the co-authors and external reviewers up to final publication.

Chapter 2.1 Geographical Variability in Paromomycin Pharmacokinetics Does Not Explain Efficacy Differences between Eastern African and Indian Visceral Leishmaniasis Patients
Author's contribution: I contributed to conception and design of the study, performed the data analysis, and contributed to the interpretation of the study results. I wrote the first version of the manuscript and implemented the contribution of the co-authors and external reviewers up to final publication.

Chapter 2.2 Paromomycin and Miltefosine Combination as an Alternative to Treat Patients with Visceral Leishmaniasis in Eastern Africa: A Randomized, Controlled, Multicountry Trial
Author's contribution: I analyzed the pharmacokinetic study data by a non-compartmental analysis. I wrote a comprehensive PK report and contributed to the summary of the main PK results described in this manuscript.

A

Chapter 2.3 Population pharmacokinetics of a combination of miltefosine and paromomycin in Eastern African children and adults with visceral leishmaniasis
Author's contribution: I contributed to conception and design of the study, performed the data analysis, and contributed to the interpretation of the study results. I wrote the first version of the manuscript and implemented the contribution of the co-authors.

Chapter 2.4 Disease-specific differences in pharmacokinetics of paromomycin and miltefosine between post-kala-azar dermal leishmaniasis and visceral leishmaniasis patients in Eastern Africa
Author's contribution: I collected and processed the data of the VL clinical trial. I contributed to the interpretation of the study results, and contributed to writing and revising the manuscript.

Chapter 3.1 Blood Parasite Load as an Early Marker to Predict Treatment Response in Visceral Leishmaniasis in Eastern Africa
Author's contribution: I contributed to conception and design of the study, performed the data analysis, and contributed to the interpretation of the study results. I wrote the first version of the manuscript and implemented the contribution of the co-authors and external reviewers up to final publication.

Chapter 3.2 *Leishmania* blood parasite dynamics during and after treatment of visceral leishmaniasis in Eastern Africa: a pharmacokinetic-pharmacodynamic model
Author's contribution: I contributed to conception and design of the study, performed the data analysis, and contributed to the interpretation of the study results. I wrote the first version of the manuscript and implemented the contribution of the co-authors.

Chapter 4 Conclusions and perspectives
After a discussion with my supervisors on the subjects and arguments to be included, I wrote the first draft of the conclusions and perspectives and implemented the input and feedback from my supervisory team.

List of publications

Admiraal R, Nierkens S, de Witte MA, Petersen EJ, Fleurke GJ, **Verrest L**, Belitser SV, Bredius RGM, Raymakers RAP, Knibbe CAJ, Minnema MC, van Kesteren C, Kuball J, Boelens JJ. Association between anti-thymocyte globulin exposure and survival outcomes in adult unrelated haemopoietic cell transplantation: a multicentre, retrospective, pharmacodynamic cohort analysis. Lancet Haematol. 2017 Apr;4(4):e183-e191.

Verrest L, Dorlo TPC. Lack of Clinical Pharmacokinetic Studies to Optimize the Treatment of Neglected Tropical Diseases: A Systematic Review. Clin Pharmacokinet. 2017 Jun;56(6):583-606.

Verrest L, Wilthagen EA, Beijnen JH, Huitema ADR, Dorlo TPC. Influence of Malnutrition on the Pharmacokinetics of Drugs Used in the Treatment of Poverty-Related Diseases: A Systematic Review. Clin Pharmacokinet. 2021 Sep;60(9):1149-1169.

Verrest L, Kip AE, Musa AM, Schoone GJ, Schallig HDFH, Mbui J, Khalil EAG, Younis BM, Olobo J, Were L, Kimutai R, Monnerat S, Cruz I, Wasunna M, Alves F, Dorlo TPC. Blood Parasite Load as an Early Marker to Predict Treatment Response in Visceral Leishmaniasis in Eastern Africa. Clin Infect Dis. 2021 Sep 7;73(5):775-782.

Verrest L, Wasunna M, Kokwaro G, Aman R, Musa AM, Khalil EAG, Mudawi M, Younis BM, Hailu A, Hurissa Z, Hailu W, Tesfaye S, Makonnen E, Mekonnen Y, Huitema ADR, Beijnen JH, Kshirsagar SA, Chakravarty J, Rai M, Sundar S, Alves F, Dorlo TPC. Geographical Variability in Paromomycin Pharmacokinetics Does Not Explain Efficacy Differences between Eastern African and Indian Visceral Leishmaniasis Patients. Clin Pharmacokinet. 2021 Nov;60(11):1463-1473.

Musa AM, Mbui J, Mohammed R, Olobo J, Ritmeijer K, Alcoba G, Muthoni Ouattara G, Egondi T, Nakanwagi P, Omollo T, Wasunna M, **Verrest L**, Dorlo TPC, Musa Younis B, Nour A, Taha Ahmed Elmukashfi E, Ismail Omer Haroun A, Khalil EAG, Njenga S, Fikre H, Mekonnen T, Mersha D, Sisay K, Sagaki P, Alvar J, Solomos A, Alves F. Paromomycin and Miltefosine Combination as an Alternative to Treat Patients with Visceral Leishmaniasis in Eastern Africa: A Randomized, Controlled, Multicountry Trial. Clin Infect Dis. 2022 Sep 27:ciac643. Epub ahead of print.

A

Author affiliations

G. Alcoba	Médecins sans Frontières, OCG, Geneva, Switzerland
J. Alvar	Drugs for Neglected Diseases Initiative, Geneva, Switzerland
F. Alves	Drugs for Neglected Diseases Initiative, Geneva, Switzerland
R. Aman	African Centre for Clinical Trials, Nairobi, Kenya
J.H. Beijnen	Department of Pharmacy & Pharmacology, Antoni van Leeuwenhoek Hospital/Netherlands Cancer Institute, Amsterdam, the Netherlands
J. Chakravarty	Institute of Medical Sciences, Banaras Hindu University, Varanasi, Uttar Pradesh, India
W. Chu	Department of Pharmacy & Pharmacology, Antoni van Leeuwenhoek Hospital/Netherlands Cancer Institute, Amsterdam, the Netherlands
I. Cruz	Foundation for Innovative New Diagnostics, Geneva, Switzerland; National School of Public Health, Instituto de Salud Carlos III, Madrid, Spain
T.P.C. Dorlo	Department of Pharmacy & Pharmacology, Antoni van Leeuwenhoek Hospital/Netherlands Cancer Institute, Amsterdam, the Netherlands; Department of Pharmacy, Uppsala University, Uppsala, Sweden
T. Egondi	Drugs for Neglected Diseases Initiative, Nairobi, Kenya
T.A. Elmukashfi	Institute of Endemic Diseases, University of Khartoum, Khartoum, Sudan
H. Fikre	Leishmaniasis Research and Treatment Center, University of Gondar, Gondar, Ethiopia
A. Hailu	College of Health Sciences, Addis Ababa University, Addis Ababa, Ethiopia
W. Hailu	College of Medicine and Health Sciences, University of Gondar, Gondar, Ethiopia
A.I.O. Haroun	Institute of Endemic Diseases, University of Khartoum, Khartoum, Sudan
A.D.R. Huitema	Department of Pharmacy & Pharmacology, Antoni van Leeuwenhoek Hospital/Netherlands Cancer Institute, Amsterdam, the Netherlands; Department of Clinical Pharmacy, University Medical Center Utrecht, Utrecht University, the Netherlands; Department of Pharmacology, Princess Máxima Center for Pediatric Oncology, Utrecht, The Netherlands
Z. Hurissa	College of Health Sciences, Arsi University, Asella, Ethiopia
E.A.G. Khalil	Institute of Endemic Diseases, University of Khartoum, Khartoum, Sudan
R. Kimutai	Centre for Clinical Research, Kenya Medical Research Institute, Nairobi, Kenya; Drugs for Neglected Diseases initiative Africa, Nairobi, Kenya

A

A.E. Kip	Department of Pharmacy & Pharmacology, Antoni van Leeuwenhoek Hospital/Netherlands Cancer Institute, Amsterdam, the Netherlands
G. Kokwaro	KEMRI Wellcome Trust Programme, Nairobi, Kenya; African Centre for Clinical Trials, Nairobi, Kenya
S.A. Kshirsagar	Department of Medicine, Stanford University Medical Center, Stanford, CA, USA
E. Makonnen	College of Health Sciences, Addis Ababa University, Addis Ababa, Ethiopia
J. Mbui	Centre for Clinical Research, Kenya Medical Research Institute, Nairobi, Kenya
T. Mekonnen	Leishmaniasis Research and Treatment Center, University of Gondar, Gondar, Ethiopia
Y. Mekonnen	College of Natural and Computational Sciences, Addis Ababa University, Addis Ababa, Ethiopia
D. Mersha	Médecins sans Frontières, Abdurafi, Ethiopia
R. Mohammed	Leishmaniasis Research and Treatment Center, University of Gondar, Gondar, Ethiopia
S. Monnerat	Drugs for Neglected Diseases Initiative, Geneva, Switzerland
M. Mudawi	Institute of Endemic Diseases, University of Khartoum, Khartoum, Sudan; Department of Pharmacology and Toxicology, Faculty of Pharmacy, Northern Border University, Arar, Saudi Arabia
A.M. Musa	Institute of Endemic Diseases, University of Khartoum, Khartoum, Sudan
P. Nakanwagi	Drugs for Neglected Diseases Initiative, Nairobi, Kenya
S. Njenga	Centre for Clinical Research, Kenya Medical Research Institute, Nairobi, Kenya
A. Nour	Institute of Endemic Diseases, University of Khartoum, Khartoum, Sudan
J. Olobo	Department of Immunology and Molecular Biology, Leishmaniasis Unit, College of Health Sciences, Makerere University, Kampala, Uganda
T. Omollo	Drugs for Neglected Diseases Initiative, Nairobi, Kenya
G.M. Ouattara	Drugs for Neglected Diseases Initiative, Nairobi, Kenya
M. Rai	Institute of Medical Sciences, Banaras Hindu University, Varanasi, Uttar Pradesh, India
K. Ritmeijer	Médecins sans Frontières, OCA, Amsterdam, The Netherlands
I.C. Roseboom	Department of Pharmacy & Pharmacology, Antoni van Leeuwenhoek Hospital/Netherlands Cancer Institute, Amsterdam, the Netherlands
P. Sagaki	Amudat Hospital, Amudat Karamoja Sub-region, Uganda

H.D.F.H. Schallig	Department of Medical Microbiology and Infection Prevention, Laboratory for Experimental Parasitology, Academic Medical Center, Amsterdam, the Netherlands
G.J. Schoone	Department of Medical Microbiology and Infection Prevention, Laboratory for Experimental Parasitology, Academic Medical Center, Amsterdam, the Netherlands
K. Sisay	Médecins sans Frontières, Abdurafi, Ethiopia
A. Solomos	Drugs for Neglected Diseases Initiative, Geneva, Switzerland
S. Sundar	Institute of Medical Sciences, Banaras Hindu University, Varanasi, Uttar Pradesh, India
S. Tesfaye	College of Health Sciences, Addis Ababa University, Addis Ababa, Ethiopia
L. Verrest	Department of Pharmacy & Pharmacology, Antoni van Leeuwenhoek Hospital/Netherlands Cancer Institute, Amsterdam, the Netherlands
M. Wasunna	Drugs for Neglected Diseases Initiative, Nairobi, Kenya
L. Were	Drugs for Neglected Diseases initiative Africa, Nairobi, Kenya
E.A. Wilthagen	Scientific Information Service, Antoni van Leeuwenhoek Hospital/Netherlands Cancer Institute, Amsterdam, the Netherlands
B.M. Younis	Institute of Endemic Diseases, University of Khartoum, Khartoum, Sudan

A

Dankwoord | Acknowledgments

Doing research is a joint effort, and the work described in this thesis could not have been realized without the help of many others. I would like to express my sincere gratitude to everyone who was involved in the realization of this thesis, with a special thank you to the people below.

Allereerst wil ik mijn (co)promotoren bedanken. Dankzij jullie heeft mijn onderzoek tot zulke mooie resultaten geleid, maar heb ik ook ontzettend veel geleerd de afgelopen vier jaar.

Thomas, het was een groot genoegen om de afgelopen jaren met je samen te werken. Na het schrijven van mijn master thesis onder jouw begeleiding wist ik al dat als ik een PhD ging doen, dan zeker in jouw onderzoeksgroep. Ik ben je dankbaar dat je me die kans hebt gegeven en heb ontzettend veel van je geleerd. Je liefde en passie voor farmacometrie en je ambitie om dit op de kaart te zetten op plekken waar het het hardst nodig is, maken je een unieke onderzoeker. Ik wil je bedanken voor je aanstekelijke enthousiasme voor het vak, de waardevolle en gezellige wekelijkse meetings en je onvermoeibare kritische blik op mijn manuscripten, die je keer op keer tot in detail bleef reviseren.

Alwin, bedankt voor je goede begeleiding. Je enthousiasme voor farmacometrie tijdens het NONMEM overleg of een van onze meetings is erg aanstekelijk en na een meeting kwam ik vaak met veel ideeën en motivatie weer naar buiten. Met je analytische blik gaf je altijd doeltreffende feedback, maar daarnaast hielp je klinische kijk me om doelgericht te blijven werken en niet in details te blijven hangen. Dit heeft mijn onderzoek en manuscripten naar een beter niveau gebracht maar heeft er ook voor gezorgd dat ik het uiteindelijk kon afronden.

Jos, wat ben ik blij dat ik mijn PhD kon doen in jouw onderzoeksgroep met zoveel enthousiaste en gedreven onderzoekers. Je wist me bij onze kennismaking meteen te enthousiasmeren over het doen van promotieonderzoek, dat was namelijk de mooiste tijd uit jouw leven. Vanaf de zijlijn heb je me altijd ondersteund bij mijn onderzoek en had je altijd ideeën om mijn manuscripten te verbeteren, bedankt daarvoor.

Besides, I would like to thank everyone from the pharmacometrics group, I learned a lot and really enjoyed our discussions during the NONMEM and NURD meetings.

Mijn OOA begeleidingscommissie, Toine, Marloes en Andre, ook jullie wil ik bedanken voor de fijne ondersteuning, vooral het afgelopen jaar.

I am very grateful for the opportunity to be involved in the Eastern African clinical trials and would like to thank everyone who contributed to my part of research in this.

First and foremost, I would like to thank all the patients and their parents/guardians for their participation in the clinical trials. Without them this research would not have been possible. Also, I would like to thank all the members of the field teams at the

A

study sites, who did such an important job to treat the patients and to follow all the study procedures.

I would like to thank the Drugs for Neglected Diseases initiative (DNDi) for the collaboration and support provided during the past years. Fabiana, your huge amount of knowledge about the VL studies is impressive and I learned a lot from you. Thank you for the interesting discussions and your valuable feedback. Alex and Séverine, thank you for providing the large amounts of data and helping me out with all my questions. I would also like to thank Jorge, Monique, Jane, Isra, and all other members of the LEAP platform for the collaboration and their feedback on my research.

I would like to thank Smita and prof. Sundar from the Institute of Medical Sciences, Baranas Hindu University, India, for providing the paromomycin data from Indian VL patients, which has been of great added value for our research.

Henk en Gerard uit het AMC, afdeling Medische Microbiologie en Infectiepreventie, ik wil jullie hartelijk bedanken voor het opsporen en aanleveren van de qPCR data van verschillende VL studies van de afgelopen jaren. Het is bewonderenswaardig hoeveel interessante inzichten we hebben verkregen uit deze data.

My leishmaniac colleagues Semra, Ignace and Wendy, thank you for the good collaboration on our projects, Ignace for measuring the many many paromomycin and miltefosine samples, and Wendy for the hard work during the last months to help me finishing in time.

Al mijn collega's van H3, ontzettend bedankt voor de leuke tijd. Dit promotietraject voelde nooit als werk wat je alleen doet, maar als iets wat we samen doen. Dankzij jullie ging ik altijd met veel plezier naar het AvL, ik vraag me af of ik ooit nog een baan vind met zoveel gezellige collega's om me heen. Ik ga alle gezelligheid tijdens de lunch, borrels en uitjes erg missen.

Mijn kamergenoten waarmee ik de afgelopen jaren zoveel tijd heb doorgebracht, Mark, Jill, Sanne, Eveline, Karin, Irene, Maarten, Hinke, Marinda, Lishi en Anke, bedankt voor de gezellige tijd. We hebben hard gewerkt maar ook vaak gelachen en stoom afgeblazen. Geniet van mijn werkplek bij het raam en mijn mooie computerschermen, ik hoop dat er veel mooie publicaties tot stand komen!

Hinke en Marinda, wat fijn dat jullie naast me willen staan bij mijn verdediging. Ik ben blij dat we elkaar zo goed hebben leren kennen en hoop jullie nog vaak te zien.

Mijn lieve familie en vrienden, bedankt voor alle steun, interesse en de welkome afleiding de afgelopen jaren. Wat is het fijn om jullie om me heen te hebben.

Jan, jou wil ik natuurlijk ook bedanken voor alles. Met jouw humor weet je mijn werk altijd te relativeren, want waarom moest ik altijd zo druk bezig zijn met "plotjes runnen". Je leuke kijk op de dingen houdt me altijd scherp. Je helpt me de juiste keuzes te maken en je staat altijd achter me, ook al was een van je adviezen "als je maar nooit een PhD gaat doen". Ook dit hebben we tot een goed eind weten te brengen en ik kijk uit naar al het volgende wat op ons pad gaat komen.

Jaap en je kleine zus, jullie hebben het afronden van deze PhD een grote uitdaging gemaakt, maar daar prijs ik mezelf erg gelukkig voor.

A

Curriculum Vitae

Luka Verrest was born on January 31st 1991 in Bergen op Zoom, the Netherlands. After graduating from high school at R.K. Gymnasium Juvenaat H. Hart in Bergen op Zoom, she started the study Pharmacy at Utrecht University in 2009. In 2013 she started the master's program Drug Innovation at the faculty of Life Sciences, where she did a nine-month research internship at the department of Translational Immunology at the University Medical Center Utrecht, focusing on modelling of exposure to Anti-Thymocyte Globulin (ATG) and reconstitution of the immune system in patients receiving allogeneic-Hematopoietic Stem Cell Transplantation (HSCT). She also did a six-month research internship at the School of Pharmacy at University College London, studying the analgesic response of gabapentin to children with chronic pain by modelling & simulation. After graduating in 2016, she started as a junior PK-PD consultant at LAP&P Consultants, Leiden. In 2018, she started her PhD at the department of Pharmacy & Pharmacology at the Netherlands Cancer Institute/Antoni van Leeuwenhoek hospital, under supervision of prof. dr. A.D.R. Huitema, prof. dr. J.H. Beijnen and dr. T.P.C. Dorlo. During her PhD she also finished the clinical pharmacology training of the Dutch Society of Clinical Pharmacology & Biopharmacy. Her PhD research resulted in this thesis, which she will defend at Utrecht University on March 16th 2023.

A